



<https://theses.gla.ac.uk/>

Theses Digitisation:

<https://www.gla.ac.uk/myglasgow/research/enlighten/theses/digitisation/>

This is a digitised version of the original print thesis.

Copyright and moral rights for this work are retained by the author

A copy can be downloaded for personal non-commercial research or study, without prior permission or charge

This work cannot be reproduced or quoted extensively from without first obtaining permission in writing from the author

The content must not be changed in any way or sold commercially in any format or medium without the formal permission of the author

When referring to this work, full bibliographic details including the author, title, awarding institution and date of the thesis must be given

Enlighten: Theses

<https://theses.gla.ac.uk/>  
[research-enlighten@glasgow.ac.uk](mailto:research-enlighten@glasgow.ac.uk)

**Cellular distribution of  $\alpha_1$ -adrenoceptors  
using visualisation and radioligand binding  
techniques.**

**Darren Caldwell**

A thesis submitted for the degree of Doctor of Philosophy (September,  
2003) from

**Institute of Biomedical & Life Sciences, University of Glasgow,  
Glasgow, G12 8QQ**

ProQuest Number: 10390440

All rights reserved

INFORMATION TO ALL USERS

The quality of this reproduction is dependent upon the quality of the copy submitted.

In the unlikely event that the author did not send a complete manuscript and there are missing pages, these will be noted. Also, if material had to be removed, a note will indicate the deletion.



ProQuest 10390440

Published by ProQuest LLC (2017). Copyright of the Dissertation is held by the Author.

All rights reserved.

This work is protected against unauthorized copying under Title 17, United States Code  
Microform Edition © ProQuest LLC.

ProQuest LLC.  
789 East Eisenhower Parkway  
P.O. Box 1346  
Ann Arbor, MI 48106 – 1346

GLASC  
UNIVERSITY  
LIBRARY:

13278

COPY 2

## Contents

Thesis contents

Acknowledgements

Declaration

List of figures and tables

Abbreviations

Summary of results

<b><u>Chapter 1. Introduction</u></b>	<b>Page No.</b>
1.1 Historical perspective	1
1.2 Pharmacological subclassification	2
1.2.1 $\alpha_{1H}$ -, and $\alpha_{1L}$ -adrenoceptors	
1.3 Molecular cloning	5
1.3.1 $\alpha_{1B}$ -adrenoceptors	
1.3.2 $\alpha_{1A}$ -adrenoceptors	
1.3.3 $\alpha_{1D}$ -adrenoceptors	
1.3.4 Splice variants	
1.4 Signal transduction mechanisms	8
1.4.1 Calcium influx	
1.4.2 cyclicAMP	
1.4.3 Arachidonic acid	
1.4.4 Phospholipase D	
1.4.5 Mitogenic responses	
1.5 G-protein coupled receptors	13
1.5.1 $\alpha_1$ -AR agonist binding	
1.5.2 Antagonist binding	
1.5.3 Inverse agonism and neutral antagonism	
1.6 Subtype-selective drugs	19
1.6.1 $\alpha_{1A}$ -AR antagonists	
1.6.2 $\alpha_{1B}$ -AR antagonists	

1.6.3	$\alpha_{1D}$ -AR antagonists	
1.6.4	$\alpha_1$ -AR agonists	
1.7	Desensitisation	25
1.7.1	Homologous desensitisation	
1.7.2	Heterologous desensitisation	
1.7.3	Phosphorylation of $\alpha_1$ -ARs	
1.8	Endocytosis	28
1.8.1	Clathrin-coated vesicles	
1.8.2	Caveolae	
1.8.3	Endocytotic rate	
1.8.4	Inhibiting endocytosis	
1.8.5	Receptor degradation	
1.8.6	Receptor trafficking	
1.9	Fluorescent ligand binding	33
1.9.1	GPCRs and GFP	
1.9.2	QAPB and subcellular localisation	
1.9.3	Extraneuronal monoamine transporter	

Figures. 1.1-1.3

## **Chapter 2. The cellular distribution of $\alpha_1$ -ARs using radioligand binding techniques**

2.0	Aims and objectives	41
	Figures. 2.1-2.2	
2.1	Methods	44
2.1.1	Cell culture	
2.1.1.1	Freezing cells	
2.1.1.2	Growing cells	
2.1.1.3	Cell splitting	
2.1.2	Membrane preparation	

2.1.3	Whole cell preparation	
2.1.4	Radioligand binding studies	
2.1.4.1	Competition binding experiments	
2.1.4.2	Displacement binding experiments	
2.1.4.3	Data analysis	
2.1.5	Materials and chemicals	
2.2	Results	51
2.2.1	Competitive inhibition of radioligand binding	
2.2.1.1	Membranes	
2.2.1.2	Whole cells	
2.2.2	New radioligand binding protocol 1	
2.2.3	New radioligand binding protocol 2	
2.2.4	New radioligand binding protocol 3	
	Figures. 2.3-2.47	
	Tables. 2.1-2.12	
2.3	Discussion	120
2.3.1	Competitive inhibition of radioligand binding	
2.3.1.1	Agonists	
2.3.1.2	Antagonists	
2.3.2	New radioligand binding protocol 1	
2.3.3	New radioligand binding protocol 2	
2.3.4	New radioligand binding protocol 3	

### **Chapter 3. The cellular distribution of $\alpha_1$ -ARs using visualisation techniques**

3.0	Aims and objectives	130
3.1	Methods	131
3.1.1	Cell culture	

- 3.1.1.1 Freezing cells
- 3.1.1.2 Growing cells
- 3.1.1.3 Cell splitting
- 3.1.2 Measurement of  $[Ca^{2+}]_i$ 
  - 3.1.2.1 Microspectrofluorimetry analysis
  - 3.1.2.2 Calcium imaging
  - 3.1.2.3 Response curves
  - 3.1.2.4 Data analysis
- 3.1.3 Materials and chemicals

Figure 3.1

## 3.2 Results

136

- 3.2.1 Microspectrofluorimetry
  - 3.2.1.1  $Ca^{2+}$  signalling mechanism
    - 3.2.1.1.1 Effect of phenylephrine on  $[Ca^{2+}]_i$
    - 3.2.1.1.2 Role of external  $Ca^{2+}$  in  $[Ca^{2+}]_i$  responses to phenylephrine
  - 3.2.2 Functional studies
    - 3.2.2.1 Agonist response
    - 3.2.2.2 Photobleaching
    - 3.2.2.3 Antagonist response
      - 3.2.2.3.1 4nM QAPB
      - 3.2.2.3.2 Removal of QAPB
      - 3.2.2.3.3 0.5nM QAPB
      - 3.2.2.3.4 2nM QAPB
      - 3.2.2.3.5 6nM QAPB
    - 3.2.2.4 Insurmountable antagonism
  - 3.2.3 Direct visualisation of fluorescent binding
    - 3.2.3.1 QAPB displacement by agonist
    - 3.2.3.2 QAPB displacement by antagonist
    - 3.2.3.3 Intracellular compartment localisation

Figures. 3.2-3.23

3.3 Discussion	165
3.3.1 Microspectrofluorimetry	
Figure 3.24	
3.3.2 Direct visualisation of fluorescent binding	
Figure 3.25	
4.0 Conclusions	176
5.0 References	179

## Acknowledgements

First and foremost, I'd like to thank Prof. McGrath for being a fantastic supervisor. You simply couldn't ask for a better person to guide you through your PhD and I'm extremely grateful for his time and wealth of knowledge. I've thoroughly enjoyed working in his lab and really appreciated both his pats on the back when I've done well and kicks up the backside when they've been needed. These things count.

I'd also like to sincerely thank John for all his time and help. He's one busy guy, but has always made time for me. I'll also say "cheers" to John for being a good mate in San Francisco. Thanks to Janet for helping me get started with the radioligand binding work. Much appreciated. Big thanks to Simon who has always helped when I can't find things and also when technical problems went wrong. Cheers mate.

Lab 440 is a great lab to work in. The best. Everybody gets on and has a good laugh. Thanks to Alison, Angela, Ann, Clare, Jillian, Joyce, Jude, Monty, Mrs K, Simon and Zeeshan for making the lab a fantastic place to work. Special thanks to Melissa, who has been my "partner in crime". I'd like to think we've caused a few smiles in the lab with our double act. Big thanks must go to Craig, who has become a good pal. We've spent endless hours talking (over a few pints) about our two favourite passions: football and music ! He's also helped and encouraged me with my guitar playing and will be rewarded with a VIP pass when I play Hampden !!

I simply cannot thank my Mum and Dad enough for their love, help and support throughout my university life. Absolutely anything I've needed, they've helped me with. I won't forget. I'd like to thank my Grandad for always helping and being very, very good to me. A mention and big thanks also to Jane, Andy and James. The last and by far the biggest thank you of the lot is for Debbie. Words simply can't do justice to what I'd like to say, so I'll keep it simple. I love you.

"The road of excess leads to the palace of wisdom"

- William Blake

## **Declaration**

The work contained within this thesis is entirely my own.

This work has not been presented in whole or as part of any other degree course.

## **Publications:**

**Caldwell, D.**, Pediani, J.D., MacKenzie, J.F. & McGrath, J.C. (2002). Competitive radioligand binding assessment of the differences between cell surface and intracellular binding sites in membranes and whole cells expressing the bovine  $\alpha_{1a}$ -adrenoceptor (AR). XIVth World Congress of Pharmacology, San Francisco, USA.

## List of figures & tables

### Chapter 1. Introduction

**Figure 1.1** Agonist chemical structures

**Figure 1.2** Prazosin and QAPB structures

**Figure 1.3** BMY7378 and RS100329 structures

### Chapter 2. The cellular distribution of $\alpha_1$ -adrenoceptors using radioligand binding techniques.

**Figure 2.1** Radioligand binding protocols

**Figure 2.2** Updated radioligand binding protocol

### Antagonists

**Figure 2.3** Displacement of 0.2 nM [ $^3\text{H}$ ]prazosin binding to bovine  $\alpha_{1a}$ -AR membranes by increasing concentrations of prazosin

**Figure 2.4** Displacement of 0.2 nM [ $^3\text{H}$ ]prazosin binding to bovine  $\alpha_{1a}$ -AR membranes by increasing concentrations of QAPB

**Figure 2.5** Displacement of 0.2 nM [ $^3\text{H}$ ]prazosin binding to bovine  $\alpha_{1a}$ -AR membranes by increasing concentrations of RS100329

**Figure 2.6** Displacement of 0.2 nM [ $^3\text{H}$ ]prazosin binding to bovine  $\alpha_{1a}$ -AR membranes by increasing concentrations of L-765314

**Figure 2.7** Displacement of 0.2 nM [ $^3\text{H}$ ]prazosin binding to bovine  $\alpha_{1a}$ -AR whole cells and membranes by increasing concentrations of prazosin

**Figure 2.8** Displacement of 0.2 nM [ $^3\text{H}$ ]prazosin binding to bovine  $\alpha_{1a}$ -AR whole cells and membranes by increasing concentrations of RS100329

**Figure 2.9** Displacement of 0.2 nM [ $^3\text{H}$ ]prazosin binding to bovine  $\alpha_{1a}$ -AR whole cells by increasing concentrations of QAPB in light surroundings and dark surroundings

**Figure 2.10** Displacement of 0.2 nM [ $^3\text{H}$ ]prazosin binding to bovine  $\alpha_{1a}$ -AR whole cells and membranes by increasing concentrations of QAPB

**Figure 2.11** Displacement of 0.2 nM [ $^3\text{H}$ ]prazosin binding to bovine  $\alpha_{1a}$ -AR whole cells and membranes by increasing concentrations of L-765314

**Figure 2.12** Displacement of 0.2 nM [ $^3\text{H}$ ]prazosin binding to bovine  $\alpha_{1a}$ -AR whole cells, membranes and to human  $\alpha_{1a}$ -AR whole cells and membranes by increasing concentrations of BMY7378

**Figure 2.13** Comparison of radioligand binding protocols using RS100329 as the competing/displacing ligand

**Figure 2.14** Comparison of radioligand binding protocols using QAPB as the competing/displacing ligand

**Figure 2.15** Comparison of radioligand binding protocols using prazosin as the competing/displacing ligand

**Figure 2.16** Displacement of 0.2 nM [<sup>3</sup>H]prazosin binding to bovine  $\alpha_{1a}$ -AR whole cells by increasing concentrations of QAPB using an updated radioligand binding protocol.

**Figure 2.17** Displacement of 0.2 nM [<sup>3</sup>H]prazosin binding to bovine  $\alpha_{1a}$ -AR whole cells by increasing concentrations of QAPB using an updated radioligand binding protocol in the presence and absence of 0.25mg/ml concanavalin A

**Figure 2.18** Effect of cold temperature on displacement of 0.2 nM [<sup>3</sup>H]prazosin binding to bovine  $\alpha_{1a}$ -AR whole cells by increasing concentrations of QAPB using an updated radioligand binding protocol

**Figure 2.19** Effect of cold temperature on displacement of 0.2 nM [<sup>3</sup>H]prazosin binding to bovine  $\alpha_{1a}$ -AR membranes by increasing concentrations of QAPB using an updated radioligand binding protocol

**Figure 2.20** Displacement of 0.2 nM [<sup>3</sup>H]prazosin binding to bovine  $\alpha_{1a}$ -AR whole cells by increasing concentrations of L-765314 using a standard and updated radioligand binding protocol

**Figure 2.21** Displacement of 0.2 nM [<sup>3</sup>H]prazosin binding to bovine  $\alpha_{1a}$ -AR whole cells by increasing concentrations of BMY7378 using a standard and updated radioligand binding protocol

### Agonists

**Figure 2.22** Displacement of 0.2 nM [<sup>3</sup>H]prazosin binding to bovine  $\alpha_{1a}$ -AR membranes by increasing concentrations of phenylephrine in the presence of and absence of 0.25 mM GTP- $\gamma$ -S

**Figure 2.23** Displacement of 0.2 nM [<sup>3</sup>H]prazosin binding to bovine  $\alpha_{1a}$ -AR membranes by increasing concentrations of A61603 in the presence of and absence of 0.25 mM GTP- $\gamma$ -S

**Figure 2.24** Displacement of 0.2 nM [<sup>3</sup>H]prazosin binding to bovine  $\alpha_{1a}$ -AR membranes by increasing concentrations of noradrenaline

**Figure 2.25** Displacement of 0.2 nM [<sup>3</sup>H]prazosin binding to bovine  $\alpha_{1a}$ -AR membranes by increasing concentrations of adrenaline

**Figure 2.26** Displacement of 0.2 nM [<sup>3</sup>H]prazosin binding to bovine  $\alpha_{1a}$ -AR whole cells by increasing concentrations of phenylephrine in the presence of and absence of 0.25 mM GTP- $\gamma$ -S

**Figure 2.27** Displacement of 0.2 nM [<sup>3</sup>H]prazosin binding to bovine  $\alpha_{1a}$ -AR whole cells and membranes by increasing concentrations of phenylephrine in the presence of 0.25 mM GTP- $\gamma$ -S

**Figure 2.28** Displacement of 0.2 nM [<sup>3</sup>H]prazosin binding to bovine  $\alpha_{1a}$ -AR whole cells by increasing concentrations of A61603

**Figure 2.29** Displacement of 0.2 nM [<sup>3</sup>H]prazosin binding to bovine  $\alpha_{1a}$ -AR whole cells by increasing concentrations of A61603 in the presence of 0.25 mM GTP- $\gamma$ -S

**Figure 2.30** Effect of temperature on displacement of 0.2 nM [<sup>3</sup>H]prazosin binding to bovine  $\alpha_{1a}$ -AR whole cells by increasing concentrations of noradrenaline

**Figure 2.31** Displacement of 0.2 nM [<sup>3</sup>H]prazosin binding to bovine  $\alpha_{1a}$ -AR whole cells and membranes by increasing concentrations of noradrenaline

**Figure 2.32** Displacement of 0.2 nM [<sup>3</sup>H]prazosin binding to bovine  $\alpha_{1a}$ -AR whole cells by increasing concentrations of noradrenaline in the absence and presence of 1 $\mu$ M corticosterone

**Figure 2.33** Effect of incubation time on displacement of 0.2 nM [<sup>3</sup>H]prazosin binding to bovine  $\alpha_{1a}$ -AR whole cells by increasing concentrations of noradrenaline

**Figure 2.34** Displacement of 0.2 nM [<sup>3</sup>H]prazosin binding to bovine  $\alpha_{1a}$ -AR whole cells and membranes by increasing concentrations of adrenaline

**Figure 2.35** Displacement of 0.2 nM [<sup>3</sup>H]prazosin binding to bovine  $\alpha_{1a}$ -AR whole cells by increasing concentrations of noradrenaline for 60 minutes at 22°C

**Figure 2.36** Displacement of 0.2 nM [<sup>3</sup>H]prazosin binding to bovine  $\alpha_{1a}$ -AR whole cells by increasing concentrations of noradrenaline using a new radioligand binding protocol and standard radioligand binding protocol

**Figure 2.37** Displacement of 0.2 nM [<sup>3</sup>H]prazosin binding to bovine  $\alpha_{1a}$ -AR membranes by increasing concentrations of adrenaline using an updated radioligand binding protocol

**Figure 2.38** Comparison of radioligand binding protocols using adrenaline as the competing/displacing ligand

**Figure 2.39** Effect of corticosterone on displacement of 0.2 nM [<sup>3</sup>H]prazosin binding to bovine  $\alpha_{1a}$ -AR whole cells by increasing concentrations of adrenaline using an updated radioligand binding protocol

**Figure 2.40** Comparison of the absence and presence of corticosterone on the displacement of 0.2 nM [<sup>3</sup>H]prazosin binding to bovine  $\alpha_{1a}$ -AR whole cells by increasing concentrations of adrenaline using an updated radioligand binding protocol

**Figure 2.41** Effect of concanavalin A on displacement of 0.2 nM [<sup>3</sup>H]prazosin binding to bovine  $\alpha_{1a}$ -AR whole cells by increasing concentrations of adrenaline using an updated radioligand binding protocol

**Figure 2.42** Displacement of 0.2 nM [<sup>3</sup>H]prazosin binding to bovine  $\alpha_{1a}$ -AR membranes by increasing concentrations of noradrenaline using an updated radioligand binding protocol

**Figure 2.43** Comparison of radioligand binding protocols using noradrenaline as the competing/displacing ligand

**Figure 2.44** Comparison of radioligand binding protocols using phenylephrine as the competing/displacing ligand

**Figure 2.45** Comparison of radioligand binding protocols using A61603 as the competing/displacing ligand

**Figure 2.46** Effect of cold temperature on displacement of 0.2 nM [<sup>3</sup>H]prazosin binding to bovine  $\alpha_{1a}$ -AR whole cells by increasing concentrations of noradrenaline using an updated radioligand binding protocol

**Figure 2.47** Effect of cold temperature on displacement of 0.2 nM [<sup>3</sup>H]prazosin binding to bovine  $\alpha_{1a}$ -AR membranes by increasing concentrations of noradrenaline using an updated radioligand binding protocol

**Table 2.1** Classic Binding Protocol: Membranes

**Table 2.2** Classic Binding Protocol: Whole Cells

**Table 2.3** Corticosterone influence on noradrenaline

**Table 2.4** BMY7378: Comparison of  $\alpha_{1a}$  and  $\alpha_{1d}$  adrenoceptors

**Table 2.5** Effect of pre-incubation time on displacement by noradrenaline: whole cells

**Table 2.6** Displacement at 37°C and 22°C: whole cells

**Table 2.7a** Displacement after [<sup>3</sup>H]prazosin for 60 minutes: Membranes and whole cells

- Table 2.7b** Displacement after [<sup>3</sup>H]prazosin for 60 minutes: Whole cells  
**Table 2.8** Corticosterone influence on adrenaline  
**Table 2.9** Concanavalin A: influence on adrenaline  
**Table 2.10** Effect of pre-incubation time on displacement by QAPB: whole cells  
**Table 2.11** Displacement from whole cells and membranes at 4°C  
**Table 2.12** Concanavalin A: influence on QAPB: whole cells

**Chapter 3.** The cellular distribution of  $\alpha_1$ -adrenoceptors using visualisation techniques.

- Figure 3.1** Diagram of experimental set-up  
**Figure 3.2** Chemical structure of Fura-2  
**Figure 3.3** Excitation spectra of fura-2 in increasing concentrations of free calcium  
**Figure 3.4** Trace showing changes in  $[Ca^{2+}]_i$  in response to phenylephrine in R-1Fs stably expressing the bovine  $\alpha_{1a}$ -AR  
**Figure 3.5** Concentration-dependant effects of phenylephrine on  $[Ca^{2+}]_i$  release  
**Figure 3.6** Maintenance of steady state equilibrium binding of QAPB (4nM) over a 4-hour time period in R-1Fs stably expressing the bovine  $\alpha_{1a}$ -AR  
**Figure 3.7** Trace showing simultaneous recording of QAPB signal and antagonised fura-2  $Ca^{2+}$  responses  
**Figure 3.8** Trace represents same experiment shown in Figure 3.7, with only the QAPB signal and antagonised ratio 340/380 Fura-2  $Ca^{2+}$  signal shown  
**Figure 3.9** Trace showing simultaneous recording of 0.5nM QAPB signal and antagonised fura-2  $Ca^{2+}$  responses  
**Figure 3.10** Trace showing simultaneous recording of 2nM QAPB signal and antagonised fura-2  $Ca^{2+}$  responses  
**Figure 3.11** Trace showing simultaneous recording of 6nM QAPB signal and antagonised fura-2  $Ca^{2+}$  responses  
**Figure 3.12** CRC to phenylephrine in the absence and presence of QAPB  
**Figure 3.13** QAPB binding to Rat-1 Fibroblasts expressing the bovine  $\alpha_{1a}$ -AR  
**Figure 3.14** Effect of reverse displacement  
**Figure 3.15** Cells incubated with 4nM QAPB in the presence of increasing concentrations of phenylephrine  
**Figure 3.16** Binding of QAPB was reversible  
**Figure 3.17** QAPB displacement by phenylephrine  
**Figure 3.18** QAPB displacement by phentolamine  
**Figure 3.19** QAPB staining in unstimulated Rat-1 fibroblasts stably expressing the bovine  $\alpha_{1a}$ -AR  
**Figure 3.20** Merged image between internal QAPB-receptor complex and early endosomal marker in Rat-1 fibroblasts  
**Figure 3.21** Co-localisation between internal QAPB-receptor complex and early endosomal marker in Rat-1 fibroblasts  
**Figure 3.22** Types of RACC  
**Figure 3.23** Constitutive recycling of the  $\alpha_{1a}$ -AR in Rat-1 fibroblasts

## Abbreviations

**5-HT:** 5-hydroxytryptamine

**A-204176:** (N-[5-(1H-imidazol-4-yl)-5,6,7,8-tetrahydro-1-naphthalenyl]methanesulfonamide

**AA:** arachidonic acid

**AH11110A:** 4-Imino-1-(2-phenylphenoxy)-4-piperidinebutan-2-ol hydrochloride

**AR:** adrenoceptor

**BAPTA:** 1,2,-bis(o-aminophenoxy)ethane-N-N'-N'-N'-tetraacetic acid

**BMY7378:** (8-[2-(4-(2-methoxyphenyl)piperazin-1-yl)ethyl]-8-azaspiro[4,5]decane-7,9-dione)

**BPH:** benign prostatic hyperplasia

**[Ca<sup>2+</sup>]<sub>er</sub>:** concentration of Ca<sup>2+</sup> in the ER lumen

**[Ca<sup>2+</sup>]<sub>i</sub>:** intracellular Ca<sup>2+</sup> concentration

**Ca<sup>2+</sup>:** calcium (II)

**CaCl<sub>2</sub>:** calcium chloride

**cAMP:** cyclic adenosine monophosphate

**CCD:** charge-coupled device

**cDNA:** complementary deoxyribonucleic acid

**CEC:** chloroethylclonidine

**CHO:** Chinese hamster ovary

**CO<sub>2</sub>:** carbon dioxide

**COMT:** catechol-O-methyltransferase

**Con A:** concanavalin A

**CRCs:** Concentration-Ca<sup>2+</sup> response curves

**DAG:** diacylglycerol

**DMEM:** Dulbecco's modified Eagle medium

**DMSO:** dimethyl sulfoxide

**DNA:** deoxyribonucleic acid

**EDTA:** ethylene-diamine tetra acidic acid

**EGTA:** ethylene-glycol tetra acetic acid

**EMT:** extraneuronal monoamine transporter

**ER:** endoplasmic reticulum

**FACS:** fluorescence activated cell sorting

**Fura-2 AM:** Fura-2 acetoxymethyl ester

**GAP:** GTPase-activating protein

**GDP:** guanosine diphosphate

**GFP:** green fluorescent protein

**GPCR:** G-protein-coupled receptor

**GRK:** G-protein-receptor kinase

**GTP:** guanosine triphosphate

**GTP- $\gamma$ -S:** guanosine 5'-O-(3-thiotriphosphate), tetralithium salt

**H<sup>+</sup>:** hydrogen (I)

**HCl:** hydrochloride

**HV732:**  $\alpha$ -ethyl-3,4,5-trimethoxy-a-(3-((2-(2-methoxyphenoxy)ethyl)-amino)propyl)-benzeneacetonitrile fumarate

**IUPHAR:** International Union of Pharmacology Committee on Receptor Nomenclature and Drug Classification

**IP<sub>3</sub>:** inositol 1,4,5-trisphosphate

**K<sup>+</sup>:** potassium (I)

**KCl:** potassium chloride

**KMD3213:** 1-(3-hydroxypropyl)-5-[2 [[2 [2 (2,2,2 trifluoroethoxy)phenoxy]ethyl]-amino]propyl]-indoline-7-carboxamide

**L-765314:** 4-Amino-2-[4-[1-(benzyloxycarbonyl)-2(S)-[[[(1,1-dimethylethyl)amino]carbonyl]-piperazinyl]-6,7-dimethoxyquinazoline

**LGCC:** ligand-gated calcium channel

**MAO:** monoamine oxidase

**MAPK:** mitogen-activated protein kinase

**MDCK:** Madine-Darby canine kidney

**MgCl<sub>2</sub>:** magnesium chloride

**mRNA:** messenger ribonucleic acid

**Na<sup>+</sup>:** sodium (I)

**NaCl:** sodium chloride

**PA<sub>2</sub>:** phospholipase A<sub>2</sub>

**PC-12:** pheochromocytoma cells

**PD-98059:** 2'-Amino-3'methoxyflavone

**pH:** negative logarithm of base 10 of the hydrogen (H) concentration

**PI:** phosphatidylinositol

**PIP<sub>2</sub>:** phosphatidylinositol 4,5-biphosphate

**PKA:** protein kinase A

**PKC:** protein kinase C

**pK<sub>i</sub>:** negative logarithm of a concentration of competing ligand in a competition assay that would occupy 50% of the receptors if no radioligand was present.

**PLC:** phospholipase C

**PLD:** phospholipase D

**PNRC:** peri-nuclear recycling compartment

**PPA:** phenylpropanolamine

**QAPB:** BODIPY FL-prazosin

**R-1Fs:** Rat-1 Fibroblasts

**R-A-61603:** (R)-enantiomer of *N*-[5-(4,5-dihydro-1 *H*-imidazol-2yl)-2-hydroxy-5,6,7,8-tetrahydronaphthalen-1-yl] methane sulphonamide

**RACC:** receptor-activated calcium channel

**REC15/2739:** 8-3-[4-(2-Methoxyphenyl)-1-piperazinyl]propylcarbonyl-3-methyl-4oxo-2,2-phenyl-4H-1-benzopyran dihydrochloride

**REC15/3039:** (8-[2-[4-(5-chloro-2-methoxyphenyl)-1-piperazinyl]ethyl]-8-azaspiro[4,5] decane-7,9-dione)

**RGS:** regulators of G-protein signalling

**RLB:** radioligand binding

**Ro 70-0004:** (3-(3-{4-[Fluoro-2-(2,2,2-trifluoroethoxy)-phenyl]-piperazin-1-yl}-propyl)-5-methyl-1H-pyrimidine-2,4-dione mono hydrochloride monohydrate)

**RS100329:** (5-methyl-3-[3-[4-[2-(2,2,2,-trifluoroethoxy)phenyl]-1-piperazinyl]propyl]-2,4-(1H)-pyrimidinedione)

**RWJ-38063:** N-(2-{4-[2-methylethoxy]phenyl]piperazinyl}ethyl)-2-(2-oxopiperidyl)acetamide

**SERCA:** sarco-endoplasmic reticulum Ca<sup>2+</sup>-ATPases

**SMCs:** smooth muscle cells

**SNAP5089:** 1,4-dihydro-2,6-dimethyl-4-(4 nitrophenyl)-3,5-pyridinedicarboxylic acid [3 (4,4 diphenyl-1-piperidinyl)propyl]amide methyl ester

**SOCC:** store-operated calcium channel

**SR/ER:** sarco-endoplasmic reticulum

**TM:** transmembrane

**VOCC:** voltage-operated calcium channel

**WB4101:** 2-(2,6-dimethoxyphenoxyethyl)aminomethyl-1,4-benzodioxane

## Summary of results

Cellular distributions of  $\alpha_1$ -adrenoceptors (ARs) were assessed using visualisation and radioligand binding techniques in Rat-1 fibroblasts stably expressing the bovine  $\alpha_{1a}$ -AR. Competitive radioligand binding (RLB) was compared in whole cell and isolated membrane preparations using both classical and updated RLB protocols. A range of agonists and antagonists displayed their known characteristics in membranes. Whole cell competitive RLB for most ligands displayed a high affinity binding site, consistent with a population of ~25% of the sites that had affinity  $\geq$  in membranes, whereas the other 75% had affinity variably lower than in membranes according to the competitor. Results suggest the high affinity component represents displacement of  $^3\text{H}$ -prazosin from cell surface receptors and the low affinity component that follows a slow sustained plateau phase represents a displacement from intracellular binding sites. Displacement by competing ligands occurred in a time-dependent, temperature-independent manner.

An early hypothesis that ligands penetrated the cell and accessed intracellular compartments via an extraneuronal monoamine transporter (EMT) was dispelled following the inability of corticosterone to block the uptake of ligands entering cells. A more likely method of how ligands access intracellular compartments is by endocytosis via clathrin-coated pits. Concanavalin A is an endocytotic blocker and exerted an inhibiting effect that could be overcome once a certain concentration of antagonist (QAPB) had been applied. It did, however, exert little effect on the ability of an agonist (adrenaline) to displace radiolabelled prazosin from intracellular binding sites.

The possibility of an endocytotic pathway for cellular penetration was supported by direct visualisation studies. Following a sustained period of time, the fluorescent  $\alpha_1$ -AR antagonist BODIPY-FL prazosin (QAPB) was detected in high fluorescent intensity "hot spots" throughout the cytosol. The intensity of the fluorescent signal steadily decreased following cumulative applications of the  $\alpha_1$ -AR agonist phenylephrine and was also reversible upon phenylephrine removal. This indicates

that not only can antagonists penetrate cells and bind to intracellular compartments, but also agonists can penetrate cells and subsequently displace antagonist from these intracellular binding sites. The ability of antagonists to selectively compete at the cell surface and intracellular regions was validated by results showing the  $\alpha$ -AR antagonist phentolamine displacing QAPB from both cell surface and intracellular binding sites. Colocalisation with fluorescent dyes that can identify subcellular compartments (Transferrin Alexa Fluor<sup>546</sup>) indicated partial localisation with the early and recycling endosomes. This strongly suggests that  $\alpha_{1a}$ -AR ligand complexes follow the endocytotic recycling pathway, via early and recycling endosomes.

Using microspectrofluorimetry techniques, phenylephrine-activated  $\text{Ca}^{2+}$  signals were recorded from single Rat-1 fibroblasts stably expressing the bovine  $\alpha_{1a}$ -AR and used to analyse functional agonist-antagonist interactions. The results demonstrate that the dominant  $\text{Ca}^{2+}$  entry pathway evoked by the bovine  $\alpha_{1a}$ -AR is store-operated, in which the  $\text{Ca}^{2+}$  content of agonist-sensitive intracellular  $\text{Ca}^{2+}$  stores governs  $\text{Ca}^{2+}$  influx. Beyond the concentration of phenylephrine that produced the maximum response ( $>3 \times 10^{-5} \text{M}$ ), the concentration-response relationships displayed fade, which could be explained by agonist-dependent depletion of  $\text{Ca}^{2+}$  stores. Antagonism exhibited by QAPB produced concentration-dependent, nonparallel, rightward displacements in the control concentration- $\text{Ca}^{2+}$  response curve to phenylephrine with a decrease in maximal response. This represents an example of insurmountable antagonism, where the antagonist dissociates very slowly (or not at all) from the receptor. It is demonstrated by a rightward shift as the antagonist concentration increases and also by a decrease in maximal response.

## 1.0 INTRODUCTION

### 1.1 Historical Perspective

Adrenoceptors (ARs) mediate the central and peripheral actions of the primary sympathetic neurotransmitter, noradrenaline, and the primary adrenal medullary hormone (and central neurotransmitter) adrenaline. Adrenoceptors are found in nearly all peripheral tissues and on many neuronal populations within the central nervous system. Adrenoceptors mediate a variety of functions and have been of major interest for many years as targets for drug action (Bylund *et al*, 1994).

It was as far back as 1895 that Oliver and Schaffer showed that *in vivo* injections of adrenal gland caused a rise in arterial blood pressure (Oliver & Schaffer, 1895). After the subsequent isolation of adrenaline as the active principle, it was as shown by Dale in 1913 that adrenaline causes two distinct kinds of effect, namely vasoconstriction (which predominates and causes the rise in arterial pressure) and vasodilation.

Following the disappearance of the vasoconstrictor component, Dale noticed that adrenaline caused a fall instead of a rise in arterial pressure, when an animal was first injected with an ergot derivative (Rang *et al*, 1995). Dale had a disagreement with JN Langley in relation to these results, refusing to interpret them in terms of a difference between categories of receptor. This variation in effect was subsequently believed to have arisen from the release of different endogenous catecholamines called sympathins (sympathin I for inhibitory and sympathin E for excitatory), with each one producing a different effect at the same receptor (Cannon & Rosenbleuth, 1933).

In 1948, Ahlquist used a quantitative approach to propose the existence of two AR subtypes, based on different rank orders of potency. He found that the potencies of various catecholamines including adrenaline, noradrenaline and isoprenaline, fell into two distinct patterns, depending on what response was being measured. Ahlquist designated the two types of ARs as  $\alpha$  and  $\beta$ , and defined them in terms of agonist potencies as follows (Rang *et al*, 1995):

$\alpha$  Noradrenaline > Adrenaline > Isoprenaline

$\beta$  Isoprenaline > Adrenaline > Noradrenaline

Following Ahlquist's findings, it was recognised that certain ergot alkaloids studied by Dale, act as selective  $\alpha$ -AR antagonists, and that Dale's adrenaline reversal experiment reflected the unmasking of the  $\beta$  effects of adrenaline by  $\alpha$ -AR blockade. Final proof of Ahlquist's subclassification scheme came in 1957 with the discovery of a compound that could block  $\beta$ -ARs (Moran & Perkins, 1958; Powell & Slater, 1958).

In 1967, Lands and colleagues, comparing rank orders of potency of agonists, in a manner similar to that of Ahlquist, concluded that there were two subtypes of the  $\beta$ -AR. The  $\beta_1$ -AR, the dominant receptor in heart and adipose tissue, was equally sensitive to noradrenaline and adrenaline, whereas the  $\beta_2$ -AR, responsible for relaxation of vascular, uterine, and airway smooth muscle, was much less sensitive to noradrenaline compared to adrenaline (Bylund *et al*, 1994).

In the early 1970s, after prejunctional  $\alpha$ -ARs had been identified, it became apparent that pre- and postjunctional  $\alpha$ -ARs had different pharmacological characteristics. Langer proposed that postsynaptic  $\alpha$ -adrenergic receptors be referred to as  $\alpha_1$ , and presynaptic receptors be referred to as  $\alpha_2$  (Langer, 1974). Soon after, it was suggested that  $\alpha_2$ -adrenergic receptors may have several nonneuronal effects and that these receptors also be classified pharmacologically (Berthelsen & Pettinger, 1977).

Finally, with the discovery of potent and highly selective  $\alpha_1$ - and  $\alpha_2$ -AR agonists and antagonists, the subdivision of  $\alpha_1$ - and  $\alpha_2$ -ARs, along with further divisions of each of these  $\alpha$ -AR subtypes, has come to rely on a pharmacological subclassification as opposed to the anatomical or functional subdivisions used previously.

## ***1.2 Pharmacological Subclassification***

It is clear that  $\alpha_1$ -ARs are heterogeneous, although the number of discrete subtypes remains controversial. All the  $\alpha_1$ -ARs subtypes are activated by the sympathetic neurotransmitters, noradrenaline and adrenaline and there remains no evidence for selective affinity of either of these catecholamines for any of the  $\alpha_1$ -AR subtypes.

The first evidence of two  $\alpha_1$ -AR subtypes came in 1982 when McGrath discovered that phenylethanolamines produced dose-response curves with a “shoulder” indicating two components, in both the rabbit basilar artery and the rat anococcygeus. However, the “non-phenylethanolamine” agonists produced virtually no response in the rabbit basilar artery, but a monophasic curve in rat anococcygeus. The “low concentration” component of the response to “non-phenylethanolamines” in the anococcygeus was mediated by one type of  $\alpha_1$ -AR ( $\alpha_{1A}$ ). The response to high concentrations of phenylethanolamines was mediated by a second type ( $\alpha_{1B}$ ), at which “non-phenylethanolamines” were relatively poor agonists. The rat basilar artery had a “low dose component” of the response to noradrenaline which corresponded more closely to the “ $\alpha_{1B}$ ” than “ $\alpha_{1A}$ ” ARs, i.e. “non-phenylethanolamines” have little agonist activity (McGrath, 1982).

Following McGrath’s discoveries, Holck and colleagues (1983) showed differential interactions of non-selective  $\alpha_1$ - and  $\alpha_2$ -AR agonists at postjunctional  $\alpha_1$ -ARs of the rabbit pulmonary artery, which again led to suggestions of multiple subtypes of the  $\alpha_1$ -AR (Holck *et al*, 1983). A number of other breakthrough findings followed suit, with Medgett and Langer’s (1984) work with the superfused tail artery displaying two populations of  $\alpha_1$ -AR, one with low and one with high affinity for the non-selective  $\alpha$ -AR agonist prazosin. Drew (1985), expanded this idea by compiling  $pA_2$  values for prazosin and discovering that the  $pA_2$  values spanned more than 2 log units, and hypothesised that this variation was due to interaction at more than one type of  $\alpha_1$ -AR.

In 1986, Morrow and Creese were the first to produce clear evidence for two subtypes of  $\alpha_1$ -AR. Using radioligand-binding techniques, they studied the ability of a series of ligands to displace [ $^3$ H] prazosin in rat brain membranes. Several ligands exhibited biphasic displacement curves, indicating low- and high-affinity binding sites, similar to the results obtained by Medgett and Langer. The two subtypes of [ $^3$ H] prazosin binding had very different rank orders of antagonist affinities: half of the sites showed the pharmacological profile of WB4101 > prazosin > phentolamine > indoramine > dihydroergocryptine. That site was termed  $\alpha_{1A}$ . In contrast, the  $\alpha_{1B}$  subtype demonstrated the rank order of prazosin > indoramine > dihydroergocryptine > WB4101 > phentolamine (Morrow & Creese, 1986).

Shortly after this, Johnson and Minneman (1987) showed that an alkylating analogue of clonidine, chloroethylclonidine (CEC), reduced, but did not eliminate the  $\alpha_1$ -AR population in rat brain membranes. Since phenoxybenzamine and other alkylating agents were able to eliminate all  $\alpha_1$ -ARs, they concluded that there were two populations of  $\alpha_1$ -ARs, one sensitive and the other insensitive to CEC. Minneman and colleagues later showed that the estimated dissociation constant for the CEC-sensitive and -insensitive  $\alpha_1$ -AR populations matched the dissociation constants for the  $\alpha_{1A}$  and  $\alpha_{1B}$ -ARs respectively (Gaurino *et al*, 1996).

Han and colleagues (1987) performed a similar work. With the knowledge that CEC inactivated a subpopulation of the  $\alpha_1$ -adrenergic receptor binding sites in rat brain, Han compared  $\alpha_1$ -adrenergic receptors in different tissues to determine whether such selective inactivation might reveal the presence of distinct receptor subtypes. He concluded that there are at least two subtypes of  $\alpha_1$ -adrenergic receptors with different pharmacological properties in mammalian tissues, only one of which is inactivated by CEC (Han *et al*, 1987). Later studies on COS-7 cells showed that CEC preferentially inactivates  $\alpha_1$ -ARs on the cell surface irrespective of their subtype and that the subtype-specific subcellular localisation rather than the receptor structure is a major determinant for CEC inactivation of  $\alpha_1$ -ARs (Iifrasawa *et al*, 1997).

Functional responses have also been attributed to each of the  $\alpha_1$ -AR subtypes and this has arisen by the identification of selective  $\alpha_{1A}$ -AR antagonists 5-methylurapidil (Gross *et al*, 1988) and (+)-niguldipine (Boer *et al*, 1989). Structural modification of the calcium channel antagonist (+)-niguldipine has led to an analogue, SNAP5089 having no activity as a calcium channel antagonist, but enhanced (100-fold) selectivity for the  $\alpha_{1A}$ -AR versus the other two  $\alpha_1$ -AR subtypes (Gluchowski *et al*, 1994). 5-methylurapidil has 30- to 100-fold higher affinity for  $\alpha_{1A}$ - than for  $\alpha_{1B}$ - and  $\alpha_{1D}$ -AR when the commonly available animal receptors ( $\alpha_{1A}$ , bovine;  $\alpha_{1B}$ , hamster or rat;  $\alpha_{1D}$ , rat) are used. However, various other studies that compared the affinity of this antagonist for the rat with human  $\alpha_1$ -AR subtypes have shown the  $\alpha_{1D}$ -AR to have affinity for 5-methylurapidil that is intermediate between the  $\alpha_{1A}$ - and  $\alpha_{1B}$ -ARs (Hieble *et al*, 1995).

### 1.2.1 $\alpha_{1H}$ , and $\alpha_{1L}$ -Adrenoceptors

It was noted that there was a wide affinity range for prazosin as an antagonist of  $\alpha_1$ -ARs. Flavahan and Vanhoutte (1986) differentiated  $\alpha_1$ -ARs into two groups, designated  $\alpha_{1H}$  and  $\alpha_{1L}$ , with high ( $\alpha_{1H}$ ) and low ( $\alpha_{1L}$ ) affinity for prazosin and yohimbine. Muramatsu and colleagues (1990) extended the  $\alpha_{1H}$ - and  $\alpha_{1L}$ -AR classification of Flavahan and Vanhoutte. They modified the  $\alpha_{1L}$  group by subdividing it into  $\alpha_{1L}$  and  $\alpha_{1N}$ . The  $\alpha_{1L}$  group was defined as having low affinity for yohimbine and the novel  $\alpha_1$ -AR competitive antagonist IIV732. The  $\alpha_{1N}$  group had a moderate affinity for yohimbine and a high affinity for IIV732. Prazosin has a higher affinity for the  $\alpha_{1H}$ -AR subtype than for the  $\alpha_{1L}$  and  $\alpha_{1N}$ -AR subtypes (Muramatsu, 1994). Support for this subclassification system came from further radioligand binding studies (Oshita *et al*, 1993; Ohmura *et al*, 1993).

The proposal of further subtypes has yet to be supported by molecular biological evidence. It has been suggested existing cloned subtypes may account for observations which led to the  $\alpha_{1H}$  versus  $\alpha_{1L}$  subdivision, in as much as cells expressing the human cloned  $\alpha_{1A}$ -AR have been shown to display an  $\alpha_{1L}$ -like pharmacology (Williams *et al*, 1996; Ford *et al*, 1997; Daniels *et al*, 1999).

### 1.3 Molecular Cloning

The cDNAs encoding three  $\alpha_1$ -AR subtypes ( $\alpha_{1a}$ ,  $\alpha_{1b}$ , and  $\alpha_{1d}$ ) have been cloned and pharmacologically characterised (Michelotti *et al*, 2000). Of note,  $\alpha_1$ -AR nomenclature has changed within the last 8 years, with the International Union of Pharmacology adopting  $\alpha_{1c}$ ,  $\alpha_{1b}$ , and  $\alpha_{1d}$  in 1995 (Hieble *et al*, 1995); the  $\alpha_{1a}$  used to be called  $\alpha_{1c}$ , the  $\alpha_{1b}$  name has not changed, and the  $\alpha_{1d}$  used to be called  $\alpha_{1a}$ ,  $\alpha_{1d}$ , or  $\alpha_{1a/d}$ ). The lower case letters, a, b, c, and d refer to the cloned receptor subtypes whereas the upper case letters A, B, and D describe pharmacologically defined receptor subtypes present in tissue.

### 1.3.1 $\alpha_{1B}$ -adrenoceptors

The  $\alpha_{1B}$ -AR subtype was the first of the  $\alpha_1$ -AR family to be cloned. This clone was isolated from a hamster vas deferens cell line (DD<sub>1</sub>MF<sub>2</sub>) and encoded a protein of 515 amino acid residues, which was predicted to have the 7 membrane-spanning domains characteristic of a G-protein-coupled receptor (Cotecchia *et al*, 1988). Expression of this clone in COS-7 cells resulted in a protein with radioligand binding properties similar to that of the native  $\alpha_{1B}$  subtype, with a high affinity for prazosin and a low affinity for phentolamine, 5-methylurapidil, and yohimbine. Also consistent with the  $\alpha_{1B}$  subtype was a high sensitivity to irreversible inactivation by CEC. Northern analysis showed mRNA expression for this clone in a variety of tissues expected to express the  $\alpha_{1B}$ -AR, including liver, spleen, heart, and cerebral cortex. It is now generally agreed that this cDNA encodes the hamster  $\alpha_{1B}$  subtype and rat (Voigt *et al*, 1990; Lomansey *et al*, 1991), dog (Libert *et al*, 1989) and human (Ramarao *et al*, 1992) homologues have been isolated.

### 1.3.2 $\alpha_{1C}$ -adrenoceptors

An additional cDNA that encoded a 466-residue polypeptide was isolated from a bovine cerebral cortex library (Schwinn *et al*, 1990). The protein expressed by the clone was different from the  $\alpha_{1B}$ -AR, with 65% amino acid identity in the membrane spanning domains. The pharmacological profile was also distinct from either the  $\alpha_{1B}$ - or  $\alpha_{1A}$ -ARs, with a relatively high affinity for 5-methylurapidil, a high affinity for WB4101, and a high sensitivity to irreversible inactivation by CEC. Northern analysis experiments showed no  $\alpha_{1C}$ -mRNA in any rat tissue examined, with noticeable quantities found only in rabbit liver and human hippocampus. With the knowledge of its unique pharmacology and limited tissue distribution, it was concluded that this clone encoded a novel subtype, which was designated  $\alpha_{1C}$  (Schwinn *et al*, 1991). Despite the lack of mRNA transcription, Southern hybridisation suggested the existence of the  $\alpha_{1C}$  gene in the rat and later, a rat homologue of the bovine  $\alpha_{1C}$ -AR was cloned by Laz and colleague (1993).

Later reports from several laboratories clearly showed that affinities of an extensive series of competitive antagonists for inhibition of radioligand binding of [<sup>3</sup>H]prazosin to the expressed  $\alpha_{1c}$ -AR correlated highly with their affinities for binding sites in native tissues that were known to possess  $\alpha_{1A}$ -ARs (Testa *et al*, 1995; Ford *et al*, 1994; Saussy *et al*, 1994; Faure *et al*, 1994; Langer *et al*, 1994). These results strongly suggested that the recombinant  $\alpha_{1c}$ -AR did in fact represent the native  $\alpha_{1A}$ -AR (Ford *et al*, 1994). There was, however, one major inconsistency that had to be explained between the  $\alpha_{1c}$ -AR clone identified by Schwinn and colleagues (1990) and the native  $\alpha_{1A}$ -AR and that was the difference in the sensitivity of the recombinant receptor to alkylation by CEC. It was concluded that the difference in sensitivity was due to varying experimental conditions, the character of the membrane in which the receptor is expressed and/or to species differences in CEC sensitivity of the recombinant  $\alpha_{1c}$ -AR (Hieble *et al*, 1995). Because of the initial confusion in nomenclature, the  $\alpha_{1c}$  designation is no longer recommended to describe the characteristics of any recombinant or native  $\alpha_1$ -AR.

### 1.3.3 $\alpha_{1D}$ -adrenoceptors

A third  $\alpha_1$ -AR, cloned by Lomansey and colleagues (1991), used homology screening from rat cerebral cortex library. The cDNA encoded a single polypeptide chain with a deduced sequence of 560 amino acids. Lomansey designated the clone  $\alpha_{1a}$  because it shared some characteristics of the pharmacological  $\alpha_{1A}$ -AR including a higher affinity for WB4101 than the cloned  $\alpha_{1b}$ -AR, resistance to inactivation by CEC and the presence of its mRNA in tissues known to contain large amounts of the  $\alpha_{1A}$ -AR. However, Perez and colleagues (1991), studying an almost identical clone (98% homologous) that was also isolated from rat brain, found low affinity for the more selective  $\alpha_{1A}$ -AR antagonists, 5-methylurapidil and (+)-niguldipine. For a time, this single recombinant receptor was referred to as either the  $\alpha_{1a}$ -AR or the  $\alpha_{1d}$ -AR. This suggestion caused a great deal of confusion in the field. The suggestion in the consensus report of the IUPHAR to refer to this receptor as the  $\alpha_{1W/d}$ -AR did little to clarify the issue (Gaurino *et al*, 1996). With the exception of two codons within the sequence of the  $\alpha_{1a}$ -AR and the  $\alpha_{1d}$ -AR, it was soon thought that these were in fact

encoding the same receptor, generally known to be the  $\alpha_{1d}$ -AR (Minneman & Esbenshade, 1994). An updated consensus report by the IUPHAR suggested the  $\alpha_{1b/d}$ -AR be replaced by the designation of  $\alpha_{1d}$ -AR for the cloned receptor and the  $\alpha_{1b}$ -AR for the pharmacological homologue found in tissue.

### ***1.3.4 Splice Variants***

The  $\alpha_1$ -AR subtypes are unusual among GPCRs in that they have an intron in their protein coding regions at the end of the putative 6<sup>th</sup> transmembrane domain (Ramarao *et al*, 1992; Chang *et al*, 1998). Three splice variants of the human  $\alpha_{1A}$ -AR have been cloned ( $\alpha_{1A-1}$ ,  $\alpha_{1A-2}$  and  $\alpha_{1A-3}$ ) which differ in length and sequence of their C-terminal domains (Hirasawa *et al*, 1995). A fourth, novel isoform ( $\alpha_{1A-4}$ ) has also been reported, which predominates in human prostate, liver, heart and bladder based upon mRNA determinations (Chang *et al*, 1998). Daniels and colleagues (1999) reported that all four isoforms display apparently identical pharmacological properties using functional analysis and that this pharmacology closely correlates with that of the  $\alpha_{1L}$ -AR. Hence, no individual isoform represents the distinct pharmacological phenotype of the  $\alpha_{1A}$ - or  $\alpha_{1L}$ -AR (Daniels *et al*, 1999; Suzuki *et al*, 2000).

## ***1.4 Signal Transduction Mechanisms***

The adrenoceptors are divided into three families, the  $\alpha_1$ -ARs, the  $\alpha_2$ -ARs and the  $\beta$ -ARs. This subdivision is suggested by the observation that each of the three receptor groups is associated with a specific second messenger system. The  $\alpha_1$ -ARs increase intracellular calcium concentrations, whereas  $\alpha_2$ -ARs and  $\beta$ -ARs inhibit and stimulate adenylyl cyclase, respectively (Bylund *et al*, 1994).

The three cloned  $\alpha_1$ -ARs couple predominately to pertussis toxin-insensitive G Proteins of the  $G_{q/11}$  family, and there is evidence of selectivity among the various  $\alpha_1$  subtypes (Wu *et al*, 1992). In intact tissue (Nebigil & Malik, 1992), as with cloned receptors (Perez *et al*, 1993), it has been shown that  $\alpha_1$  subtypes can activate multiple

effectors via distinct pertussis toxin-sensitive ( $G_i$  or  $G_o$  family) and -insensitive G Proteins (Gaurino *et al*, 1996).

Stimulation of  $\alpha_1$ -ARs results in the activation of various effector enzymes including PLC,  $PA_2$  and PLD, as well as activation of  $Ca^{2+}$  channels,  $Na^+$ - $H^+$  and  $Na^+$ - $Ca^{2+}$  exchange and activation or inhibition of  $K^+$  channels. In most cells, the primary functional response to activation of all  $\alpha_1$ -AR subtypes is an increase in intracellular  $Ca^{2+}$ . Activation or inhibition of the receptor-coupled effectors involves coupling via G Proteins (Graham *et al*, 1996).

In 1975, Michell proposed that all receptors that increase  $Ca^{2+}$  levels also increase turnover of phosphatidylinositol (PI), and proposed that this effect might be involved in the opening of  $Ca^{2+}$  gates. This hypothesis was strongly supported by Fain and Berridge (1979) whose results made it clear that breakdown of PI was probably an important pathway for the formation of second messengers involved in the control of cytosolic  $Ca^{2+}$  levels (Minneman, 1988). Fain and Garcia-Sainz (1980) postulated that this was the major mechanism of signal transduction for  $\alpha_1$ -adrenergic receptors.

$\alpha_1$ -ARs are one of the many types of cell surface receptors that produce changes in cellular activity by increasing intracellular level of free  $Ca^{2+}$  (Summers & McMartin, 1993). Activation of  $\alpha_1$ -ARs stimulates PLC- $\beta$  via  $G_{q/11}$ , which hydrolyses  $PIP_2$  to yield DAG and  $IP_3$ .  $IP_3$  then interacts with specific receptors on intracellular organelles, such as the sarcoplasmic reticulum, to release stored  $Ca^{2+}$  (Graham *et al*, 1996). DAG is a highly lipophilic substance which remains in the membrane and stimulates PKC in the presence of  $Ca^{2+}$  ions and phospholipids. PKC is located in the cytosol and in the membrane fractions of the cell, but only the membrane bound pool of the enzyme is active (Szmigielski *et al*, 1997). PKC then phosphorylates a variety of cellular substrates, including  $Ca^{2+}$  channels, that may regulate intracellular  $Ca^{2+}$  or activate transcription of various genes (Graham *et al*, 1996).

#### **1.4.1 Calcium Influx**

Activation of  $\alpha_1$ -ARs can increase  $Ca^{2+}$  influx via voltage-dependant (Ljung & Kjellstedt, 1987) as well as voltage-independent  $Ca^{2+}$  channels (Han *et al*, 1992).

Initially this was believed to be a discriminating criterion for classification of the  $\alpha_1$ -AR subtypes. Han and colleagues (1987) worked with isolated smooth muscle and reported evidence for two types of  $\alpha_1$ -ARs, which caused contractile responses through different mechanisms. They proposed the  $\alpha_{1b}$ -AR stimulated IP<sub>3</sub> formation and caused contractions independent of extracellular Ca<sup>2+</sup> and that the  $\alpha_{1a}$ -AR did not stimulate IP<sub>3</sub> formation and caused contractions, which required the influx of extracellular Ca<sup>2+</sup> through dihydropyridine-sensitive channels (Han *et al*, 1987). With the cloning of receptors and the use of many other cell types, there are now numerous exceptions to proposals such as Han's. For example, the  $\alpha_{1b}$ -ARs are linked to Ca<sup>2+</sup> influx in rat vena cava (Sayct *et al*, 1993) and in MDCK-D1 cells (Klijn *et al*, 1991). Expressed receptors in COS-1 cells demonstrate that all three  $\alpha_1$ -AR subtypes can mobilise intracellular calcium and increase Ca<sup>2+</sup> influx via voltage-operated Ca<sup>2+</sup> channels (Perez *et al*, 1993; Lomansey *et al*, 1993).

Extracellular Ca<sup>2+</sup> can enter animal cells via three main pathways. These are VOCCs (Putney Jnr & Bird, 1993; Berridge, 1995; Clapham, 1995), LGCCs (Berridge, 1997) and RACCs (Catterall, 1995; Dunlap *et al*, 1995; Fasolato *et al*, 1994). The broad physiological functions of these channels are to provide extracellular Ca<sup>2+</sup> for increases in [Ca<sup>2+</sup>]<sub>c</sub> in given regions of the cytoplasmic space, and to replenish Ca<sup>2+</sup> stores in the sarcoplasmic reticulum and ER by replacing Ca<sup>2+</sup> which is released from these stores and subsequently pumped out of the cell (Barritt, 1999). The members of all of these families of plasma-membrane channels exhibit the electrophysiological properties usually attributed to a cation channel (Hille, 1992). That is, when induced to open, the channel remains open for a short period of time (usually microseconds) before closing as the result of an inactivation mechanism.

The subgroups of RACCs that have been of interest in recent years are the SOCCs (capacitative Ca<sup>2+</sup> channels) (Putney Jnr & Bird, 1993; Berridge, 1995; Clapham, 1995). These are defined as plasma-membrane Ca<sup>2+</sup> channels that are opened in response to a decrease in the concentration of Ca<sup>2+</sup> in the lumen of the ER ([Ca<sup>2+</sup>]<sub>er</sub>) (Putney Jnr & Bird, 1993). Under physiological conditions, the decrease in [Ca<sup>2+</sup>]<sub>er</sub> that leads to channel opening is caused by the binding of IP<sub>3</sub> to IP<sub>3</sub>-receptor Ca<sup>2+</sup> channels and possibly also by the binding of Ca<sup>2+</sup> to ryanodine-receptor Ca<sup>2+</sup> channels

(Wayman *et al*, 1998; Bennett *et al*, 1998). The key event that initiates the opening of SOCCs is the decrease in  $[Ca^{2+}]_{cr}$  (Barritt, 1999).

#### **1.4.2 cyclicAMP**

Stimulation of  $\alpha_1$ -ARs has been reported to increase cAMP accumulation and to potentiate cAMP levels elicited through other receptors (Schultz & Daly, 1973; Johnson & Minneman, 1986). Activation of  $\alpha_{1A}$ -ARs in COS-7 and HeLa cells (Schwinn *et al*, 1991) or  $\alpha_{1B}$ -ARs or  $\alpha_{1D}$ -ARs in COS-1 and CHO cells was also shown to increase cAMP levels (Perez *et al*, 1993). The cAMP accumulation most likely occurs via a PKC-mediated potentiation of adenylyl cyclase activity, although there is also evidence for  $\alpha_1$ -AR-mediated inhibition of cAMP degradation (Buxton *et al*, 1985).

Studies by Ruan and colleagues (1998) showed that all  $\alpha_1$ -AR subtypes are coupled to PLD and that activation of these receptors increases AA release and cAMP levels in rat-1 fibroblasts. The  $\alpha_{1A}$ -ARs seemed to be coupled more effectively to AA release, PLD activity and cAMP system than either  $\alpha_{1B}$ - or  $\alpha_{1D}$ -ARs. This conclusion arose after the finding that the  $\alpha_1$ -AR agonist phenylephrine produced a much greater increase in AA release, PLD activity and cAMP accumulation in rat-1 fibroblasts stably expressing the  $\alpha_{1A}$ -AR than in those expressing the  $\alpha_{1B}$ - or  $\alpha_{1D}$ -AR. Furthermore, cAMP generated by  $\alpha_{1A}$ -AR stimulation acted as an inhibitory modulator of PLD activity and AA release via PKC (Ruan *et al*, 1998).

#### **1.4.3 Arachidonic Acid**

It was Burch and colleagues in 1986 that showed that stimulation of  $\alpha_1$ -ARs in a rat thyroid cell line increased release of AA, which in turn mediated a noradrenaline-stimulated cell replication. Other studies have shown that stimulation of  $\alpha_1$ -ARs can cause AA release in many cells (Kanterman *et al*, 1990; Blue *et al*, 1994), either through activation of PA<sub>2</sub> (Kanterman *et al*, 1990; Nishio *et al*, 1996) or PLD (Ruan *et al*, 1998). Some evidence suggests that such increases in AA release require

extracellular  $\text{Ca}^{2+}$ , but are independent of increases in intracellular  $\text{Ca}^{2+}$ , suggesting a role for  $\text{PA}_2$  (Zhong & Minneman, 1999). The involvement of a pertussis toxin sensitive G Protein have been supported by studies in rabbit aortic smooth muscle (Nishio *et al*, 1996), while other studies provide evidence for the involvement of PKC or MAPK pathways.

In more recent years, activation of AA release has been shown to be downstream of MAPK pathways (Xing & Insel, 1996). In MDCK cells, immunoprecipitation studies combined with specific inhibitor showed that an 85-kD cytosolic  $\text{PA}_2$  was activated by  $\alpha_1$ -AR stimulation. PD 98059, a specific inhibitor of MAPK pathways, blocked this activation and also inhibited adrenaline-promoted AA release. Down-regulation or inhibition of PKC also blocked MAPK activation and AA release, hence  $\alpha_1$ -AR appear to regulate AA release through phosphorylation-dependant activation of  $\text{PA}_2$  by MAPK, subsequent to activation of PKC in these cells (Zhong & Minneman, 1999).

#### **1.4.4 Phospholipase D**

Activation of PLD also appears to be involved in the action of  $\alpha_1$ -ARs (Lahi & Fain, 1992; Balboa & Insel, 1998; Ruan *et al*, 1998). Such activation seems to be secondary to the initial signalling, i.e., it may be induced by increases in  $\text{Ca}^{2+}$  or PKC activation. Balboa and Insel (1998) studied activation of PLD stimulated by adrenaline in MDCK cells. They discovered that even though adrenaline stimulated PKC  $\alpha$  and PKC  $\epsilon$ , this was not related to PLD activation. Furthermore, blocking PLC with neomycin did not significantly decrease adrenaline-stimulated PLD activity. A role for  $\text{Ca}^{2+}$  in PLD activation by  $\alpha_1$ -ARs was suggested after chelation of extracellular  $\text{Ca}^{2+}$  noticeably inhibited PLD activation. All three  $\alpha_1$ -AR subtypes appear to be able to activate PLD, although the mechanisms may differ in different cell types (Ruan *et al*, 1998; Zhong & Minneman, 1999).

### **1.4.5 Mitogenic Responses**

Signalling to the nucleus has become a major area of research in recent years. It is clear that  $\alpha_1$ -AR activation may result in mitogenesis and that constitutively active mutants are tumorigenic (Allen *et al*, 1991), that is,  $\alpha_1$ -AR genes could be considered as protooncogenes. Mitogenic responses are caused by a conserved cascade of events including receptor phosphorylation, binding of adaptor proteins, such as Shc and Grb2, and eventually recruitment and activation of the small molecular weight G Proteins Ras. Raf is then activated by Ras and this activates downstream MAPK cascades (Davis, 1993). It is now clear that GPCRs can rapidly activate MAPK pathways and this activation is an important factor in the regulation of cell proliferation and growth (Zhong & Minneman, 1999).

$\alpha_1$ -AR stimulated DNA synthesis and activation of MAPK involves activation of phosphatidylinositol 3-kinase via a pertussis toxin-sensitive G Protein (Hu *et al*, 1996). Differences in the signalling pathways of  $\alpha_{1A}$ - and  $\alpha_{1B}$ -ARs have been observed involving phosphatidylinositol 3-kinase, p21<sup>ras</sup> and MAPK (Hu *et al*, 1999). Neither  $\text{Ca}^{2+}$  nor PKC appears to mediate  $\alpha_{1A}$ -AR activation of MAPK in transfected PC12 cells (Berts *et al*, 1999; Garcia-Sainz *et al*, 1999).

### **1.5 G-protein coupled receptors**

Adrenoceptors are part of the superfamily of receptors that exert their physiological effects by coupling to guanine nucleotide-binding proteins (G Proteins). The G-protein coupled receptor (GPCR) family comprises many of the receptors that are familiar to pharmacologists, such as muscarinic Ach receptors, adrenoceptors, opiate receptors and receptors for many peptides. A large number of these receptors have been isolated and purified, and some have been cloned, revealing a remarkably coherent pattern of their molecular structure (Rang *et al*, 1995).

G Proteins contain three subunits, the  $\beta$  and  $\gamma$  subunits of 35-37 and 8-10kDa and  $\alpha$  subunits of 45-52kDa. The  $\beta$  and  $\gamma$  subunits are tightly associated with each other and do not differ greatly among the G Proteins. In the basal state, G Proteins have GDP bound to the catalytic state of GTPase on the  $\alpha$  subunit, and interaction of agonists

with a coupled receptor induces release of GDP and its replacement by GTP. The dissociated GTP- $\alpha$  and  $\beta/\gamma$  subunits, interact with effector proteins to modulate cellular responses including second messenger metabolism and ion channel function (Freissmuth *et al*, 1989; Ikeda, 1996; Clapham & Neer, 1993). The  $\alpha$  subunit is reassociated with the  $\beta/\gamma$  subunit by the hydrolysis of GTP to GDP due to the activity of the  $\alpha$  subunit GTPase. The spontaneous GDP release rate corresponds to a tonic activation rate in the absence of activated receptors (Remmers *et al*, 1999).

G protein activity is regulated both by receptor-catalysed GTP binding to the  $\alpha$  subunit and by the rate of GTP hydrolysis. Regulators of G protein signalling (RGS) proteins are a recently identified family of intracellular GTPase-activating proteins (GAPs) (Dolman & Thorner, 1997; Berman & Gilman, 1998) that accelerate GTP hydrolysis by G $\alpha$  subunits (Berman *et al*, 1996; Hunt *et al*, 1996; Heximer *et al*, 1997), thus limiting the duration of G protein activation. RGS proteins can regulate signalling by uncoupling the cycle of GTP binding and hydrolysis from effector protein activation by the G $\alpha$  subunit, even in the presence of persistent agonist stimulation (Xu *et al*, 1999).

G Protein subtypes are currently defined by their  $\alpha$  subunits, of which 23 (including splice variants) are known, and up to 5 different  $\beta$  and 11 different  $\gamma$  subunits have been identified (Neer, 1995). This means that a greater number of heterotrimers composed of specific  $\alpha$ ,  $\beta$  and  $\gamma$  subunits may exist and be involved in signal transduction pathways. In many cases, the coupling between receptor and G Protein may seem unselective since one receptor may activate more than one G Protein and thus initiate more than one signal transduction pathway (Macrez-Lepretre *et al*, 1997). However, there are many examples showing that different receptors activate the same effector system (Offermanns & Schultz, 1994; Gudermann *et al*, 1996).

Despite their diverse biological functions, GPCRs share many common characteristics. They possess seven domains of 20-25 hydrophobic residues in the form of  $\alpha$  helices, which span the plasma membrane (Grady *et al*, 1997). They have an extracellular NH<sub>2</sub> terminus, three intracellular loops, and an intracellular COOH terminus. The three intracellular loops have been shown to bind and activate the G Proteins (Franke *et al*, 1990). It is thought that upon agonist binding, these loops

either become more exposed or undergo conformational changes transduced through transmembrane movements. The aminergic binding receptors, such as the  $\alpha_1$ -AR family, appear to bind ligands within the membrane-spanning domain (Strader *et al*, 1987).

The structure of  $\alpha_1$ -ARs is very similar to that of rhodopsin, the light-activated retinal receptor involved in visual transduction; bacteriorhodopsin, the light-activated proton pump of *Halobacterium halobium*, and  $\beta$ -ARs (Riek *et al*, 1995). However, there is little amino acid identity between  $\alpha_1$ -ARs and either rhodopsin or bacteriorhodopsin and only a low degree of identity (20%-30%) with the  $\beta$ -AR, even though both  $\alpha_1$ -ARs and  $\beta$ -ARs are activated by the catecholamines, adrenaline and noradrenaline (Graham *et al*, 1996). All models for adrenergic structure are based on the structure of bacteriorhodopsin and as a result, a great deal of data for mammalian adrenoceptors has come from mutational studies that alter critical amino acids involved in receptor function (Gaurino *et al*, 1996; Piascik *et al*, 1996; Michelotti *et al*, 2000).

Like other members of the GPCR family,  $\alpha_1$ -ARs are single polypeptide chains, ranging from 355 to 511 amino acids that fold into a highly conserved structure of seven predicted membrane-spanning regions, TM1-7 (Michelotti *et al*, 2000). The seven TM regions fold into a conformation that creates a hydrophilic ligand-binding pocket surrounded by a hydrophobic core for the physiological agonists adrenaline and noradrenaline (Piascik *et al*, 1996). The TM regions are most likely arranged in a juxtaposed, counter-clockwise cluster that forms the binding pocket (Gaurino *et al*, 1996). However, the ligand-binding pocket is distinct in each of the different subtypes, since they can discriminate between a wide variety of synthetic agonists and antagonists (Hwa *et al*, 1995).

The amino termini of  $\alpha_1$ -ARs are located extracellularly and possess several consensus sites for modification by N-linked glycosylation. The amino termini vary significantly in length, with the terminus for the  $\alpha_{1D}$ -AR being much longer (~90 amino acids) than the terminus for the  $\alpha_{1A}$ -AR (25 amino acids) or the  $\alpha_{1B}$ -AR (42 amino acids). The longer amino terminus of the  $\alpha_{1D}$ -AR may limit efficient translation or membrane insertion as this subtype is more poorly expressed in the

plasma membrane than the other two subtypes, despite abundant production of  $\alpha_{1D}$  mRNA (Graham *et al*, 1996).

The carboxy termini are located intracellularly and possess consensus sites for phosphorylation by serine/threonine protein kinases and modification of protein at these sites is involved in receptor desensitisation (Garcia-Sainz, 1993). The carboxy termini contain a conserved cysteine residue, approximately 16 amino acids after the end of TM-7 that is most likely post-translationally modified by thioesterification with palmitic acid.

### 1.5.1 $\alpha_1$ -AR Agonist Binding

The binding of catecholamines to the  $\alpha_1$ -ARs seems to occur in a different manner than with the  $\beta_2$ -AR, where an aspartic acid residue (Asp<sup>113</sup>) in TM-3 is involved in forming a salt bridge with the protonated amine of the catecholamine (Strader *et al*, 1987). In the  $\beta_2$ -AR, two serine residues, Ser<sup>204</sup> and Ser<sup>207</sup>, have been shown to be involved in hydrogen-bond interactions with the hydroxyl groups on the catechol ring and both residues are required for the high affinity binding of agonists and for full activation of the receptor. Two serine residues in TM-5 of the  $\alpha_1$ -AR, Ser<sup>188</sup> and Ser<sup>192</sup>, are partly responsible for the agonist binding affinity of this receptor subtype (Hwa & Perez, 1996). Unlike the  $\beta_2$ -AR, the catechol hydroxyl groups are not located an equal distance from their respective serine residues. Both hydroxyl groups appear closer to Ser<sup>188</sup>, with the *meta*-hydroxyl group forming the closest interaction. It is only the Ser<sup>188</sup> that is required for full agonist action upon receptor activation. The  $\alpha_{1B}$  and  $\alpha_{1D}$ -ARs have an extra serine located at the analogous position to residue 189 in the  $\alpha_{1A}$ -AR, and a Ser<sup>208</sup> Ala mutation in the  $\alpha_{1B}$ -AR was found to have no effect on the binding affinity, or functional responsiveness of this receptor (Hwa *et al*, 1995). This showed that the two key serine residues involved in catecholamine binding to the  $\alpha_1$ -AR are located three amino acid residues apart in the helix, while the  $\beta_2$ -AR serines are located two residues apart.

The aromatic interactions of the phenyl ring of the agonist and the phenylalanine residue in TM-6 are also different in the  $\alpha_1$ - than the  $\beta_2$ -AR. In the  $\beta_2$ -AR, Phe<sup>290</sup>

(equivalent to Phe<sup>311</sup> in the  $\alpha_1$ -AR) was suggested to be involved in an aromatic interaction with the agonist (Strader *et al.*, 1989). In contrast, a study in the  $\alpha_{1B}$ -AR using various techniques showed that only Phe<sup>310</sup> (equivalent to Phe<sup>289</sup> in the  $\beta_2$ -AR) is critically involved in both binding and activation (Chen *et al.*, 1999; Piascik & Perez, 2001).

Waugh and colleagues (2000) unexpectedly discovered two additional phenylalanine residues involved in the binding of agonists. Phe<sup>163</sup> in TM-4 and Phe<sup>187</sup> in TM-5 of the  $\alpha_{1A}$ -AR are involved in agonist-specific binding interactions. Mutation of both of these residues contributes to a 150-fold loss of affinity for the endogenous agonist. An interesting observation is that the  $\beta_2$ -AR does not conserve these aromatic residues, further highlighting differences in the agonist binding pocket between these two receptors.

The  $\alpha_{1A}$ -AR shows a 10- to 100-fold higher binding affinity for nonselective agonists compared with the  $\alpha_{1B}$ -AR subtype. There are two residues responsible for this selectivity, Ala<sup>204</sup> in TM-5 and Met<sup>313</sup> in TM-6 of the  $\alpha_{1B}$ -AR (Hwa *et al.*, 1995). Although the interactions were direct, the mechanism of this selectivity was due to the specific packing interactions of these two residues as mismatched combinations of the  $\alpha_{1B}$ - and  $\alpha_{1A}$ -AR residues resulted in constitutive activity.

### 1.5.2 Antagonist Binding

There is a limited knowledge of how antagonists bind to the  $\alpha_1$ -ARs. Piascik and colleagues (2001) have shown using mutagenesis studies that the subtype-selectivity of two  $\alpha_{1A}$ -AR-selective antagonists phentolamine and WB4101 are conferred by interactions with three consecutive residues (Gln<sup>177</sup>, Ile<sup>178</sup>, Asn<sup>179</sup>) of the second extracellular loop (Zhao *et al.*, 1996; Piascik & Perez, 2001). A phenylalanine residue (Phe<sup>86</sup>) at the surface of TM-2 in the  $\alpha_{1A}$ -AR accounts for the  $\alpha_{1A}$ - versus  $\alpha_{1D}$ -selectivity of dihydropyridine antagonists such as nifedipine, although the studies mentioned here involve residues involved in selectivity and with a limited set of antagonists. Waugh and colleagues (2001) reported that two conserved phenylalanine residues near the extracellular surface of TM-7 are involved in nonselective binding

for nearly all  $\alpha_1$ -antagonists. This indicates the first case of a common site of antagonist binding for members of the adrenergic receptor family. Waugh's study supported the hypothesis that imidazoline agonists bind in a different manner than phenethylamine agonists after discovering the two residues also altered imidazoline binding such as cirazoline. It seems imidazolines bind similarly to antagonists, which may explain their partial agonist properties.

### 1.5.3 Inverse Agonism and Neutral Antagonism

When GPCRs exist in a spontaneously active form in the absence of an agonist, the term used is ligand-independent or constitutive receptor activation. This has been observed in cell lines in which receptors are overexpressed or mutated (Barker *et al*, 1994; Bond *et al*, 1995; Newman-Tancredi *et al*, 1997). A two-state receptor model may explain this where GPCRs exist in equilibrium between two conformations, an active form ( $R^*$ ) and an inactive form ( $R$ ) (Lefkowitz *et al*, 1993; Samama *et al*, 1993). Based on this model, agonists shift the equilibrium to the active conformation ( $R^*$ ), hence increasing receptor activity, whereas some antagonists, called inverse agonists, lead preferentially to the inactive conformational state ( $R$ ), resulting in reduced basal receptor activity (Leff, 1995; Zhu *et al*, 2000). There is also another type of antagonist called a neutral antagonist, which is believed to bind equally to both  $R^*$  and  $R$  without affecting the equilibrium. In such a case, the neutral antagonist can inhibit the effects of both agonists (reducing the receptor signal) and inverse agonists (thereby increasing receptor signalling in the simultaneous presence of an inverse agonist) (Zhu *et al*, 2000).

It was reported that Recordati compounds such as REC 15/3039, REC 15/2739 and REC 15/3011, act as neutral antagonists at the wild-type  $\alpha_{1a}$ -AR, but as inverse agonists at the wild-type  $\alpha_{1b}$ -AR in COS-7 cells (Rossier *et al*, 1999). Using the same cell type, Zhu and colleagues (2000) constructed a constitutively active mutant of the  $\alpha_{1a}$ -AR by changing the Ala<sup>271</sup> to Thr in TM-3 and found prazosin to act as an inverse agonist and KMD-3213 behaving as a neutral antagonist. Their results found that a neutral antagonist can reverse the action of an inverse agonist at the receptor site (Zhu *et al*, 2000).

## 1.6 Subtype-Selective Drugs

The affinities and selectivities of drugs for  $\alpha_1$ -AR subtypes have been determined mostly by competition for radioligand binding to heterologously expressed recombinant subtypes. The majority of antagonists, including the prototype  $\alpha_1$ -AR selective antagonist prazosin, display little or no selectivity between the three  $\alpha_1$ -AR subtypes (Hancock, 1996). However, a wide range of drugs with varying degrees of selectivity has been identified. A significant effort in drug design that is directed at obtaining selective compounds will be advantageous in studying the interactions and functional roles of these subtypes and may have potential therapeutic applications.

### 1.6.1 $\alpha_{1A}$ -AR Antagonists

The development of  $\alpha_{1A}$ -AR selective antagonists has proved to be the most fruitful. The first  $\alpha_{1A}$ -AR antagonist to be identified was WB4101, which displays a 20-fold higher affinity for the  $\alpha_{1A}$  than  $\alpha_{1B}$  subtype (Morrow & Creese, 1986). Along with an intermediate affinity for the  $\alpha_{1D}$  subtype, this limited selectivity confines its use in differentiating between subtypes.

Following the discovery of this property of WB4101 came the identification of 5-methylurapidil (Gross *et al*, 1988) and (+)-niguldipine (Boer *et al*, 1989) as selective  $\alpha_{1A}$ -AR antagonists. Both of these antagonists had a greater selectivity (80-500-fold) between  $\alpha_{1A}$  and  $\alpha_{1H}$  subtype and a low affinity for the  $\alpha_{1D}$  subtype, making them useful as tools for distinguishing subtypes in radioligand binding assays (Han & Minneman, 1991). A problem with both these antagonists is that 5-methylurapidil is a partial agonist at serotonin 5-HT<sub>1A</sub> receptors, while (+)-niguldipine is a dihydropyridine Ca<sup>2+</sup> channel antagonist. These actions do not complicate radioligand binding studies, but limit their use in functional experiments. This is especially true in smooth muscle, in which both serotonin receptors and dihydropyridine sensitive Ca<sup>2+</sup> channels play major functional roles, and where defining the functional roles of  $\alpha_1$ -AR subtypes is of significant interest (Minneman & Esbenshade, 1994). The (+)-niguldipine derivative, SNAP5089 has been

developed and is highly  $\alpha_{1A}$ -selective, but has a much lower affinity for voltage-gated  $\text{Ca}^{2+}$  channels (Wetzel *et al*, 1995).

Interest in  $\alpha_{1A}$ -AR selective antagonists has been strong as it has been postulated that these antagonists may have significant therapeutic advantages over non-subtype selective  $\alpha_1$ -AR antagonists in the treatment of BPH. The  $\alpha_{1A}$ -AR subtype predominates in the urethra and prostate of man (Price *et al*, 1993; Faure *et al*, 1994) and has been claimed to be the receptor mediating noradrenaline induced smooth muscle contraction in these tissues (Hatano *et al*, 1994; Marshall *et al*, 1995). The moderately  $\alpha_{1A}$ -AR selective antagonist tamsulosin has been introduced for treatment of BPH (Foglar *et al*, 1995). Studies by Blue and colleagues (1997) have assessed the *in vitro* and *in vivo* pharmacology of tamsulosin and dismissed the proposal that the compound is uroselective based on a degree of  $\alpha_{1A}$ -subtype selectivity.

Williams and colleagues (1999) reported the profiles of two novel  $\alpha_{1A}$ -AR selective antagonists, Ro 70-0004 and a structurally related compound, RS-100329 (for chemical structure, see Fig. 1.3). They found both compounds to be high affinity antagonists at the  $\alpha_{1A}$ -AR, with a considerable selectivity over the  $\alpha_{1B}$ - and  $\alpha_{1D}$ -subtypes. They both potently inhibit *in vitro* and *in vivo*  $\alpha_{1A}$ -AR mediated contractions of lower urinary tract tissue and appear to exhibit only weak cardiovascular effects when compared to standard non-selective  $\alpha_1$ -AR antagonists such as prazosin (for chemical structure, see Fig. 1.2) and tamsulosin. The clinical use of Ro 70-0004 in the symptomatic treatment of BPH is currently being assessed (Williams *et al*, 1999)

Another compound that has potential use in the treatment of BPH is RWJ-38063. Pulito and colleagues (2000) compared the *in vitro* and *in vivo* uroselective properties of four novel arylpiperazine compounds with those of tamsulosin. The binding activities of RWJ-38063, RWJ-68141, RWJ-68157, RWJ-69736 and tamsulosin were examined at each of the three cloned  $\alpha_1$ -AR subtypes to determine their affinities and receptor subtype selectivities. All the RWJ compounds showed significantly higher binding affinities for the  $\alpha_{1A}$ -AR subtype than either the  $\alpha_{1B}$ - or  $\alpha_{1D}$ -AR subtype. Although tamsulosin had the highest affinity for the  $\alpha_{1A}$ -AR subtype of all the

compounds tested, it showed the lowest level of selectivity for this subtype (Pulito *et al.*, 2000)

### 1.6.2 $\alpha_{1B}$ -AR Antagonists

Finding selective antagonists for  $\alpha_{1B}$  and  $\alpha_{1D}$ -ARs has been more difficult. CEC was originally thought of as an  $\alpha_{1B}$ -AR selective alkylating agent (Han *et al.*, 1987), but complications in the use of site directed alkylating agents and controversies over its selectivity in inactivating the recombinant  $\alpha_1$ -AR subtypes have pushed it into disfavour (Hirasawa *et al.*, 1997). There have been some cases of competitive antagonists being moderately  $\alpha_{1B}$ -AR selective, such as spiperone and cyclazosin or its (+)-enantiomer (Giardina *et al.*, 1996), but the extremely limited selectivity of these compounds has hindered their use in subclassifying receptors (Eltze *et al.*, 2001).

Patane and colleagues (1998) reported the discovery of a potent and selective  $\alpha_{1B}$ -AR antagonist, L-765,314. The group had intended to incorporate new structural elements into the prazosin piperazine subunit. The effects induced by the modest structural changes to the 2-*N*-piperazinyl-4-aminoquinazoline containing  $\alpha_1$  antagonist suggested a potential strategy for introducing subtype selectivity in other series of nonselective or less-selective  $\alpha_1$ -AR antagonists (Patane *et al.*, 1998).

A novel  $\alpha_{1B}$ -AR-selective compound with no direct chemical resemblance to other  $\alpha_1$ -AR antagonists was characterised through binding experiments with native or cloned  $\alpha_1$ -AR subtypes in different animal and human tissues (King *et al.*, 1994). This compound, named AH11110A, displayed an approximately 10- and 20-fold selectivity to subtype B relative to A and D, respectively, and an affinity rank order at these subtypes of B > A > D (King *et al.*, 1994; Giardina *et al.*, 1996; Saussy *et al.*, 1996). The case for AH11110A being listed as the only recommended  $\alpha_{1B}$ -AR-selective antagonist (Alexander & Peters, 2000) was dismissed by Eltze and colleagues (2001). The group characterised AH11110A as a low affinity, unselective and in most cases non-competitive antagonist with respect to the  $\alpha_{1A}$ -,  $\alpha_{1B}$ - and  $\alpha_{1D}$ -AR subtypes. They also found AH11110A to be almost equipotent at  $\alpha_1$ - and  $\alpha_2$ -ARs,

hence the claimed usefulness of AH11110A for  $\alpha_{1B}$ -AR subtype characterisation, at least by means of functional experiments, seems to be unjustified (Eltze *et al.*, 2001).

### 1.6.3 $\alpha_{1D}$ -AR Antagonists

The partial serotonin 5-HT<sub>1A</sub> receptor agonist BMY 7378 (for chemical structure, see Fig. 1.3), has been shown to be a selective antagonist at the  $\alpha_{1D}$  subtype with approximately 100-fold higher affinity for the  $\alpha_{1D}$  than the  $\alpha_{1A}$  or  $\alpha_{1B}$  subtype. Goetz and colleagues (1995) compared the binding affinities in the three recombinant subtypes expressed in fibroblast cells rather than nonhomogeneous subtypes in tissues. BMY 7378 is more selective than (-)-discretamine, which Ko and colleagues (1994) described as a selective  $\alpha_{1D}$ -AR antagonist (15- to 25-fold). The cystamine-bearing quinazoline cystazosin, displayed a high affinity for the  $\alpha_{1D}$ -AR subtype and when compared with BMY 7378, cystazosin had a much better specificity profile since it has lower affinity for D<sub>2</sub> and 5-HT<sub>1A</sub> receptors (Minarini *et al.*, 1998). Buspirone, a close structural analogue of BMY 7378 has been reported as another compound with the ability to functionally discriminate the  $\alpha_{1D}$ -AR from the other known  $\alpha_1$ -AR subtypes in various tissues (Eltze *et al.*, 1999). Another substituted 8-azapiro[4,5]decane-7,9-dione, MDL 73005EF was also found to have significant selectivity for the  $\alpha_{1D}$ -AR (Saussy *et al.*, 1996).

### 1.6.4 $\alpha_1$ -AR Agonists

Little is known about the subtype selectivity of  $\alpha_1$ -AR agonists. Comparing the affinities of agonists for receptors is much more difficult than comparing the affinities of antagonists due to problems in determining agonist affinities in both radioligand binding and functional studies. There is some information available on the comparative potencies and efficacies of agonists at the cloned  $\alpha_1$ -AR subtypes. Oxymetazoline is a partial agonist that displays selectivity in radioligand binding assays, with an approximately 20-fold higher apparent affinity for the  $\alpha_{1A}$  than  $\alpha_{1B}$  or  $\alpha_{1D}$  subtypes (Minneman *et al.*, 1988; Hancock, 1996; Zhong & Minneman, 1999).

Tsujimoto and colleagues (1989) reported that methoxamine is selective for the  $\alpha_{1A}$  subtype in both affinity and efficacy.

Using hepatocytes from guinea pigs, rats and rabbits, which express  $\alpha_{1D}$ -,  $\alpha_{1B}$  and  $\alpha_{1A}$ -ARs respectively, Garcia-Sainz and colleagues (1993) investigated the agonist pharmacology of these subtypes. After the labelling of phosphatidylinositol, they discovered that methoxamine had a high intrinsic activity in guinea pig liver ( $\alpha_{1D}$ -) but not in rat or rabbit liver, whilst oxymetazoline displayed a high intrinsic activity in rabbit liver ( $\alpha_{1A}$ -) but not in guinea pig or rat liver (Garcia-Sainz *et al*, 1993). These results suggested methoxamine as a possible  $\alpha_{1D}$ -selective agonist and oxymetazoline as a possible  $\alpha_{1A}$ -selective agonist. The results were interpreted with caution however, as the receptor reserves of the different subtypes in the various liver preparations were unknown and efficacy cannot be obtained directly from intrinsic activity. Nevertheless, these results did suggest that commonly used agonists could show different efficacies at different  $\alpha_1$ -AR subtypes (Minneman & Esbenshade, 1994).

Minneman and colleagues (1994) studied the potencies of a range of full and partial agonists at the recombinant subtypes. Using radioligand binding studies, the group confirmed that full agonists such as adrenaline and noradrenaline showed about a 20-fold higher apparent affinity for the  $\alpha_{1D}$  subtype compared to the other two. This potency difference was not apparent when receptor-mediated second messenger responses were measured in intact cells, which was of some surprise. Noradrenaline, adrenaline, 6-fluoronoradrenaline and phenylephrine had similar potencies and apparent intrinsic activities for stimulating inositol phosphate formation mediated by all three recombinant  $\alpha_1$ -AR subtypes in human embryonic kidney (HEK) 293 cells (Minneman *et al*, 1994). Methoxamine was most potent at the  $\alpha_{1A}$ -AR subtype, but had a significant intrinsic activity at all three subtypes, while various imidazolines, including cirazoline, displayed a significantly higher intrinsic activity at the  $\alpha_{1A}$ -AR subtype compared to the other two.

There have been other  $\alpha_{1A}$ -AR selective agonists reported. Knepper and colleagues (1995) reported that A-61603 is a member of the tetrahydro-1-naphthyl imidazoline

agonists and is a potent agonist at  $\alpha_1$ -ARs. A-61603 is 35-fold more potent at human cloned  $\alpha_{1A}$ - than at  $\alpha_{1B}$ - or  $\alpha_{1D}$ -ARs in radioligand binding studies and 100- to 300-fold more potent than noradrenaline and phenylephrine in isolated canine prostate strips and rat vas deferens ( $\alpha_{1A}$ -ARs). In contrast, A-61603 is only 40-fold more potent than phenylephrine at  $\alpha_{1B}$ -ARs (rat spleen) and 35-fold less potent at  $\alpha_{1D}$ -ARs (rat aorta) (Knepper *et al*, 1995; Meyer *et al*, 1996; Willems *et al*, 2001). Even though A-61603 shows a low affinity for other receptors, it displays a reasonable affinity and agonist property at  $\alpha_2$ -AR subtypes (Willems *et al*, 2001). Chemical structures for adrenaline, noradrenaline, phenylephrine and A-61603 are shown in Figure 1.1.

More recently, O'Neill and colleagues (2001) described the pharmacological properties of a potent and selective  $\alpha_{1A}$ -AR agonist, A-204176. Following functional studies using rabbit urethra, the group reported that A-204176 shows selectivity for  $\alpha_{1A}$  *in vitro* and enhanced urethral selectivity in comparison to the non-selective adrenergic agonist PPA. However, despite its selectivity for  $\alpha_{1A}$  versus  $\alpha_{1B}$  and  $\alpha_{1D}$  subtypes, A-204176 did not show the degree of urethral selectivity *in vivo* that would have been expected from its *in vitro* functional profile (O'Neill *et al*, 2001). These results were in contrast to the development of selective  $\alpha_{1A}$  antagonists for the treatment of BPH where compounds lacking  $\alpha_{1B}$  activity produce little cardiovascular effect (Kirkby, 1999; Takeda *et al*, 1999). The data indicates that A-204176 may be a useful pharmacological tool to investigate the functional role of the  $\alpha_{1A}$  adrenergic subtype in the urethra.

It is clear that there is a need for more selective agonists and antagonists, especially for the  $\alpha_{1B}$  and  $\alpha_{1D}$  subtypes. The discovery of such compounds would help by allowing quantitative assessment of subtype distribution by radioligand binding studies and in defining their functional roles. This remains unlikely, however, due to the lack of clearly defined potential therapeutic applications for such compounds.

## **1.7 Desensitisation**

Adrenoceptors are subject to regulation by a variety of mechanisms including phosphorylation, protein-protein interactions, protein trafficking and transcription. One of the most intensively studied of these mechanisms is desensitisation, a general phenomenon where the intensity of a biological response diminishes over a period of time, despite continued stimulus (Michelotti *et al*, 2000). The concept of desensitisation is based mainly on exhaustive studies performed with the Gs-coupled  $\beta_2$ -ARs (Lefkowitz *et al*, 1998; Pitcher *et al*, 1998; Krupnick & Benovic, 1998; Goodman *et al*, 1996; Krueger *et al*, 1997). Desensitisation can be homologous, where receptor response wanes upon continuous exposure to its agonist or heterologous, where the activation of one receptor can result in reduced responses to activation of other unrelated receptors, particularly when there is activation of signalling pathways or effectors common to the receptor types (Freedman & Lefkowitz, 1996; Bunemann *et al*, 1999). Both phosphorylation of agonist-occupied receptor and uncoupling of the phosphorylated receptor from G Protein by  $\beta$ -arrestins are involved in the mechanism of desensitisation. Two distinct arrestin like genes have been cloned, termed  $\beta$ -arrestin 1 and  $\beta$ -arrestin 2 (Lohse *et al*, 1990; Attramadal *et al*, 1992).

### **1.7.1 Homologous Desensitisation**

The process of receptor desensitisation has been most extensively characterised for the  $\beta_2$ -adrenergic receptor, although many of the mechanisms operative for  $\beta_2$ -receptor desensitisation are being observed for other GPCRs (Hein & Kobilka, 1997). It is generally accepted that homologous desensitisation involves receptor phosphorylation by GRKs (Ferguson *et al*, 1997; Krupnick & Benovic, 1998; Garcia-Sainz *et al*, 2000). The sites for GRK phosphorylation seem to be in the carboxyl terminus for the  $\beta$ -adrenergic receptors (Bouvier *et al*, 1988) or in the third intracellular loop of  $\alpha_2$ -ARs (Eason *et al*, 1995). GRKs are a family of at least six serine/threonine protein kinases that phosphorylate GPCRs only in the agonist bound state. Receptors with bound agonist activate heterotrimeric G-Proteins, releasing G $\beta$

complexes. These membrane-bound G $\beta$  $\gamma$  heterodimers and PIP<sub>2</sub> bind to the carboxyl terminal domain of soluble GRKs that targets the kinase to the receptor (Pitcher *et al*, 1998).

There are hundreds to thousands of GPCRs and only a limited number of GRKs, suggesting that different GRKs recognise different subsets of GPCRs as substrates *in vivo* (Bunemann *et al*, 1999). Six GRKs have been identified from mammalian cDNA libraries: GRK1 (rhodopsin kinase), GRK2 and GRK3 (formerly referred to as the  $\beta$ -adrenergic receptor kinases  $\beta$ -ARK1 and  $\beta$ -ARK2), GRK4, GRK5 and GRK6 (Chuang *et al*, 1996). GRK1 and GRK4 are localised in a tissue-specific manner, restricting their interaction with many types of GPCR, whereas the other GRKs are widely distributed, and in the cardiovascular system, GRK2, 3 and 5 have been suggested to regulate a number of GPCRs (Chuang *et al*, 1996; Bunemann *et al*, 1999).

Evidence has recently suggested that GRKs may also inhibit receptor signalling via phosphorylation-independent mechanisms. Using kinase-negative mutants of GRKs and truncated receptors, it has been shown that binding of GRKs to the receptors inhibits signalling (Dicker *et al*, 1999). Mukherjee and colleagues (1999) also provided evidence that arrestins may bind and desensitise some GPCRs in the absence of receptor phosphorylation and that receptor activation seems to start these processes (Garcia-Sainz *et al*, 2000).

### ***1.7.2 Heterologous Desensitisation***

Many GPCRs are desensitised via feedback regulation by second messenger-stimulated kinases, such as PKA and PKC. This is an example of heterologous desensitisation since, in principle, any stimulant that can increase cAMP or DAG has the potential to induce the phosphorylation and desensitisation of any GPCR containing the consensus phosphorylation sites for PKA or PKC (Garcia-Sainz *et al*, 2000). Other proteins involved in signalling and possessing such consensus sites can also be phosphorylated and their function can be modified as a result of this.

Similarly, a single receptor type is susceptible to phosphorylation and desensitisation by multiple protein kinases (Nambi *et al*, 1985).

There is evidence that PKA-dependant phosphorylation of the  $\beta_2$ -AR can strengthen the coupling of the receptor to the inhibitory G Protein  $G_i$  (Daaka *et al*, 1997) and promote activation of the MAP kinase pathway via a process that has been suggested to be pertussis toxin sensitive and to require receptor endocytosis (Daaka *et al*, 1998). This shows that even though PKA-mediated phosphorylation of the  $\beta_2$ -AR can switch off signalling via the receptor's normal partner,  $G_s$ , at the same time it helps to couple the receptor to an inhibitory G Protein (Bunemann *et al*, 1999).

### 1.7.3 Phosphorylation of $\alpha_1$ -ARs

The information on  $\alpha_1$ -ARs phosphorylation/desensitisation is more limited than that available for  $\alpha_2$ - and  $\beta$ -ARs. There is information available on  $\alpha_{1B}$ -AR phosphorylation/desensitisation, but more information is needed on the possible phosphorylation of other subtypes. There appears to be little, if no information on the possible phosphorylation of  $\alpha_{1D}$ -ARs. When transfected into Rat-1 fibroblasts,  $\alpha_1$ -ARs are differentially regulated by activation of PKC. Activation of PKC with phorbol esters clearly inhibited the actions mediated through  $\alpha_{1B}$ - and  $\alpha_{1D}$ -ARs, whereas those mediated through  $\alpha_{1A}$ -ARs were unaltered (Vazquez-Prado & Garcia-Sainz, 1996).

Studies on  $\alpha_{1A}$ -ARs stably expressed in Rat-1 fibroblasts show that these receptors are phosphorylated in response to noradrenaline and when PKC is activated by phorbol esters (Vazquez-Prado *et al*, 2000; Garcia-Sainz *et al*, 2000). This was something of a surprising result as there is very little effect of active phorbol esters on the adrenergic modulation of cellular parameters ( $\alpha_{1A}$ -AR-mediated increases in intracellular  $Ca^{2+}$  concentration or phosphoinositide hydrolysis). There was however, a small effect of active phorbol esters on noradrenaline-stimulated [ $^{35}S$ ]GTP $\gamma$ S binding (Vazquez-Prado *et al*, 2000). It must also be noted however, that  $\alpha_{1A}$ -ARs are much less sensitive (or more resistant) to desensitisation and are phosphorylated to

a lesser extent than  $\alpha_{1\beta}$ -ARs. A major future issue is the identification of the isoforms of PKC and phosphatidylinositol 3-kinase that play important roles in heterologous desensitisation. These kinases are now extremely important in the regulation of receptor function and unfortunately there are no pharmacological agents with sufficient selectivity to address these aspects. Molecular biological techniques will probably be used and once these aspects have been clarified, there will be a window for drug design, which may be of therapeutic potential (Garcia-Sainz *et al*, 2000).

## **1.8 Endocytosis**

Mammalian cells have evolved a variety of mechanisms to internalise small molecules, macromolecules and particles and target them to specific sealed organelles within the cytoplasm. Together, these processes are known as “endocytosis”, a term proposed by de Duve in 1963. Under its broad definition, endocytosis includes various methods of uptake of extracellular material by cells, including phagocytosis (or “cell eating”), pinocytosis (or “cell drinking”), clathrin-dependent receptor-mediated endocytosis and clathrin-independent endocytosis (Mukherjee *et al*, 1997).

Receptor-mediated endocytosis via clathrin-coated pits is a shared pathway used for the internalisation of a variety of ligand-receptor complexes. Roth and Porter (1964) were the first to describe these coated pits and vesicles in mosquito oocytes and proposed that these structures help in yolk formation by taking up absorbed proteins from the extracellular fluid. Kanaseki and Kadota (1969) first reported the fact that the coat actually corresponds to a baselike structure. Receptor-mediated endocytosis of molecules that concentrate in the coated pits leads to their extremely efficient clearance from the cell surface.

### **1.8.1 Clathrin-Coated Vesicles**

Clathrin-coated pits are ~150nm invaginated structures on the plasma membrane (Willingham *et al*, 1981) that occupy approximately 2% of the plasma membrane

surface on human fibroblasts (Anderson *et al*, 1977). These pits assemble on the cytoplasmic face of the plasma membrane by the recruitment of the adaptor complex AP-2, a heterotetramer comprising two large subunits,  $\alpha$  and  $\beta$ 2 (each of ~100kDa), and two smaller chains,  $\mu$ 2 (50kDa) and  $\sigma$ 2 (20kDa). The function of such adaptors is to link clathrin to the membrane and to organise the structural assembly of the coat with the selection of cargo proteins and lipids (Takei & Haucke, 2001).

Endocytosis of plasma membrane or synaptic vesicle components is affected by the gathering of clathrin-coated vesicles that serve to concentrate cargo proteins and lipids into the emerging vesicle and provide a mechanical means to deform the membrane into a vesicular bud (Takei & Haucke, 2001). This bud then matures and subsequently pinches off, forming a free clathrin-coated vesicle. Energy-dependant uncoating restores a vesicle (Braell *et al*, 1984), which can either fuse with endosomes and be routed to lysosomes for degradation or, in the case of a synaptic vesicle, be refilled with neurotransmitter and recycled back to the cell surface for another round of delivery (Gruenberg & Maxfield, 1995; Brodin *et al*, 2000).

Clathrin-coated vesicles formed at the plasma membrane fuse with early, but not late endosomes, even though there are late endosomes present next to early endosomes. This specificity must reflect the presence of a specific receptor on the early endosome membrane (Gruenberg & Maxfield, 1995).

### 1.8.2 Caveolae

The definition of caveolae has expanded in recent years to include vesicles detached from the plasma membrane proper, associated in groups as grape-like clusters or rosettes or even in fused form as elongated tubules or *trans*-cellular channels (Razani *et al*, 2002). Since their discovery in the 1950s, caveolae were given the exclusive electron microscope description of membrane invaginated “smooth” vesicles of approximately 50 to 100nm in size (as opposed to the more dense clathrin-coated pits). As more is learned about these structures, caveolae can no longer be classed as static in-pocketings of the plasma membrane, but can take on disparate shapes and forms by conglomerating and/or fusing with one another (Razani *et al*, 2002).

Caveolae have also been implicated in endocytotic processes. Clathrin-coated vesicular transport has been almost entirely associated with endocytosis (Takei & Haucke, 2001), but it has become apparent that certain receptors and extracellular macromolecules are exclusively transported via caveolae rather than the clathrin-coated pits. The first example of this came when caveolae bound and internalised cholera and tetanus toxins (Montesano *et al.*, 1982). Biochemical evidence supported these findings when it was shown that treatment of cell with cholesterol binding agents (nystatin or filipin) cancelled the endocytosis of certain macromolecules (e.g., albumin) without affecting the uptake of clathrin-dependent ones (Schnitzer *et al.*, 1994; Razani *et al.*, 2002).

It is unclear where the endocytosed caveolar vesicle targets in the cell. Among the possibilities is direct transport to endosomes with or without further trafficking to other intracellular compartments. For example, in the case of cholera toxin, it is believed that caveolar endocytosis on the apical membrane is followed by retrograde transport to endosomes, the Golgi apparatus, the ER and finally resorting to the basolateral membrane (Lencer *et al.*, 1999). However, this trafficking scheme does not apply to all caveolae-mediated endocytosis. The budded caveolae containing the simian virus 40 (SV40) eventually merges with larger, non-endosomal, non-lysosomal caveolin-1 containing organelles that target to the ER (Pelkmans *et al.*, 2001). These organelles were named “caveosomes” and provide the first evidence of distinct compartments formed from internalised caveolae. This correlates with earlier work, which stated that under specific conditions, caveolins can either directly traffic from the plasma membrane to Golgi/ER compartments or localise to non-endosomal vesicles (Conrad *et al.*, 1996; Roy *et al.*, 1999).

### **1.8.3 Endocytotic Rate**

In unstimulated cells, there is a relatively slow endocytosis of receptors from the cell surface into endosomes, but in the presence of agonist, the rate of endocytosis is increased dramatically (Koenig & Edwardson, 1997). It seems that when agonist binds, the receptor is activated and becomes liable to endocytosis. If the ligand dissociates, the receptor can still be associated with the endocytotic machinery and be

endocytosed minus the ligand. This means that when the agonist is present, it enhances the rate of receptor endocytosis, but the amount of agonist endocytosed depends on both its dissociation rate and the receptor endocytosis rate. For the lower affinity ligands, such as the muscarinic acetylcholine receptor agonists, it appears unlikely that they are internalised at all (Koenig & Edwardson, 1997).

#### ***1.8.4 Inhibiting Endocytosis***

Endocytosis and recycling of GPCRs are both extremely temperature and energy dependent with both these processes almost completely prevented below 16°C (Von Zastrow & Kobilka, 1994). Other ways to inhibit receptor endocytosis include increased extracellular hyperosmolarity (normally achieved with 0.45M sucrose), depletion of intracellular K<sup>+</sup> and acidification of the cytosol (Roettger *et al*, 1995). Treatment with phenylarsine oxide also inhibits endocytosis (Hunyady *et al* 1991), although it is known to have many effects on cellular function through interactions with sulphhydryl groups. These properties described are characteristic of endocytosis via clathrin-coated pits, and in some cases agonist-stimulated accumulation of GPCRs in these pits. Their budding from the cell surface to form clathrin-coated vesicles were directly visualised by Koenig and Edwardson (1997). There have also been reports of endocytosis via uncoated pits (Roettger *et al*, 1995).

#### ***1.8.5 Receptor Degradation***

Receptor degradation is also important when modelling intracellular movement, especially since the rate of degradation increases dramatically in the presence of agonist (Koenig and Edwardson, 1997). It is common for receptor density to decrease after agonist concentrations have been elevated for a considerable time and this change shows an important component of the response to chronic drug treatment (Sleight *et al*, 1995).

Following endocytosis, receptors enter a tubulo-vesicular endosomal compartment (Tooze & Hollinshead, 1991). As mentioned previously, once in the endosome, GPCRs can either be recycled to the plasma membrane or directed to other destinations on the endocytotic pathway, such as the lysosome. The different extents of recycling and degradation for different GPCRs suggest that signals operate in early endosomes to determine the later fate of the endocytosed receptor, with recycling to the plasma membrane being the default pathway (Koenig and Edwardson, 1997). It is possible that the activation state of the receptor once it reaches the endosome plays some part in its fate. Evidence for this was proved using the thrombin receptor, which was directly activated by a unique proteolytic mechanism (Hein *et al*, 1994). Thrombin cleaves the receptor's amino terminus to expose a new terminus, which then acts as a tethered peptide ligand.

For GPCRs where agonists are of low affinity (i.e. micromolar), such as the  $\beta$ -AR and the muscarinic receptor, it is unlikely that sufficient agonist will be endocytosed to cause significant receptor activation in endosomes (Sorensen *et al*, 1997). On the other hand, peptides often have higher affinity for their respective GPCRs (i.e. nanomolar to picomolar) and it is possible that the agonist concentration in the endosome's lumen could be high enough to cause receptor activation. If constant activation does target GPCRs to lysosomes, it would be expected that the receptors' fates depend on the affinity of the agonist (Koenig and Edwardson, 1997).

### ***1.8.6 Receptor Trafficking***

Michelotti and colleagues (2000) reported that a green fluorescent protein-tagged  $\alpha_{1a}$ -AR undergoes constitutive (agonist-independent) cycling between the cell surface and nonlysosomal intracellular compartments. This finding of agonist-independent cellular trafficking may provide a potential means for continuous  $\alpha_{1a}$ -AR signalling, which could possibly contribute to the development of myocardial hypertrophy (Price & Schwinn, 1998). This was supported by earlier findings where transiently expressed, green fluorescent protein- or FLAG-tagged  $\alpha_{1a}$ -AR and  $\alpha_{1b}$ -AR subtypes displayed differential sensitivity to CEC as a result of differences in subcellular

localisation and not differences in structural determinants (Hirasawa *et al*, 1997). This should increase the chance of pharmacologic manipulation of  $\alpha_1$ -ARs as differences in subtype-specific trafficking are clarified.

The  $\alpha_{1a}$ -AR is unique in that agonist exposure in a rat neonatal myocyte model results in continued signalling, while  $\alpha_{1b}$ - and  $\alpha_{1d}$ -ARs undergo desensitisation (Rokosh *et al*, 1996). All three  $\alpha_1$ -ARs are expressed in neonatal rat cardiac myocytes and these myocytes maintain full  $\alpha_1$ -AR responsiveness to noradrenaline exposure, even following 24-72 hour continuous stimulation, suggesting that persistent  $\alpha_1$ -AR signalling results from  $\alpha_{1a}$ -AR expression and signalling (Rokosh *et al*, 1996; Michelotti *et al*, 2000). Signalling differences between subtypes do not dictate these results as  $\alpha_1$ -ARs mainly couple to the same second messenger cascade, albeit with  $\alpha_{1a} \approx \alpha_{1b} > \alpha_{1d}$  efficacy (Schwinn *et al*, 1995).

## **1.9 Fluorescent Ligand Binding**

### **1.9.1 GPCRs and GFP**

Cell surface GPCRs are extremely difficult to localise accurately, even in fixed tissue, due to the nonspecificity of antibodies, in turn due to the high degree of conservation of sequence, and to the inherent low resolution of autoradiography (Daly *et al*, 1998). The gene encoding green fluorescent protein (GFP) from the jellyfish *Aequoria victoria* was first isolated in 1992 (Prasher *et al*, 1992) and has quickly become a popular reporter molecule for monitoring protein expression and localisation (Kallal & Benovic, 2000). The introduction of GFP for use as an autofluorescent epitope tag (Cubit *et al*, 1995) has allowed the visualisation of GPCRs and their regulatory proteins in real-time with a precision not afforded by fluorescent antibody staining of fixed cells (Ferguson, 1998).

GFP is a 238 amino acid protein that emits green light with an emission maximum of 509nm upon fluorescent excitation at 488nm. GFP fluorescence is stable and has been measured non-invasively in living cells of many species including mammals,

*Drosophila*, *C.elegans*, yeast and *E.coli* (Milligan, 1999). GFP fluorescence can be detected by fluorimetry, by fluorescence activated cell sorting (FACS) and by microscopy. No cofactors or substrates are required, making the attractiveness of GFP as a reporter protein apparent (Chalfie & Kain, 1998).

There have been various attempts at conjugating fluorescent molecules to receptor ligands in the hope of identifying their binding sites. The reason was to study the localisation of the receptors rather than studying their properties. The aim was to produce a fluorescent compound that would remain fluorescent when bound to the receptor and would remain bound when the free drug was washed away (McGrath *et al*, 1996). Problems seemed likely to occur with the latter, as washing would probably cause the ligand to dissociate and diffuse away, unless it has very high affinity.

The fluorescent ligand-receptor complex can be studied particularly effectively with confocal microscopy. This allows localisation of the receptive site within a cell, tissue or organ giving much higher spatial resolution than autoradiography and offers high resolution and quantitative analysis in three dimensions. Also, temporal resolution is achievable: binding can be followed in real-time in live tissue with the consequent advantages of studying the kinetic properties of the receptors and their relationship to cellular activation processes (Daly *et al*, 1998).

Not all GPCRs are effectively delivered to the plasma membrane of cells. Hirasawa and colleagues (1997) examined the subcellular localisation of native  $\alpha_{1A}$ - and  $\alpha_{1B}$ -ARs and compared it with CEC sensitivity of each subtype. Flow cytometry analysis and immunocytochemical and GFP-fluorescent localisation analysis by confocal microscopy showed that  $\alpha_{1A}$ -ARs predominately localise intracellularly, whereas most of  $\alpha_{1B}$ -ARs localise on the cell surface, and that CEC preferentially inactivates the cell surface  $\alpha_1$ -AR irrespective of the subtype (Hirasawa *et al*, 1997). Recent work has confirmed these cellular localisation findings by use of flow cytometry and confocal microscopy techniques (Sugawara *et al*, 2002; Koshimizu *et al*, 2002). The long held suggestion that CEC can be used as a selective pharmacological discriminator for the  $\alpha_{1B}$ -AR was re-examined. Inactivation of the two GPCR subtypes by CEC was

equivalent in membrane preparations, but displayed selective inactivation of the  $\alpha_{1B}$ -AR in intact cell studies. It was concluded that CEC is not essentially a selective alkylating agent between these two closely related GPCRs if provided with equal access, but that the observed differential effects of CEC might instead relate to uneven subcellular distribution of the two GPCRs (Hirasawa *et al*, 1997; Milligan, 1999).

### 1.9.2 QAPB and Subcellular Localisation

An example of a fluorescent ligand for  $\alpha_1$ -ARs is BODIPY FL-prazosin, alternatively known as QAPB (McGrath & Daly, 1995). This compound is related to the  $\alpha_1$ -AR antagonists doxazosin, prazosin and terazosin (Ruffolo *et al*, 1995). QAPB has been used to visualise  $\alpha$ -ARs on live cells and intact pieces of tissue. The punctate fluorescence found confirms the punctate nature of  $\alpha$ -AR distribution reported by Uhlen and colleagues (1995) in MDCK cells. This is an example of the ligand-receptor complex being more fluorescent than the unbound ligand (McGrath *et al*, 1996). The chemical structure of QAPB is shown in Figure 1.2.

Daly and colleagues (1998) visualised QAPB at concentrations equivalent to those used for radioligand binding, in real time, at kinetic equilibrium, with a defined receptor subtype on live cells. The cells used were rat-1 fibroblasts expressing the recombinant  $\alpha_{1d}$ -AR. QAPB was validated as a competitive antagonist against the  $\alpha_1$ -AR agonist phenylephrine's production of inositol phosphates and as a competitive ligand against [ $^3$ H] prazosin, confirming that it is a ligand for functional  $\alpha_{1d}$ -ARs. The binding and functional antagonism data showed that despite the modification of the molecule to incorporate the fluorescent tag, it retains the properties required of a high affinity pharmacological "antagonist" ligand. QAPB entered live cells and hence reported spatial distribution of binding sites throughout the cell, not only at the expected functional locations on the plasma membrane. It was assumed that QAPB entered the cells because it is lipophilic. It showed no fluorescence in the aqueous phase and so could be employed at equilibrium. It was, however, fluorescent when bound to the receptor, allowing estimation of receptor occupation under equilibrium conditions (Daly *et al*, 1998; MacKenzie *et al*, 2000).

Following Daly's studies, MacKenzie and colleagues (2000) confirmed QAPB as a high affinity nonsubtype-selective competitive antagonist at  $\alpha_1$ -AR-binding sites. QAPB bound to the cell membrane and intracellular perinuclear sites in all three recombinant  $\alpha_1$ -AR subtypes expressed in rat-1 fibroblasts, although it was more prominent around the perinuclear area of the cell in the  $\alpha_{1b}$ -AR subtype (MacKenzie *et al*, 2000). This is an example of different subtypes adopting different locations in the same host cell. Previous work by Hrometz and colleagues (1999) had reported that in fibroblasts expressing each of the receptors,  $\alpha_1$ -ARs are expressed not only on the cell surface, but also in intracellular compartments. Immunostaining in these fibroblasts was noted on the cell surface and also in the perinuclear region (Hrometz *et al*, 1999). MacKenzie's group also reported that quantitative three-dimensional mapping of QAPB-associated fluorescence binding in native human cells showed that 40% of high affinity binding sites were found in intracellular compartments. The binding in these prostatic smooth muscle cells was found particularly around the nucleus, which could represent binding in the Golgi and may include both newly synthesised and recycling stores of receptors. This demonstrates that the vast quantity of intracellular binding sites previously shown in recombinant cells is not an artifact of artificial systems, but a natural phenomenon (MacKenzie *et al*, 2000).

### ***1.9.3 Extraneuronal Monoamine Transporter***

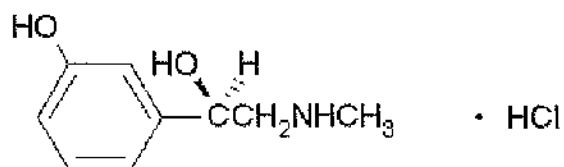
The discovery by MacKenzie and colleagues (2000) that  $\alpha_1$ -AR subtypes bind ligands at intracellular sites raises the possibility that this may be a general property of heptahelical receptors and this has important implications for drug action. If intracellular receptors transduce signals, then activators or blockers might act at these differentially with regard to whether they can penetrate the cells, by means of diffusion/lipophilicity or whether they are substrates for membrane carriers.

The catecholamine noradrenaline, is taken up and accumulated by smooth muscle cells that express  $\alpha_1$ -ARs (Avakian & Gillespie, 1968). The transporter responsible, known as the extraneuronal monoamine transporter (EMT), has been cloned (Grundemann *et al*, 1998). This transporter was previously known as Uptake<sub>2</sub>.

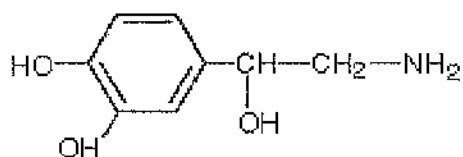
Iversen (1965) had concluded that Uptake<sub>2</sub> lacked stereoselectivity based on the comparison of (-)- with (+)-noradrenaline and (-)- with (±)-adrenaline in the isolated rat heart. It was soon discovered that the naturally secreted glucocorticoid in the rat, corticosterone, was a potent inhibitor of Uptake<sub>2</sub> (Iversen & Salt, 1970). When the transporter is blocked, the metabolism of noradrenaline is attenuated which implies that the purpose of the carrier is to eliminate noradrenaline from the extracellular space (Eisenhofer *et al*, 1996; MacKenzie *et al*, 2000). The presence of intracellular  $\alpha_1$ -ARs with the ability to bind ligands, raises the possibility that a function of the transporter is to deliver catecholamines to intracellular receptors.

Extraneuronal uptake, like metabolism of catecholamines by COMT, exists almost exclusively in non-neuronal cells (Karhunen *et al*, 1994), and monoamine oxidases (MAO-A and MAO-B). Grundemann and colleagues (1998) cloned the EMT and reported its use as a widely distributed second line of defence, inactivating the fraction of released monoamine transmitters that escape neuronal uptake and hence stopping uncontrolled spreading of the signal (Grundemann *et al*, 1998). Amino acid sequence analysis identified EMT as a new member of the recently defined family of amphiphilic solute facilitators (ASF) (Schomig *et al*, 1998). The cloning of EMT provides a new candidate not just for diseases based on autonomic dysfunction, but also for neuropsychiatric disorders.

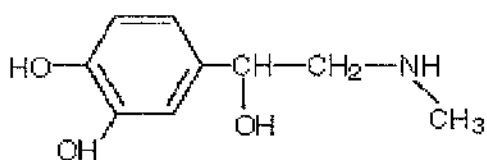
**Phenylephrine**



**Noradrenaline**



**Adrenaline**



**A61603**

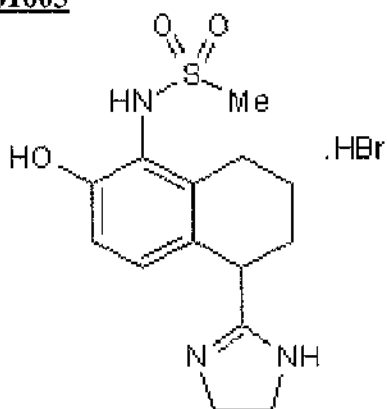
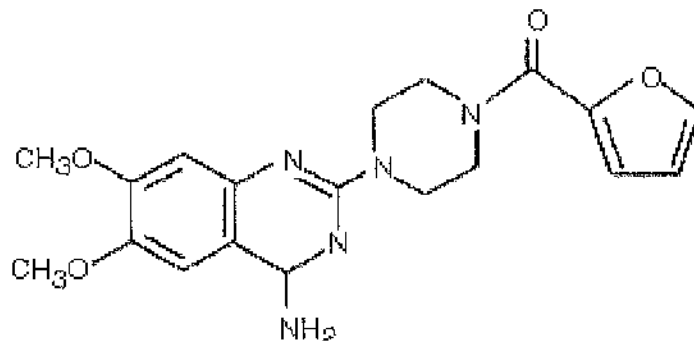


**Figure 1.1** Agonist chemical structures:  $\alpha_1$ -AR agonist phenylephrine,  $\alpha_{1a}$ -AR agonist A61603 and catecholamines; noradrenaline and adrenaline.

## Prazosin



## QAPB

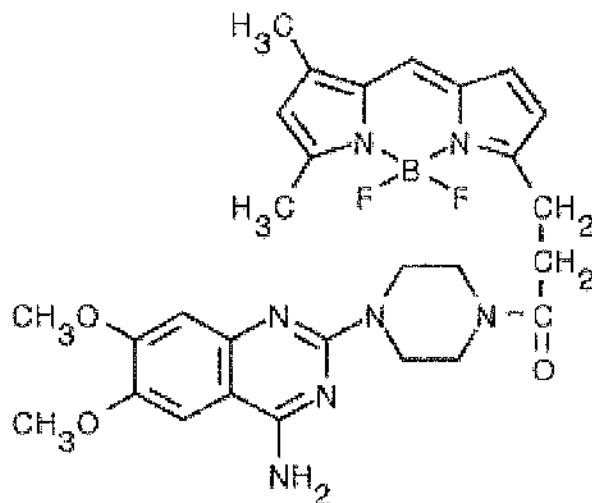
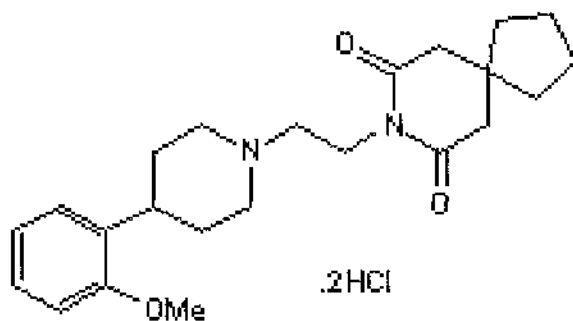


**Figure 1.2** Prazosin and QAPB structures. Chemical structure of the  $\alpha_1$ -AR antagonist prazosin and a fluorescent derivative of prazosin, BODIPY FL-prazosin (QAPB).

**BMY7378**



**RS100329**

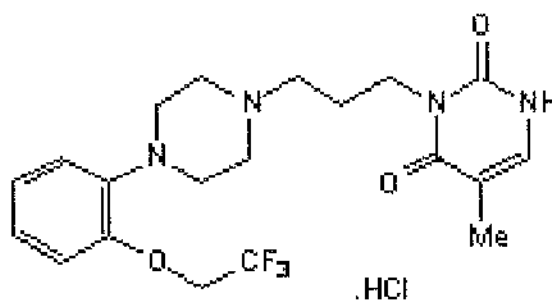


**Figure 1.3** BMY7378 and RS100329 structures: Chemical structures of the  $\alpha_{1d}$ -AR antagonist BMY7378 and the  $\alpha_{1a}$ -AR antagonist RS100329.

## *2.0 Aims & objectives*

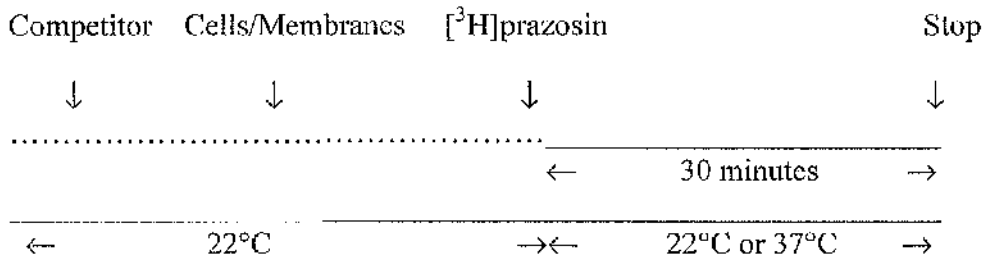
The lab has been using fluorescent ligands such as BODIPY FL-prazosin (QAPB) to visualise a subset of receptors ( $\alpha_1$ -ARs) that belong to the GPCR family. Initial expectations were that  $\alpha_1$ -ARs are exclusively membrane bound receptors.

Subsequent experiments presented in Chapter 3 of the present study revealed a high proportion of fluorescent ligand could be found inside cells. Other antagonists can displace these fluorescent ligands; hence competitive binding takes place inside cells.

Using classical and updated radioligand binding techniques (for detailed diagrams of protocols, see Figures 2.1 & 2.2), we could make a comparison of binding to isolated cell membranes and whole cells. Any differences would indicate differences in intracellular binding or issues related to penetration of cells by ligands. A number of questions were addressed.

1. Is binding inside cell similar or different from binding at the cell surface?
2. Do antagonists bind similarly inside cells and is this influenced by their ability to penetrate cells?
3. Are there ways to selectively block receptors on the cell membrane or inside the cell?
4. Can  $\alpha$ -AR agonists cross cell membranes and act on intracellular sites?

# A



# B

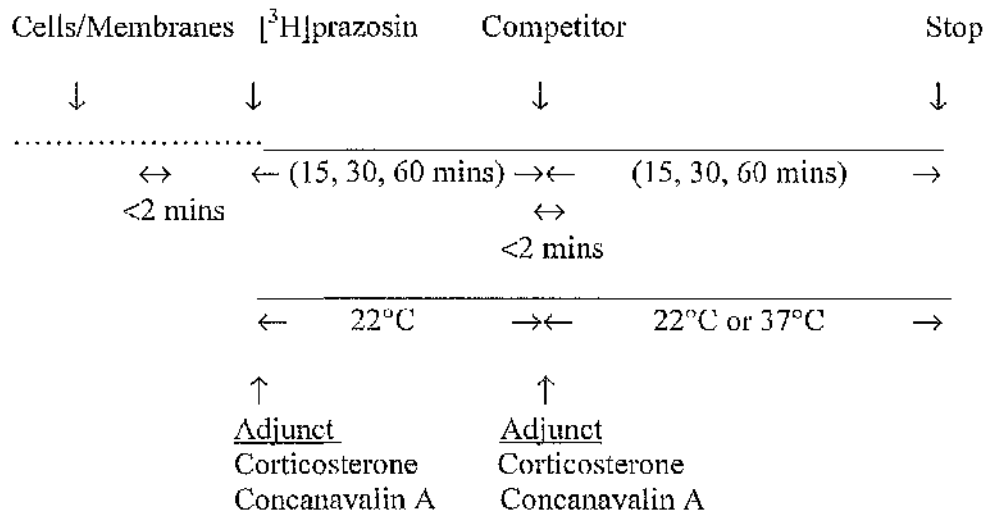


**Figure 2.1** Radioligand binding protocols. **A**, shows the “classical” radioligand binding protocol and **B**, shows a new radioligand binding protocol.

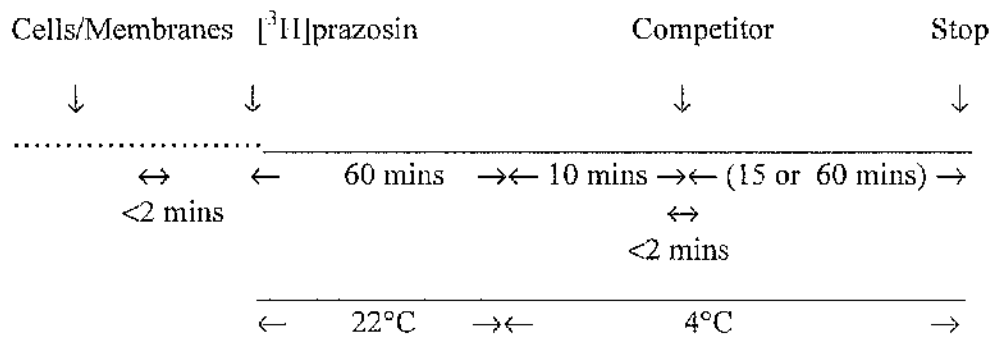


**Figure 2.2** Updated radioligand binding protocol. Diagram shows a new “cold” radioligand binding protocol.

## **2.1 METHODS**

### **2.1.1 Cell Culture.**

Rat-1 Fibroblasts stably expressing the bovine  $\alpha_{1a}$ -AR and human  $\alpha_{1d}$ -AR were used. Cells were grown in monolayers in DMEM containing 10% (v/v) foetal bovine serum, 100 I.U./ml penicillin, 100 $\mu$ g/ml streptomycin and 1mM L-glutamine in a 95% air and 5% CO<sub>2</sub> atmosphere at 37°C. Selection was maintained by adding geneticin (G418) (400 $\mu$ g/ml) to the growth media.

#### **2.1.1.1 Freezing cells.**

Cells are grown to confluence in 75cm<sup>3</sup> tissue culture flasks, growth media removed and replaced with fresh growth media containing 10% DMSO. Cells are removed from the base of the flask by gentle agitation and aliquoted into 1.5ml cryovials. The cryovials are stored at -70°C for 24 hours, then labelled in cryocanes and frozen down in liquid nitrogen.

#### **2.1.1.2 Growing cells**

Single cryovials containing the cells were removed from cryocanes and left in the incubator at 37°C for 5-7 minutes. Once defrosted, cells were carefully triturated twice and added to a 25cm<sup>3</sup> tissue culture flask. 10mls of DMEM was slowly added to the flask, the flask cap was loosened and the suspension left in the incubator for 40 minutes to allow cells to adhere to the base of the flask. The media was then removed, replaced with 5mls fresh media and flask placed in incubator to be maintained as normal.

### ***2.1.1.3 Cell splitting***

Cells were maintained using a “splitting” process. Once cells reached confluence, growth media was removed and cells washed with 2mls 0.25% trypsin/EDTA solution. The wash solution was removed, replaced with 2.5mls fresh trypsin/EDTA and 2.5mls fresh DMEM, then transferred to a 13ml centrifuge tube and centrifuged at 4000rpm for 3 minutes at 22°C. The solution was discarded, leaving a pellet. Using a Pasteur pipette, 1ml DMEM was added and carefully triturated 15-20 times before adding a further 9mls DMEM. After resuspending, 1ml of the cell suspension was added to a 25cm<sup>3</sup> tissue culture flask along with 4mls fresh DMEM. The cells were then placed in the incubator and maintained as normal.

### ***2.1.2 Membrane Preparation***

Cells were grown to confluence and harvested using a rubber policeman followed by centrifugation at 4000rpm for 3 minutes at 22°C. The cell pellet was resuspended in 5ml of Tris-HCl assay buffer (150mM NaCl, 50mM Tris-HCl, 10mM MgCl<sub>2</sub>, 5mM EDTA, pH 7.4) then stored for 24 hours at -80°C. After defrosting on ice, the cells were homogenised using a pre-chilled Teflon-in-glass homogeniser. The homogenate was centrifuged at 4000rpm for 5 minutes at 4°C, the supernatant recovered and centrifuged at 26000rpm for 30 minutes at 4°C. The resulting membrane pellet was resuspended in 1ml of ice-cold Tris-HCl assay buffer and sheared by passage through a 26-gauge needle. The homogenate was processed for protein estimation using a BCA™ Protein Assay Kit (Pierce) using bovine serum albumin as the standard. Aliquots not used immediately for ligand binding studies were stored at -80°C.

### ***2.1.3 Whole Cell Preparation***

Similar to membrane preparations, cells were grown to confluence and harvested using a rubber policeman followed by centrifugation at 4000rpm for 3 minutes at 22°C. The resulting pellets were pooled, supernatant discarded and replaced with 8mls ice-cold Tris-assay buffer. After a brief resuspension, cells were drawn through

a 26-gauge needle into a universal tube 10-12 times. A small amount of cell suspension was administered into the haemocytometer channel beneath a coverslip to determine the cell number. Cells were viewed under a microscope and a counter used to count cells in the 25(5x5) grid. Cells were then immediately ready for use in ligand binding studies.

#### ***2.1.4 Radioligand binding studies***

##### ***2.1.4.1 Competition binding experiments***

Estimates of binding affinity ( $pK_i$ ) for [ $^3H$ ]-prazosin (0.2nM) in the presence of a range of increasing concentrations of competing ligands were made using rat-1 fibroblast membranes (0.05mg/ml) or whole cells ( $6.5 \times 10^4$  cells/tube) in a total volume of 0.5ml Tris-HCl assay buffer. All equilibrations were carried out for 30 minutes at 22°C, or at 37°C in a heated water bath, and reactions terminated by rapid cold vacuum filtration. Non-specific binding was defined as the concentration of bound ligand in the presence of 10 $\mu$ M phentolamine. Throughout all competition binding experiments, the amount of radioactivity bound remained consistent.

##### ***2.1.4.2 Displacement binding experiments***

These experiments employed slightly different protocols to those used for standard competition experiments. [ $^3H$ ]-prazosin (0.2nM) was incubated with rat-1 fibroblast membranes (0.05mg/ml) or whole cells ( $6.5 \times 10^4$  cells/tube) for 15, 30 or 60 minutes at 22°C or at 37°C in a heated water bath. A range of increasing concentrations of competing ligands were then added and left to incubate for 15, 30, 60 and 120 minutes at 22°C or at 37°C in a heated water bath or at 4°C in a cold room. Reactions were terminated by rapid cold vacuum filtration as described previously. Non-specific binding was defined as the concentration of bound ligand in the presence of 10 $\mu$ M phentolamine. Ligands used in competition and displacement binding studies included prazosin, QAPB, adrenaline, noradrenaline, BMY7378, L-765314,

phenylephrine HCl, (R)-A-61603 and RS100329. Throughout all displacement binding experiments, the amount of radioactivity bound remained consistent.

### 2.1.4.3 Data analysis

Competition and displacement binding experiments were carried out in duplicate, repeated a minimum of three times and the results from each pooled and expressed as mean  $\pm$  s.e.m. Non-specific binding (determined in the presence of 10 $\mu$ M phentolamine) was defined as 0% and total binding (in the absence of any competitor) was defined as 100%. Specific binding is then calculated accordingly and expressed as % specific binding of maximum.

Competitive and displacement binding curves can be described by the equation:

$$Y = \text{NSB} + \frac{(\text{Total} - \text{NSB})}{1 + 10^{(\log[D] - \log[IC_{50}])}}$$

Y = total binding in the presence of the competitor

Log[D] = logarithm of the concentration of competitor

NSB = non-specific binding in the presence of a saturating concentration of D

Total = binding in the absence of competitor

[logIC<sub>50</sub>] = logarithm to the base 10 of the concentration of the competitor which inhibits the binding of the radioligand by 50%

The above equation describes a situation in which the radiolabel and the competing ligand compete for only 1 receptor type. However, in many tissues there are 2 classes of binding sites, which may represent 2 subtypes of receptor. This can be described by a more complicated equation:

$$Y = \text{NSB} + (\text{Total} - \text{NSB}) \cdot \left( \frac{F}{1 + 10^{(\log[D] - \log[IC_{50}]_1)}} + \frac{1 - F}{1 + 10^{(\log[D] - \log[IC_{50}]_2)}} \right)$$

Y, NSB, Total and [D] are the same as for the previous equation and F = the fraction of binding to receptors of the first type of receptor.

Data from competition and displacement experiments were analysed using both the one-site and two-site models. Results of these were compared to determine which gave the more accurate fit. This was achieved in a number of ways. Firstly, the graphs were compared visually to assess which equation appeared to be fitting the data better, after which a number of statistical parameters were determined, which are provided by GraphPad when performing nonlinear regression. The curve-fitting program Prism version 3.0 (GraphPad Software, San Diego, CA) was used throughout. (All definitions taken from GraphPad guide to Nonlinear Regression by Dr. Harvey Motulsky, 1996).

**95% Confidence Intervals:** if all the assumptions of non-linear regression are true, then there is a 95% chance that the true value of the variable lies within the interval. Therefore the narrower the confidence interval, the better the fit.

**Sum of Squares (SS):** the sum of squares is defined as the sum of the square of the vertical distances of the points from the curve. So the smaller the value of SS, then the closer the points are to the curve and the more accurate the fit.

**$r^2$ :** a measure of the goodness of the fit. It is a fraction between 0 and 1 and has no units. When  $r^2 = 0$  the best-fit curve fits the data no better than a horizontal line going through the mean of all the y values, i.e. knowing x does not help you predict y. When  $r^2 = 1$ , all points lie exactly on the curve with no scatter i.e. if you know x, you can predict y.

GraphPad Prism also performs a test called the F test that directly compares the fits of 2 equations and reports which is statistically better suited to the data. The results are presented in the form of an F Ratio that is calculated as follows:

$$F = \frac{(SS1 - SS2)/SS2}{(DF1 - DF2)/DF2}$$

SS = sum of squares

DF = degrees of freedom

If the simpler equation (i.e. the one-site model) is correct, then  $F \approx 1$  because the relative increase in the sum of squares is approximately equal to the relative increase in the degrees of freedom. However, if  $F$  is much greater than 1, then the more complicated equation is correct because the relative increase in the sum of squares (going from the complicated to the simpler model) is greater than the relative increase in the degrees of freedom. For the purposes of the present study, a two-site model was accepted only when the  $F$  Ratio was much greater than 1 and produced a  $p$  value of  $< 0.05$ .

The  $K_i$  or inhibition constant is defined as the concentration of unlabelled drug that will bind half the receptors at equilibrium, in the absence of radioligand or any other competitors and can be calculated using the Cheng-Prusoff equation (Cheng & Prusoff, 1973). For each competition and displacement experiment, a  $K_i$  was calculated and then converted to a  $pK_i$  value, which is the negative logarithm to the base 10 of the  $K_i$ .

Nonlinear regression was also carried out using the Hill equation in order to determine the Hill slope, which allows for the quantification of the slope steepness.

$$Y = \frac{NSB + (Total - NSB)}{1 + 10^{(\log IC_{50} - \log [R]) \cdot \text{slope factor}}}$$

A one-site competitive binding curve that follows the law of mass action will have a slope of  $-1$  (it is negative because the curves go downhill). If the slope differs significantly from  $-1$  then the binding does not follow the law of mass action. One possible explanation may be that there is a heterogeneous population of receptors for which the competing drug has different affinities or it could be a result of heterogeneity in the receptor coupling to other molecules such as G proteins. A Hill slope was calculated for each competition and displacement experiment in order to provide further information about the nature of the binding.

### **2.1.5 Materials and Chemicals**

Cell culture plastics were supplied by Falcon. DMEM with sodium pyruvate, foetal bovine serum, L-glutamine, penicillin, streptomycin and trypsin/EDTA were purchased from Gibco Life Technologies (Paisley, Scotland); Phenylephrine HCl, adrenaline, noradrenaline, HEPES and EDTA were purchased from Sigma (Dorset, UK); The (*R*)-enantiomer of A-61603 was a gift from Dr Michael Meyer (Abbott Laboratories, Abbott Park, IL); L-765314 was a gift from Dr Michael Patane (Merck & Co. Inc, NJ); RS100329 (Dr. Michelson, Roche Bioscience, Palo Alto, CA); Phentolamine, QAPB, prazosin HCl, BMY7378 dihydrochloride from Research Biochemicals Inc. (Natick, MA); [<sup>3</sup>H]Prazosin (0.2nM; specific activity, 76 Ci/mmol) was ordered from Amersham Corp. (Arlington Heights, IL)

Stock solutions for each chemical were prepared in distilled water or dimethyl sulfoxide and subsequently aliquoted and stored at -20°C. These stock solutions were diluted to working concentrations in the physiological salt solution on each experimental day.

## 2.2 RESULTS

### 2.2.1 Competitive Inhibition of Radioligand Binding.

#### 2.2.1.1 Membranes.

The binding affinities ( $pK_i$ ) of various ligands for the bovine  $\alpha_{1a}$ -AR were first assessed in standard membrane preparation assays versus [ $^3$ H]prazosin (Table 2.1). This is the common method used to determine  $\alpha_1$ -AR affinity (Kenny *et al*, 1996). All incubation times were a standard 30 minutes at room temperature (22°C) unless stated otherwise. Non-specific binding was determined in the presence of phentolamine (10  $\mu$ M)

Binding affinities for the non-subtype selective  $\alpha_1$ -AR agonist phenylephrine were determined in the presence and absence of the non-hydrolysable GTP analogue GTP- $\gamma$ -S (0.25mM). In the presence of GTP- $\gamma$ -S, the curve was monophasic with one low affinity component ( $pK_i = 5.6$ ) and a Hill coefficient close to unity. In the absence of GTP- $\gamma$ -S, the curve was biphasic with a high ( $pK_i = 7.9$ ) and low ( $pK_i = 5.2$ ) affinity component (Fig. 2.22). This biphasic behaviour is generally observed for agonist binding on isolated membranes in the absence of GTP due to a complex two-stage binding process (Bockaert *et al*, 1997).

The specific  $\alpha_{1a}$ -AR agonist (*R*)-A-61603 displayed a higher affinity for the  $\alpha_{1a}$ -ARs compared with phenylephrine in the presence and absence of GTP- $\gamma$ -S (0.25mM). In the presence of GTP- $\gamma$ -S, the curve was monophasic with one low affinity component ( $pK_i = 6.85$ ) and in the absence of GTP- $\gamma$ -S, the curve was biphasic with a high ( $pK_i = 10.26$ ) and low ( $pK_i = 6.82$ ) affinity component (Fig. 2.23) consistent with (*R*)-A-61603 being a high affinity agonist at  $\alpha_{1a}$ -AR binding sites.

The catecholamines noradrenaline and adrenaline displayed similar agonist profiles on membrane preparations (Fig. 2.24 & 2.25). For these two ligands, the incubation temperature was changed to 37°C in anticipation of subsequent experiments on binding to whole cells. The experiments were performed in the absence of GTP- $\gamma$ -S.

Both showed similar low affinity components with adrenaline displaying a slightly higher affinity ( $pK_i = 5.80$ ) than noradrenaline ( $pK_i = 5.05$ ).

The subtype selective  $\alpha_{1a}$ -AR antagonist RS100329 showed a high affinity by displacing specific [ $^3$ H]prazosin binding to  $\alpha_{1a}$ -AR membranes with a  $pK_i$  value of 9.63 (Fig. 2.5) and also displayed a small low affinity component ( $pK_i = 8.16$ ). The non-selective  $\alpha$ -AR antagonist prazosin displayed a lower affinity to  $\alpha_{1a}$ -AR membranes than RS100329 as shown previously (Fig. 2.3), with a  $pK_i$  value of 8.57 and a Hill coefficient close to unity. The fluorescent analogue of prazosin, BODIPY-FL prazosin (QAPB), is a non-subtype selective competitive antagonist at  $\alpha_1$ -AR binding sites. As expected, QAPB displayed a similar antagonist profile to prazosin (Fig. 2.4) with a slightly lower affinity ( $pK_i = 8.37$ ) and a Hill coefficient of unity. The subtype selective  $\alpha_{1b}$ -AR antagonist L-765314 displayed a lower affinity for  $\alpha_{1a}$ -AR membranes (Fig. 2.6) with a  $pK_i$  value of 6.29.

### **2.2.1.2 Whole Cells.**

The binding affinities for [ $^3$ H]prazosin sites of various agonist and antagonists were then assessed on whole-cell preparations (Table 2.2) harbouring the recombinant bovine  $\alpha_{1a}$ -AR as this is the modality in which visualisation of ligand-ligand competition is assessed. A specific group of binding experiments was also performed using the recombinant human  $\alpha_{1a}$ -AR.

Similarly to the membrane experiments, binding affinities for phenylephrine were determined in the presence and absence of GTP- $\gamma$ -S (0.25mM). In whole-cell preparations, curves should appear monophasic. As the high affinity binding state is not observed in the presence of GTP, all receptors in whole cells containing natural levels of GTP should be under the low affinity binding state. This was confirmed using phenylephrine (Fig. 2.26), which displayed a single low affinity component in the absence ( $pK_i = 4.97$ ) and presence ( $pK_i = 4.88$ ) of the GTP analogue. A comparison of phenylephrine membrane and whole-cell curves in the presence of GTP- $\gamma$ -S is shown in Figure 2.27.

In the absence of GTP- $\gamma$ -S, (*R*)-A-61603 displayed a biphasic curve (Fig. 2.28) with a high ( $pK_i = 8.25$ ) and low ( $pK_i = 5.85$ ) component. Interestingly, there was not a full displacement by (*R*)-A-61603 and approximately 25% of binding sites were not displaced from. To increase the probability of maximum displacement, the experiment was repeated with a longer incubation period of 2 hours at room temperature (Fig. 2.28). This longer incubation resulted in a full displacement and curve showing high ( $pK_i = 6.82$ ) and low ( $pK_i = 5.63$ ) components. Similarly to membrane experiments, these results showed (*R*)-A-61603 to be a specific agonist at  $\alpha_{1a}$ -AR binding sites. As the previous results had hinted at a time-dependant displacement, the next set of experiments using (*R*)-A-61603 in the presence of GTP- $\gamma$ -S were performed using various incubation times of 15, 30 and 120 minutes (Fig. 2.29). Contrary to the expected monophasic curves, each curve for separate incubations displayed both high and low affinity components and in a manner similar to previous results, there were approximately 25% of binding sites that had not been accessed.

Experiments using noradrenaline as the competing ligand were carried out for the standard incubation time of 30 minutes, but the temperature was changed to 37°C. Our early hypothesis regarding cell penetration by catecholamines was that it occurred via the extraneuronal monoamine transporter (EMT) (Grundemann *et al*, 1998). The EMT could deliver catecholamines to intracellular receptors. This transporter reportedly functions optimally at temperature 37°C. A comparison of incubation temperatures (22°C and 37°C) was the focus of an initial binding experiment using noradrenaline as the competing ligand (Fig. 2.30). Both curves were biphasic, displaying high and low affinity binding sites and  $pK_i$  values of similar value (Table 2.3). A comparison of noradrenaline binding profiles in membranes and whole-cells at incubation temperature 37°C is shown in Figure 2.31. To test the hypothesis that noradrenaline and other ligands may penetrate the cells via the EMT, binding experiments were performed (Fig. 2.32) in the presence of the Uptake<sub>2</sub> inhibitor corticosterone (1  $\mu$ M) (Iversen & Salt, 1970). The result was a high ( $pK_i = 7.72$ ) and low ( $pK_i = 4.24$ ) affinity component, but still almost a full displacement (Table 2.3). Although in the absence of corticosterone, the results presented a two-site binding curve, the curve did not appear as biphasic as the curve in the presence of

corticosterone. The initial high affinity component (25% of binding sites) was followed by a small plateau phase before the low affinity component (75% of binding sites). This could suggest an initial displacement from cell membranes and the plateau phase may represent a difficulty of the ligand to penetrate the cell. The low affinity phase would therefore represent the ability of ligands to displace the radiolabel from intracellular binding sites. This suggested corticosterone had little, if any effect. However, the biphasic effect of noradrenaline was particularly clear in the presence of corticosterone, so this deserves further investigation (see discussion).

In pursuit of the concept that the uptake of the ligand into the cell may occur in a time-dependant manner, the binding affinities for noradrenaline were determined by comparing an incubation time of 15 minutes with a 30-minute period (Fig. 2.33). This showed that a greater displacement occurred following the 30-minute incubation. The 30-minute incubation produced higher affinity values ( $pK_i = 6.71$  &  $4.42$ ) than those observed with a 15-minute incubation ( $pK_i = 5.81$  &  $3.94$ ) (Table 2.3).

Adrenaline displayed a low affinity by displacing specific [ $^3$ H]prazosin binding to  $\alpha_{1a}$ -AR whole cells with a  $pK_i$  value of 4.96 (Fig. 2.34 & Table 2.2). Interestingly, adrenaline produced a monophasic, one-site curve and a lower affinity value compared with noradrenaline. RS100329 again demonstrated a high affinity to  $\alpha_{1a}$ -AR whole cells with a  $pK_i$  value of 10.99 and also a low affinity value of 7.35 (Fig. 2.8 & Table 2.2). Similar to the phenomenon observed with the noradrenaline experiment in the presence of corticosterone, RS100329 high affinity component (approx. 20% of binding sites) was followed by a slow sustained plateau phase before the low affinity component (approx. 80% of binding sites), which again raised the possibility of a difficulty of cellular penetration.

Prazosin and QAPB were expected to display a similar binding profile for the displacement of [ $^3$ H]prazosin, but prazosin displayed a one-site affinity with a  $pK_i$  value of 8.72 (Fig. 2.7 & Table 2.2). The curve shows that prazosin has a similar profile in cells and in membrane preparations. This suggests that prazosin itself has no apparent difficulty penetrating the cell. QAPB is a light-sensitive compound and therefore a series of experiments were carried out under light and dark conditions to

test the effect of light on QAPB binding (Fig. 2.9). The binding affinity was almost identical under both circumstances, but a higher affinity value was observed under normal light conditions ( $pK_i = 9.94$ ) than in darkness ( $pK_i = 9.26$ ). Subsequent experiments with QAPB would be carried out under normal light conditions. A comparison of QAPB membrane and whole-cell curves under light conditions is shown in Figure 2.10. QAPB continued the trend of a high affinity component preceding a slow sustained plateau and low affinity component. A difficulty in cellular penetration for QAPB and not for prazosin could be caused by the size or chemical properties of the fluorescent component of the compound. The antagonist L-765314 also displayed a high ( $pK_i = 7.27$ ) and low affinity component ( $pK_i = 4.72$ ) separated by a plateau phase (Fig. 2.11 & Table 2.2). There was not full displacement, although the curve shows there would have been full displacement at higher concentrations of the antagonist. L-765314 had a much lower affinity than the other antagonists to  $\alpha_{1a}$ -AR whole cells consistent with its specificity for  $\alpha_{1b}$ -ARs (Patane *et al.*, 1998).

The binding affinities for [ $^3$ H]prazosin sites of the subtype selective  $\alpha_{1d}$ -AR antagonist BMY7378 were then assessed on membrane and whole-cell preparations harbouring the recombinant bovine  $\alpha_{1a}$ -AR and also the recombinant human  $\alpha_{1d}$ -AR (Fig. 2.12). BMY7378 displayed a lower affinity than prazosin, QAPB and RS100329 at bovine  $\alpha_{1a}$ -AR whole cells with a  $pK_i$  value of 6.36, but produced subnanomolar affinity ( $pK_i = 9.48$ ) for the displacement of [ $^3$ H]prazosin at human  $\alpha_{1d}$ -AR whole cells (Table 2.4).

### **2.2.2 New Radioligand Binding Protocol 1.**

A new series of protocols for competitive RLB experiments were devised that were slightly different from the 'classical' binding approach used for earlier experiments in the thesis. These earlier experiments allow competition between a test compound and [ $^3$ H]prazosin in which the test compound is given a few minutes before [ $^3$ H]prazosin and a period of 30 minutes is then allowed for equilibrium to be established. This assumes that there is equal access of test compound and [ $^3$ H]prazosin and that the two

compounds and the receptor come to equilibrium, with the extra few minutes for the test compound conferring no advantage. However, in whole cell experiments these conditions may not apply. Some receptors may be less accessible than others e.g. intracellular cf. cell surface and some ligands may penetrate cells more easily than others. Receptor location or other cell characteristics may be modified by the ligands. For those reasons, the timing and order of addition of competitive ligands may influence the final 'equilibrium'. Furthermore, in our experiments to visualise fluorescence binding and verify its properties with competing ligands, the compounds are given sequentially to allow comparison with and without a competitor. A new displacement protocol was therefore devised that would recreate a more 'real' context of visualisation experiments than in standard ligand-ligand competition. All non-specific binding was still determined in the presence of phentolamine (10  $\mu$ M).

Essentially cells are equilibrated with [ $^3$ H]prazosin and then competitors are added for a further period. This means that competitors must displace [ $^3$ H]prazosin from its pre-equilibrated location(s). The first set of new experiments was performed with noradrenaline as the displacing ligand on bovine  $\alpha_{1a}$ -AR whole cells. The cells and [ $^3$ H]prazosin were incubated together at room temperature (22°C) for varying time periods of 15, 30 and 60 minutes before noradrenaline was added at a range of concentrations and left to incubate at 37°C for a fixed time period of 60 minutes before reaction termination. The hypothesis was that 60 minutes would provide sufficient time for [ $^3$ H]prazosin equilibrium binding to whole cells as opposed to 15 or 30 minutes (Fig. 2.35). There was a greater displacement by noradrenaline after cells have been left to incubate with the radiolabel for 60 minutes. The three time courses provided results with high and low affinity components and similar binding affinities (Table 2.5). A comparison of noradrenaline binding curves using the 'classical' and new RLB approaches are shown in Figure 2.36. When [ $^3$ H]prazosin binding was pre-established (new protocol), noradrenaline was less effective at displacing it.

### **2.2.3 New Radioligand Binding Protocol 2.**

After devising a new RLB displacement protocol as previously explained, this protocol was expanded to provide a more consistent comparison with visualisation studies. Previous imaging experiments demonstrated that 60 minutes was sufficient time for [<sup>3</sup>H]prazosin binding to reach equilibrium to bovine  $\alpha_{1a}$ -AR whole cells both on cell surface and at intracellular binding sites. All subsequent experiments would now have a time course of 60 minutes at room temperature for the radiolabel to equilibrate with the cells before the displacing ligand was added.

As RS100329 had displayed a pronounced two-site biphasic response using the 'classical' RLB protocol, it was the subject of the first experiment using the updated displacement protocol. After a 60-minute equilibration between cells and radiolabel, RS100329 was applied for 30 minutes at a temperature of 22°C or 37°C. This was a test to determine if the incubation temperature had a direct effect on the ability of the ligand to displace the radiolabel. Altering the temperature had no effect on the total amount of <sup>3</sup>H-prazosin bound. Figure 2.13 shows that altering the temperature had very little effect on the ability of RS100329 to displace radiolabel. Subsequent experiments would be performed at 37°C as there was a marginally greater displacement at this temperature and since it was considered that any transport processes that might be involved would be more likely to be active at this temperature. Both curves were monophasic with a low affinity component (Table 2.6). The same experiment was repeated using QAPB as the competing ligand (Fig. 2.14 & Table 2.6). Similar to RS100329, there was a greater displacement at 37°C at the biphasic concentrations of ligand. Both curves were biphasic with a very high affinity site followed by a sustained plateau phase until 10<sup>-7</sup>M QAPB where a low affinity component was observed, reinforcing the concept that QAPB has difficulty penetrating the cells.

As equilibration between cells and radiolabel and incubation temperature for maximum displacement had been resolved, the next series of experiments was to determine if the displacement was time-dependant once the displacing ligand had been added.

The new protocol was first performed on bovine  $\alpha_{1a}$ -AR membranes, as the differences in incubation times should have made no difference to the displacement from the cell surface. Following incubation with adrenaline for 15, 30 and 60 minutes at 37°C, the three curves were almost superimposed and displayed similar one-site binding affinities (Fig. 2.37 & Table 2.7a). The same experiments were performed, but this time on bovine  $\alpha_{1a}$ -AR whole cells. There was a greater displacement at 30 minutes than after 15 minutes and a greater displacement than both these times after 60 minutes (Fig. 2.38). The displacement curves were biphasic with both high and low affinity  $pK_i$  values (Table 2.7a). This indicated a time-dependant implement to displacement of [ $^3$ H]prazosin by adrenaline.

To test the hypothesis that ligands may be entering cells and accessing intracellular binding sites via an EMT, a series of experiments was performed using the new displacement protocol in the presence of 1  $\mu$ M corticosterone. In the first set of experiments, corticosterone was present only after pre-equilibrium with [ $^3$ H]prazosin (Fig. 2.39). This would show if the corticosterone had a direct single effect on the ability of adrenaline to penetrate the cells. Adrenaline was used rather than noradrenaline, as the former is believed to be a better substrate for the EMT (Grundemann *et al.*, 1998). Both 15 and 30-minute incubation curves were monophasic with similar binding affinity values (Table 2.8), but the 60-minute incubation displacement curve showed both high and low affinity components, suggesting that corticosterone may have a small effect after a certain period of time, but there was still a near maximum displacement. To determine if corticosterone had any effect on the uptake of [ $^3$ H]prazosin into cells, the experiment was repeated where the whole experiment was carried out in the presence of corticosterone (Fig. 2.40). All displacement curves were monophasic, demonstrating a near maximum displacement and similar  $pK_i$  binding values (Table 2.8). This confirmed that corticosterone had no effect on the ability of adrenaline to displace from intracellular binding sites. Data also showed that  $^3$ H-prazosin uptake was not reduced by corticosterone.

A second hypothesised mechanism by which ligands might penetrate cells is via an endocytotic pathway. This was tested using an endocytotic blocker concanavalin A.

In a series of experiments similar to the first set performed with corticosterone, the equilibrium between cells and [<sup>3</sup>H]prazosin was established in the absence of concanavalin A. Con A (0.25 mg/ml) was added at the same time as adrenaline and left for 30 minutes at 37°C to determine whether endocytosis was directly responsible for adrenaline uptake into the cell (Fig. 2.41). To determine if concanavalin A had any effect on the uptake of [<sup>3</sup>H]prazosin into cells, the experiment was repeated where the whole experiment was carried out in the presence of concanavalin A (Fig. 2.41). Both sets of experiments produced biphasic displacement curves with high and low affinity pK<sub>i</sub> values (Table 2.9) and a near maximum displacement. This confirmed that concanavalin A was having little or no effect. The same experiment was performed with QAPB as the displacing ligand. The whole experiment was performed in the presence of concanavalin A. The binding curve was monophasic with a pK<sub>i</sub> value of 7.71 (Table 2.12). Surprisingly, there was a full displacement by QAPB (Fig. 2.17). There appears to be difficulty of cellular penetration until 10<sup>-8</sup>M QAPB when there was a pronounced fall in the binding curve. Using GraphPad Prism statistical analysis, an F test showed the binding curve changed from biphasic in the absence of concanavalin A to monophasic in the presence of concanavalin A. In the absence of concanavalin A, the F ratio was 12.98 and had a p value of 0.0002. In the presence of concanavalin A, the F ratio was 0.43 and had a p value of 0.66. Using the F-test (as described in the data analysis section), a two-site model is only accepted when the F ratio is much greater than 1 and produces a p value of <0.05. This suggests that concanavalin A may be exerting an inhibiting effect that can be overcome once a certain concentration of QAPB is applied. Comparing the amount of radiolabel bound for both protocols, there is more <sup>3</sup>H-prazosin bound when half the experiment is performed in the presence of concanavalin A, as opposed to the whole experiment in concanavalin A. This would be expected, as it shows that concanavalin A is exerting a small inhibiting effect on the uptake of <sup>3</sup>H-prazosin.

An identical series of experiments to those using adrenaline (Figs. 2.37 & 2.38) was performed on bovine α<sub>1a</sub>-AR membranes and whole cells using noradrenaline as the displacing ligand. As with adrenaline, the noradrenaline displacement curves were monophasic and superimposed on top of each other in membrane preparations (Fig. 2.42 & Table 2.7a). In whole cells, the curves displayed both high and low affinity

components (Fig. 2.43 & Table 2.7a). There was a greater displacement at 30 minutes than after 15 minutes and a greater displacement than both these times after 60 minutes. A similar protocol was followed with a series of other displacing ligands on whole cells. Phenyneprine displayed an unusual set of results in that a 15-minute incubation provided the greatest displacement. The most clearly biphasic curve was observed after 30 minutes (Fig. 2.44 & Table 2.7b). A biphasic displacement curve was also observed with (*R*)-A-61603 (Fig. 2.45). The phenomenon of approximately 20-25% of binding sites being inaccessible to (*R*)-A-61603 was similar to that found with previous experiments (Fig. 2.28). Inspection of the curve shows that a maximum displacement might have been achieved given higher concentrations of the agonist. After a 30-minute displacement period, (*R*)-A-61603 again displayed a high affinity for the  $\alpha_{1a}$ -AR (Table 2.7b). Both phenylephrine and (*R*)-A-61603 had displayed a difficulty in penetrating the cell. The earlier trend continued where the initial high affinity component may represent a displacement from the cell surface and the plateau phase represents a difficulty of the ligand to penetrate the cell.

Prazosin was used as the displacing ligand using the new displacement protocol on both bovine  $\alpha_{1a}$ -AR membranes and whole cells (Fig. 2.15). After 30 minutes displacement, prazosin had penetrated the cell and displayed a monophasic binding curve and  $pK_i$  value of 7.18 (Table 2.7a). Both L-765314 (Fig. 2.20) and BMY7378 (Fig. 2.21) displayed a much lower affinity at  $\alpha_{1a}$ -ARs compared with the other antagonists as expected, but after 30-minute displacement periods, both the antagonists showed single site components (Table 2.7b) with Hill coefficients close to unity. This demonstrated that both these antagonists had an apparent ease in penetrating the cell. BMY7378 did show a slightly higher affinity ( $pK_i = 6.39$ ) than L-765314 ( $pK_i = 5.48$ ).

The next set of experiments involved altering the incubation time between the  $\alpha_{1a}$ -AR cells and [ $^3$ H]prazosin. Figure 2.16 shows two sets of experiments where one protocol had the cells incubating with the radiolabel at room temperature for 60 minutes and the other for 90 minutes. QAPB was the displacing ligand and was left for 60 minutes at room temperature before terminating the reaction. The curve with a first incubation time of 60 minutes was more monophasic with a  $pK_i$  of 6.63 (Table

2.10) and there was not a full displacement with approximately 30% of binding sites unaccounted for. The curve with a first incubation time of 90 minutes was clearly biphasic with high ( $pK_i = 11.01$ ) and low ( $pK_i = 7.54$ ) affinity components.

### ***2.2.4 New Radioligand Binding Protocol 3.***

The updated radioligand binding protocol was further expanded to determine the effect cold temperature had on displacement from whole cells and membranes. The  $\alpha_{1a}$ -AR cells or membranes were pre-incubated with [ $^3\text{H}$ ]prazosin for one hour at room temperature. The displacing ligand was then added for 15 or 60 minutes at 4°C. If displacing ligands do penetrate cells and access intracellular compartments by endocytosis, they should fail to penetrate cells at 4°C as a result of the endocytotic mechanism being halted by cold temperatures. In whole cells preparations, noradrenaline (Fig. 2.46) and QAPB (Fig. 2.18) displayed similar curves, with only approximately 25% of all sites displaced. There is a marginally greater displacement after 60 minutes using noradrenaline. This would suggest that the 25% of displaced sites might represent cell surface receptors. However, a full displacement by noradrenaline (Fig. 2.47) and QAPB (Fig. 2.19) was not observed in membranes. Following addition of displacing ligand, an incubation time of 15 minutes (Fig. 2.19) or 60 minutes (Fig. 2.47) caused only an approximate 15% displacement. QAPB displayed a higher affinity at  $\alpha_{1a}$ -AR whole cells and membranes than noradrenaline (Table 2.11).

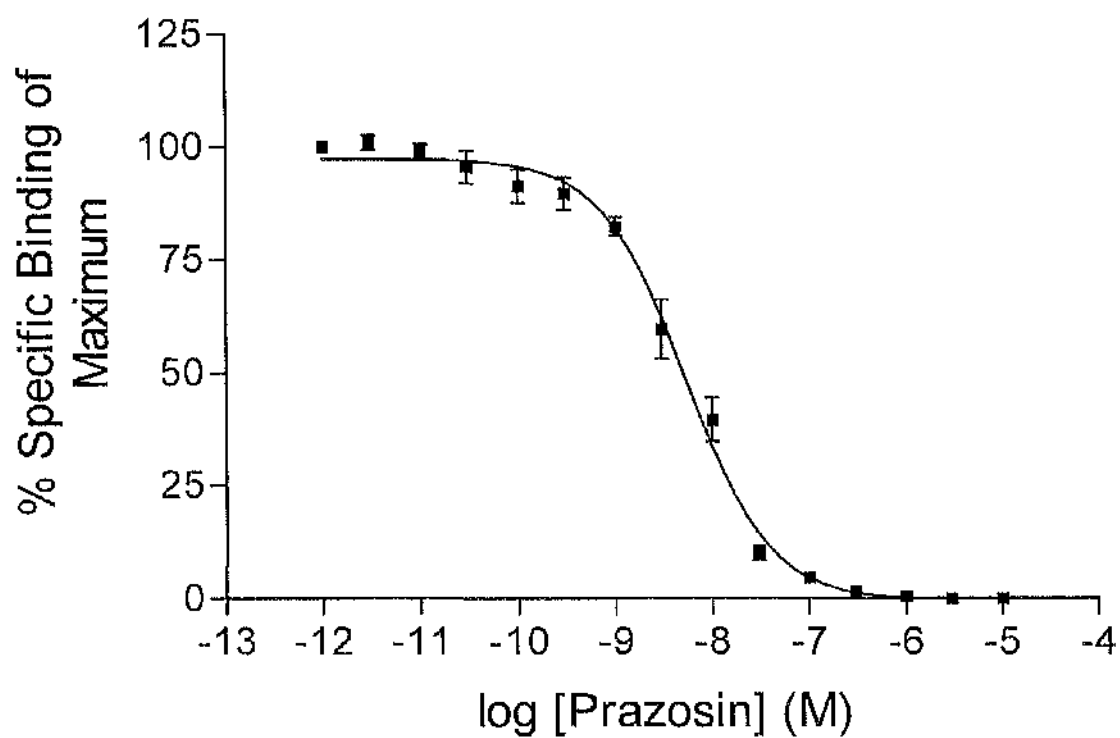


**Figure 2.3** Displacement of 0.2 nM [<sup>3</sup>H]prazosin binding to bovine  $\alpha_{1a}$ -AR membranes by increasing concentrations of prazosin. Non-specific binding was determined in the presence of 10  $\mu$ M phentolamine. Values are the mean ( $\pm$  S.E.) of four experiments performed in duplicate.

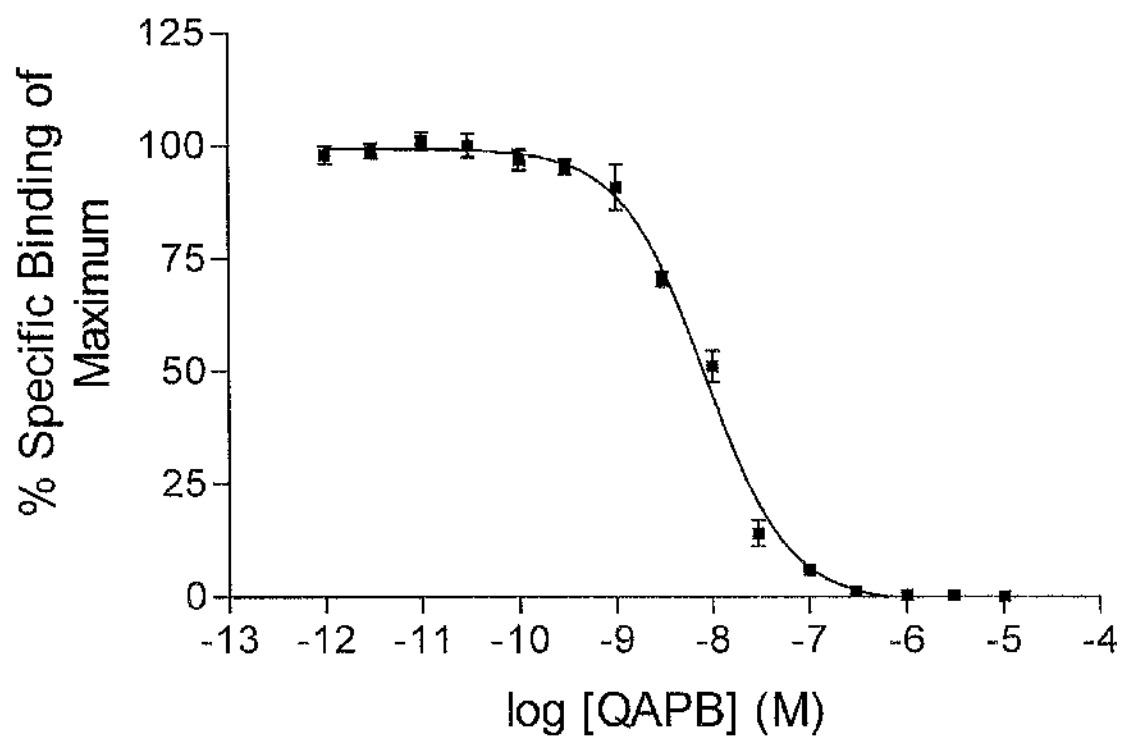


**Figure 2.4** Displacement of 0.2 nM [<sup>3</sup>H]prazosin binding to bovine  $\alpha_{1a}$ -AR membranes by increasing concentrations of QAPB. Non-specific binding was determined in the presence of 10  $\mu$ M phentolamine. Values are the mean ( $\pm$  S.E.) of four experiments performed in duplicate.

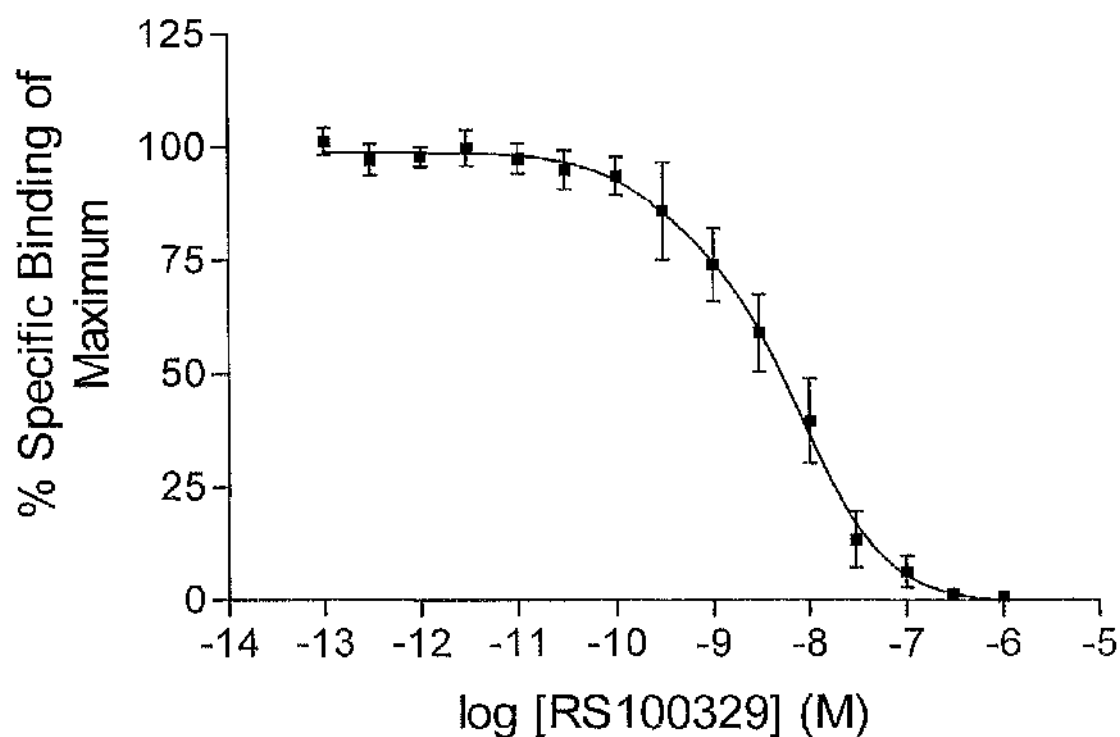


**Figure 2.5** Displacement of 0.2 nM [ $^3\text{H}$ ]prazosin binding to bovine  $\alpha_{1a}$ -AR membranes by increasing concentrations of RS100329. Non-specific binding was determined in the presence of 10  $\mu\text{M}$  phentolamine. Values are the mean ( $\pm$  S.E.) of five experiments performed in duplicate.

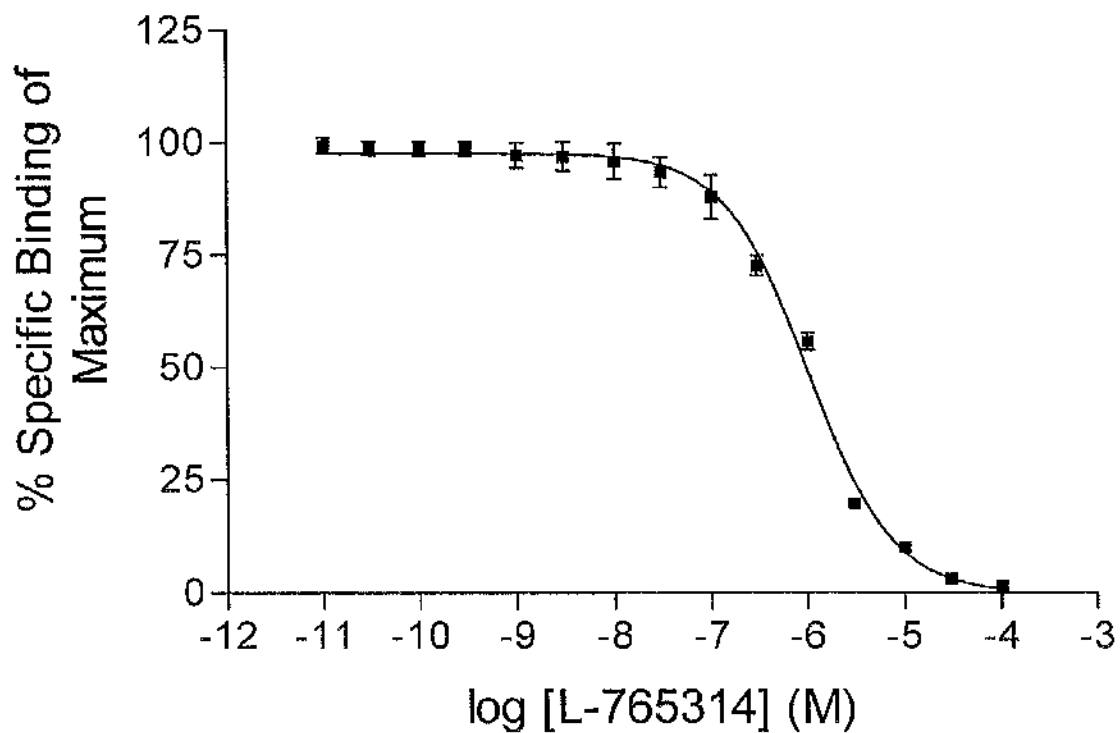


**Figure 2.6** Displacement of 0.2 nM [<sup>3</sup>H]prazosin binding to bovine  $\alpha_{1a}$ -AR membranes by increasing concentrations of L-765314. Non-specific binding was determined in the presence of 10  $\mu$ M phentolamine. Values are the mean ( $\pm$  S.E.) of four experiments performed in duplicate.

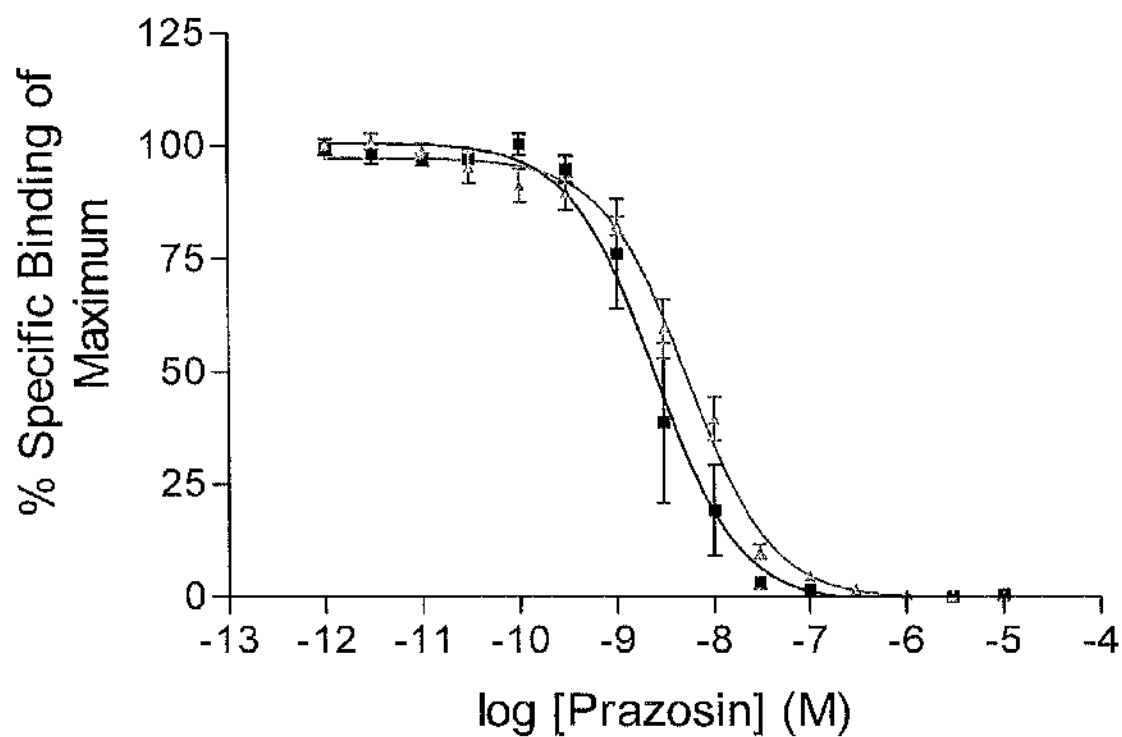


**Figure 2.7** Displacement of 0.2 nM [<sup>3</sup>H]prazosin binding to bovine  $\alpha_{1a}$ -AR (■) whole cells and (△) membranes by increasing concentrations of prazosin. Non-specific binding was determined in the presence of 10  $\mu$ M phentolamine. Values are the mean ( $\pm$  S.E.) of (■) four and (△) four experiments performed in duplicate.

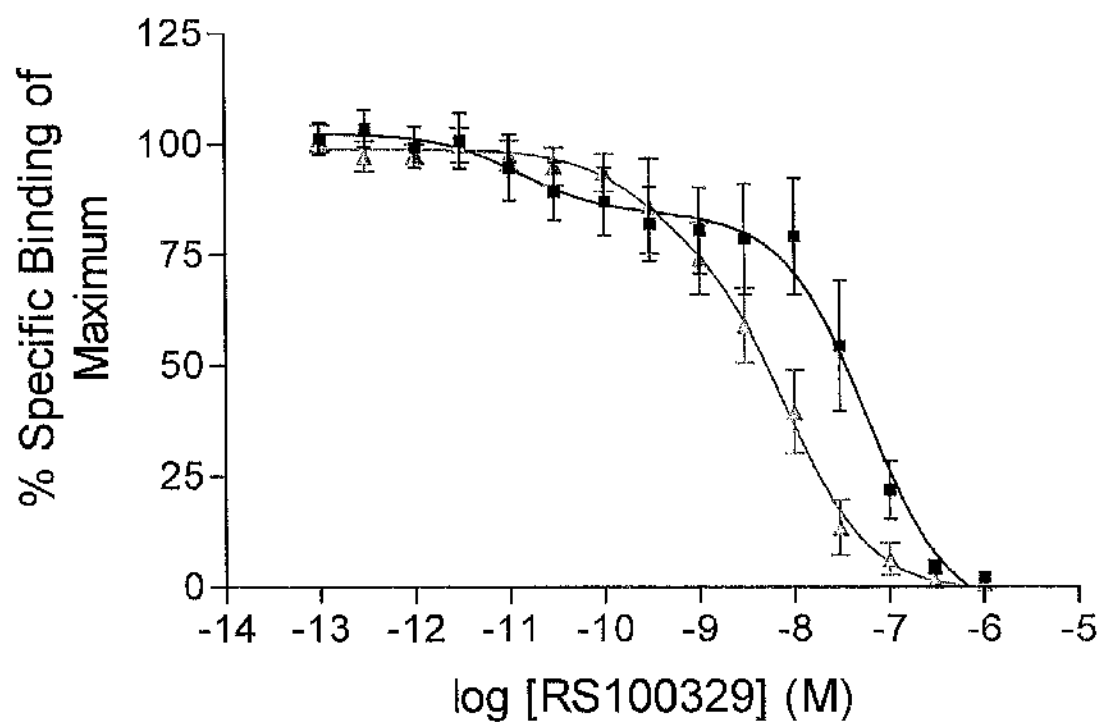


**Figure 2.8** Displacement of 0.2 nM [<sup>3</sup>H]prazosin binding to bovine  $\alpha_{1a}$ -AR (■) whole cells and (△) membranes by increasing concentrations of RS100329. Non-specific binding was determined in the presence of 10  $\mu$ M phentolamine. Values are the mean ( $\pm$  S.E.) of (■) four and (△) five experiments performed in duplicate.

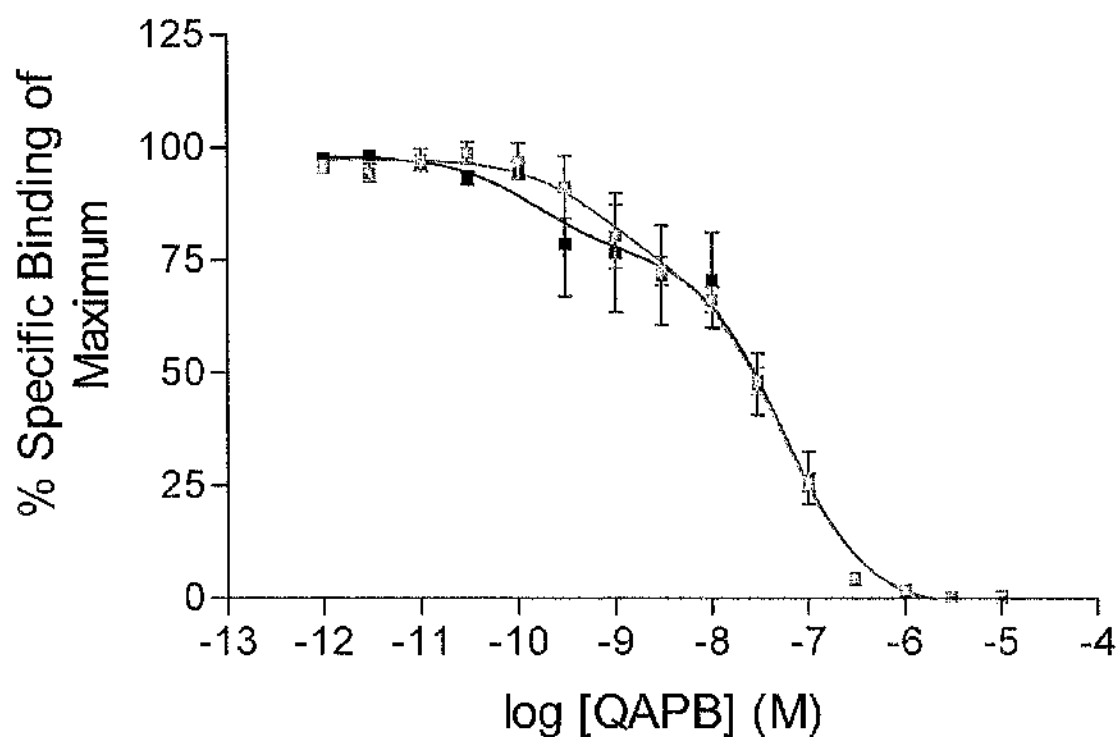


**Figure 2.9** Displacement of 0.2 nM [<sup>3</sup>H]prazosin binding to bovine  $\alpha_{1a}$ -AR whole cells by increasing concentrations of QAPB in (■) light surroundings and (□) dark surroundings. Non-specific binding was determined in the presence of 10  $\mu$ M phentolamine. Values are the mean ( $\pm$  S.E.) of (■) four and (□) four experiments performed in duplicate.

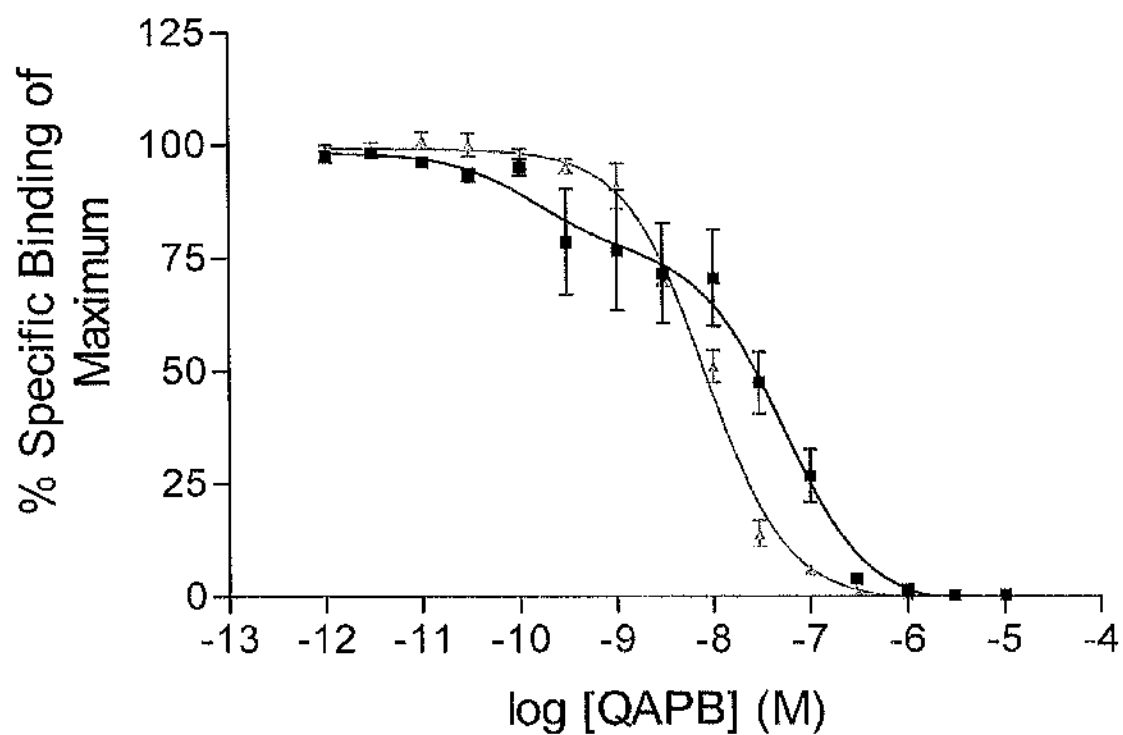


**Figure 2.10** Displacement of 0.2 nM [<sup>3</sup>H]prazosin binding to bovine  $\alpha_{1a}$ -AR (■) whole cells and (△) membranes by increasing concentrations of QAPB. Non-specific binding was determined in the presence of 10  $\mu$ M phentolamine. Values are the mean ( $\pm$  S.E.) of (■) four and (△) four experiments performed in duplicate.

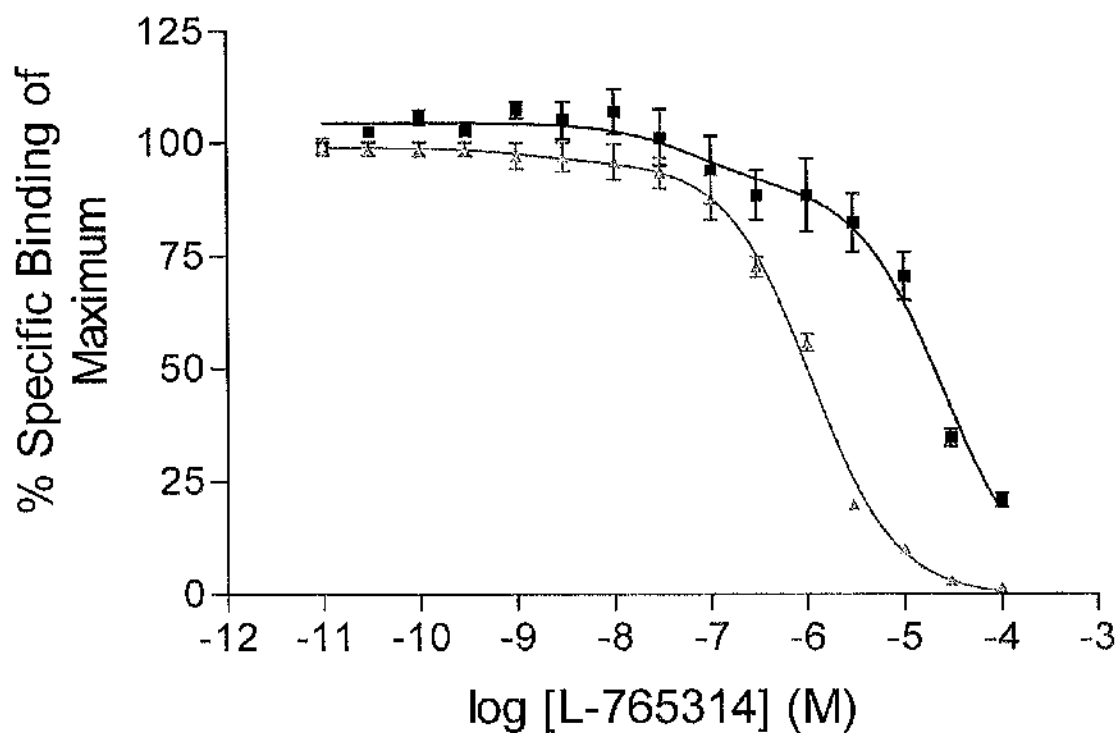


**Figure 2.11** Displacement of 0.2 nM [<sup>3</sup>H]prazosin binding to bovine  $\alpha_{1a}$ -AR (■) whole cells and (△) membranes by increasing concentrations of L-765314. Non-specific binding was determined in the presence of 10  $\mu$ M phentolamine. Values are the mean ( $\pm$  S.E.) of (■) five and (△) four experiments performed in duplicate.

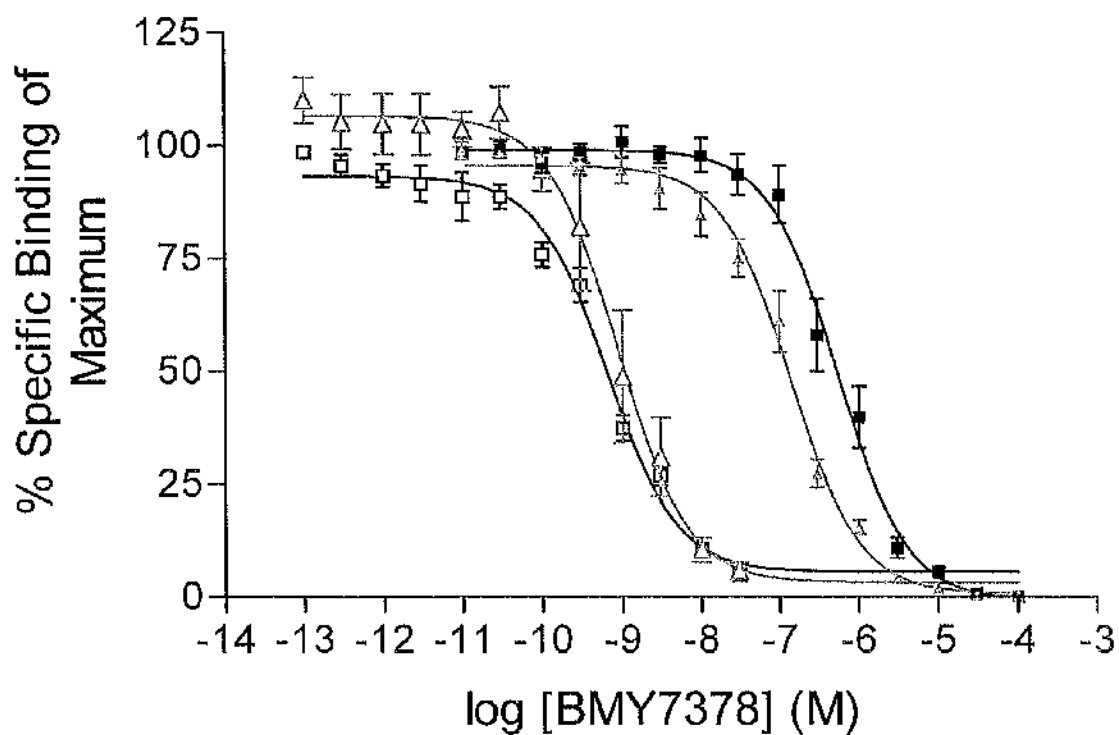


**Figure 2.12** Displacement of 0.2 nM [ $^3$ H]prazosin binding to bovine  $\alpha_{1a}$ -AR (■) whole cells, ( $\Delta$ ) membranes and to human  $\alpha_{1d}$ -AR (□) whole cells and ( $\Delta$ ) membranes by increasing concentrations of BMY7378. Non-specific binding was determined in the presence of 10  $\mu$ M phentolamine. Values are the mean ( $\pm$  S.E.) of (■) four, ( $\Delta$ ) four, (□) four and ( $\Delta$ ) six experiments performed in duplicate.

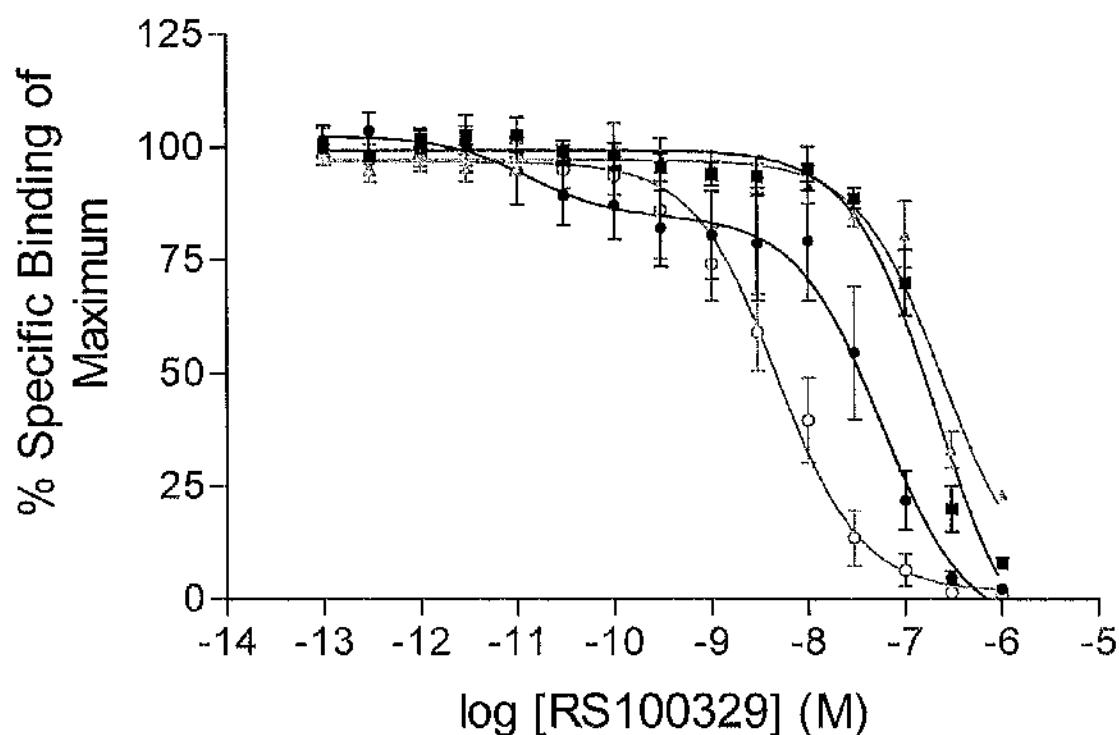


**Figure 2.13** Comparison of radioligand binding protocols using RS100329 as the competing/displacing ligand. Displacement of 0.2 nM [<sup>3</sup>H]prazosin binding to bovine  $\alpha_{1a}$ -AR whole cells by increasing concentrations of RS100329 using an updated radioligand binding protocol. Both second incubations were 30 minutes at a temperature of (■) 37°C and (△) 22°C. Also shown is the displacement of 0.2 nM [<sup>3</sup>H]prazosin binding to bovine  $\alpha_{1a}$ -AR (□) whole cells and (○) membranes by increasing concentrations of RS100329 using the standard radioligand binding protocol. Non-specific binding was determined in the presence of 10  $\mu$ M phentolamine. Values are the mean ( $\pm$  S.E.) of (■) three, (△) three, (□) four and (○) five experiments performed in duplicate.

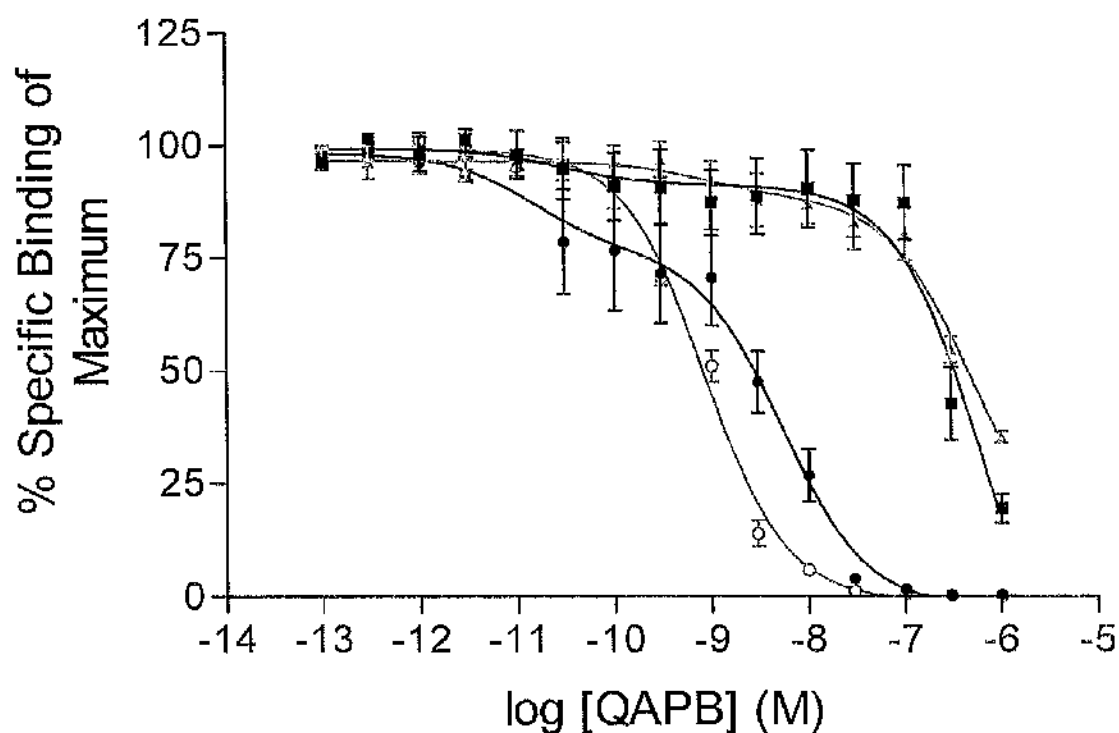


**Figure 2.14** Comparison of radioligand binding protocols using QAPB as the competing/displacing ligand. Displacement of 0.2 nM [<sup>3</sup>H]prazosin binding to bovine  $\alpha_{1a}$ -AR whole cells by increasing concentrations of QAPB using an updated radioligand binding protocol. Both second incubations were 30 minutes at a temperature of (■) 37°C and (△) 22°C. Also shown is the displacement of 0.2 nM [<sup>3</sup>H]prazosin binding to bovine  $\alpha_{1a}$ -AR (■) whole cells and (○) membranes by increasing concentrations of QAPB using the standard radioligand binding protocol. Non-specific binding was determined in the presence of 10  $\mu$ M phentolamine. Values are the mean ( $\pm$  S.E.) of (■) four, (△) four, (●) four and (○) four experiments performed in duplicate.

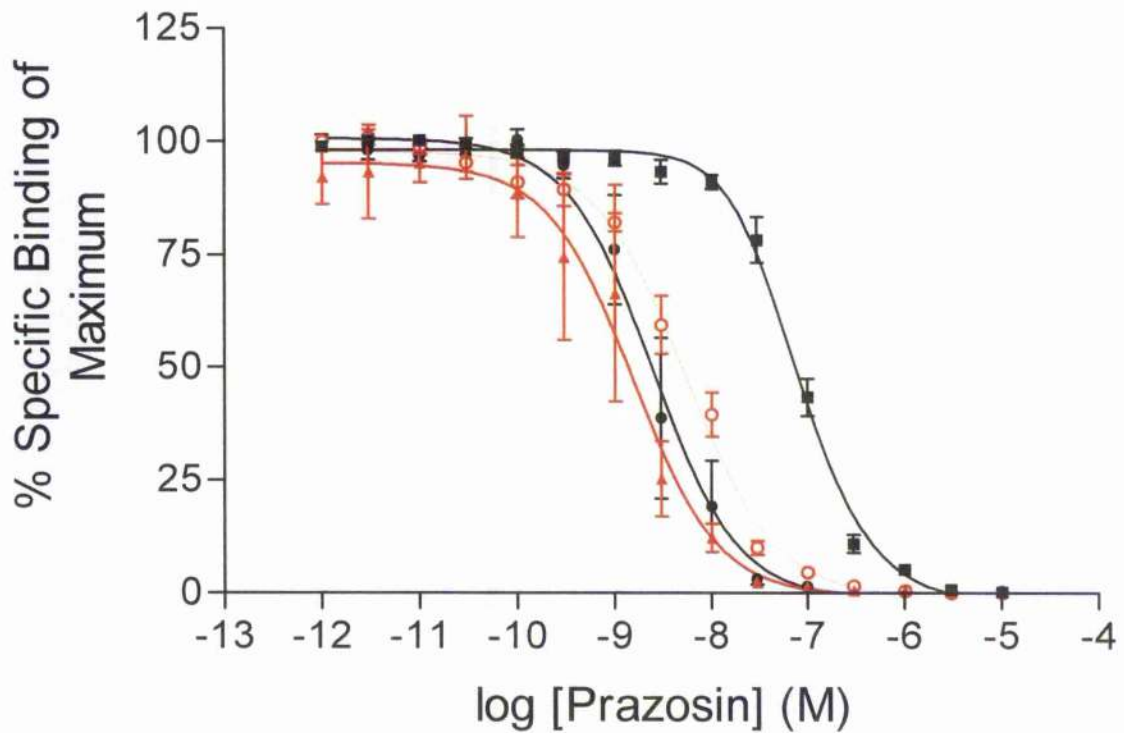


**Figure 2.15** Comparison of radioligand binding protocols using prazosin as the competing/displacing ligand. Displacement of 0.2 nM [<sup>3</sup>H]prazosin binding to bovine  $\alpha_{1a}$ -AR whole cells by increasing concentrations of prazosin using an (■) updated and (□) standard radioligand binding protocol and in membranes using an (▲) updated and (△) standard radioligand binding protocol. Both second incubations were 30 minutes at a temperature of 37°C for the updated protocol. Non-specific binding was determined in the presence of 10  $\mu$ M phentolamine. Values are the mean ( $\pm$  S.E.) of (■) four, (▲) two, (□) four and (△) four experiments performed in duplicate.

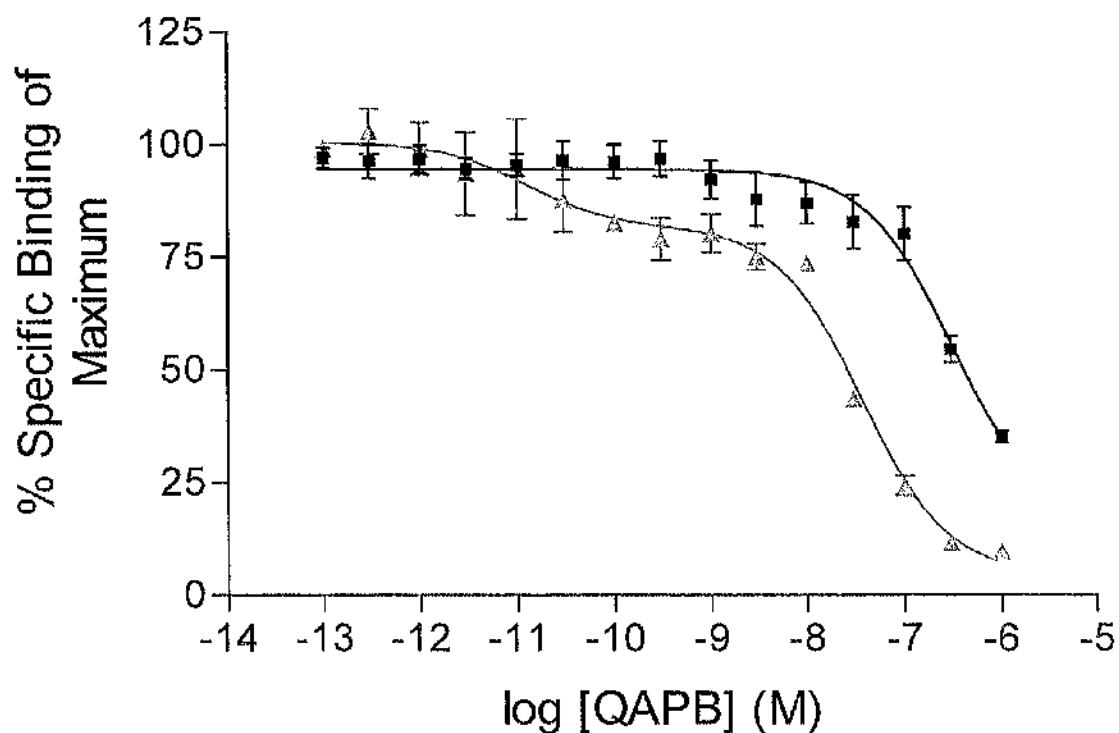


**Figure 2.16** Displacement of 0.2 nM [<sup>3</sup>H]prazosin binding to bovine  $\alpha_{1a}$ -AR whole cells by increasing concentrations of QAPB using an updated radioligand binding protocol. First incubation time was (■) 60 and (△) 90 minutes at a temperature of 22°C. Second incubation time was 60 minutes at a temperature of 22°C. Non-specific binding was determined in the presence of 10  $\mu$ M phentolamine. Values are the mean ( $\pm$  S.E.) of (■) four and (△) two experiments performed in duplicate.

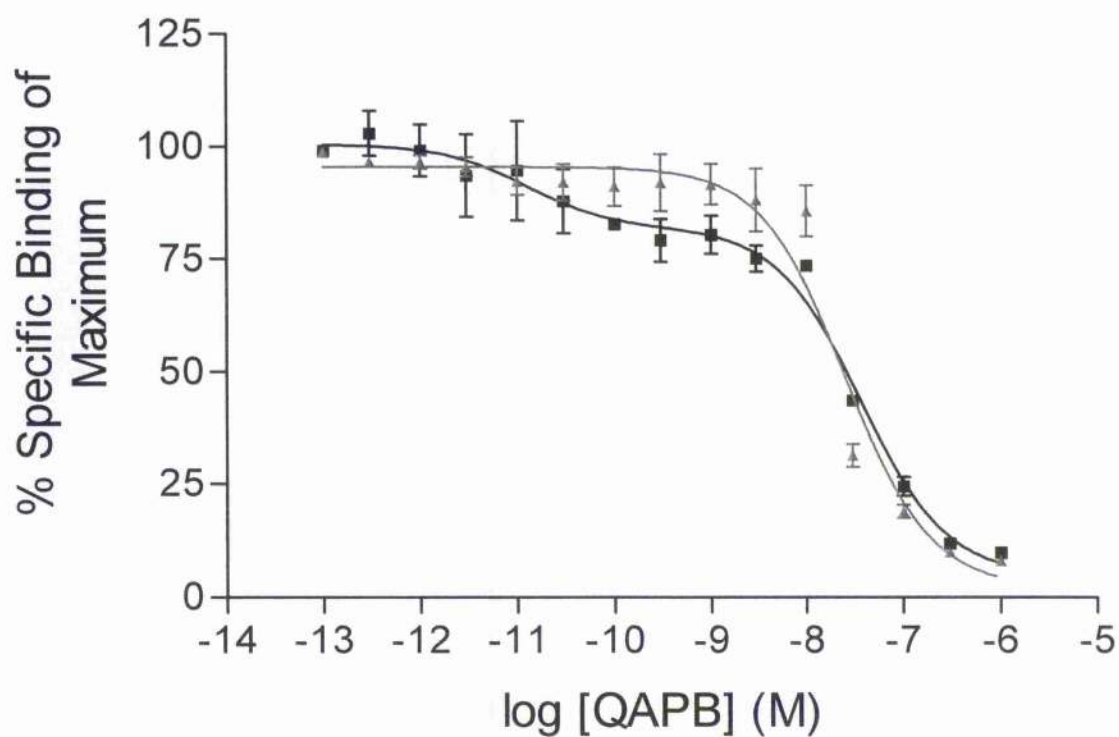


**Figure 2.17** Displacement of 0.2 nM [<sup>3</sup>H]prazosin binding to bovine  $\alpha_{1a}$ -AR whole cells by increasing concentrations of QAPB using an updated radioligand binding protocol in the (●) presence and (■) absence of 0.25mg/ml concanavalin A. Second incubation time was 60 minutes at a temperature of 22°C. Non-specific binding was determined in the presence of 10  $\mu$ M phentolamine. Values are the mean ( $\pm$  S.E.) of four (●) and (■) four experiments performed in duplicate.

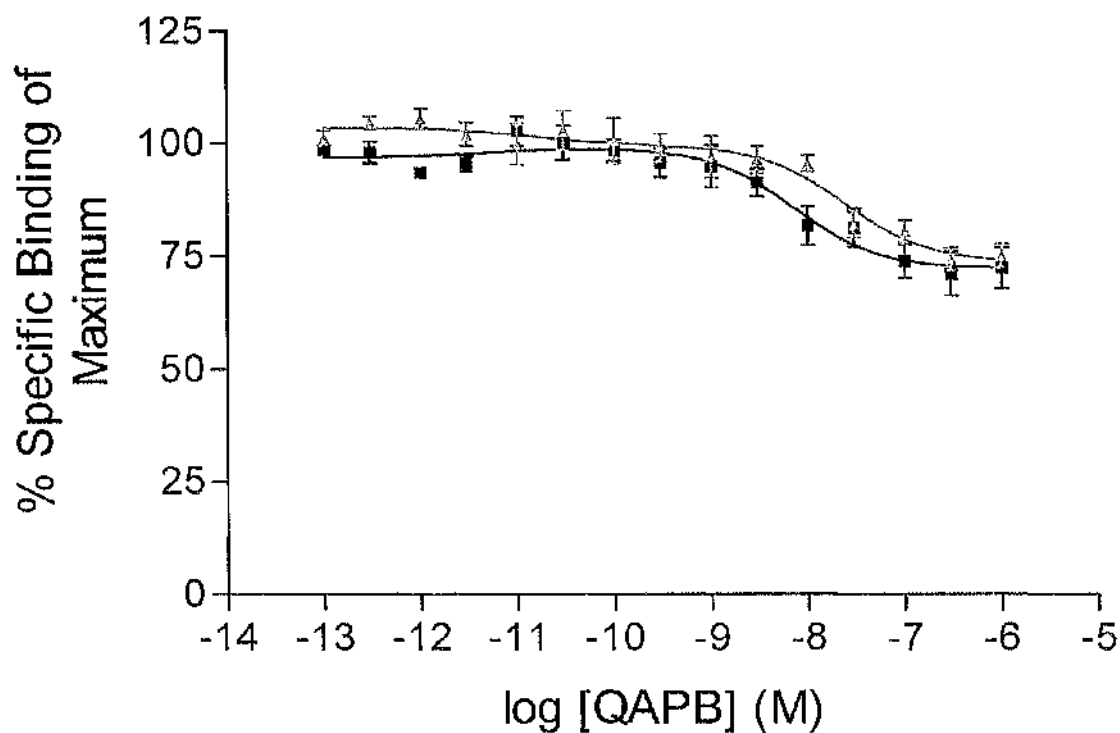


**Figure 2.18** Effect of cold temperature on displacement of 0.2 nM [<sup>3</sup>H]prazosin binding to bovine  $\alpha_{1a}$ -AR whole cells by increasing concentrations of QAPB using an updated radioligand binding protocol. Second incubation time was (■) 15 and (△) 60 minutes at a temperature of 4°C. Non-specific binding was determined in the presence of 10  $\mu$ M phentolamine. Values are the mean ( $\pm$  S.E.) of (■) four and (△) four experiments performed in duplicate.

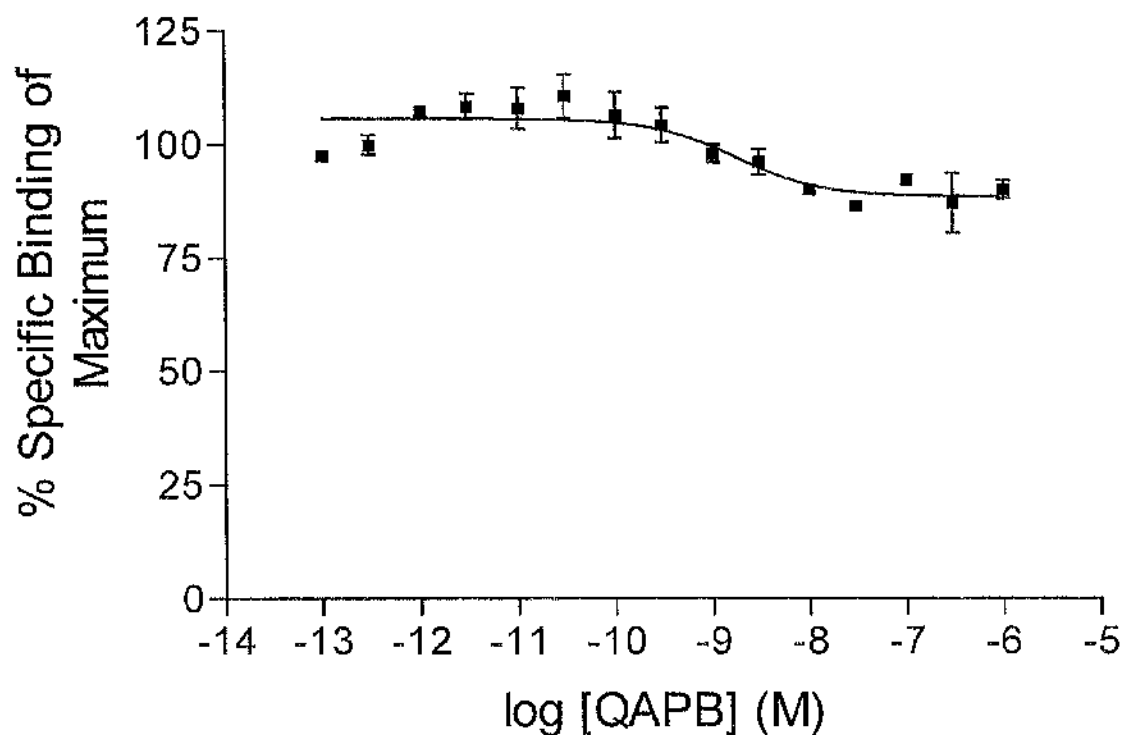


**Figure 2.19** Effect of cold temperature on displacement of 0.2 nM [<sup>3</sup>H]prazosin binding to bovine  $\alpha_{1a}$ -AR membranes by increasing concentrations of QAPB using an updated radioligand binding protocol. Second incubation time was 15 minutes at a temperature of 4°C. Non-specific binding was determined in the presence of 10  $\mu$ M phentolamine. Values are the mean ( $\pm$  S.E.) of two experiments performed in duplicate.

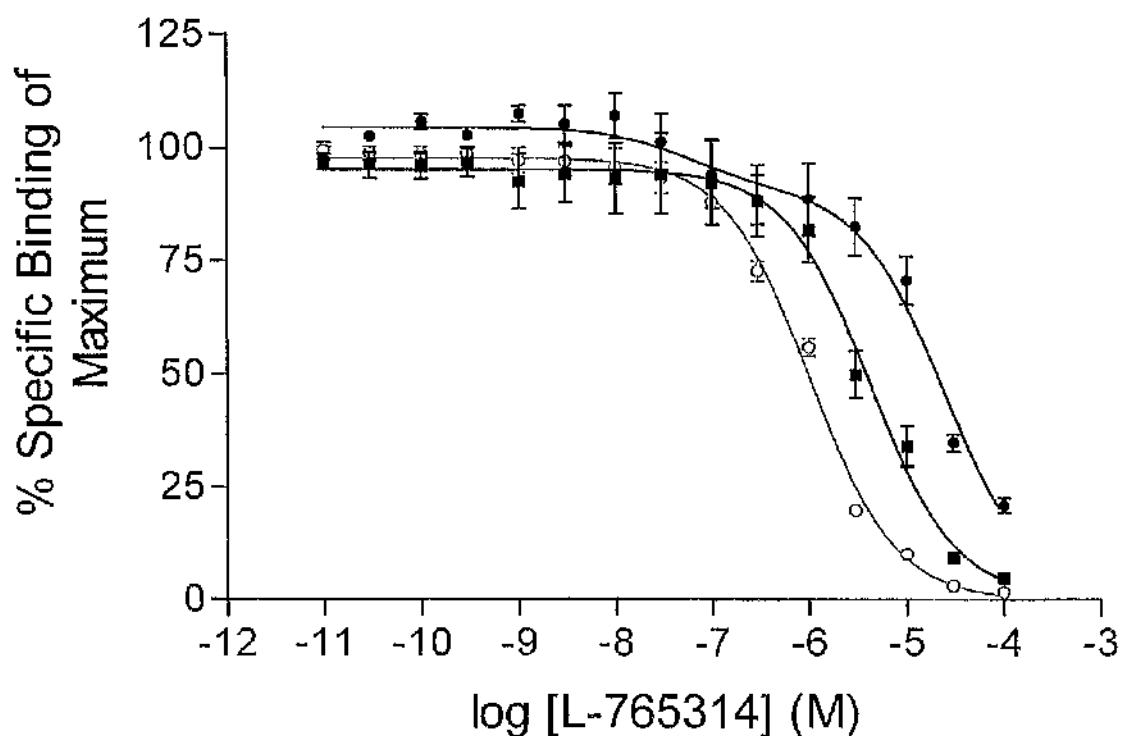


**Figure 2.20** Displacement of 0.2 nM [<sup>3</sup>H]prazosin binding to bovine  $\alpha_{1a}$ -AR whole cells by increasing concentrations of L-765314 using a (○) standard and (■) updated radioligand binding protocol. Membrane data is also shown (□) for standard binding protocol. Second incubation time was 30 minutes at a temperature of 37°C for updated protocol. Non-specific binding was determined in the presence of 10  $\mu$ M phentolamine. Values are the mean ( $\pm$  S.E.) of (■) five, (□) five and (○) four experiments performed in duplicate.

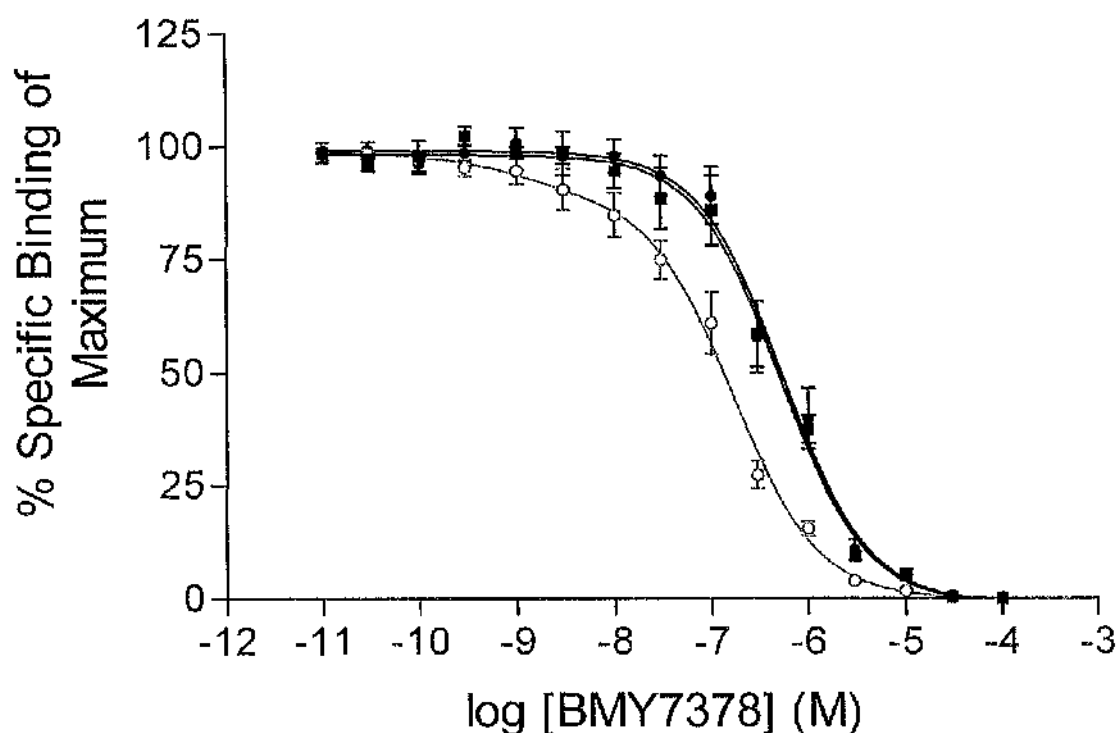


**Figure 2.21** Displacement of 0.2 nM [<sup>3</sup>H]prazosin binding to bovine  $\alpha_{1a}$ -AR whole cells by increasing concentrations of BMY7378 using a (□) standard and (■) updated radioligand binding protocol. Membrane data is also shown (○) for standard binding protocol. Second incubation time was 30 minutes at a temperature of 37°C for updated protocol. Non-specific binding was determined in the presence of 10  $\mu$ M phentolamine. Values are the mean ( $\pm$  S.E.) of (■) four, (□) four and (○) four experiments performed in duplicate.

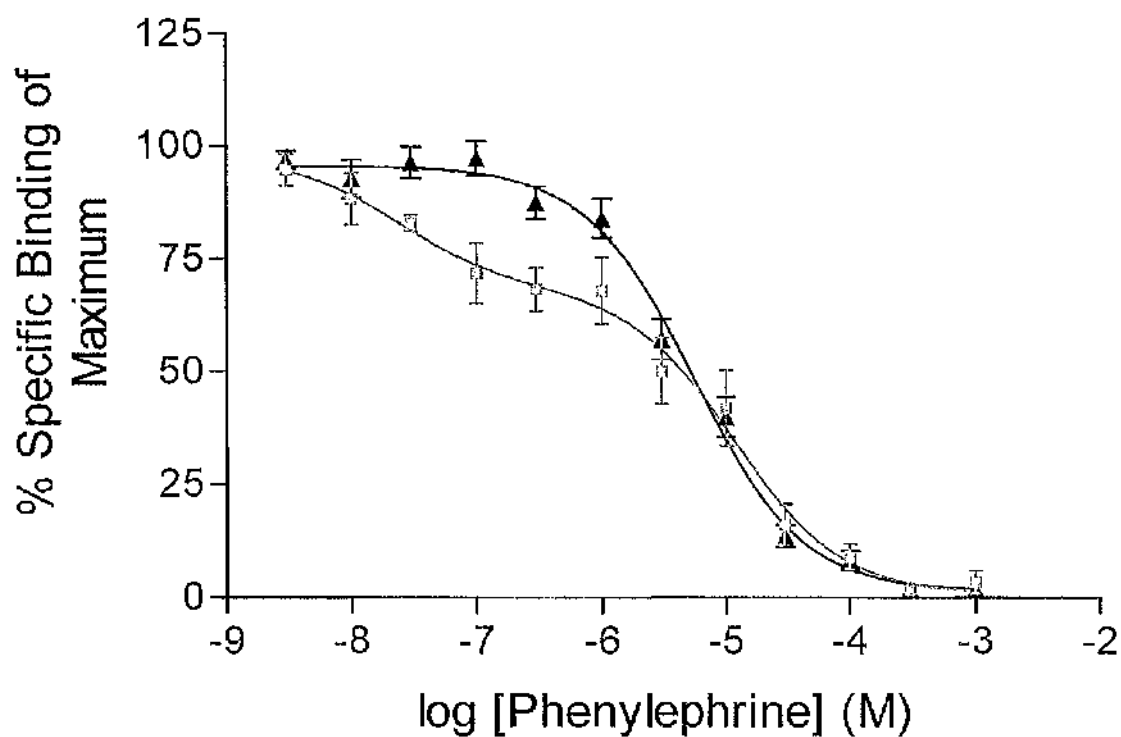


**Figure 2.22** Displacement of 0.2 nM [ $^3\text{H}$ ]prazosin binding to bovine  $\alpha_{1a}$ -AR membranes by increasing concentrations of phenylephrine in the (▲) presence of and (□) absence of 0.25 mM GTP- $\gamma$ -S. Non-specific binding was determined in the presence of 10  $\mu\text{M}$  phentolamine. Values are the mean ( $\pm$  S.E.) of (▲) six experiments and (□) three experiments performed in duplicate.

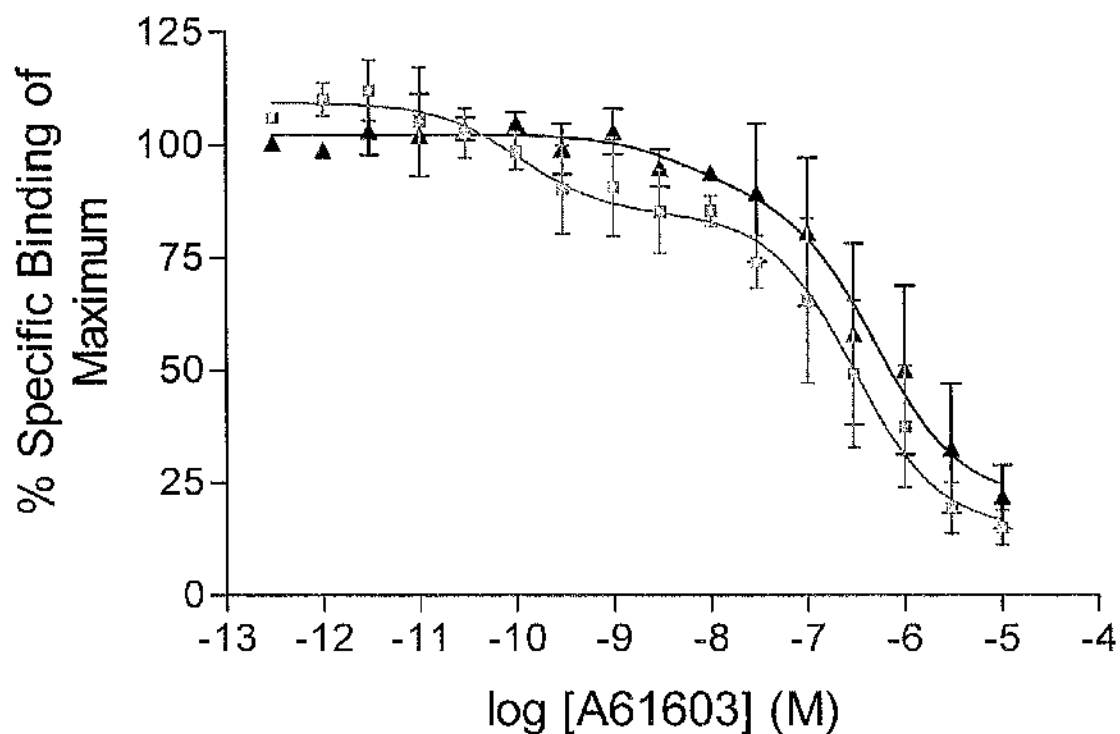


**Figure 2.23** Displacement of 0.2 nM [<sup>3</sup>H]prazosin binding to bovine  $\alpha_{1a}$ -AR membranes by increasing concentrations of A61603 in the (▲) presence of and (◻) absence of 0.25 mM GTP- $\gamma$ -S. Non-specific binding was determined in the presence of 10  $\mu$ M phentolamine. Values are the mean ( $\pm$  S.E.) of (▲) two experiments and (◻) three experiments performed in duplicate.

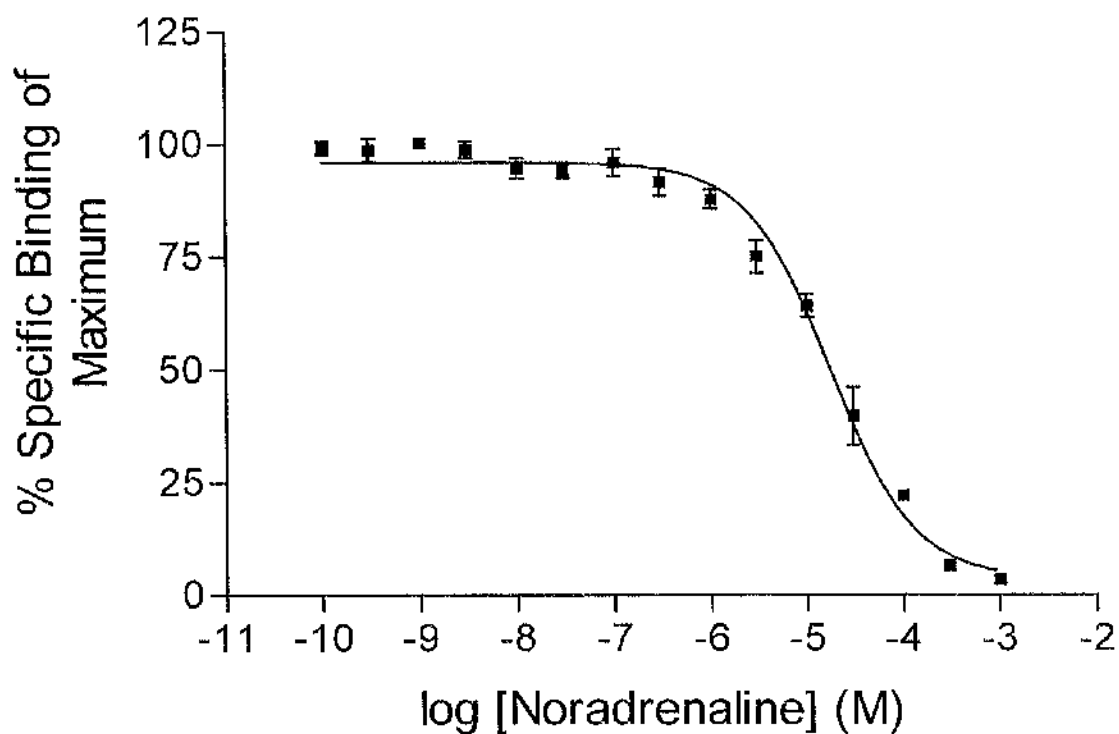


**Figure 2.24** Displacement of 0.2 nM [<sup>3</sup>H]prazosin binding to bovine  $\alpha_{1a}$ -AR membranes by increasing concentrations of noradrenaline. Incubation temperature was 37°C. Non-specific binding was determined in the presence of 10  $\mu$ M phentolamine. Values are the mean ( $\pm$  S.E.) of four experiments performed in duplicate.

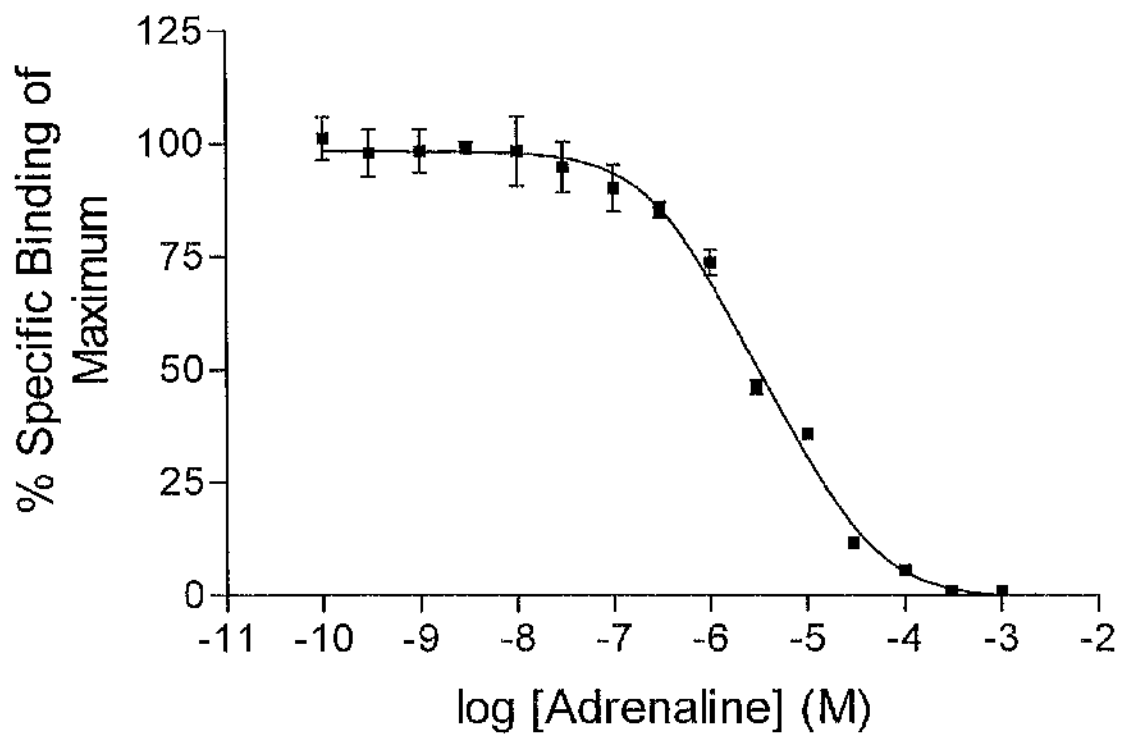


**Figure 2.25** Displacement of 0.2 nM [<sup>3</sup>H]prazosin binding to bovine  $\alpha_{1a}$ -AR membranes by increasing concentrations of adrenaline. Non-specific binding was determined in the presence of 10  $\mu$ M phentolamine. Values are the mean ( $\pm$  S.E.) of three experiments performed in duplicate.

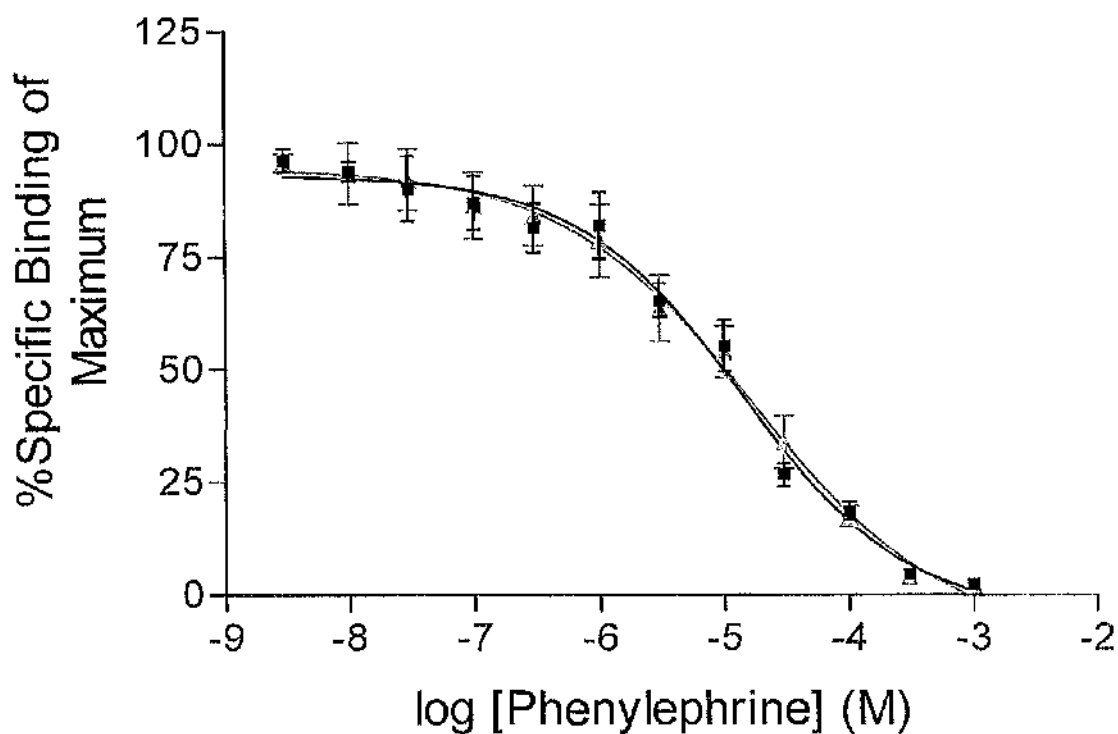


**Figure 2.26** Displacement of 0.2 nM [ $^3$ H]prazosin binding to bovine  $\alpha_{1a}$ -AR whole cells by increasing concentrations of phenylephrine in the ( $\Delta$ ) presence of and ( $\blacksquare$ ) absence of 0.25 mM GTP- $\gamma$ -S. Non-specific binding was determined in the presence of 10  $\mu$ M phentolamine. Values are the mean ( $\pm$  S.E.) of ( $\Delta$ ) three and ( $\blacksquare$ ) three experiments performed in duplicate.

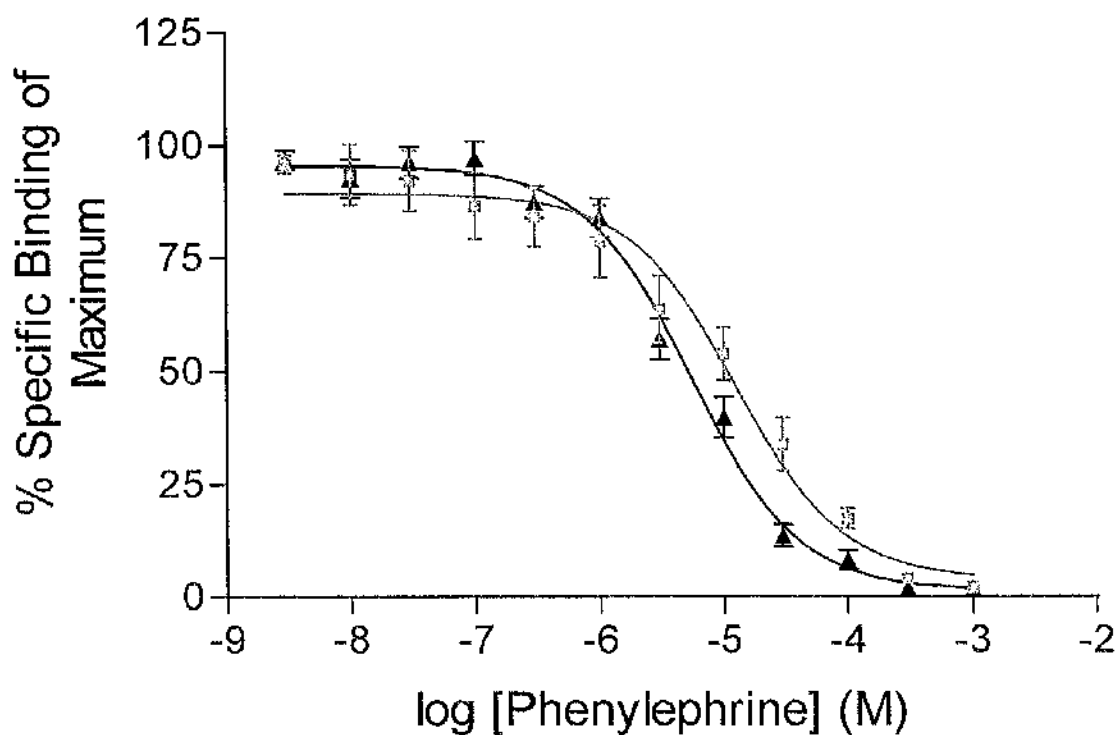


**Figure 2.27** Displacement of 0.2 nM [<sup>3</sup>H]prazosin binding to bovine  $\alpha_{1a}$ -AR (□) whole cells and (▲) membranes by increasing concentrations of phenylephrine in the presence of 0.25 mM GTP- $\gamma$ -S. Non-specific binding was determined in the presence of 10  $\mu$ M phentolamine. Values are the mean ( $\pm$  S.E.) of (□) three and (▲) six experiments performed in duplicate.

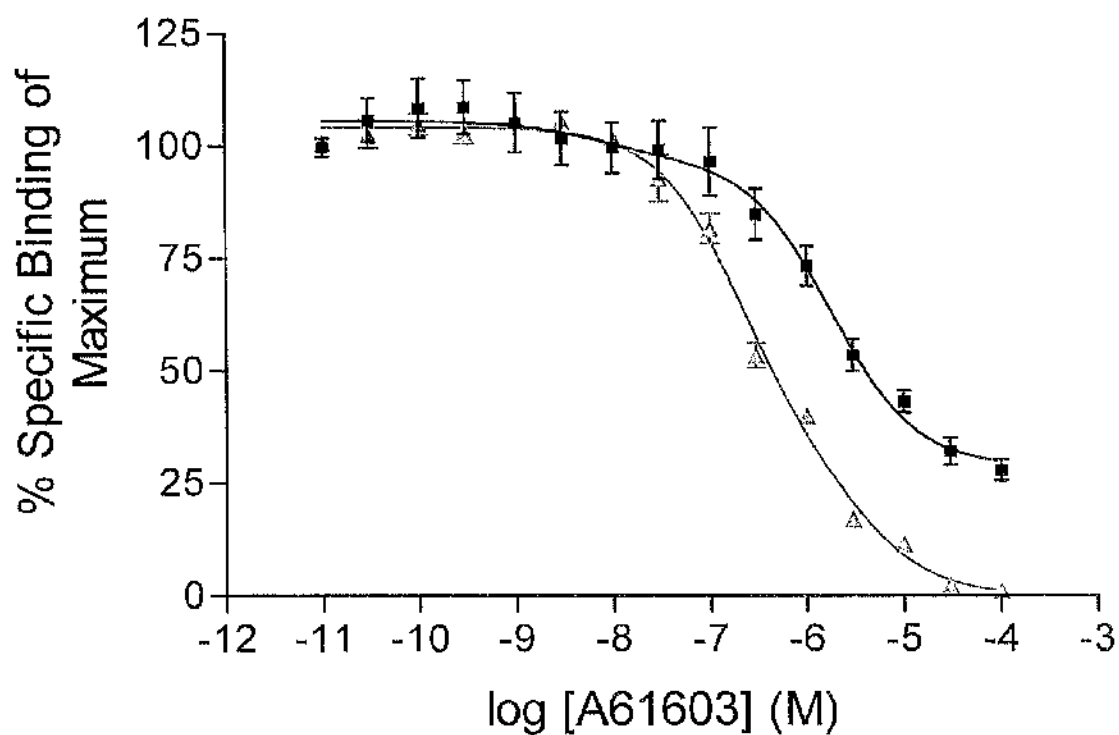


**Figure 2.28** Displacement of 0.2 nM [<sup>3</sup>H]prazosin binding to bovine  $\alpha_{1a}$ -AR whole cells by increasing concentrations of A61603. Incubation times are (■) 30 and (△) 120 minutes. Non-specific binding was determined in the presence of 10  $\mu$ M phentolamine. Values are the mean ( $\pm$  S.E.) of (■) four and (△) two experiments performed in duplicate.

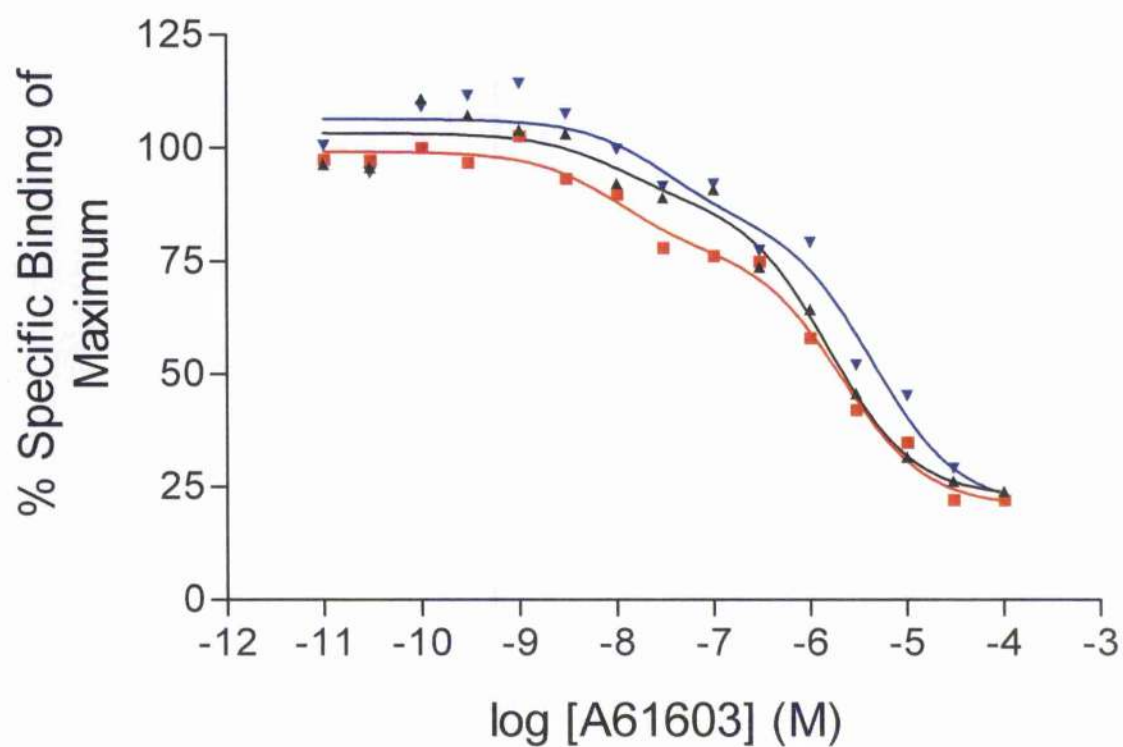


**Figure 2.29** Displacement of 0.2 nM [ $^3\text{H}$ ]prazosin binding to bovine  $\alpha_{1a}$ -AR whole cells by increasing concentrations of A61603 in the presence of 0.25 mM GTP- $\gamma$ -S. Incubation times are ( $\blacktriangle$ ) 15 minutes, ( $\blacksquare$ ) 30 minutes and ( $\blacktriangledown$ ) 120 minutes. Non-specific binding was determined in the presence of 10  $\mu\text{M}$  phentolamine. Values are for one single experiment performed in duplicate.

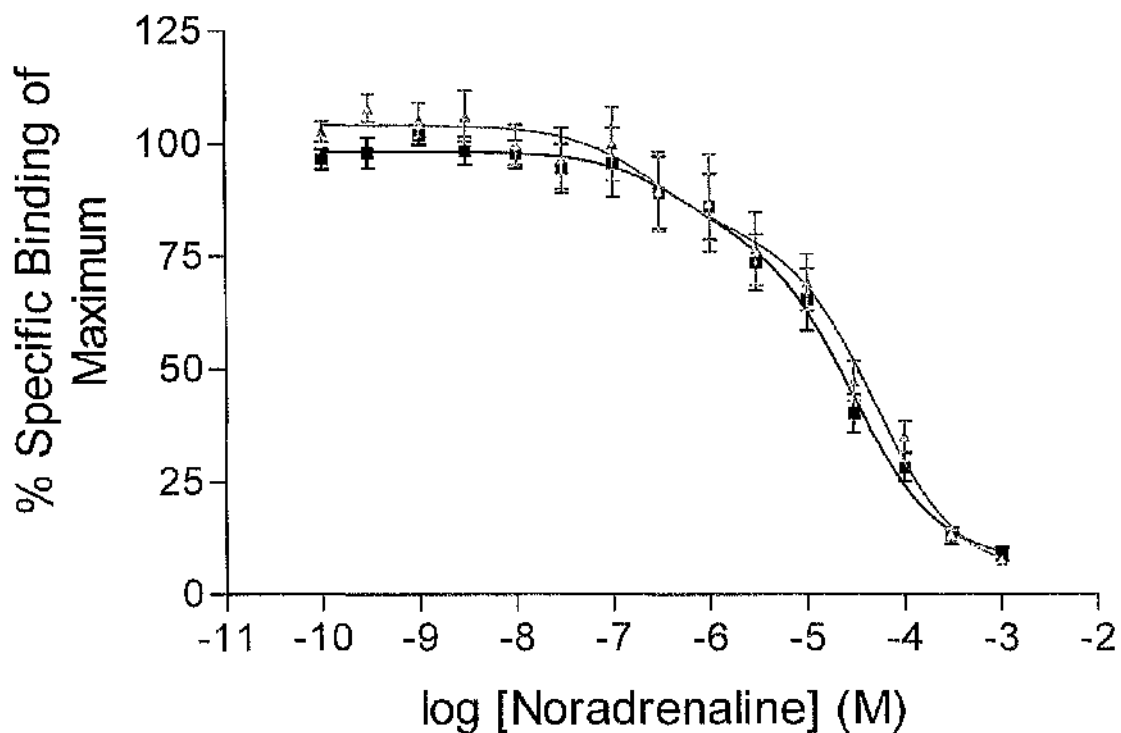


**Figure 2.30** Effect of temperature on displacement of 0.2 nM [<sup>3</sup>H]prazosin binding to bovine  $\alpha_{1a}$ -AR whole cells by increasing concentrations of noradrenaline. Incubation temperatures were (■) 22°C and (△) 37°C. Non-specific binding was determined in the presence of 10  $\mu$ M phentolamine. Values are the mean ( $\pm$  S.E.) of (■) four and (△) four experiments performed in duplicate.

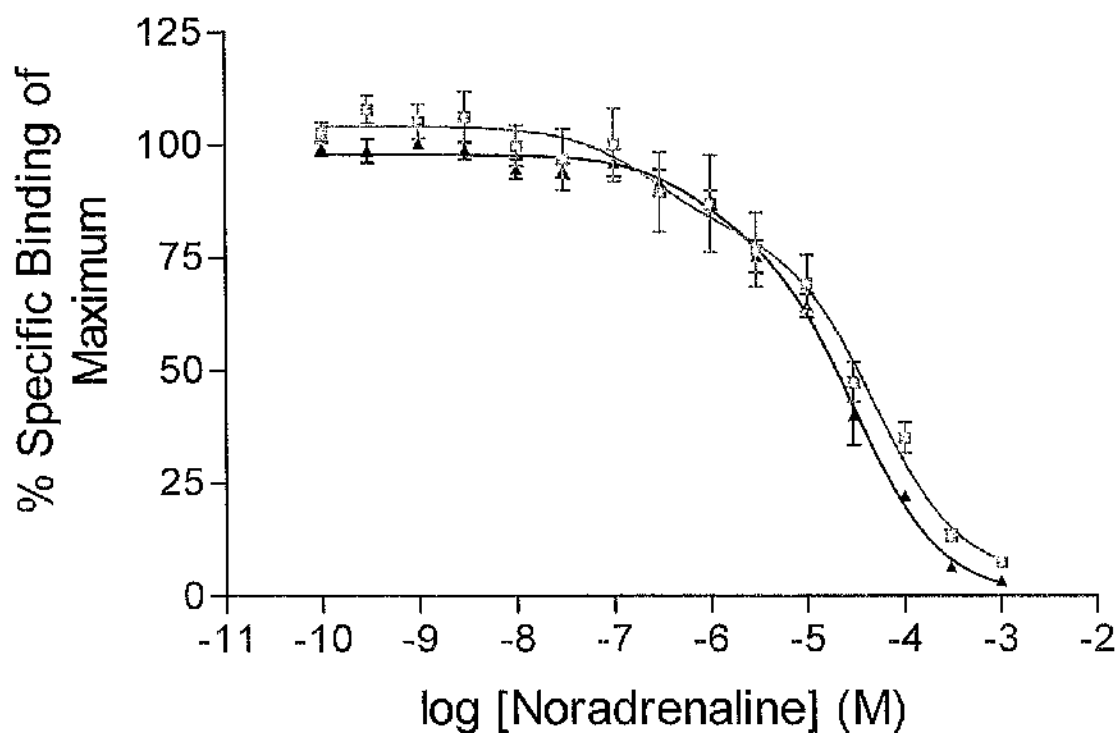


**Figure 2.31** Displacement of 0.2 nM [<sup>3</sup>H]prazosin binding to bovine  $\alpha_{1a}$ -AR (□) whole cells and (▴) membranes by increasing concentrations of noradrenaline. Both incubation temperatures were 37°C. Non-specific binding was determined in the presence of 10  $\mu$ M phentolamine. Values are the mean ( $\pm$  S.E.) of (□) four and (▴) four experiments performed in duplicate.

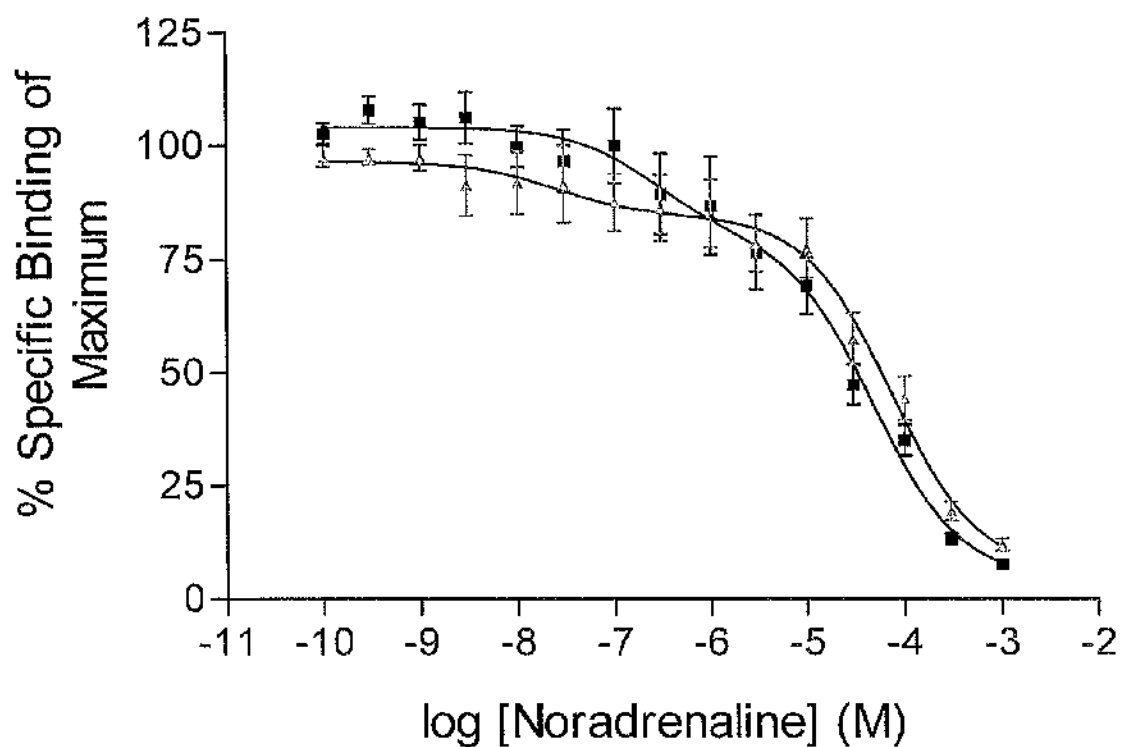


**Figure 2.32** Displacement of 0.2 nM [ $^3\text{H}$ ]prazosin binding to bovine  $\alpha_{1a}$ -AR whole cells by increasing concentrations of noradrenaline in the (■) absence and (Δ) presence of 1  $\mu\text{M}$  corticosterone. Incubation temperature for both sets of experiments was 37°C. Non-specific binding was determined in the presence of 10  $\mu\text{M}$  phentolamine. Values are the mean ( $\pm$  S.E.) of (■) four and (Δ) four experiments performed in duplicate.

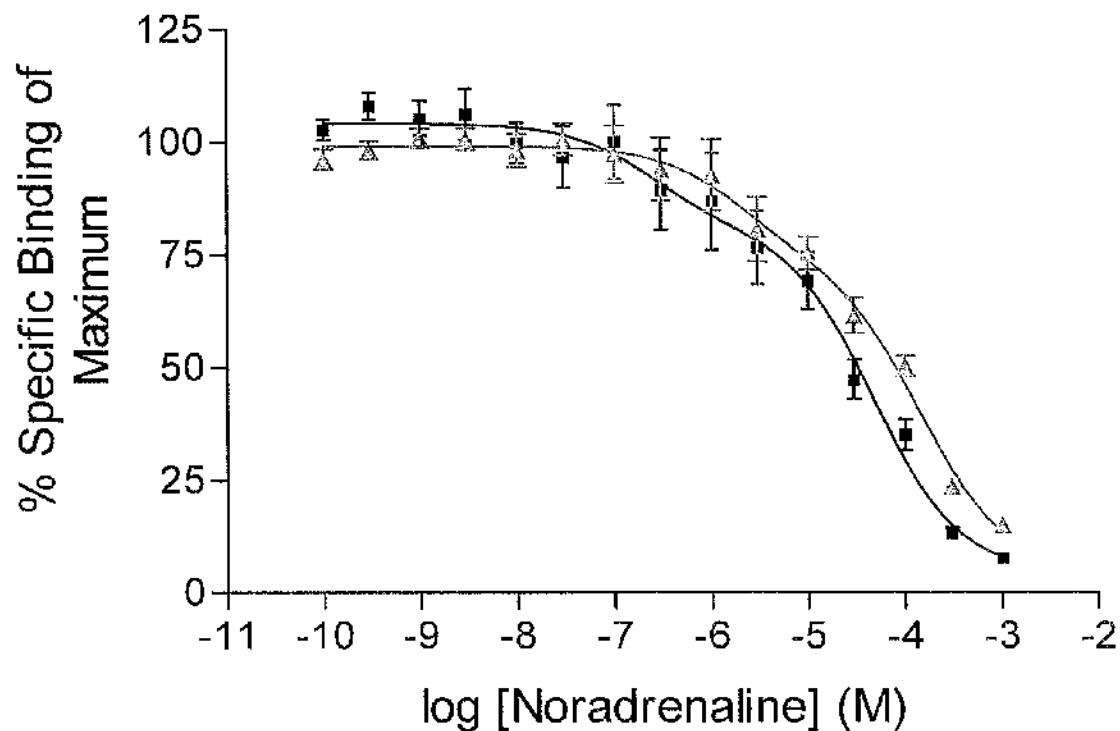


**Figure 2.33** Effect of incubation time on displacement of 0.2 nM [ $^3\text{H}$ ]prazosin binding to bovine  $\alpha_{1a}$ -AR whole cells by increasing concentrations of noradrenaline. Incubation times were (■) 30 minutes and (△) 15 minutes. Incubation temperature for both sets of experiments was 37°C. Non-specific binding was determined in the presence of 10  $\mu\text{M}$  phentolamine. Values are the mean ( $\pm$  S.E.) of (■) four and (△) four experiments performed in duplicate.

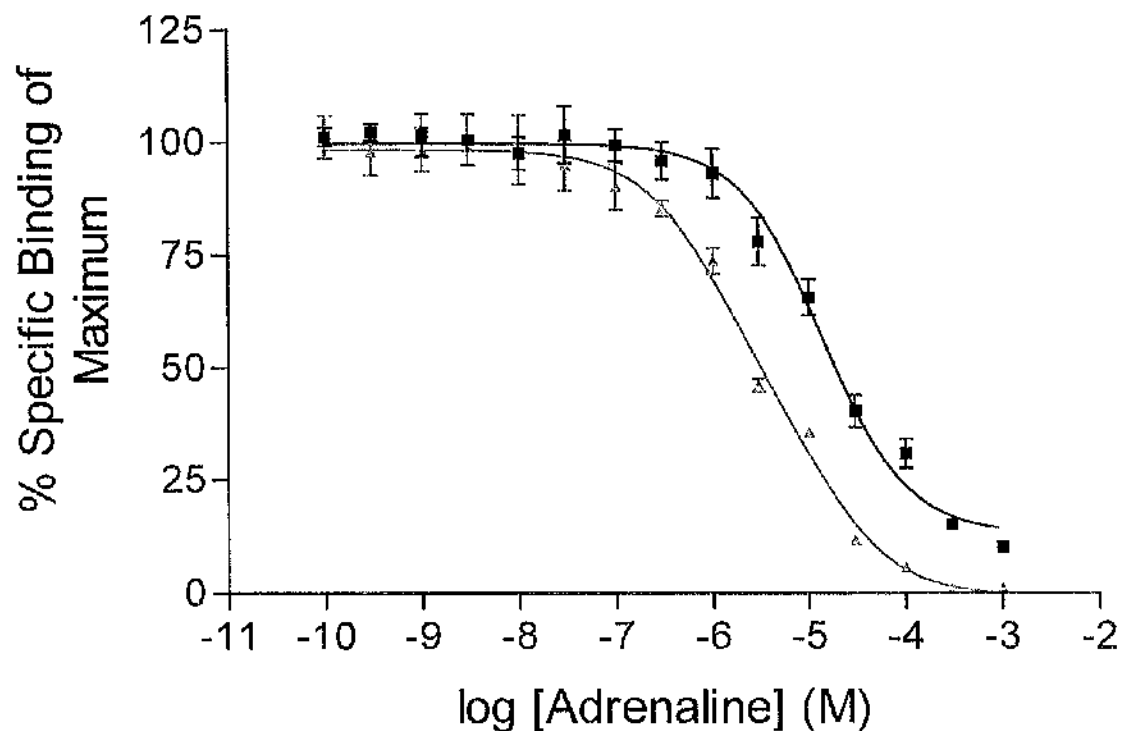


**Figure 2.34** Displacement of 0.2 nM [<sup>3</sup>H]prazosin binding to bovine  $\alpha_{1a}$ -AR (■) whole cells and (△) membranes by increasing concentrations of adrenaline. Both incubation temperatures were 37°C. Non-specific binding was determined in the presence of 10  $\mu$ M phentolamine. Values are the mean ( $\pm$  S.E.) of (■) four and (△) two experiments performed in duplicate.

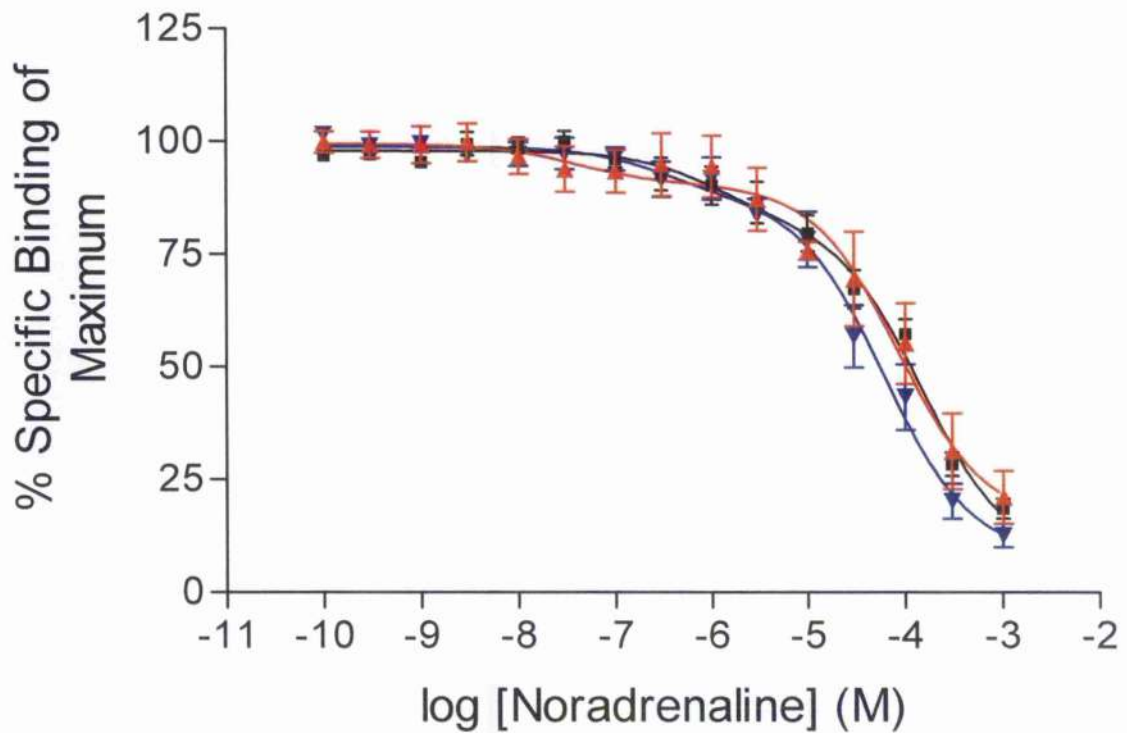


**Figure 2.35** Displacement of 0.2 nM [ $^3\text{H}$ ]prazosin binding to bovine  $\alpha_{1a}$ -AR whole cells by increasing concentrations of noradrenaline for 60 minutes at 22°C. First incubation times ([ $^3\text{H}$ ]prazosin alone) were ( $\blacktriangle$ ) 15 minutes, ( $\blacksquare$ ) 30 minutes and ( $\blacktriangledown$ ) 60 minutes at 22°C. Non-specific binding was determined in the presence of 10  $\mu\text{M}$  phentolamine. Values are the mean ( $\pm$  S.E.) of ( $\blacktriangle$ ) four, ( $\blacksquare$ ) four and ( $\blacktriangledown$ ) four experiments performed in duplicate.

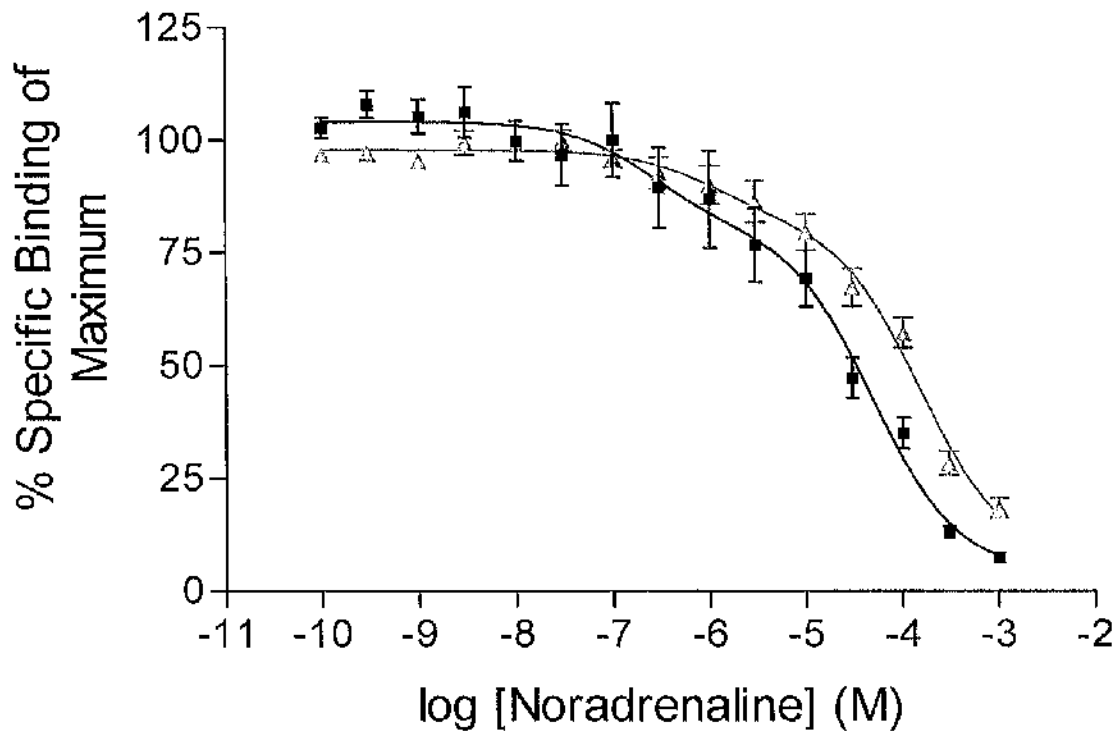


**Figure 2.36** Displacement of 0.2 nM [ $^3\text{H}$ ]prazosin binding to bovine  $\alpha_{1a}$ -AR whole cells by increasing concentrations of noradrenaline using a ( $\Delta$ ) new radioligand binding protocol and ( $\blacksquare$ ) standard radioligand binding protocol. Both incubations were 30 minutes at a temperature of 37°C. Non-specific binding was determined in the presence of 10  $\mu\text{M}$  phentolamine. Values are the mean ( $\pm$  S.E.) of ( $\Delta$ ) four and ( $\blacksquare$ ) four experiments performed in duplicate.

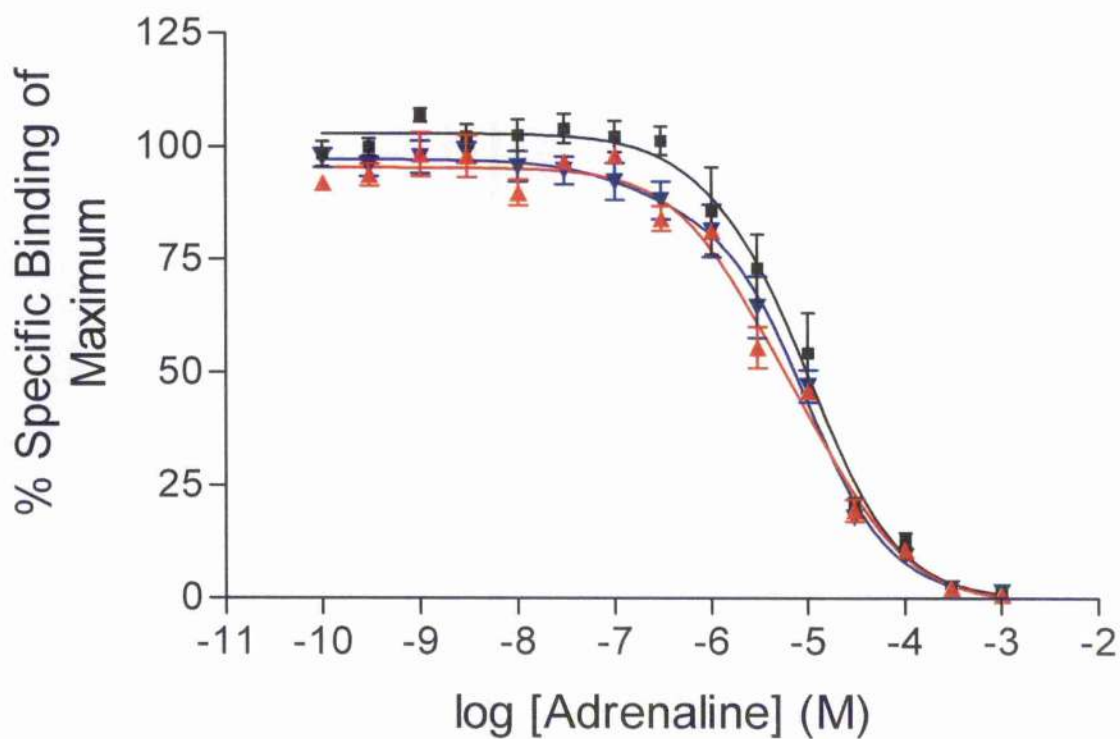


**Figure 2.37** Displacement of 0.2 nM [<sup>3</sup>H]prazosin binding to bovine α<sub>1a</sub>-AR membranes by increasing concentrations of adrenaline using an updated radioligand binding protocol. Second incubation times were (▲) 15, (■) 30 and (▼) 60 minutes at a temperature of 37°C. Non-specific binding was determined in the presence of 10 μM phentolamine. Values are the mean (± S.E.) of (▲) two, (■) four and (▼) four experiments performed in duplicate.

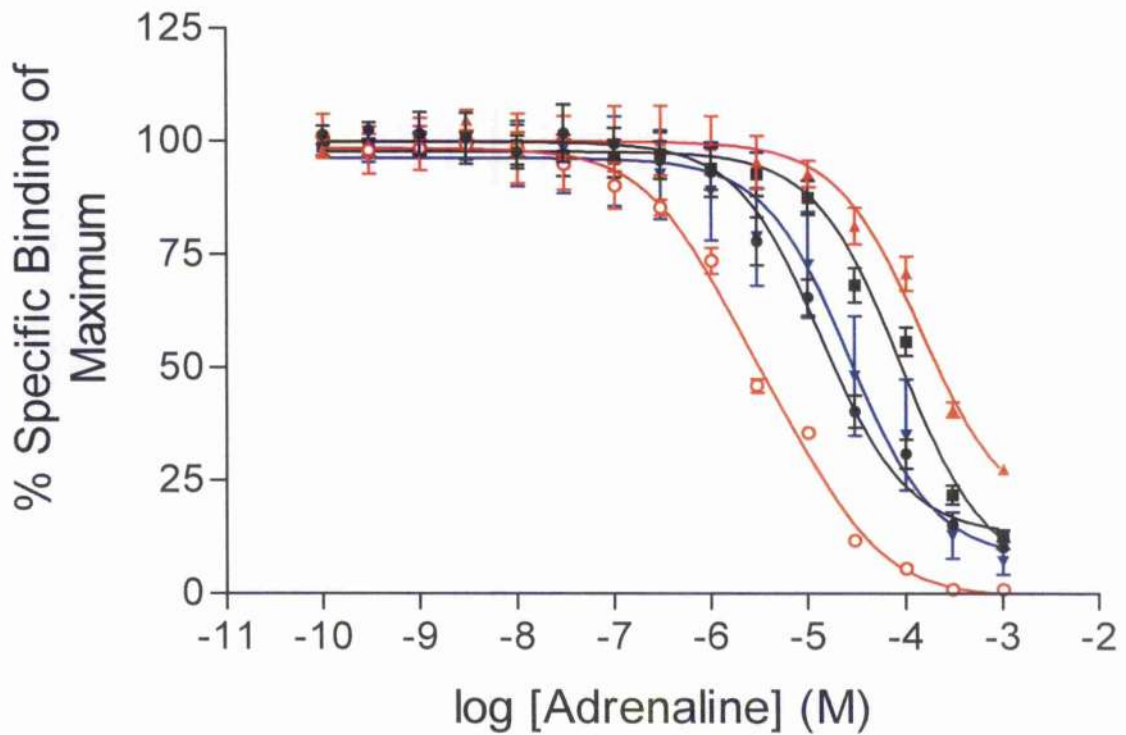


**Figure 2.38** Comparison of radioligand binding protocols using adrenaline as the competing/displacing ligand. Displacement of 0.2 nM [ $^3\text{H}$ ]prazosin binding to bovine  $\alpha_{1a}$ -AR whole cells by increasing concentrations of adrenaline using an updated radioligand binding protocol. Second incubation times were (▲) 15, (■) 30 and (▼) 60 minutes at a temperature of 37°C. Also shown is the displacement of 0.2 nM [ $^3\text{H}$ ]prazosin binding to bovine  $\alpha_{1a}$ -AR (◼) whole cells and (◻) membranes by increasing concentrations of adrenaline using a standard binding protocol. Non-specific binding was determined in the presence of 10  $\mu\text{M}$  phentolamine. Values are the mean ( $\pm$  S.E.) of (▲) four, (■) six, (▼) four, (◼) four and (◻) two experiments performed in duplicate.

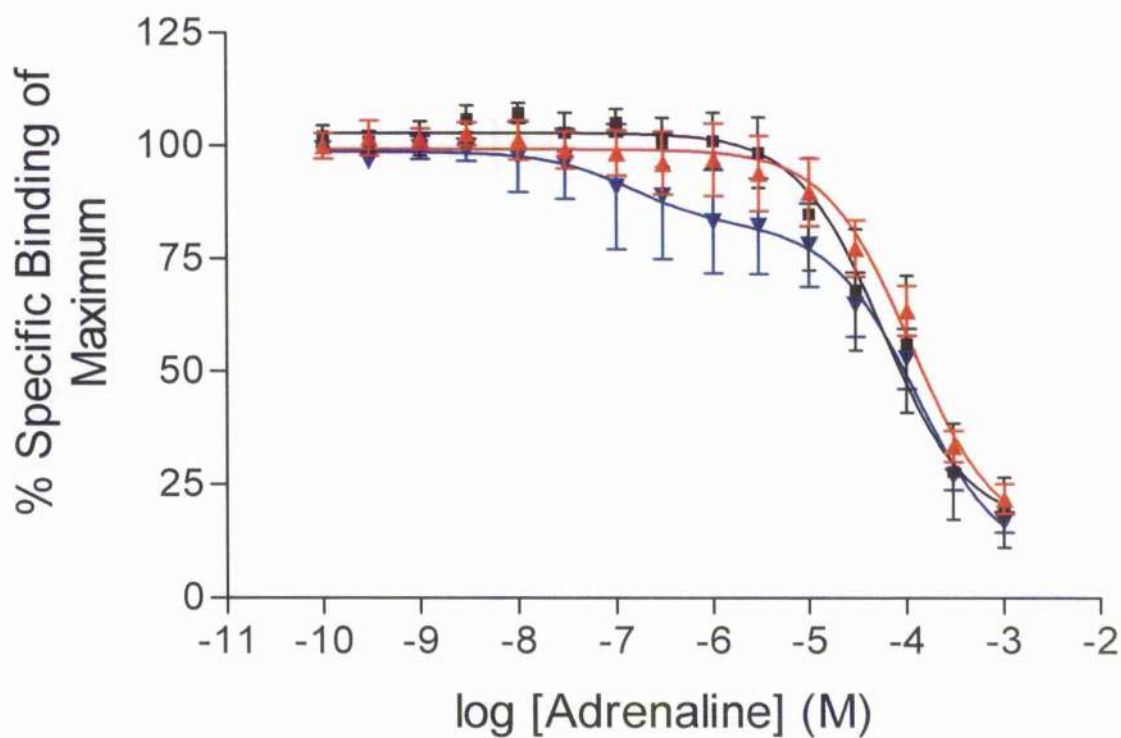


**Figure 2.39** Effect of corticosterone on displacement of 0.2 nM [<sup>3</sup>H]prazosin binding to bovine  $\alpha_{1a}$ -AR whole cells by increasing concentrations of adrenaline using an updated radioligand binding protocol. Second incubation times were ( $\blacktriangle$ ) 15, ( $\blacksquare$ ) 30 and ( $\blacktriangledown$ ) 60 minutes at a temperature of 37°C in the presence of 1  $\mu$ M corticosterone. Non-specific binding was determined in the presence of 10  $\mu$ M phentolamine. Values are the mean ( $\pm$  S.E.) of ( $\blacktriangle$ ) four, ( $\blacksquare$ ) four and ( $\blacktriangledown$ ) three experiments performed in duplicate.

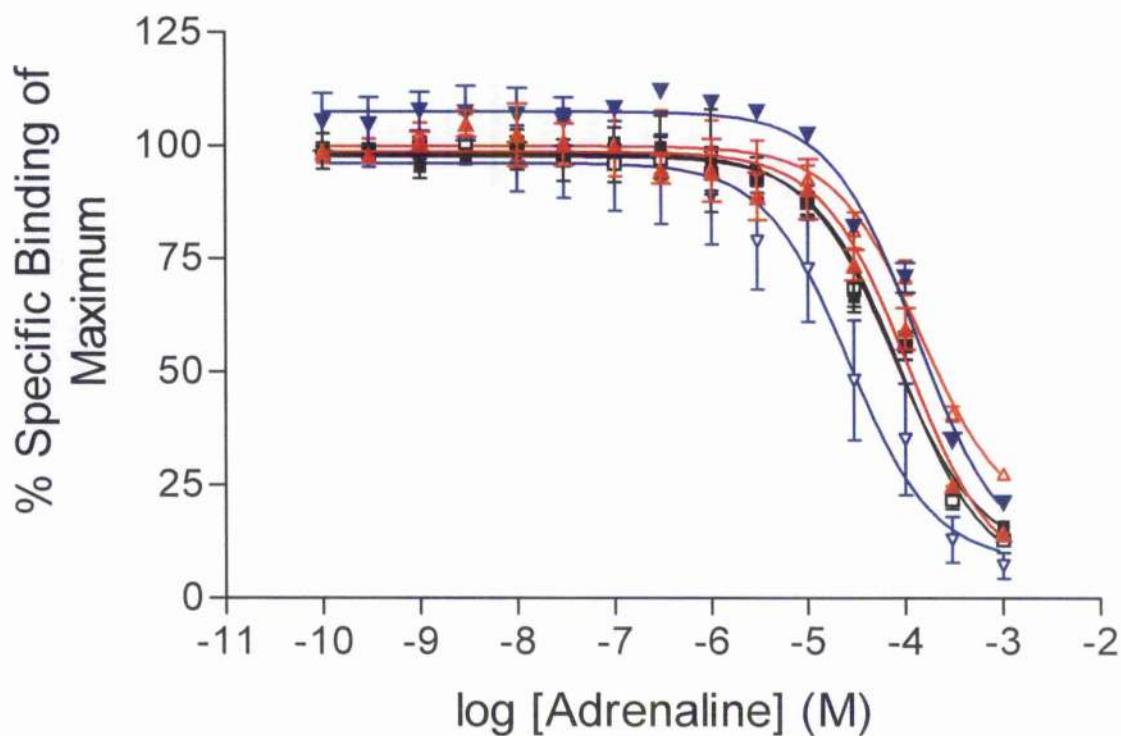


**Figure 2.40** Comparison of the absence and presence of corticosterone on the displacement of 0.2 nM [ $^3\text{H}$ ]prazosin binding to bovine  $\alpha_{1a}$ -AR whole cells by increasing concentrations of adrenaline using an updated radioligand binding protocol. Second incubation times were ( $\blacktriangle$ ) 15, ( $\blacksquare$ ) 30 and ( $\blacktriangledown$ ) 60 minutes at a temperature of 37°C. The whole experiment performed in the presence of 1  $\mu\text{M}$  corticosterone. Also shown are the control experiments in the absence of corticosterone. Second incubations were ( $\triangle$ ) 15, ( $\square$ ) 30 and ( $\triangledown$ ) 60 minutes at 37°C. Non-specific binding was determined in the presence of 10  $\mu\text{M}$  phentolamine. Values are the mean ( $\pm$  S.E.) of ( $\blacktriangle$ ) two, ( $\blacksquare$ ) two, ( $\blacktriangledown$ ) two, ( $\triangle$ ) four, ( $\square$ ) six and ( $\triangledown$ ) four experiments performed in duplicate.

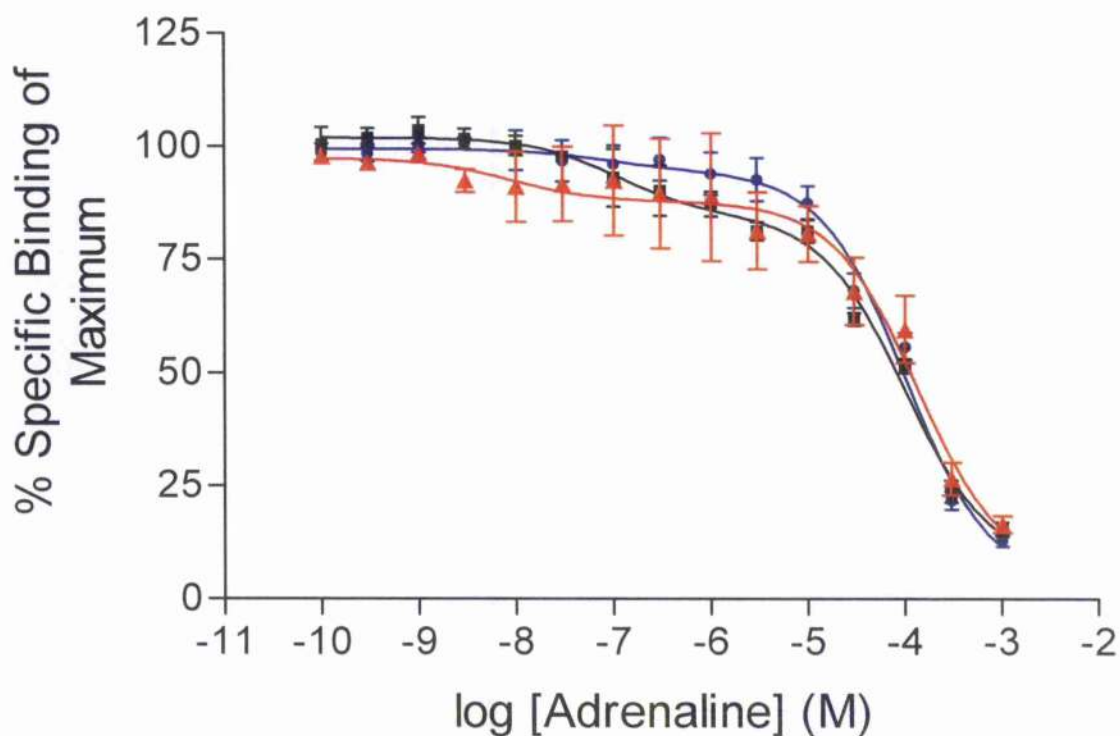


**Figure 2.41** Effect of concanavalin A on displacement of 0.2 nM [ $^3\text{H}$ ]prazosin binding to bovine  $\alpha_{1a}$ -AR whole cells by increasing concentrations of adrenaline using an updated radioligand binding protocol. (■) Half and (▲) whole experiment performed in presence of 0.25mg/ml concanavalin A. Also shown is the (◼) control experiment in the absence of concanavalin A. Second incubation times were 30 minutes at a temperature of 37°C. Non-specific binding was determined in the presence of 10  $\mu\text{M}$  phentolamine. Values are the mean ( $\pm$  S.E.) of (■) two, (▲) two and (◼) six experiments performed in duplicate.

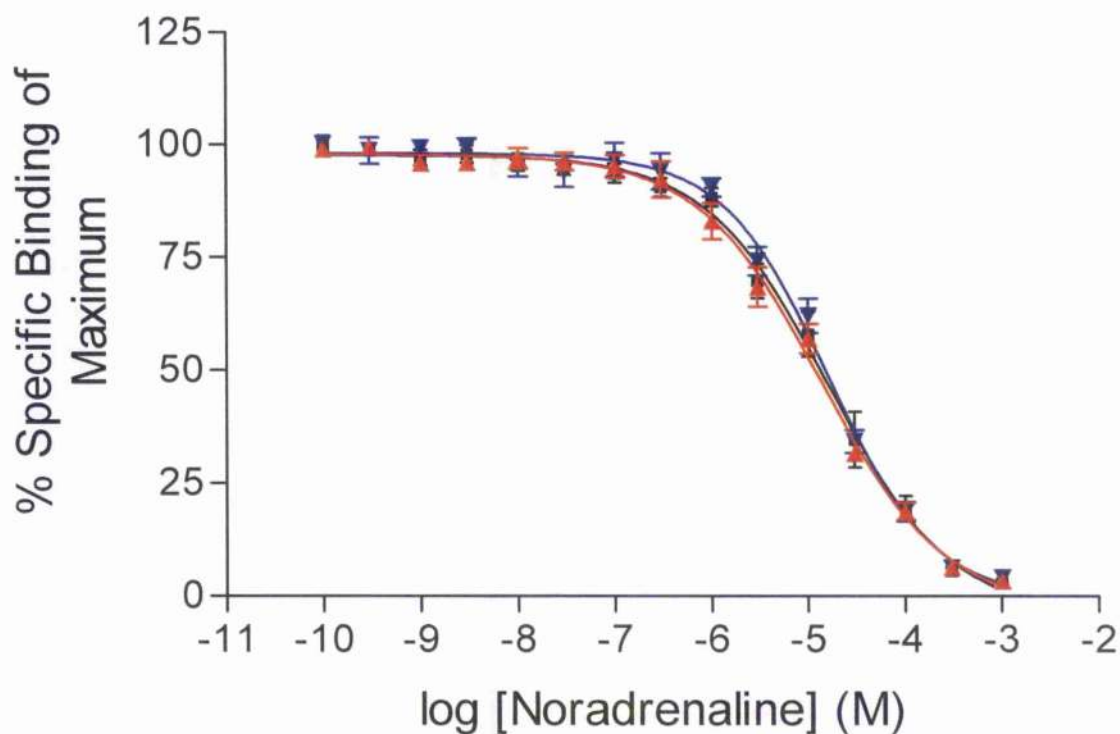


**Figure 2.42** Displacement of 0.2 nM [<sup>3</sup>H]prazosin binding to bovine  $\alpha_{1a}$ -AR membranes by increasing concentrations of noradrenaline using an updated radioligand binding protocol. Second incubation times were (▲) 15, (■) 30 and (▼) 60 minutes at a temperature of 37°C. Non-specific binding was determined in the presence of 10  $\mu$ M phentolamine. Values are the mean ( $\pm$  S.E.) of (▲) four, (■) four and (▼) four experiments performed in duplicate.

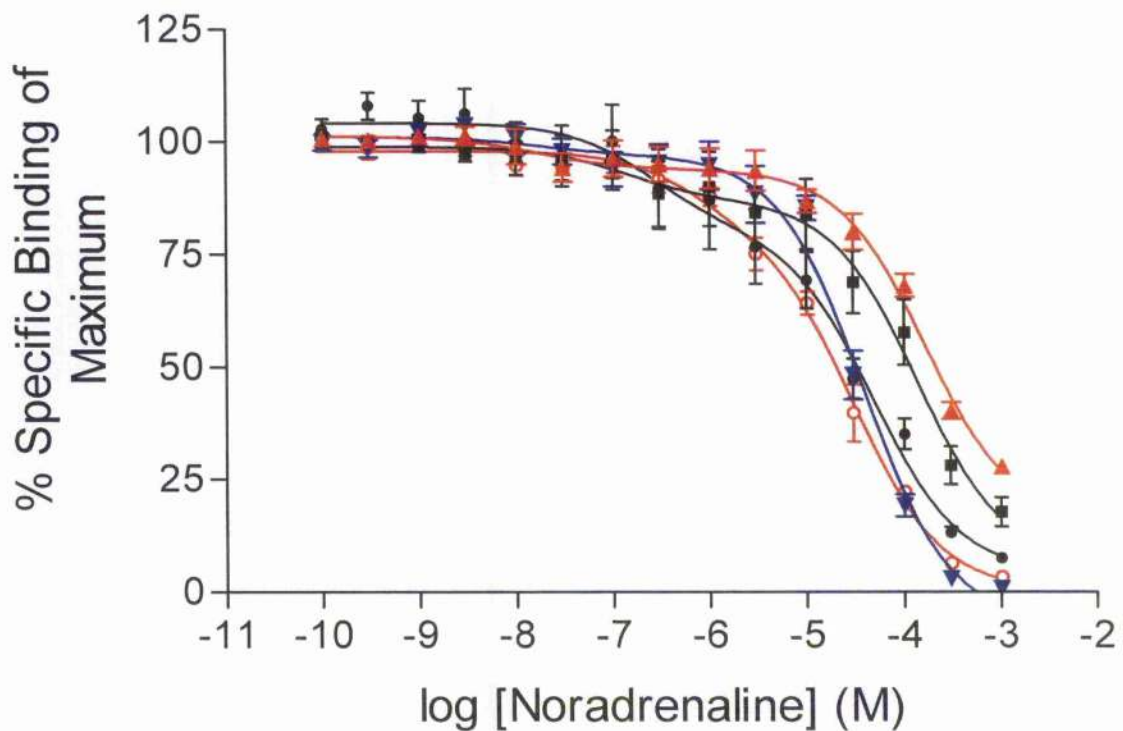


**Figure 2.43** Comparison of radioligand binding protocols using noradrenaline as the competing/displacing ligand. Displacement of 0.2 nM [ $^3\text{H}$ ]prazosin binding to bovine  $\alpha_{1a}$ -AR whole cells by increasing concentrations of noradrenaline using an updated radioligand binding protocol. Second incubation times were (▲) 15, (■) 30 and (▼) 60 minutes at a temperature of 37°C. Also shown is the displacement of 0.2 nM [ $^3\text{H}$ ]prazosin binding to bovine  $\alpha_{1a}$ -AR (□) whole cells and (○) membranes by increasing concentrations of noradrenaline using a standard binding protocol. Non-specific binding was determined in the presence of 10  $\mu\text{M}$  phentolamine. Values are the mean ( $\pm$  S.E.) of (▲) four, (■) four, (▼) four, (□) four and (○) four experiments performed in duplicate.

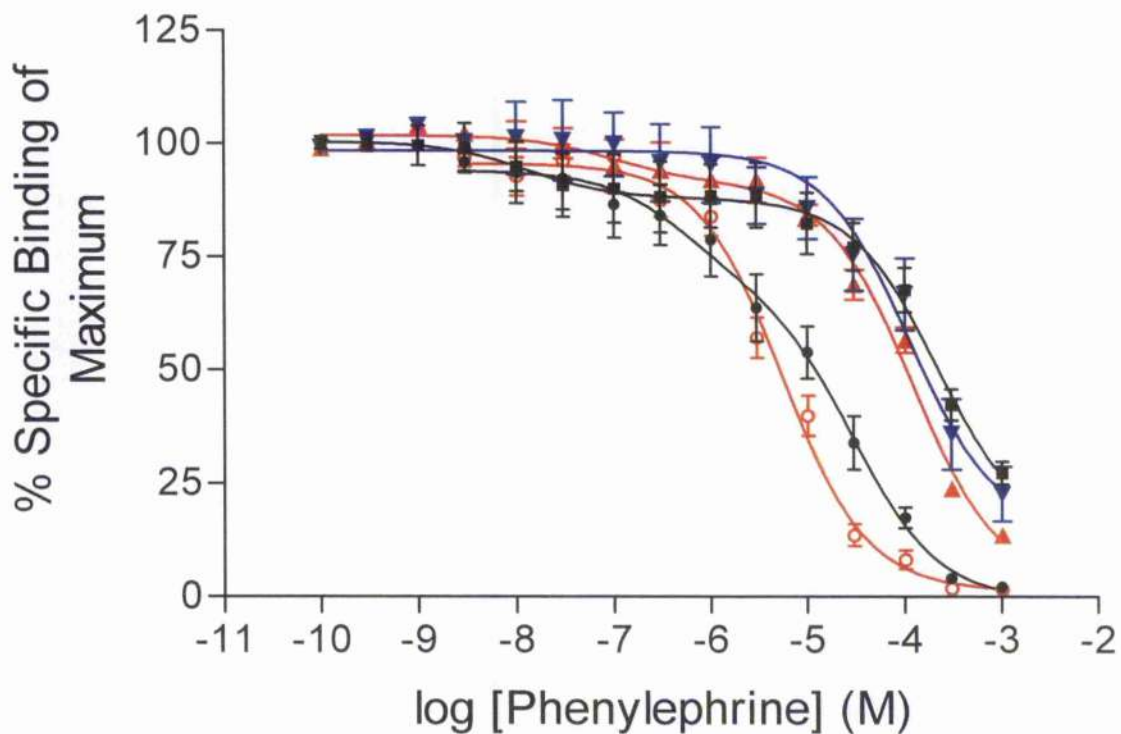


**Figure 2.44** Comparison of radioligand binding protocols using phenylephrine as the competing/displacing ligand. Displacement of 0.2 nM [<sup>3</sup>H]prazosin binding to bovine  $\alpha_{1a}$ -AR whole cells by increasing concentrations of phenylephrine using an updated radioligand binding protocol. Second incubation times were (▲) 15, (■) 30 and (▼) 60 minutes at a temperature of 37°C. Also shown is the displacement of 0.2 nM [<sup>3</sup>H]prazosin binding to bovine  $\alpha_{1a}$ -AR (◻) whole cells and (◻) membranes by increasing concentrations of phenylephrine using a standard binding protocol. Non-specific binding was determined in the presence of 10  $\mu$ M phentolamine. Values are the mean ( $\pm$  S.E.) of (▲) four, (■) four, (▼) four, (◻) three and (◻) six experiments performed in duplicate.

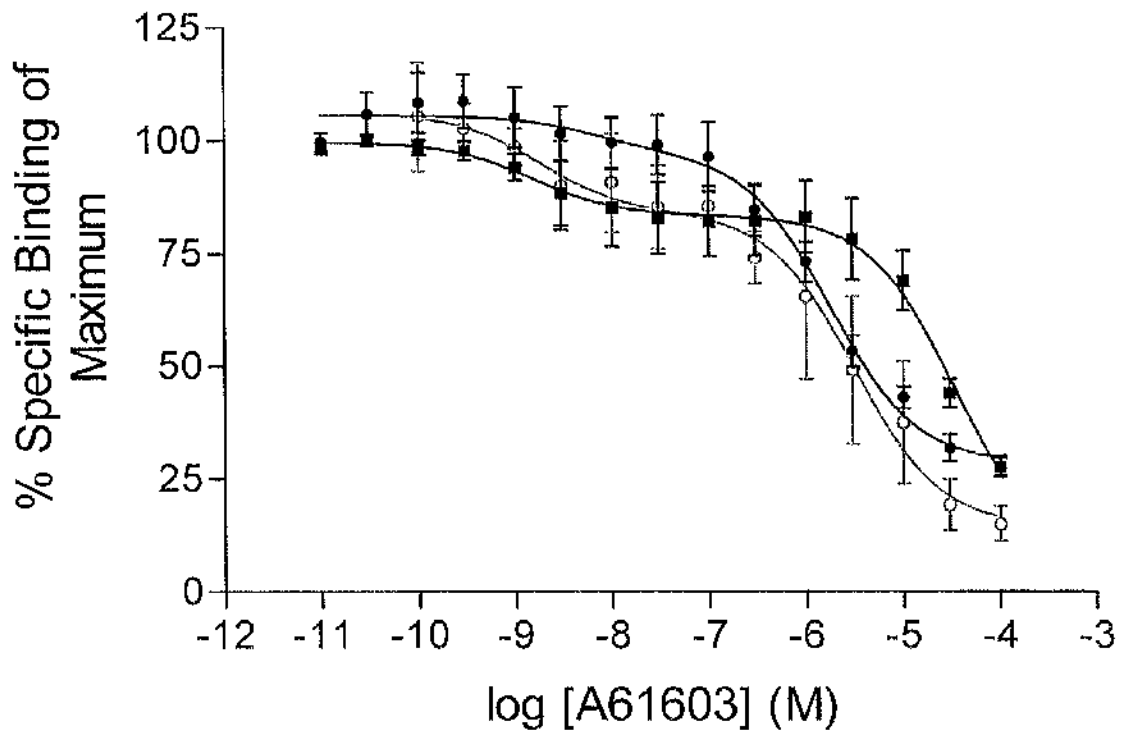


**Figure 2.45** Comparison of radioligand binding protocols using A61603 as the competing/displacing ligand. Displacement of 0.2 nM [<sup>3</sup>H]prazosin binding to bovine  $\alpha_{1a}$ -AR (■) whole cells by increasing concentrations of A61603 using an updated radioligand binding protocol. Second incubation time was 30 minutes at a temperature of 37°C. Also shown is the displacement of 0.2 nM [<sup>3</sup>H]prazosin binding to bovine  $\alpha_{1a}$ -AR (◼) whole cells and (○) membranes by increasing concentrations of A61603 using a standard binding protocol. Non-specific binding was determined in the presence of 10  $\mu$ M phentolamine. Values are the mean ( $\pm$  S.E.) of (■) four, (◼) four and (○) three experiments performed in duplicate.

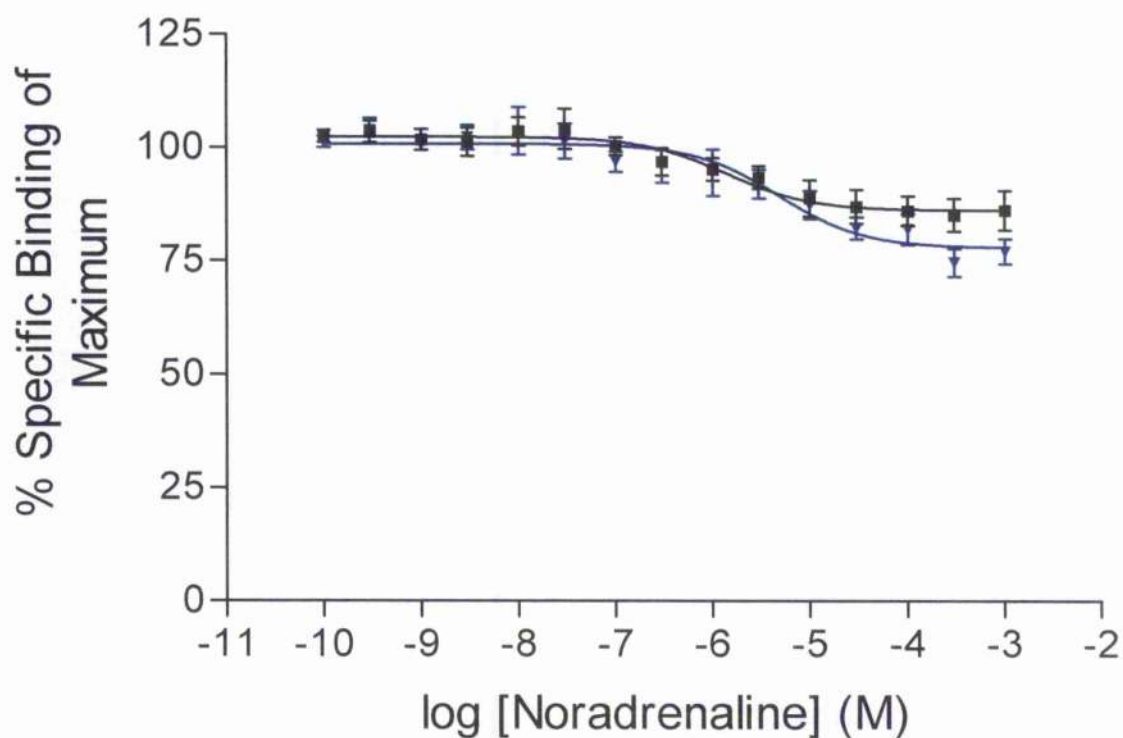


**Figure 2.46** Effect of cold temperature on displacement of 0.2 nM [ $^3\text{H}$ ]prazosin binding to bovine  $\alpha_{1a}$ -AR whole cells by increasing concentrations of noradrenaline using an updated radioligand binding protocol. Second incubation time was (■) 15 and (▼) 60 minutes at a temperature of 4°C. Non-specific binding was determined in the presence of 10  $\mu\text{M}$  phentolamine. Values are the mean ( $\pm$  S.E.) of (■) four and (▼) four experiments performed in duplicate.

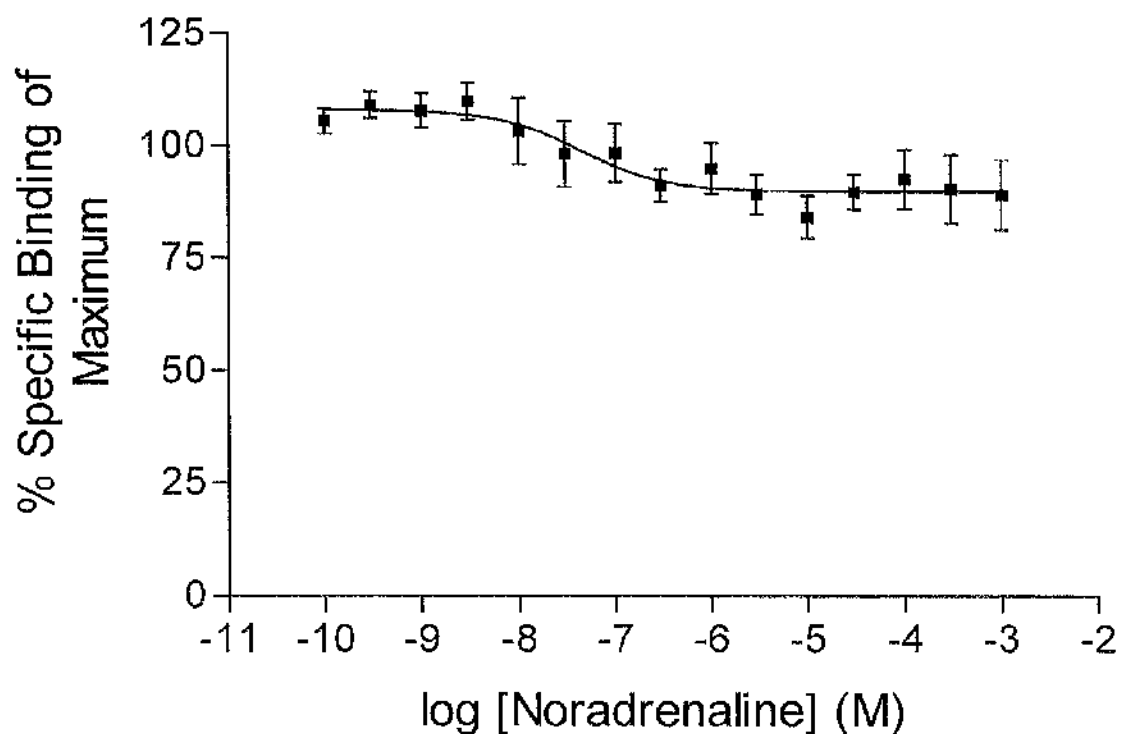


**Figure 2.47** Effect of cold temperature on displacement of 0.2 nM [<sup>3</sup>H]prazosin binding to bovine  $\alpha_{1n}$ -AR membranes by increasing concentrations of noradrenaline using an updated radioligand binding protocol. Second incubation time was 60 minutes at a temperature of 4°C. Non-specific binding was determined in the presence of 10  $\mu$ M phentolamine. Values are the mean ( $\pm$  S.E.) of four experiments performed in duplicate.

**TABLE 2.1****Classic Binding Protocol: Membranes**

Comparison of affinity estimates from rat-1 fibroblasts expressing bovine  $\alpha_{1A}$ -AR in membranes. Displacement of [ $^3$ H]prazosin (0.2nM) was determined with increasing concentrations of competing ligand from at least three experiments performed in duplicate ( $\pm$  S.E.M) in the presence or absence of 0.25 mM GTP- $\gamma$ -S. All incubations were 30 minutes at temperature 22°C unless stated otherwise. Nonspecific binding was determined in the presence of 10  $\mu$ M phentolamine.

Ligands	-GTP- $\gamma$ -S			+GTP- $\gamma$ -S		
	$pK_i$	$n_H$	Fig.	$pK_i$	$n_H$	Fig.
Phenylephrine	$7.9 \pm 0.6$ $5.2 \pm 1.1$	$0.4 \pm 0.1$	2.22	$5.6 \pm 1.6$	$0.9 \pm 0.1$	2.22, 2.27
(R)-A-61603	$10.26 \pm 0.58$ $6.82 \pm 1.0$	$0.2 \pm 0.1$	2.23	$6.85 \pm 0.99$	$0.6 \pm 0.3$	2.23
Noradrenaline	$5.05 \pm 1.61$	$0.7 \pm 0.1$	2.24, 2.31			
Adrenaline	$5.80 \pm 1.52$	$0.7 \pm 0.1$	2.25, 2.31			
RS100329	$9.63 \pm 0.22$ $8.16 \pm 0.77$	$0.7 \pm 0.1$	2.5, 2.8			
Prazosin	$8.57 \pm 1.68$	$0.9 \pm 0.1$	2.3, 2.7			
QAPB	$8.37 \pm 1.77$	$1.0 \pm 0.1$	2.4, 2.10			
L-765314	$6.29 \pm 1.70$	$1.0 \pm 0.1$	2.6, 2.11			

**TABLE 2.2****Classic Binding Protocol: Whole Cells**

Comparison of affinity estimates from rat-1 fibroblasts expressing bovine  $\alpha_{1A}$ -AR in whole cells. Displacement of [ $^3$ H]prazosin (0.2nM) was determined with increasing concentrations of competing ligand from at least three experiments performed in duplicate ( $\pm$  S.E.M) in the presence or absence of 0.25 mM GTP- $\gamma$ -S. Incubation times were altered for experiments with (*R*)-A-61603 and experiments with QAPB were performed under light and dark conditions. Nonspecific binding was determined in the presence of 10  $\mu$ M phentolamine.

Ligand	-GTP- $\gamma$ -S			+GTP- $\gamma$ -S		
	p <i>K</i> <sub>i</sub>	<i>n</i> <sub>H</sub>	Fig.	p <i>K</i> <sub>i</sub>	<i>n</i> <sub>H</sub>	Fig.
Phenylephrine	4.97 $\pm$ 1.0	0.7 $\pm$ 0.1	2.26	4.88 $\pm$ 0.82	0.6 $\pm$ 0.1	2.26, 2.27
<i>(R)</i> -A-61603				(15min) 8.07 $\pm$ 0.28	0.6 $\pm$ 0.1	2.29
				5.91 $\pm$ 0.85		
	8.25 $\pm$ 0.05	0.7 $\pm$ 0.1	2.28	(30min) 8.10 $\pm$ 0.66	0.5 $\pm$ 0.1	2.29
	5.85 $\pm$ 0.92			5.78 $\pm$ 1.0		
	6.82 $\pm$ 0.92	0.8 $\pm$ 0.1	2.28	(120min) 7.61 $\pm$ 0.32	0.5 $\pm$ 0.2	2.29
5.63 $\pm$ 0.49			5.45 $\pm$ 0.66			
Noradrenaline	6.44 $\pm$ 0.31	0.6 $\pm$ 0.1	2.30, 2.31			
	4.64 $\pm$ 0.84					
Adrenaline	4.96 $\pm$ 1.27	0.7 $\pm$ 0.1	2.34			
RS100329	10.99 $\pm$ 0.27	0.6 $\pm$ 0.2	2.8			
	7.35 $\pm$ 0.89					
Prazosin	8.72 $\pm$ 1.21	1.2 $\pm$ 0.2	2.7			
QAPB	(dark) 9.26 $\pm$ 0.59	0.7 $\pm$ 0.1	2.9			
	7.38 $\pm$ 1.10					
	(light) 9.94 $\pm$ 0.37	0.6 $\pm$ 0.1	2.9, 2.10			
	7.37 $\pm$ 0.94					
L-765314	7.27 $\pm$ 0.33	0.5 $\pm$ 0.2	2.11			
	4.72 $\pm$ 0.92					

**TABLE 2.3****Corticosterone influence on noradrenaline**

Comparison of affinity estimates from rat-1 fibroblasts expressing bovine  $\alpha_{1A}$ -AR in whole cells. Displacement of [ $^3$ H]prazosin (0.2nM) was determined with increasing concentrations of noradrenaline from at least three experiments performed in duplicate ( $\pm$  S.E.M). Incubation times and temperatures were altered for specific experiments that were also performed in the presence or absence of 1  $\mu$ M corticosterone. Nonspecific binding was determined in the presence of 10  $\mu$ M phentolamine.

Noradrenaline experiment	37°C			22°C		
	p <i>K</i> <sub>i</sub>	n <sub>H</sub>	Fig	p <i>K</i> <sub>i</sub>	n <sub>H</sub>	Fig.
30 mins	6.71 $\pm$ 0.44 4.42 $\pm$ 0.85	0.4 $\pm$ 0.1	2.30	6.44 $\pm$ 0.31 4.64 $\pm$ 0.84	0.6 $\pm$ 0.1	2.30
30 mins + 1 $\mu$ M corticosterone	7.72 $\pm$ 0.25 4.24 $\pm$ 0.98	0.5 $\pm$ 0.1	2.32			
15 mins	5.81 $\pm$ 0.52 3.94 $\pm$ 0.77	0.5 $\pm$ 0.1	2.33			

**TABLE 2.4**BMY7378: Comparison of  $\alpha_{1a}$  and  $\alpha_{1d}$  adrenoceptors.Comparison of affinity estimates from rat-1 fibroblasts expressing bovine  $\alpha_{1a}$ -AR and human  $\alpha_{1d}$ -AR in membranes and whole cells. Displacement of [ $^3$ H]prazosin (0.2nM) was determined with increasing concentrations of BMY7378 from at least four experiments performed in duplicate ( $\pm$  S.E.M).Nonspecific binding was determined in the presence of 10  $\mu$ M phentolamine.

Subtype	Whole cells			Membranes		
	$pK_i$	$n_H$	Fig.	$pK_i$	$n_H$	Fig.
$\alpha_{1a}$ -AR	$6.36 \pm 1.38$	$1.0 \pm 0.1$	2.12	$7.16 \pm 1.64$	$0.9 \pm 0.1$	2.12
$\alpha_{1d}$ -AR	$9.48 \pm 1.54$	$0.8 \pm 0.1$	2.12	$9.30 \pm 1.20$	$1.0 \pm 0.2$	2.12

**TABLE 2.5**

Effect of pre-incubation time on displacement by noradrenaline; whole cells

Comparison of affinity estimates from rat-1 fibroblasts expressing bovine  $\alpha_{1a}$ -AR in whole cells.Displacement of noradrenaline was determined using a different RLB binding protocol with increasing concentrations of noradrenaline from at least four experiments performed in duplicate ( $\pm$  S.E.M). Pre-incubations with [ $^3$ H]prazosin (0.2nM) were of varying times at 22°C, followed by second incubations of 60 minutes at 37°C. Nonspecific binding was determined in the presence of 10  $\mu$ M phentolamine.

$\alpha_{1a}$ -AR whole cells			
1st incubation	$pK_i$	$n_H$	Fig.
15 mins	$7.51 \pm 0.09$	$0.6 \pm 0.1$	2.35
	$4.17 \pm 0.89$		
30 mins	$6.07 \pm 0.51$	$0.5 \pm 0.1$	2.35
	$3.93 \pm 1.01$		
60 mins	$6.58 \pm 0.29$	$0.6 \pm 0.1$	2.35
	$4.32 \pm 1.01$		

**TABLE 2.6****Displacement at 37°C and 22°C: whole cells**

Comparison of affinity estimates from rat-1 fibroblasts expressing bovine  $\alpha_{1A}$ -AR in whole cells. Displacement of [<sup>3</sup>H]prazosin (0.2nM) was determined using an updated RLB binding protocol with increasing concentrations of competing ligands from at least four experiments performed in duplicate ( $\pm$  S.E.M). First incubation of 60 minutes at 22°C was followed by a second incubation of 30 minutes at varying temperature. Nonspecific binding was determined in the presence of 10  $\mu$ M phentolamine.

Ligand	37°C			22°C		
	$pK_i$	$n_H$	Fig	$pK_i$	$n_H$	Fig.
RS100329	6.78 $\pm$ 1.19	1.0 $\pm$ 0.1	2.13	6.72 $\pm$ 1.08	0.9 $\pm$ 0.1	2.13
QAPB	10.89 $\pm$ 0.03 6.33 $\pm$ 0.71	0.6 $\pm$ 0.2	2.14	8.96 $\pm$ 0.18 6.39 $\pm$ 0.76	0.5 $\pm$ 0.2	2.14

**TABLE 2.7a**Displacement after [<sup>3</sup>H]prazosin for 60 minutes: Membranes and whole cells

Comparison of affinity estimates from rat-1 fibroblasts expressing bovine  $\alpha_{1b}$ -AR in membranes and whole cells. Displacement of [<sup>3</sup>H]prazosin (0.2nM) was determined using an updated RLB binding protocol with increasing concentrations of competing ligands from at least four experiments performed in duplicate ( $\pm$  S.E.M). First incubation of 60 minutes at 22°C was followed by a second incubation of varying time at 37°C. Nonspecific binding was determined in the presence of 10  $\mu$ M phentolamine.

Ligand + incubation	Whole cells			Membranes		
	$pK_i$	$n_H$	Fig.	$pK_i$	$n_H$	Fig.
<b>Adrenaline</b>						
15 mins	5.75 $\pm$ 0.09 3.84 $\pm$ 0.82	0.6 $\pm$ 0.2	2.38	5.51 $\pm$ 1.51	0.8 $\pm$ 0.1	2.37
30 mins	7.23 $\pm$ 0.03 4.10 $\pm$ 1.15	0.5 $\pm$ 0.2	2.38	5.36 $\pm$ 1.48	0.9 $\pm$ 0.1	2.37
60 mins	6.11 $\pm$ 0.08 4.37 $\pm$ 0.58	0.6 $\pm$ 0.2	2.38	5.44 $\pm$ 1.58	0.8 $\pm$ 0.1	2.37
<b>Noradrenaline</b>						
15 mins	7.90 $\pm$ 0.32 3.89 $\pm$ 1.15	0.5 $\pm$ 0.2	2.43	5.26 $\pm$ 1.62	0.7 $\pm$ 0.1	2.42
30 mins	6.97 $\pm$ 0.24 3.96 $\pm$ 0.89	0.5 $\pm$ 0.1	2.43, 2.36	5.09 $\pm$ 1.44	0.7 $\pm$ 0.1	2.42
60 mins	7.86 $\pm$ 0.06 4.52 $\pm$ 1.30	0.6 $\pm$ 0.2	2.43	5.10 $\pm$ 1.54	0.8 $\pm$ 0.1	2.42
<b>Prazosin</b>						
30 mins	7.18 $\pm$ 1.57	1.4 $\pm$ 0.1	2.15	9.12 $\pm$ 1.26	1.10 $\pm$ 0.3	2.15

**TABLE 2.7b****Displacement after [<sup>3</sup>H]prazosin for 60 minutes: Whole cells**

Comparison of affinity estimates from rat-1 fibroblasts expressing bovine  $\alpha_{1a}$ -AR in whole cells. Displacement of [<sup>3</sup>H]prazosin (0.2nM) was determined using an updated RLB binding protocol with increasing concentrations of competing ligands from at least three experiments performed in duplicate ( $\pm$  S.E.M). First incubation of 60 minutes at 22°C was followed by a second incubation of varying time at 37°C. Nonspecific binding was determined in the presence of 10  $\mu$ M phentolamine.

Ligand + incubation	$\alpha_{1a}$ -AR whole cells		
	$pK_i$	$n_H$	Fig.
Phenylephrine			
15 mins	7.12 $\pm$ 0.37	0.6 $\pm$ 0.2	2.44
	4.04 $\pm$ 1.15		
30 mins	8.00 $\pm$ 0.29	0.5 $\pm$ 0.2	2.44
	3.77 $\pm$ 0.85		
60 mins	4.06 $\pm$ 0.93	0.9 $\pm$ 0.3	2.44
	4.32 $\pm$ 1.01		
<hr/>			
<i>(R)</i> -A-61603			
30 mins	8.92 $\pm$ 0.39	0.3 $\pm$ 0.2	2.45
	4.59 $\pm$ 0.77		
<hr/>			
L-765314			
30 mins	5.48 $\pm$ 1.12	1.0 $\pm$ 0.2	2.20
<hr/>			
BMY7378			
30 mins	6.39 $\pm$ 1.36	0.9 $\pm$ 0.1	2.21
<hr/>			

**TABLE 2.8****Corticosterone influence on adrenaline**

Comparison of affinity estimates from rat-1 fibroblasts expressing bovine  $\alpha_{1a}$ -AR in whole cells. Displacement of [ $^3$ H]prazosin (0.2nM) was determined using an updated RLB binding protocol with increasing concentrations of adrenaline from at least three experiments performed in duplicate ( $\pm$  S.E.M). Experiments performed in the presence and part-presence of 1 $\mu$ M corticosterone. First incubation of 60 minutes at 22°C was followed by a second incubation of varying time at 37°C. Nonspecific binding was determined in the presence of 10  $\mu$ M phentolamine.

Ligand + incubation	Corticosterone			Part-Corticosterone		
	$pK_i$	$n_H$	Fig	$pK_i$	$n_H$	Fig.
Adrenaline						
15 mins	4.08 $\pm$ 1.36	0.7 $\pm$ 0.1	2.40	4.06 $\pm$ 1.05	0.8 $\pm$ 0.2	2.39
30 mins	4.23 $\pm$ 1.40	0.8 $\pm$ 0.1	2.40	4.36 $\pm$ 0.92	0.9 $\pm$ 0.1	2.39
60 mins	4.00 $\pm$ 1.21	1.0 $\pm$ 0.2	2.40	6.95 $\pm$ 0.24 4.01 $\pm$ 0.74	0.4 $\pm$ 0.2	2.39

**TABLE 2.9****Concanavalin A: influence on adrenaline**

Comparison of affinity estimates from rat-1 fibroblasts expressing bovine  $\alpha_{1A}$ -AR in whole cells. Displacement of [ $^3$ H]prazosin (0.2nM) was determined using an updated RLB binding protocol with increasing concentrations of adrenaline from at least three experiments performed in duplicate ( $\pm$  S.E.M). Experiments performed in the presence and part-presence of 0.25 mg/ml concanavalin A. First incubation of 60 minutes at 22°C was followed by a second incubation of 30 minutes at 37°C. Nonspecific binding was determined in the presence of 10  $\mu$ M phentolamine.

Ligand + incubation	Concanavalin A			Part-Concanavalin A		
	$pK_i$	$n_H$	Fig	$pK_i$	$n_H$	Fig.
Adrenaline						
30 mins	$8.37 \pm 0.07$	$0.5 \pm 0.2$	2.41	$7.06 \pm 0.63$	$0.4 \pm 0.1$	2.41
	$3.98 \pm 0.86$			$4.10 \pm 1.14$		

**TABLE 2.10**

Effect of pre-incubation time on displacement by QAPB: whole cells

Comparison of affinity estimates from rat-1 fibroblasts expressing bovine  $\alpha_{1a}$ -AR in whole cells. Displacement of [ $^3$ H]prazosin (0.2nM) was determined using an updated RLB binding protocol with increasing concentrations of QAPB from at least three experiments performed in duplicate ( $\pm$  S.E.M.). First incubation of varying time at 22°C was followed by a second incubation of 60 minutes at 22°C. Nonspecific binding was determined in the presence of 10  $\mu$ M phentolamine.

$\alpha_{1a}$ -AR whole cells			
Ligand + incubation	$pK_i$	$n_H$	Fig.
QAPB			
60 mins	$6.63 \pm 0.96$	$0.5 \pm 0.2$	2.16
90 mins	$11.01 \pm 0.51$ $7.54 \pm 1.07$	$0.4 \pm 0.1$	2.16

**TABLE 2.11****Displacement from whole cells and membranes at 4°C**

Comparison of affinity estimates from rat-1 fibroblasts expressing bovine  $\alpha_{1a}$ -AR in membranes and whole cells. Displacement of [<sup>3</sup>H]prazosin (0.2nM) was determined using an updated R1.B binding protocol with increasing concentrations of competing ligands from at least three experiments performed in duplicate ( $\pm$  S.E.M). First incubation of 60 minutes at 22°C was followed by a second incubation of varying time at 4°C. Nonspecific binding was determined in the presence of 10  $\mu$ M phentolamine.

Ligand + incubation	Whole cells			Membranes		
	$pK_i$	$n_H$	Fig.	$pK_i$	$n_H$	Fig.
Noradrenaline						
15 mins	5.96 $\pm$ 0.70	0.7 $\pm$ 0.3	2.46			
60 mins	5.41 $\pm$ 0.81	0.4 $\pm$ 0.2	2.46	7.64 $\pm$ 0.69	0.8 $\pm$ 0.6	2.47
QAPB						
15 mins	8.25 $\pm$ 0.91	0.7 $\pm$ 0.3	2.18	9.16 $\pm$ 0.96	1.1 $\pm$ 0.5	2.19
60 mins	7.90 $\pm$ 0.64	0.6 $\pm$ 0.3	2.18			

**TABLE 2.12****Concanavalin A: influence on QAPB: whole cells**

Comparison of affinity estimates from rat-1 fibroblasts expressing bovine  $\alpha_{1A}$ -AR in whole cells. Displacement of [<sup>3</sup>H]prazosin (0.2nM) was determined using an updated RLB binding protocol with increasing concentrations of QAPB from at least four experiments performed in duplicate ( $\pm$  S.E.M). Experiments performed in the presence and absence of 0.25-mg/ml concanavalin A. Cells pre-treated with con A for 90 minutes at 22°C before first incubation of 60 minutes at 22°C with [<sup>3</sup>H]prazosin. This was followed by a second incubation of 30 minutes at 37°C. Nonspecific binding was determined in the presence of 10  $\mu$ M phentolamine.

Ligand + incubation	Concanavalin A			No Concanavalin A		
	$pK_i$	$n_H$	Fig.	$pK_i$	$n_H$	Fig.
QAPB						
60 mins	$7.71 \pm 1.22$	$0.5 \pm 0.05$	2.17	$11.01 \pm 0.51$ $7.54 \pm 1.07$	$0.4 \pm 0.1$	2.17

## 2.3 DISCUSSION

### 2.3.1 Competitive inhibition of radioligand binding

#### 2.3.1.1 Agonists

Radioligand binding is now a standard technique used for analysis of the interactions of ligands with their receptors. The technique is fast, simple and allows the investigation of the pharmacological properties of many drugs within a short time. Used in conjunction with modern analysis techniques (Uhlen & Wikberg, 1991; Wikberg *et al*, 1998), the results obtained are generally very accurate and highly reproducible. The most commonly used radioligand binding technique is the membrane filtration receptor assay. A variation on the membrane assay, the intact cell radioligand binding assay, has specific advantages in certain circumstances, such as screening large numbers of small cell samples and studies of receptor internalisation (Bylund & Toews, 1993).

The present study determined the binding affinities of various ligands in a series of competition-binding experiments with the  $\alpha_1$ -AR-selective antagonist [ $^3$ H]prazosin as the radioligand. The binding affinities of agonists and antagonists for the bovine  $\alpha_{1a}$ -AR were first assessed in standard membrane preparation assays. This is the common method used to determine  $\alpha_1$ -AR affinity (Kenny *et al*, 1996).

A well-studied example of agonist interaction with receptors linked to GPCRs is by comparing the competition of agonists with radio-labelled antagonist in the presence or absence of GTP (or its analogues). When the competing ligand used is an agonist, the situation becomes more complex than using an antagonist, as an agonist will interact with its G protein. The first step in this interaction is a decrease in the affinity of the nucleotide-binding site for GDP and the formation of a ternary complex (agonist-receptor- $\alpha$  empty  $\beta\gamma$ ). When GTP is absent, the activated receptor is unable to dissociate from the  $\alpha$ -subunit and so the receptor and G protein are essentially locked together or frozen (Bockaert *et al*, 1997). This frozen state increases the stability of the agonist-receptor complex and so increase the agonist's affinity for the receptor,

hence a high affinity state. However, when GTP is present, this transient state disappears, the activated receptor is able to dissociate from the  $\alpha$ -subunit and the GPCR cycle proceeds as normal, i.e. the activated  $\alpha$ -GTP subunit interacts with the effector protein. This represents the low affinity state. When the G protein concentration is limiting or when some receptors cannot associate to G proteins, then a mixture of agonist-receptor and agonist-receptor-G protein complexes can accumulate to give rise to a heterogeneous binding curve. This behaviour is generally only observed for agonist binding on membranes in the absence of GTP. The heterogeneous binding curve will become homologous when GTP is present.

Binding affinities for the non-subtype selective  $\alpha_1$ -AR agonist phenylephrine were determined in the presence and absence of the non-hydrolysable GTP analogue GTP- $\gamma$ -S in the present study. The results were consistent with the aforementioned GTP theory. In the absence of the GTP analogue, the binding curve was biphasic, displaying both high and low affinity components. When GTP- $\gamma$ -S was present, the binding curve was monophasic. This phenomenon was reproduced using the specific  $\alpha_{1a}$ -AR agonist (*R*)-A-61603 as the competing ligand. (*R*)-A-61603 displayed a higher affinity for the bovine  $\alpha_{1a}$ -AR than phenylephrine, which would be expected due to its specificity for  $\alpha_{1a}$ -ARs. Knepper and colleagues (1995) had previously reported that (*R*)-A-61603 was highly selective for the cloned bovine  $\alpha_{1a}$ -AR expressed in mouse fibroblasts.

As mentioned previously, the high affinity state is not observed in the presence of GTP; therefore in whole cells containing GTP, all receptors should be under the low affinity state. Binding is heterogeneous in membranes (high and low affinity states), but homogeneous in whole cells (low affinity state). The binding affinities for [<sup>3</sup>H]prazosin sites of various agonists and antagonists were assessed on whole-cell preparations harbouring the recombinant bovine  $\alpha_{1a}$ -AR in the present study, as this is the modality in which visualisation of ligand-ligand competition is assessed. With phenylephrine as the competing ligand in the presence and absence of GTP- $\gamma$ -S, the whole cell binding curve was consistent with the literature. Both curves almost superimposed on top of each other, displaying a monophasic nature and low affinity  $pK_i$  values.

The situation was slightly different when (*R*)-A-61603 was used as the competitor in whole cell binding assays in the absence and presence of GTP- $\gamma$ -S. In the absence of the GTP analogue, the curve was biphasic and there was only an approximate 75% of displacement. This suggested that there were binding sites inaccessible to (*R*)-A-61603. A possible explanation was that the uptake of the ligand into the cell was time dependant and subsequent experiments with a 2-hour incubation period resulted in a full displacement. According to the literature, in the presence of GTP- $\gamma$ -S, binding curves were expected to be monophasic. To investigate further the thought that (*R*)-A-61603 might displace the radiolabel, a series of experiments were performed with incubation times of 15, 30 and 120 minutes. All three binding curves were biphasic and repeated the phenomenon where 25% of binding sites seemed inaccessible. The various incubation times had no real effect on the binding curves and it appears that (*R*)-A-61603 can cause full displacement after 2 hours in the absence of GTP- $\gamma$ -S, but not in the presence of the analogue. Visualisation experiments where (*R*)-A-61603 could displace QAPB from intracellular compartments may help resolve this issue.

Both noradrenaline and adrenaline displayed similar low affinity binding curves in membrane preparations. In whole cells, noradrenaline displayed both high and low affinity components whereas adrenaline displayed only a low affinity component. Our early hypothesis was that catecholamines were delivered to intracellular receptors via an extraneuronal monoamine transporter (EMT) (Grundemann *et al*, 1998). The EMT (previously known as Uptake<sub>2</sub>) reportedly functions optimally at 37°C. The present study compared competition-binding experiments at 22°C and 37°C using noradrenaline as the competing ligand. Both curves were biphasic, displaying high and low affinity binding sites and similar pK<sub>i</sub> values. Literature maintains that incubation temperature can be varied as desired, although 37°C is the usual choice since the goal is to maintain physiological conditions (Bylund & Toews, 1993).

Extraneuroal transport is the predominant pathway for terminating the actions of circulating adrenaline and noradrenaline (Eisenhofer *et al*, 1996). Although neuronal and extraneuronal uptakes compete for released catecholamines, these transport systems have distinct pharmacological profiles, that is, affinity for substrates and

sensitivity to various drugs (Grundmann *et al*, 1998). Iversen & Salt discovered in 1970 that corticosterone was a potent inhibitor of Uptake<sub>2</sub>. When the transporter is blocked, the metabolism of noradrenaline is attenuated. To test the hypothesis that noradrenaline and other ligands may penetrate the cells via the EMT, binding experiments were performed in the presence of corticosterone. The result was a biphasic binding curve where a high affinity component was followed by a small plateau phase before the low affinity component. This curve was evidently more biphasic than the binding curve where no corticosterone was present. The high affinity component may represent an initial displacement from cell membranes and the plateau phase may correspond to a difficulty of the ligand to penetrate the cell. The low affinity phase would therefore represent the ability of ligands to displace the radiolabel from intracellular binding sites. Although corticosterone did not prevent total displacement, one could speculate that it caused greater difficulty in the cellular penetration process by the ligand, as represented by a more pronounced plateau phase on the binding curve.

Altering the incubation times in binding experiments using noradrenaline as the competitor reinforced the concept that the uptake of a ligand into the cell may be time dependant. A 30-minute incubation achieved a greater displacement than a 15-minute incubation.

### **2.3.1.2 Antagonists**

The binding affinities of various antagonists were also determined in the present study in a series of competition-binding experiments with [<sup>3</sup>H]prazosin as the radioligand. Similar to agonist experiments, the binding affinities were determined in membrane and whole cell preparations.

Prazosin displayed a similar binding profile in cells and membrane preparations. The binding curves were monophasic and suggest prazosin has no difficulty penetrating the cell. QAPB (BODIPY FL-prazosin) was expected to display a similar binding profile to prazosin as it is structurally related to prazosin. The binding curve for QAPB was monophasic and it shared similar affinity for bovine  $\alpha_{1A}$ -AR membranes

as prazosin. In whole cells, QAPB continued the trend of a high affinity component preceding a slow sustained plateau and low affinity component. The difficulty in cellular penetration by QAPB may be related to the size or chemical properties of the fluorescent component of the compound. Light surroundings had no effect on the ability of QAPB to displace the radiolabel. QAPB is apparently a light-sensitive compound (McGrath *et al*, 1996) and a comparison of binding curves for QAPB in dark and light surroundings were made. Both curves were almost identical; hence QAPB is fully operational under light conditions.

Consistent with its specificity for  $\alpha_{1a}$ -ARs (Williams *et al*, 1999), RS100329 displayed the highest affinity binding values out of all antagonists tested. In whole cells preparations, RS100329 continued the trend of a high affinity component (approx. 20% of binding sites) followed by a slow sustained plateau phase before the low affinity component (approx. 80% of binding sites), which again raised the possibility of a difficulty of cellular penetration. The selective  $\alpha_{1b}$ -AR antagonist L-765314 displayed a much lower affinity for the bovine  $\alpha_{1a}$ -AR than prazosin, QAPB and RS100329, consistent with its specificity for  $\alpha_{1b}$ -ARs (Patane *et al*, 1998). The curve was biphasic, which again suggests that this antagonist has difficulty with regards to cellular penetration.

The binding affinities for [ $^3$ H]prazosin sites of the subtype selective  $\alpha_{1d}$ -AR antagonist BMY7378 were assessed on membrane and whole-cell preparations harbouring the recombinant bovine  $\alpha_{1a}$ -AR and also the recombinant human  $\alpha_{1d}$ -AR. BMY7378 displayed a lower affinity than prazosin, QAPB and RS100329 at bovine  $\alpha_{1a}$ -AR whole cells, but produced subnanomolar affinity for the displacement of [ $^3$ H]prazosin at human  $\alpha_{1d}$ -AR whole cells. Both whole cell curves were monophasic suggesting BMY7378 has no difficulty penetrating cells. These results relate to work by Piascik and Perez (2001), who studied the cellular distribution of the  $\alpha_1$ -AR subtypes in stably transfected fibroblasts as well as cultured vascular smooth muscle cells. They detected very little cell surface expression of the  $\alpha_{1D}$ -AR. Most of the  $\alpha_{1D}$ -AR immunoreactivity was detected intracellularly in a perinuclear orientation. The groups also found, using  $\alpha_1$ -AR/GFP fusion proteins, that  $\alpha_{1A}$ -AR fluorescence was detected on the cell surface and intracellularly, whereas  $\alpha_{1D}$ -AR fluorescence was

detected intracellularly. This lends weight to the theory that  $\alpha_1$ -ARs are expressed, to one degree or another, in intracellular compartments (Hrometz *et al.*, 1999; Piascik & Percz, 2001).

There is an interesting observation in the present study when comparing membrane and whole-cell binding curves for agonists and antagonists. There is higher affinity for membrane preparations compared with whole cells for nearly all agonists and antagonist tested. The only notable exception is that of prazosin. MacKenzie and colleagues (2000) reported similar results. The group found binding affinities were greater in membrane preparations than in cells, but also is greater in native prostatic tissues or cells compared with recombinant receptors. This supported, for native prostatic tissue, the theory of Ford (1998) who proposed that receptors expressed in cells displayed lower binding affinities than those in membrane preparations.

### ***2.3.2 New radioligand binding protocol 1***

A new displacement protocol was devised that would recreate a more 'real' context of visualisation experiments than in standard ligand-ligand competition. The "classical" RLB approach dealt more with the 30-minute competition between competitor and radiolabel. The timing and order of addition of competitive ligands were now very important. The time of incubation has to be sufficient to ensure that equilibrium (or at least steady state) has been achieved. Most radioligands appear to reach steady state at room temperature within 20-60 minutes (Bylund & Toews, 1993). The new protocol therefore pre-equilibrated cells with [ $^3$ H]prazosin for varying time periods, followed by the addition of displacing ligand for a further time course. This meant that competitors had to displace [ $^3$ H]prazosin from its pre-equilibrated location(s).

A 60-minute pre-incubation between cells and radiolabel at room temperature resulted in the greatest displacement by noradrenaline. Noradrenaline was added for 60 minutes at 37°C following pre-incubation between cells and [ $^3$ H]prazosin. This was consistent with Bylund & Toews (1993) theory that radioligands appear to reach

steady state at room temperature within 20-60 minutes. A 15- and 30-minute pre-incubation between cells and radiolabel resulted in similar results. There was a lesser displacement of radiolabel. A comparison of noradrenaline binding curves using the 'classical' and new RLB approaches revealed that noradrenaline was less effective at displacing [<sup>3</sup>H]prazosin after binding was pre-established (new RLB protocol).

### *2.3.3 New radioligand binding protocol 2*

Imaging results from the present study had revealed that 60 minute was sufficient time for an analogue of prazosin to reach and maintain steady state. These results coupled with results from the previous displacement RLB protocol helped establish that 60 minutes was indeed sufficient time for [<sup>3</sup>H]prazosin binding to reach equilibrium to bovine  $\alpha_{1a}$ -AR whole cells both on cell surface and at intracellular binding sites. An expanded version of the aforementioned displacement protocol provides a more consistent comparison with visualisation studies. A fixed 60-minute pre-incubation between cells (or membranes) and [<sup>3</sup>H]prazosin at room temperature was followed by addition of the displacing ligand for varying times.

Before any further investigations using the new displacement protocol, the initial aim was to determine if incubation temperature had any effect on ligands ability to displace [<sup>3</sup>H]prazosin following the pre-incubation period. A 30-minute incubation with RS100329 at 37°C caused a slightly greater displacement of [<sup>3</sup>H]prazosin than the same time period at 22°C. The same result was confirmed using QAPB as displacing ligand. A comparison of RS100329 and QAPB binding curves using the 'classical' and new displacement approaches revealed that the antagonists were less effective at displacing [<sup>3</sup>H]prazosin after binding was pre-established (new displacement protocol). This new displacement protocol would suggest that both antagonists find it much harder to penetrate cells, although both curves are less biphasic than their respective "classical" binding curves. Similar to its binding profile with the "classical" RLB approach, prazosin displayed no apparent difficulty penetrating the cell, but consistent with RS100329 and QAPB, prazosin was less

effective at displacing [<sup>3</sup>H]prazosin using the new displacement protocol. Both L-765314 and BMY7378 displayed ease in cellular penetration. L-765314 had a higher binding affinity value using the displacement protocol than the "classical" RLB protocol. BMY7378 displayed exactly the same binding profile when comparing both protocols. These differences in cellular penetration by various antagonists may be structurally related.

As the equilibration between cells, [<sup>3</sup>H]prazosin and incubation temperature for maximum displacement had been resolved, a new series of experiments determined whether displacement was time-dependant once the displacing ligand had been added. Following pre-incubation between radiolabel and membranes, a series of adrenaline concentrations were added for 15, 30 and 60 minutes at 37°C. The three curves were almost superimposed and displayed similar one-site binding affinities, consistent with our thought that varying incubation times should have no effect on displacement from the cell surface. The same results were obtained on membrane preparations using noradrenaline as the displacing ligand. The same protocol in whole cell preparations produced an expected response with adrenaline as displacing ligand. The smallest displacement occurred after a 15-minute incubation and the 60-minute incubation produced the greatest displacement. Again, the same results were obtained with noradrenaline as the displacing ligand. Phenylephrine produced an unusual set of results in that a 15-minute incubation provided the greatest displacement. (*R*)-A-61603 experienced obvious difficulty penetrating the cells as noted by the extremely biphasic binding curve. In a continuing trend, there were approximately 20-25% of binding sites being inaccessible to (*R*)-A-61603. One common trend with agonists and antagonists when using the new displacement protocol was the lower affinity values than when used with the "classical" RLB approach.

Zhu and Toews (1995) proposed that the low affinity for agonists observed in assays with whole cells was a result of receptor internalisation. Exposure of cells to agonist for the time required to achieve "equilibrium" during competition binding assay would lead to receptor internalisation. As [<sup>3</sup>H]prazosin is relatively lipophilic, it can cross cell membranes and label internalised receptors. In contrast, agonists such as adrenaline are quite hydrophilic and cross cell membranes poorly. Adrenaline would

have limited accessibility to the internalised receptors and therefore inhibit binding to internalised receptors only at high concentrations. Zhu and Toews (1995) modified their hypothesis for whole cell low affinity binding to propose that either sequestration within the plasma membrane or endocytosis into intracellular vesicles resulted in low affinity binding.

Corticosterone was again used to investigate our proposal that ligands may penetrate cells and access intracellular binding sites via an EMT. Adrenaline was used as the displacing ligand rather than noradrenaline as adrenaline is believed to be a better substrate for the EMT (Grundemann *et al*, 1998). These results gave a more "real" displacement result than experiments carried out with corticosterone using the "classical" RLB protocol. With corticosterone present only after pre-equilibrium with [<sup>3</sup>H]prazosin, this would reveal whether corticosterone had any direct single effect on the ability of adrenaline to penetrate the cells. The only displacement curve that suggested corticosterone might be having some, if any effect, was following the 60-minute incubation with adrenaline, which produced a biphasic curve, although a full displacement was still achieved. With corticosterone present for the entire experiment, the only difference noted was again following the 60-minute incubation with adrenaline. When compared with the same control experiment, there was a lower affinity in the presence of corticosterone and also a greater displacement in the control experiment. This is still not strong enough evidence to suggest that ligands are crossing the cell membrane and accessing intracellular binding sites via the EMT. One thing is definite from the displacement protocols and that is that agonists and antagonist can both cross the cell membrane by a certain mechanism and displace [<sup>3</sup>H]prazosin from intracellular binding sites throughout the cytosol.

To test the theory proposed by Zhu and Toews (1995) that ligands access intracellular compartments via an endocytotic mechanism, the present study investigated the effects of the endocytotic blocker concanavalin A on displacement by agonists and antagonists. Using protocols identical to the corticosterone experiments, it was clear that concanavalin A was having no effect on the displacement of radiolabel by adrenaline. There was still a near full displacement using both protocols suggesting that the endocytotic blocker was exerting no effect. QAPB, when used as the displacing ligand, produced a slightly more positive result in similar experiments

using concanavalin A. When compared with the biphasic control displacement curve, the QAPB displacement curve in the presence of concanavalin A appeared monophasic which suggested a difficulty in cellular penetration. There seemed to be difficulty of cellular penetration until  $10^{-8}$ M, where only approximately 15% of radiolabel had been displaced. There was then a sharp fall in the displacement curve and at the next QAPB concentration ( $3 \times 10^{-8}$ M), approximately 75-80% of radiolabel had been displaced. It was apparent something crucial had occurred between the two concentrations. A possible explanation is that concanavalin A is blocking the endocytotic pathway until a certain high QAPB concentration is applied which can overcome this blockade and hence allow QAPB access to intracellular binding sites.

### ***2.3.4 New radioligand binding protocol 3***

If displacing ligands do penetrate cells and access intracellular binding sites by endocytosis, they should fail to penetrate cells at  $4^{\circ}\text{C}$  as a result of the endocytotic mechanism being halted by cold temperatures. This proposal formed the basis of altering the displacement protocol to investigate the effects cold temperature has on displacement. It has been previously reported that endocytosis is temperature dependent and that the internalisation process is blocked at  $4^{\circ}\text{C}$  (Von Zastrow & Kobilka, 1994).

In the present study, using whole cells preparations, noradrenaline and QAPB displayed similar curves, with only approximately 25% of all sites displaced. There was a marginally greater displacement after 60 minutes using noradrenaline. This would suggest that the 25% of displaced sites might represent cell surface receptors. These whole cell results correlate with the theory that endocytosis is blocked at low temperature. Surprisingly, there were only 25% of sites displaced when the experiments were repeated in membrane preparations. A full displacement from the cell surface had been expected and these different results prove difficult to explain.

### 3.0 Aims & objectives

To investigate whether quantitative agonist/antagonist pharmacology could be carried out at the single cell level on  $\alpha_1$ -adrenoceptors using a Rat-1 fibroblast cell line that stably expresses the recombinant  $\alpha_{1a}$ -adrenoceptor. Using microspectrofluorimetry techniques, this would be determined by:

1. Defining the nature of the  $[Ca^{2+}]_i$  signal for the bovine  $\alpha_{1a}$ -AR
2. Evaluating functional Fura-2  $Ca^{2+}$  responses to  $\alpha_{1a}$ -AR activation that allows us to make a quantitative analysis for the interaction of agonists and antagonists.

Another aim was to use direct visualisation techniques to investigate:

1. The ability of a fluorescent antagonist to enter cells and bind to intracellular compartments throughout the cytoplasm.
2. Can ligands penetrate cells and displace the fluorescent antagonist from such intracellular binding sites?
3. To determine the identity of these intracellular compartments and hence comment on the process of cellular penetration by ligands.

### **3.1 METHODS**

#### **3.1.1 Cell Culture.**

Rat-1 Fibroblasts stably expressing the bovine  $\alpha_{1a}$ -AR were used. Cells were grown in monolayers in DMEM containing 10% (v/v) foetal bovine serum, 100 IU./ml penicillin, 100 $\mu$ g/ml streptomycin and 1mM L-glutamine in a 95% air and 5% CO<sub>2</sub> atmosphere at 37°C. Selection was maintained by adding geneticin (G418) (400 $\mu$ g/ml) to the growth media.

##### **3.1.1.1 Freezing cells.**

Cells are grown to confluence in 75cm<sup>3</sup> tissue culture flasks, growth media removed and replaced with fresh growth media containing 10% DMSO. Cells are removed from the base of the flask by gentle agitation and aliquoted into 1.5ml cryovials. The cryovials are stored at -70°C for 24 hours, then labelled in cryocanes and frozen down in liquid nitrogen.

##### **3.1.1.2 Growing cells**

Single cryovials containing the cells were removed from cryocanes and left in the incubator at 37°C for 5-7 minutes. Once defrosted, cells were carefully triturated twice and added to a 25cm<sup>3</sup> tissue culture flask. 10mls of DMEM was slowly added to the flask, the flask cap was loosened and the suspension left in the incubator for 40 minutes to allow cells to adhere to the base of the flask. The media was then removed, replaced with 5mls fresh media and flask placed in incubator to be maintained as normal.

### 3.1.1.3 Cell splitting

Cells were maintained using a "splitting" process. Once cells reached confluence, growth media was removed and cells washed with 2mls 0.25% trypsin/EDTA solution. The wash solution was removed, replaced with 2.5mls fresh trypsin/EDTA and 2.5mls fresh DMEM, then transferred to a 13ml centrifuge tube and centrifuged at 4000rpm for 3 minutes at 22°C. The solution was discarded, leaving a pellet. Using a Pasteur pipette, 1ml DMEM was added and carefully triturated 15-20 times before adding a further 9mls DMEM. After resuspending, 1ml of the cell suspension was added to a 25cm<sup>3</sup> tissue culture flask along with 4mls fresh DMEM. The cells were then placed in the incubator and maintained as normal.

### 3.1.2 Measurement of $[Ca^{2+}]_i$

#### 3.1.2.1 Microspectrofluorimetry analysis

Rat-1 fibroblasts stably expressing the bovine  $\alpha_{1a}$ -AR were removed from culture flasks using trypsin/EDTA and washed by centrifugation-resuspension in fresh DMEM. Aliquots of this suspension were plated onto 22mm circular coverslips and grown overnight. Cells were then loaded (15 minutes at 37°C) with the dual excitation  $Ca^{2+}$ -sensitive dye Fura-2 AM (1 $\mu$ M). A rise or fall in  $[Ca^{2+}]_i$  causes a corresponding effect in the Fura-2 fluorescence ratio recorded from cells loaded with this dye and this allows receptor/voltage-mediated changes in  $[Ca^{2+}]_i$  to be microspectrofluorimetrically monitored (Grynkiewicz *et al.*, 1985). Fura-2 fluorescence ratios (excitation wavelengths, 340 and 380nm) were recorded at 4-Hz intervals from single cells at room temperature. Experimental set-up is shown in Figure 3.1. Data was digitised and recorded directly to computer disk using an interface and associated software (Version 5.2) obtained from Cairn Research Ltd (Faversham, Kent, UK).

### *3.1.2.2 Calcium Imaging*

After 15 minutes loading with Fura-2 at 37°C, the cells were mounted in a chamber attached to the stage of a Nikon Diaphot inverted microscope where the cells were superfused with physiological saline solution (130mM NaCl, 5mM KCl, 20mM HEPES, 10mM D-glucose, 1mM MgCl<sub>2</sub> and 1mM CaCl<sub>2</sub>, pH 7.4). An Optoscan monochromator (Cairn Research, Faversham, Kent, UK) positioned between a 70W Xenon lamp and the epifluorescence port of the microscope was used to alternate the excitation wavelength between 340, 380 and 488nm (band pass 10nm) and to control the excitation frequency. Excitation light was reflected from a custom designed dichroic mirror through a Nikon 40x oil immersion FLUOR objective (NA=1.3). Fura-2 emitted fluorescence emitted light at 515nm was monitored either by a low noise COHU CCD camera or a photomultiplier tube with a bialkali photocathode. Using Meta Fluor imaging software (Universal Imaging Corp, West Chester, PA, USA), the images obtained using the CCD camera were stored and analysed digitally. Images obtained for each excitation wavelength were collected every 1second; exposure to excitation light was always 80ms/image and the time interval between the acquisition of each image was approximately 2 milli seconds. Cells were delimited by producing a mask that contained pixel values above a threshold applied to the 380nm image and time dependant changes in  $[Ca^{2+}]_i$  were calculated from the ratio of two background subtracted images.

### *3.1.2.3 Response curves*

A desired group of cells was selected using cell autofluorescence and the focal plane fixed by locking the focus motor. The system was then set to acquire images at 30-second intervals. After a baseline had been established for 5-7 minutes in every experiment, a 30-second pulse of agonist (1µM phenylephrine in all experiments) was applied to determine the maximum Fura-2 Ca<sup>2+</sup>-signal in control solution alone. The initial experiments involved a test for cell photobleaching where 4nM QAPB was applied for approximately 4 hours. The subsequent experiments looked at the time to equilibrium between QAPB and the cells, along with the simultaneous recording of the antagonised fura-2 Ca<sup>2+</sup> signals. In such experiments 0.5, 2, 4 or 6nM QAPB was

equilibrated with the cells for a period of 1.5 hours before construction of concentration- $\text{Ca}^{2+}$  response curves. The concentration- $\text{Ca}^{2+}$  response curves to phenylephrine were constructed by noncumulative addition (10-minute pulses of increasing concentrations of phenylephrine applied at 15-minute intervals).

#### **3.1.2.4 Data analysis**

Agonist-evoked  $[\text{Ca}^{2+}]_i$  signals were quantified as the difference between the baseline resting ratio level and that attained at the peak response. The effect of QAPB on the concentration- $\text{Ca}^{2+}$  response to phenylephrine was analysed by expressing the data as a fraction of the maximal peak response elicited by phenylephrine in control solution alone.

#### **3.1.3 Materials and Chemicals**

Cell culture plastics were supplied by Falcon. DMEM with sodium pyruvate, foetal bovine serum, L-glutamine, penicillin, streptomycin and trypsin/EDTA were purchased from Gibco Life Technologies (Paisley, Scotland); Fura 2-AM, phenylephrine HCl, adrenaline, noradrenaline, HEPES and EDTA were purchased from Sigma (Dorset, UK); The (*R*)-enantiomer of A-61603 was a gift from Dr Michael Meyer (Abbott Laboratories, Abbott Park, IL); L-765314 was a gift from Dr Michael Patane (Merck & Co. Inc, NJ); RS100329 (Dr. Michelson, Roche Bioscience, Palo Alto, CA); Phentolamine, QAPB, prazosin HCl, BMY7378 dihydrochloride from Research Biochemicals Inc. (Natick, MA); [ $^3\text{H}$ ]Prazosin (0.2nM; specific activity, 76 Ci/mmol) was ordered from Amersham Corp. (Arlington Heights, IL).

Stock solutions for each chemical were prepared in distilled water or dimethyl sulfoxide and subsequently aliquoted and stored at  $-20^\circ\text{C}$ . These stock solutions were diluted to working concentrations in the physiological salt solution on each experimental day.

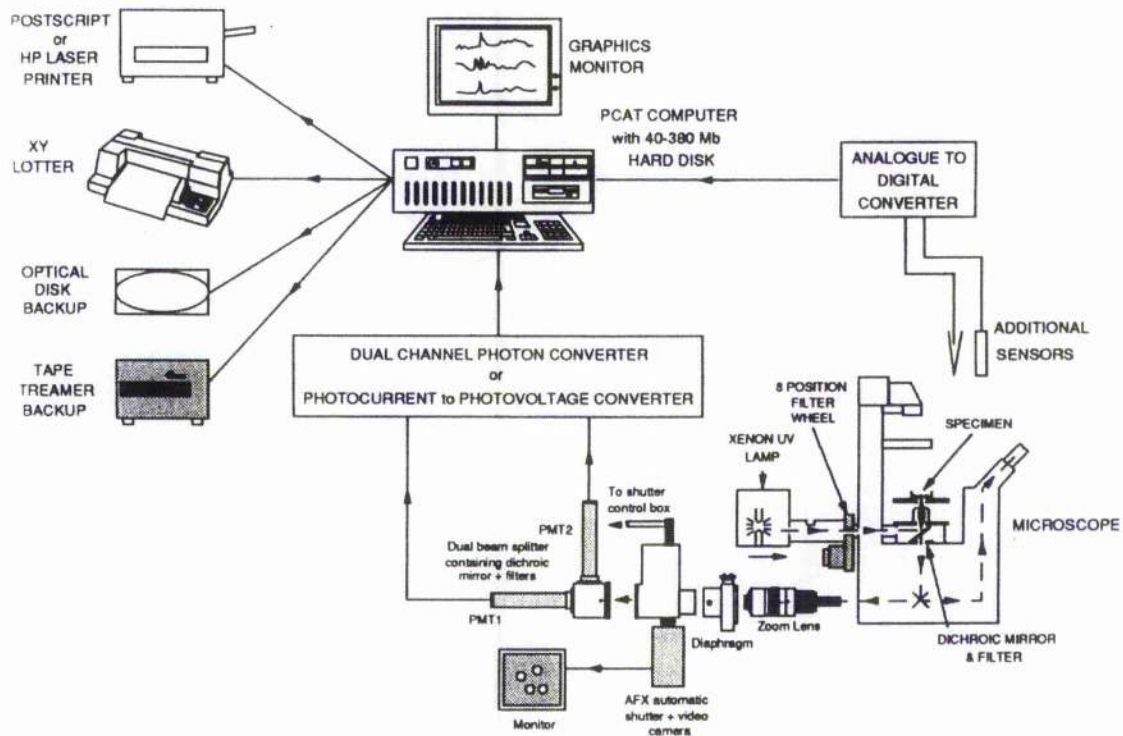


Figure 3.1 Diagram of experimental set-up.

## 3.2 RESULTS

### 3.2.1 Microspectrofluorimetry

The objective was to investigate whether quantitative agonist/antagonist pharmacology could be carried out at the single cell level on  $\alpha_1$ -ARs using a Rat-1 fibroblast cell line that stably expresses the recombinant  $\alpha_{1a}$ -AR. Schwinn and colleagues (1995) reported that an  $\alpha_1$ -AR cloned from bovine brain (e.g. bovine  $\alpha_{1a}$ -AR) activates IP formation in R-1Fs, suggesting that this receptor raises  $[Ca^{2+}]_i$  in this cell-line by mobilising intracellular  $Ca^{2+}$  stores via the PLC- $\beta$ /IP<sub>3</sub> pathway. In the present study, microspectrofluorimetry analysis using the dual excitation  $Ca^{2+}$ -sensitive fluorescent dye Fura-2 AM was used to monitor  $[Ca^{2+}]_i$ . Fura-2 (Fig. 3.2) is a fluorescent derivative of the  $Ca^{2+}$ -chelator BAPTA which itself is an aromatic analogue of the  $Ca^{2+}$ -selective chelator EGTA. The fluorescence excitation spectrum of Fura-2 is shown in Figure 3.3. The excitation wavelengths for Fura-2 are 340 and 380nm and its  $K_d$  value is 220, when 50% of Fura is bound to 50% of free calcium ions.

#### 3.2.1.1 $Ca^{2+}$ signalling mechanism

##### 3.2.1.1.1 Effect of phenylephrine on $[Ca^{2+}]_i$

The first experiments determined the nature of the  $[Ca^{2+}]_i$  signal for the bovine  $\alpha_{1a}$ -AR. Figure 3.4A shows the rise in  $[Ca^{2+}]_i$  in response to a 3 minute pulse of the  $\alpha_1$ -AR agonist, phenylephrine (1 $\mu$ M). The response was transient, followed by a rapid decline and small plateau phase, despite the continued presence of phenylephrine.

##### 3.2.1.1.2 Role of external $Ca^{2+}$ in $[Ca^{2+}]_i$ responses to phenylephrine

Phenylephrine (1 $\mu$ M) evoked a transient rise in  $[Ca^{2+}]_i$  without the sustained phase when applied under  $Ca^{2+}$ -free conditions (Fig. 3.4B). Subsequent elevation of

external  $\text{Ca}^{2+}$  (1mM), in the continued presence of phenylephrine, resulted in a maintained rise in  $[\text{Ca}^{2+}]_i$ . Once the nature of the functional  $[\text{Ca}^{2+}]_i$  signal had been determined, we wanted to make a quantitative analysis of agonist and antagonist pharmacology at this recombinant subtype in single R-1Fs by evaluating functional  $\text{Ca}^{2+}$ -responses to receptor-activation, which would allow us to predict a relationship for the interaction of agonists and antagonists.

### **3.2.2 Functional pharmacology studies**

#### **3.2.2.1 Agonist response**

Concentration- $\text{Ca}^{2+}$  response curves (CRCs) were recorded to cells stimulated noncumulatively with 30-second exposures (applied at 5-minute intervals) to increasing concentrations ( $10^{-8} \rightarrow 10^{-3}\text{M}$ ) of phenylephrine (Fig. 3.5). Phenylephrine caused a concentration-dependant peak increase in  $[\text{Ca}^{2+}]_i$ . Beyond the concentration of phenylephrine that produced the maximum response ( $> 3 \times 10^{-5}\text{M}$ ), the concentration-response relationship displayed an inverse phase (i.e., smaller peak responses to increasing concentrations of phenylephrine).

#### **3.2.2.2 Photobleaching**

Before studying any interaction between phenylephrine and the fluorescently labelled  $\alpha_1$ -AR antagonist QAPB, the possibility of a "photobleaching" effect by QAPB was tested. Initially, a 30 second pulse of phenylephrine was applied to evoke an increase in  $[\text{Ca}^{2+}]_i$  (Fig. 3.6). QAPB (4nM) was then applied for a 4 hour and 10 minute period. The trace in Figure 3.6 shows that no degradation/photobleaching of QAPB intensity existed, hence a steady state equilibrium binding of QAPB could be maintained over a 4 hour time period. This had no effect on the Fura-2  $\text{Ca}^{2+}$  signal.

### 3.2.2.3 Antagonist response

#### 3.2.2.3.1 4nM QAPB

Antagonism versus phenylephrine by QAPB was assessed across the concentration ranges indicated by its RLB affinities. Figure 3.7 shows the time to equilibrium between QAPB (4nM) and the recombinant  $\alpha_{1a}$ -AR along with the simultaneous recording of the antagonised Fura-2  $\text{Ca}^{2+}$  signals.

The cells were loaded (15 minutes at 37°C) with Fura-2 (1 $\mu\text{M}$ ). A control 30 second pulse of phenylephrine (1 $\mu\text{M}$ ) was applied to evoke an increase in  $[\text{Ca}^{2+}]_i$  (not shown). This was followed by a 60-minute incubation at room temperature with 4nM QAPB. This is shown as the initial part of the trace in Figure 3.7, representing the time for QAPB to reach equilibrium binding. A series of phenylephrine concentrations (0.1  $\rightarrow$  1000 $\mu\text{M}$ ) were then applied, each for 3 minutes, followed by a 6-minute washout. The top trace in Figure 3.7 shows the QAPB signal, which has an excitation wavelength of 490nm. The middle two traces show the two Fura-2 signals, one excited at 380nm and the other at 340nm. The bottom trace shows the ratio 340/380nm Fura-2  $\text{Ca}^{2+}$  signal. Subsequent traces show only the ratio  $\text{Ca}^{2+}$  signal.

The experiment shown in Figure 3.7 is reproduced in Figure 3.8A with only the QAPB signal and ratio Fura-2  $\text{Ca}^{2+}$  signal shown. The first three concentrations of phenylephrine (0.1  $\rightarrow$  1 $\mu\text{M}$ ) produced no rise in  $[\text{Ca}^{2+}]_i$ , but as each subsequent concentration increased, so did the  $[\text{Ca}^{2+}]_i$  until a maximum response was elicited by 1000 $\mu\text{M}$ . Despite the first three concentrations producing no rise in  $[\text{Ca}^{2+}]_i$ , they did cause a decrease in QAPB fluorescent intensity. The intensity increased following each washout period. The  $\text{Ca}^{2+}$  signal associated with each increasing phenylephrine concentration ( $\square$  3 $\mu\text{M}$ ) reached a maximal response before the corresponding decrease in QAPB intensity had reached its maximum. Throughout the experiment, the intensity of the QAPB signal remained constant.

### **3.2.2.3.2 Removal of QAPB**

The graph shown in Figure 3.8B represents the end of the experiment shown in Figure 3.8A when QAPB was removed from the control saline solution and left for 60 minutes until the QAPB intensity had maximally decreased. A 3-minute pulse of phenylephrine (1000 $\mu$ M) was applied and the resulting rise in  $[Ca^{2+}]_i$  was far greater than the corresponding phenylephrine concentration elicited in the presence of 4nM QAPB.

### **3.2.2.3.3 0.5nM QAPB**

The following experiments studied the time to equilibrium between the recombinant  $\alpha_{1a}$ -AR and varying concentrations of QAPB, along with the simultaneous recording of the antagonised Fura-2  $Ca^{2+}$  signals.

The lowest concentration of QAPB studied was 0.5nM. After incubation with Fura-2, a control 30 second pulse of phenylephrine (1 $\mu$ M) was applied to evoke an increase in  $[Ca^{2+}]_i$  (not shown). Cells were then incubated with QAPB (0.5nM) until equilibrium binding was achieved (Fig. 3.9). A series of phenylephrine concentrations (0.1  $\rightarrow$  300 $\mu$ M) were then applied, each for 3 minutes, followed by a 5-minute washout. The first two concentrations of phenylephrine (0.1  $\rightarrow$  0.3 $\mu$ M) produced no rise in  $[Ca^{2+}]_i$ , but as each subsequent concentration increased, so did the  $[Ca^{2+}]_i$  until a maximum response was achieved by 300 $\mu$ M. Despite the initial two phenylephrine concentrations producing no rise in  $[Ca^{2+}]_i$ , they did cause a small decrease in QAPB fluorescent intensity. For each phenylephrine concentration tested, the corresponding decrease in QAPB fluorescence intensity remained minimal. After phenylephrine concentrations above and including 1 $\mu$ M, the  $Ca^{2+}$  responses were transient, followed by a rapid decline and small plateau phase that continued into each washout period. Throughout the experiment, the intensity of the QAPB signal remained unaltered.

#### **3.2.2.3.4 2nM QAPB**

The next concentration of QAPB studied was 2nM. Following incubation with Fura-2, a control 30 second pulse of phenylephrine (1 $\mu$ M) was applied to evoke an increase in  $[Ca^{2+}]_i$  (shown on left of Fig. 3.10). Once equilibrium binding had been achieved between the cells and QAPB, 10-minute phenylephrine concentrations (0.1  $\rightarrow$  3000 $\mu$ M) were applied, each followed by a 15-minute washout (Fig. 3.10). Although the first two phenylephrine concentrations produced no  $Ca^{2+}$  response, there was a decrease in QAPB fluorescence intensity. The following  $Ca^{2+}$  responses were all transient, followed by small, sustained plateau phases. For each phenylephrine concentration, the maximum rise in  $[Ca^{2+}]_i$  had occurred before the corresponding decrease in QAPB fluorescent intensity had started. Throughout the experiment, the intensity of the QAPB signal remained unaltered.

#### **3.2.2.3.5 6nM QAPB**

The highest concentration of QAPB studied was 6nM. Following incubation with Fura-2, a control 30 second pulse of phenylephrine (1 $\mu$ M) was applied to evoke an increase in  $[Ca^{2+}]_i$  (shown on left of Fig. 3.11). Cells were then incubated with QAPB (6nM) for 75 minutes, until equilibrium binding was achieved. Phenylephrine concentrations (1  $\rightarrow$  300 $\mu$ M) were applied, each for 10 minutes, followed by a 15-minute washout (Fig. 3.11). There was no  $Ca^{2+}$  response to 1 $\mu$ M phenylephrine, but a decrease in QAPB intensity was observed. From 3 to 30 $\mu$ M phenylephrine, the  $Ca^{2+}$  response was transient, followed by a small, sustained plateau phase and then a rapid decline upon washout. The final two  $Ca^{2+}$  responses were transient followed by a rapid decline and then a small increase before declining upon washout. For each phenylephrine concentration, the maximum rise in  $[Ca^{2+}]_i$  had occurred before the corresponding decrease in QAPB fluorescent intensity had started. Following every washout, the QAPB signal recovered, but its intensity diminished with every corresponding phenylephrine concentration.

### **3.2.2.4 Insurmountable Antagonism**

Phenylephrine-evoked  $[Ca^{2+}]_i$  signals were quantified as the difference between the baseline resting ratio level and that attained at the peak response. The effect of QAPB on the CRC to phenylephrine was analysed by expressing the data as a fraction of the maximal peak response elicited by phenylephrine in control solution alone.

QAPB produced concentration-dependant, nonparallel, rightward displacements in the control CRC to phenylephrine with a decrease in the maximal response (Fig. 3.12). This represents an example of insurmountable antagonism, where the antagonist dissociates very slowly (or not at all) from the receptor. It is demonstrated by a rightward shift as the antagonist concentration increases and also by a decrease in maximal response.

### **3.2.3 Direct visualisation of fluorescent binding**

#### **3.2.3.1 QAPB displacement by agonist**

Using our knowledge from radioligand binding studies, competitive binding was visualised in cells using QAPB. Rat-1 fibroblasts were mounted in a chamber attached to the stage of an inverted microscope and superfused with physiological saline containing 4nM QAPB for 60 minutes at room temperature until equilibrium binding was achieved. Cells were imaged by exciting at 490nm and 515nm and QAPB fluorescence was monitored by a CCD camera.

Pediani and colleagues had demonstrated, using HEK293T cells, that QAPB is specific for intracellular human  $\alpha_{1a}$ -AR binding sites (results not published). HEK293T cells are very similar to Rat-1 fibroblasts in that they are secretory cells. Using non-transfected HEK293T cells, there was no evidence of intracellular QAPB binding after cells had been stained with the nuclear dye Hoechst 33342 and 20nM QAPB. Using transiently transfected HEK293T cells, there was clear evidence of

intracellular binding to human  $\alpha_{1a}$ -AR binding sites around the perinuclear region when nuclear staining and QAPB images were merged.

Figure 3.13 shows 4nM QAPB equilibrium binding after 60 minutes at room temperature. Within minutes of QAPB application, diffuse low intensity fluorescent signals were observed in punctate intracellular sites that were scattered throughout the cell cytoplasm. After a period of 60 minutes, higher intensity fluorescent signals were observed in larger punctate structures. This suggests a pattern of fluorescence evolves from a small particulate distribution towards larger structures with time.

Following 4nM QAPB equilibrium binding, three 15-minute applications of the  $\alpha_1$ -AR agonist phenylephrine, were added cumulatively (Figs 3.14 & 3.15). The first concentration of 0.1 $\mu$ M phenylephrine caused a large decrease in QAPB fluorescent intensity, but the following 1 $\mu$ M caused only a small decrease. The application of 10 $\mu$ M produced a further decrease in QAPB intensity. Following the 15-minute application of the 10 $\mu$ M concentration, phenylephrine was removed from the perfusion system and a reversal of QAPB fluorescent intensity was observed (Figs 3.14 & 3.16). This is an example of reverse displacement. Figure 3.17 compares the fluorescent intensity of QAPB in the absence and presence of phenylephrine. Following three consecutive applications of phenylephrine, there was a clear, large decrease in fluorescent intensity. Phenylephrine can therefore penetrate the cells and cause displacement from these intracellular sites of high fluorescent intensity.

### 3.2.3.2 *QAPB displacement by antagonist*

A similar series of experiments was performed to determine if antagonists could penetrate cells and displace QAPB in a manner similar to that of agonists.

Cells were incubated with 5nM QAPB at room temperature for 75 minutes. The cells exhibited fluorescence at punctate intracellular sites and more diffusely over the cell surface (Fig. 3.18A). All of the fluorescent sites could be totally displaced by phentolamine (0.1mM). Phentolamine was present for 150 minutes after equilibrium

binding was established (Fig. 3.18B), thus establishing that the fluorescent receptor ligand complexes were accessible to competitive ligands.

### 3.2.3.3 *Intracellular compartment localisation*

It was now clear that QAPB entered the cell and could be detected within intracellular compartments throughout the cytoplasm. When reconstructed as a short movie, the motions of individual fluorescent signals observed in punctate structures were very characteristic of endocytosis. Some were inert and displayed short range, bi-directional motion, whereas others appeared to move with great speed. To visualise and determine the identity of these intracellular compartments, a fluorescently tagged agonist was used that could identify subcellular compartments. Transferrin Alexa Fluor<sup>546</sup> is an early and recycling endosomal marker for endocytosis via clathrin-coated pits (Anderson, 1998). This was used to identify the endocytotic recycling pathway. Transferrin Alexa Fluor<sup>546</sup> also binds to the constitutively active Transferrin receptor, which localises predominantly in the perinuclear-recycling compartment (PNRC). Hence, the red dye is ideal for labelling the PNRC. Constitutively active receptors can be transported to the PNRC and then recycled back to the cell surface independent of agonist activation.

Unstimulated Rat-1 fibroblasts expressing the bovine  $\alpha_{1a}$ -AR were labelled with the nuclei dye Hoechst 33342. This corresponds with the blue coloured panel in Figure 3.19. Cells were then labelled with 4nM QAPB for 75 minutes at room temperature and the corresponding green image is shown in Figure 3.19. The image shows that QAPB fluorescence corresponding to intracellular binding sites was scattered throughout the cytoplasm. Cells were further labelled with Transferrin-Alexa Fluor<sup>546</sup> for 75 minutes. This corresponds with the red panel shown in Figure 3.19. The merged images for all three labels are shown in Figure 3.20. Areas of yellow/orange colour represent overlapping sites of co-localisation. The areas of co-localisation appear to be found around the perinuclear region, thus implying that  $\alpha_{1a}$ -AR ligand complexes follow the endocytotic recycling pathway, via early and recycling endosomes. A similar experiment is shown with a larger field of cells in Figure 3.21.

Again, the areas of overlap appear to be of a perinuclear nature. Although in both experiments a small proportion of fluorescent sites overlapped with the Transferrin-Alexa Fluor<sup>546</sup>, there was a large proportion of the QAPB binding sites that were spatially distinct from the recycling endosomal marker. These sites can be clearly identified as single green "hotspots".

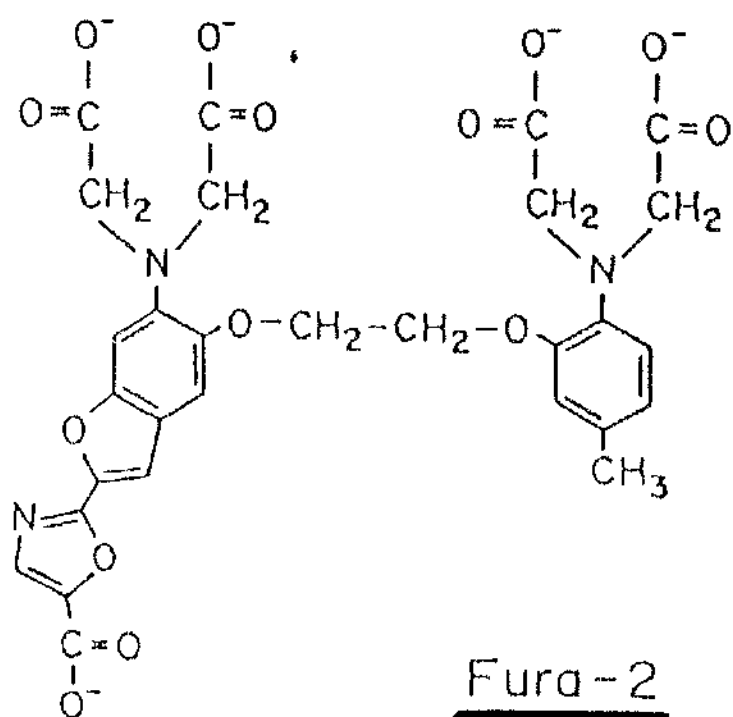


**Figure 3.2** Chemical structure of fura-2

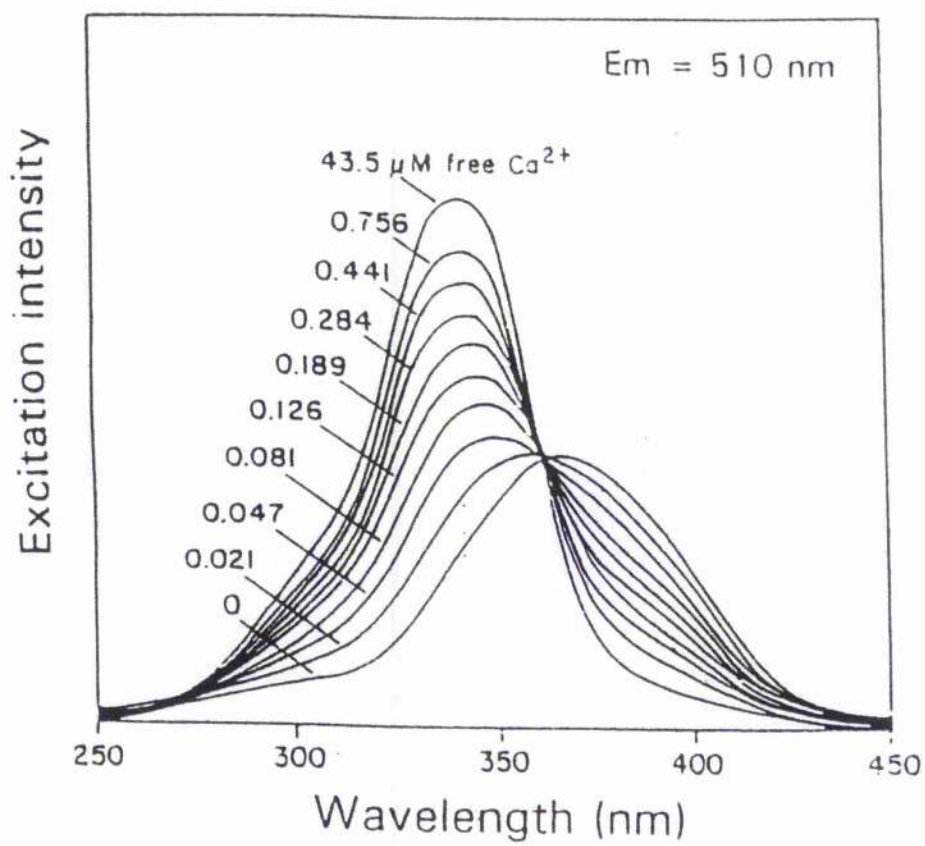


**Figure 3.3** Excitation spectra of fura-2 in increasing concentrations of free calcium

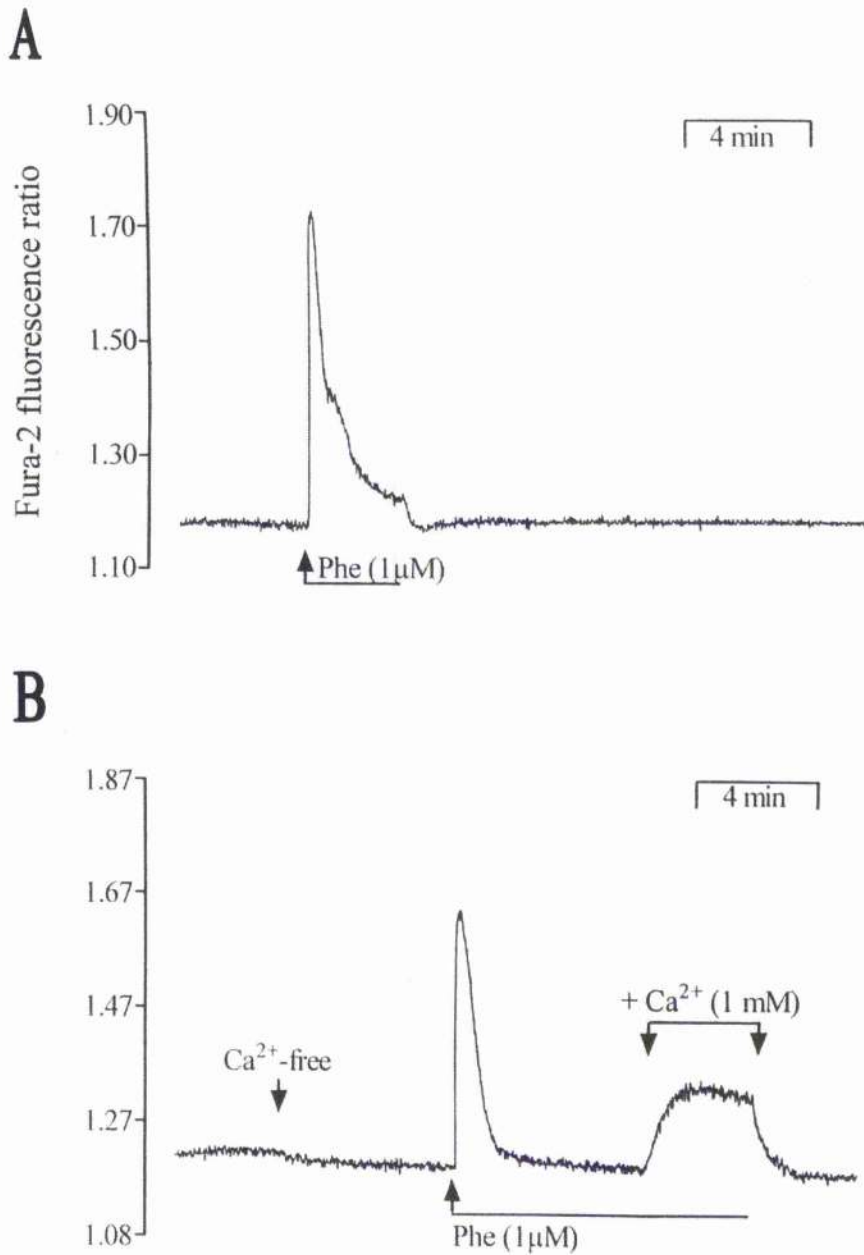


**Figure 3.4** Trace showing changes in  $[Ca^{2+}]_i$  in response to phenylephrine in R-1Fs stably expressing the bovine  $\alpha_{1a}$ -AR. **A**, effects of phenylephrine ( $1\mu M$ ; 3-minute pulse) on  $[Ca^{2+}]_i$  in the presence of external  $Ca^{2+}$  (1mM). **B**, resolution of the initial  $Ca^{2+}$  release phase from the sustained  $Ca^{2+}$  entry phase. Cells were superfused with  $Ca^{2+}$ -free saline solution and exposed to phenylephrine ( $1\mu M$ ) before external  $Ca^{2+}$  was restored to 1mM for the indicated period.

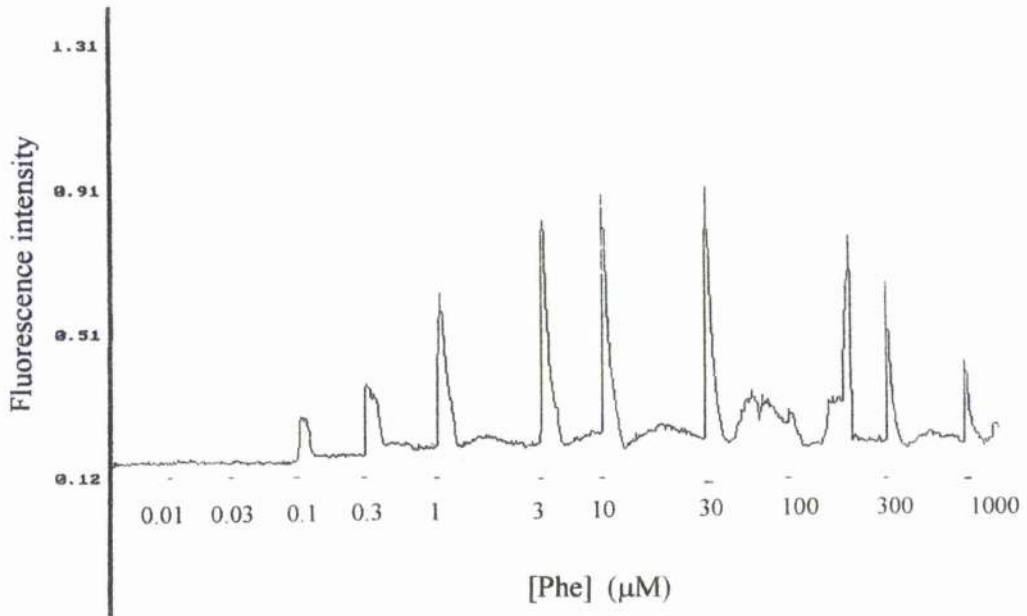


**Figure 3.5** Concentration-dependant effects of phenylephrine on  $[Ca^{2+}]_i$  release. Phenylephrine was applied for 30 seconds and delivered at 5-minute intervals. Trace shows effects evoked by increasing concentration of phenylephrine on  $[Ca^{2+}]_i$ .

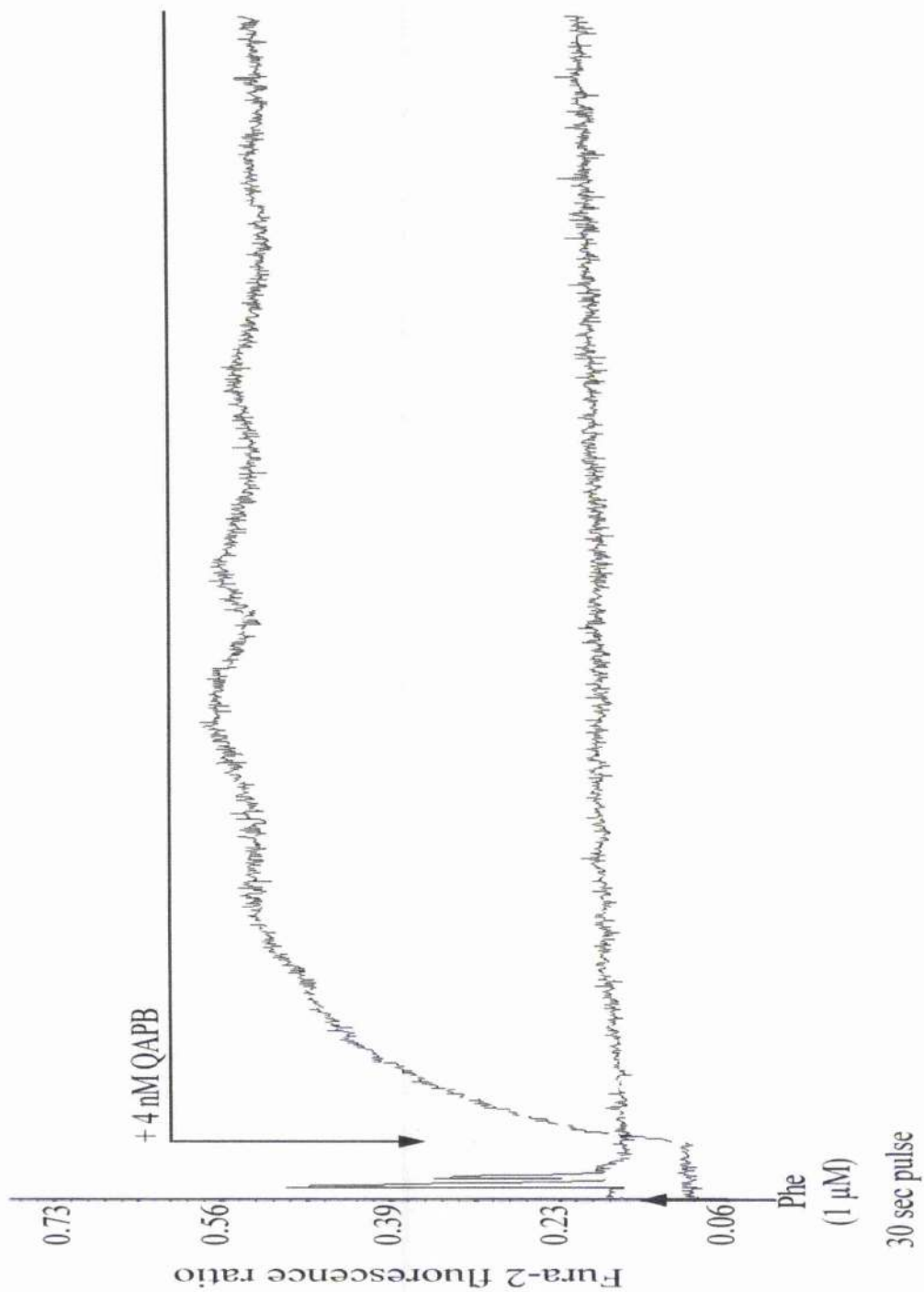


**Figure 3.6** Maintenance of steady state equilibrium binding of QAPB (4nM) over a 4-hour time period in R-1Fs stably expressing the bovine  $\alpha_{1a}$ -AR. Cells were exposed to 30-second pulse of phenylephrine (1 $\mu$ M) before QAPB was applied. Trace shows no degradation/photobleaching of QAPB intensity existed.

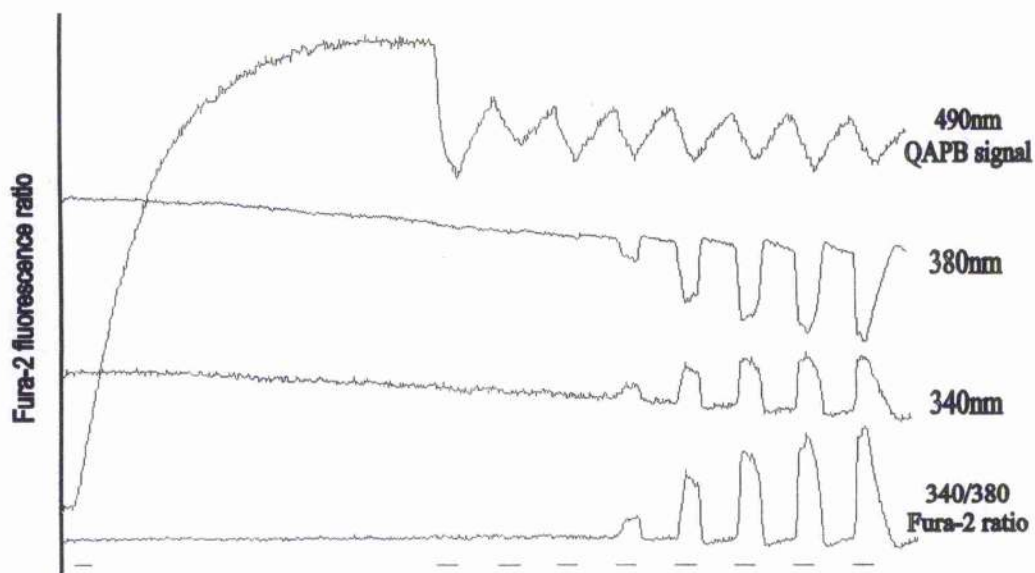


**Figure 3.7** Trace showing simultaneous recording of QAPB signal and antagonised fura-2  $\text{Ca}^{2+}$  responses. Top trace shows 4nM QAPB signal, which has an excitation wavelength of 490nm. Middle two traces show two Fura-2 signals, one excited at 380nm and the other at 340nm. Bottom trace shows ratio 340/380nm Fura-2  $\text{Ca}^{2+}$  signal.

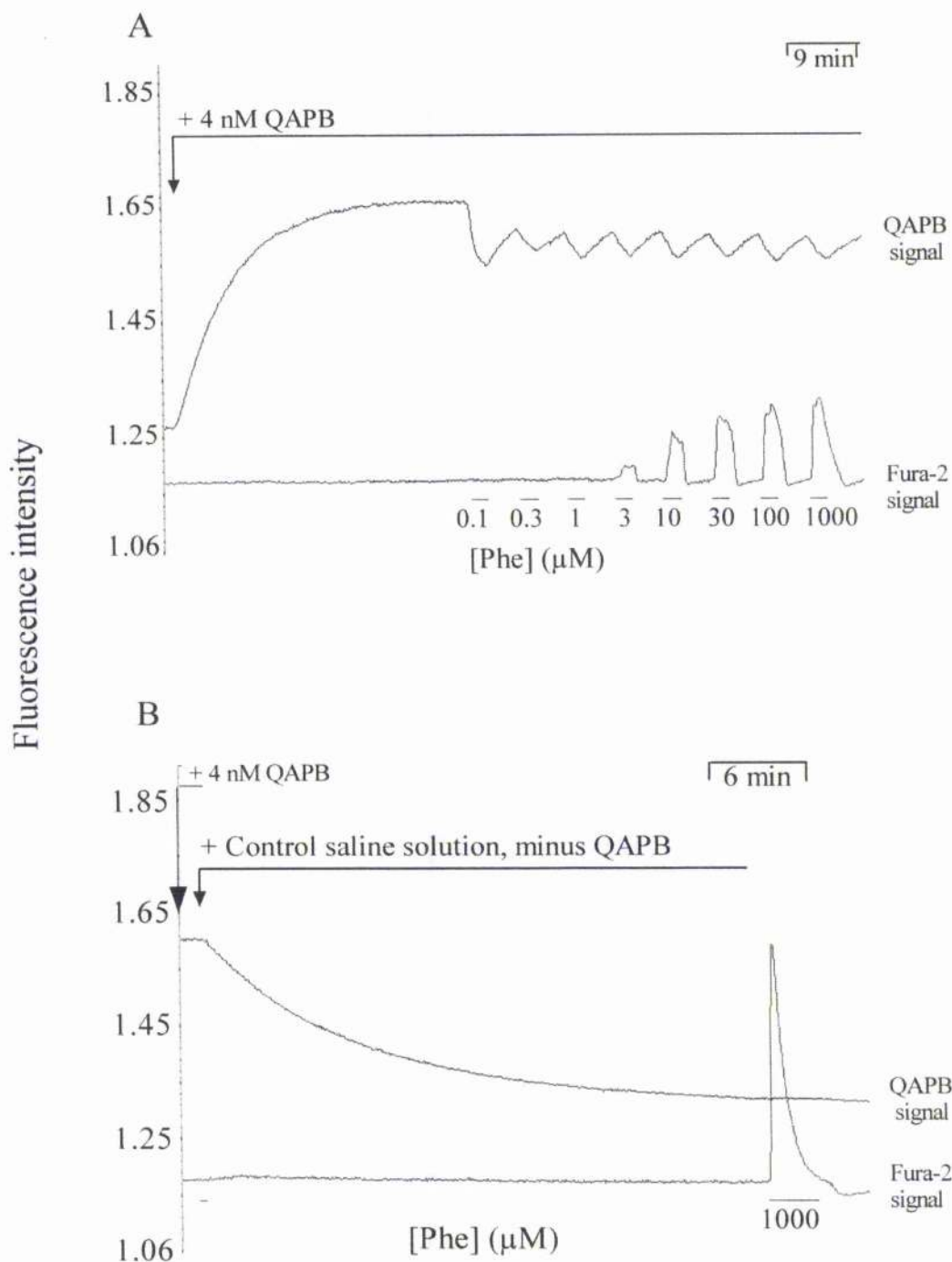


**Figure 3.8** Trace represents same experiment shown in Figure 3.7, with only the QAPB signal and antagonised ratio 340/380 Fura-2  $Ca^{2+}$  signal shown. **A**, trace shows time to equilibrium between cells and 4nM QAPB and the subsequent effect of phenylephrine (0.1  $\rightarrow$  1000 $\mu$ M) applications (3-minutes at 6-minute intervals) on  $[Ca^{2+}]_i$ . **B**, trace shows removal of 4nM QAPB from control saline solution, the subsequent decrease in QAPB intensity signal and rise in  $[Ca^{2+}]_i$  following a 3-minute pulse of phenylephrine (1000 $\mu$ M).

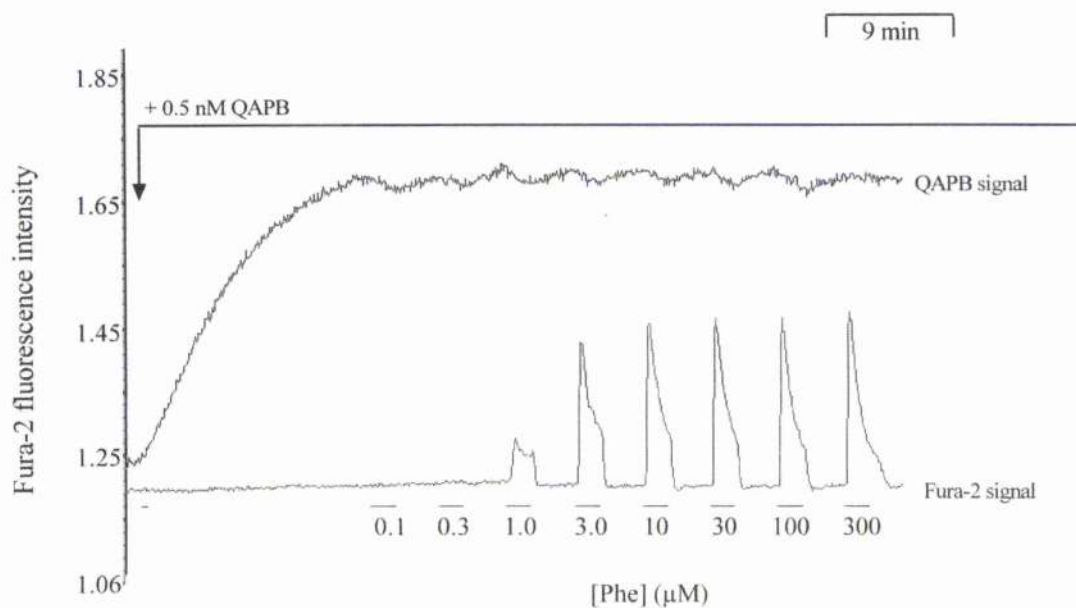


**Figure 3.9** Trace showing simultaneous recording of 0.5nM QAPB signal and antagonised fura-2  $\text{Ca}^{2+}$  responses. Trace shows time to equilibrium between cells and 0.5nM QAPB and the subsequent effect of phenylephrine (0.1  $\rightarrow$  300 $\mu\text{M}$ ) applications (3-minutes at 5-minute intervals) on  $[\text{Ca}^{2+}]_i$ .

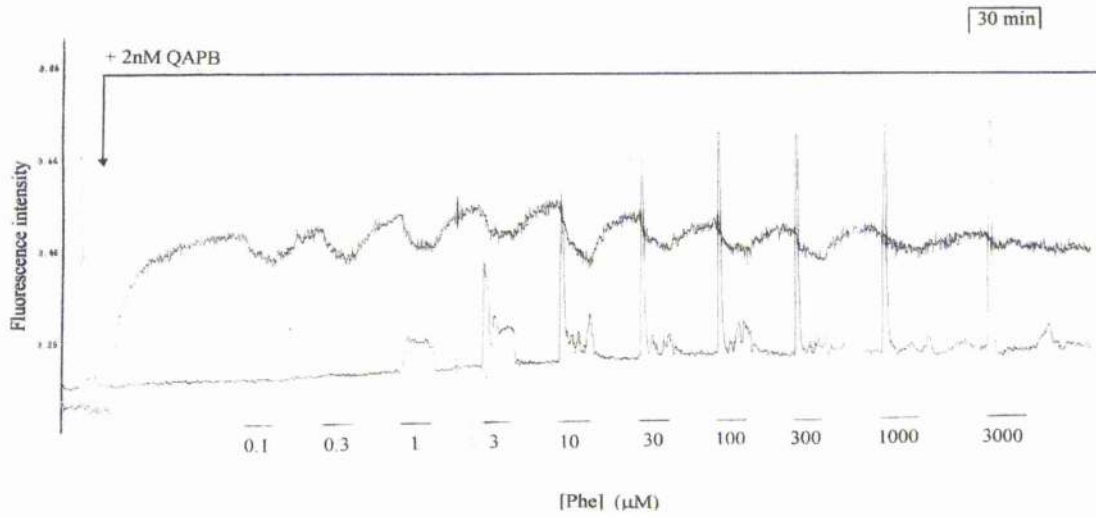


**Figure 3.10** Trace showing simultaneous recording of 2nM QAPB signal and antagonised fura-2  $\text{Ca}^{2+}$  responses. Trace shows time to equilibrium between cells and 2nM QAPB and the subsequent effect of phenylephrine (0.1  $\rightarrow$  3000 $\mu\text{M}$ ) applications (10-minutes at 15-minute intervals) on  $[\text{Ca}^{2+}]_i$ .

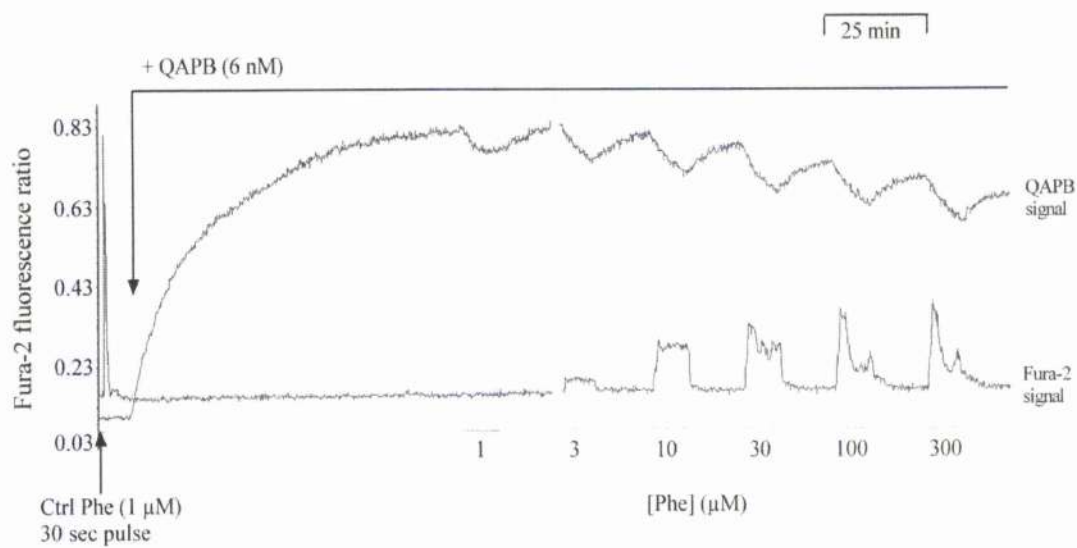


**Figure 3.11** Trace showing simultaneous recording of 6nM QAPB signal and antagonised fura-2  $\text{Ca}^{2+}$  responses. Trace shows time to equilibrium between cells and 6nM QAPB and the subsequent effect of phenylephrine (1  $\rightarrow$  300 $\mu\text{M}$ ) applications (10-minutes at 15-minute intervals) on  $[\text{Ca}^{2+}]_i$ .

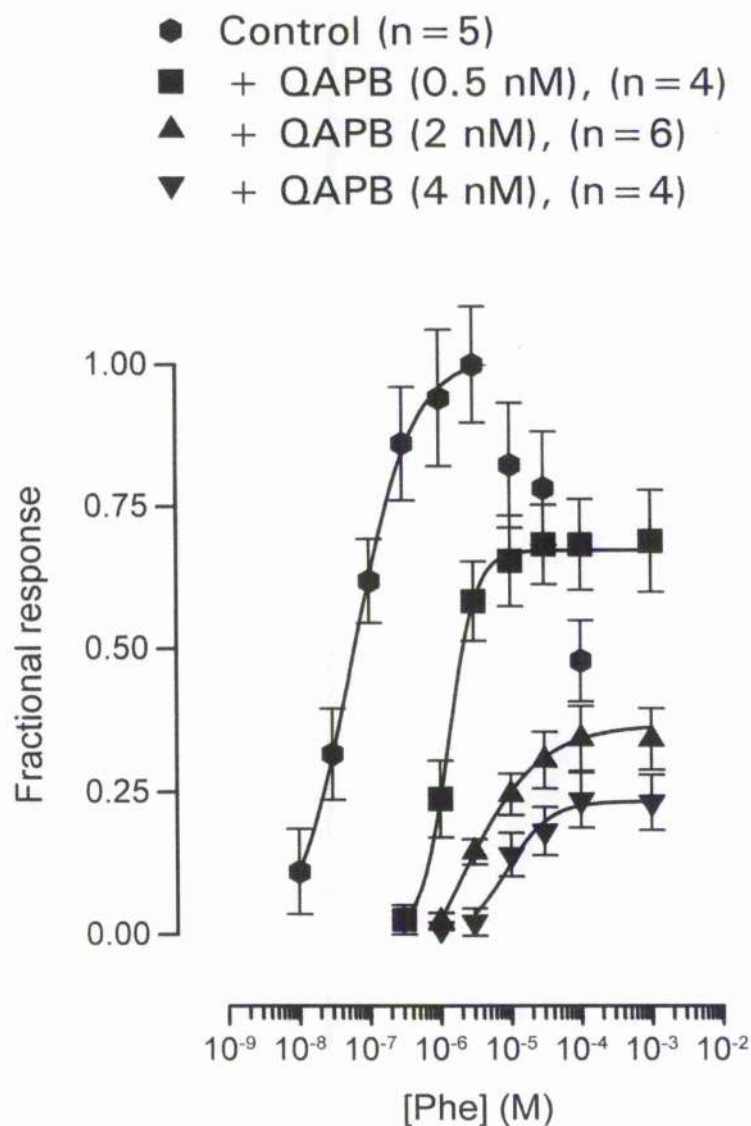


**Figure 3.12** CRC to phenylephrine in the absence (●) and presence of QAPB (0.5nM,  $n=4$ , ■; 2nM,  $n=6$ , ▲; and 4nM,  $n=4$ , ▼). Pooled data (mean  $\pm$  S.E. for each test concentration) presented as fraction of maximal response evoked by phenylephrine in control saline solution alone.

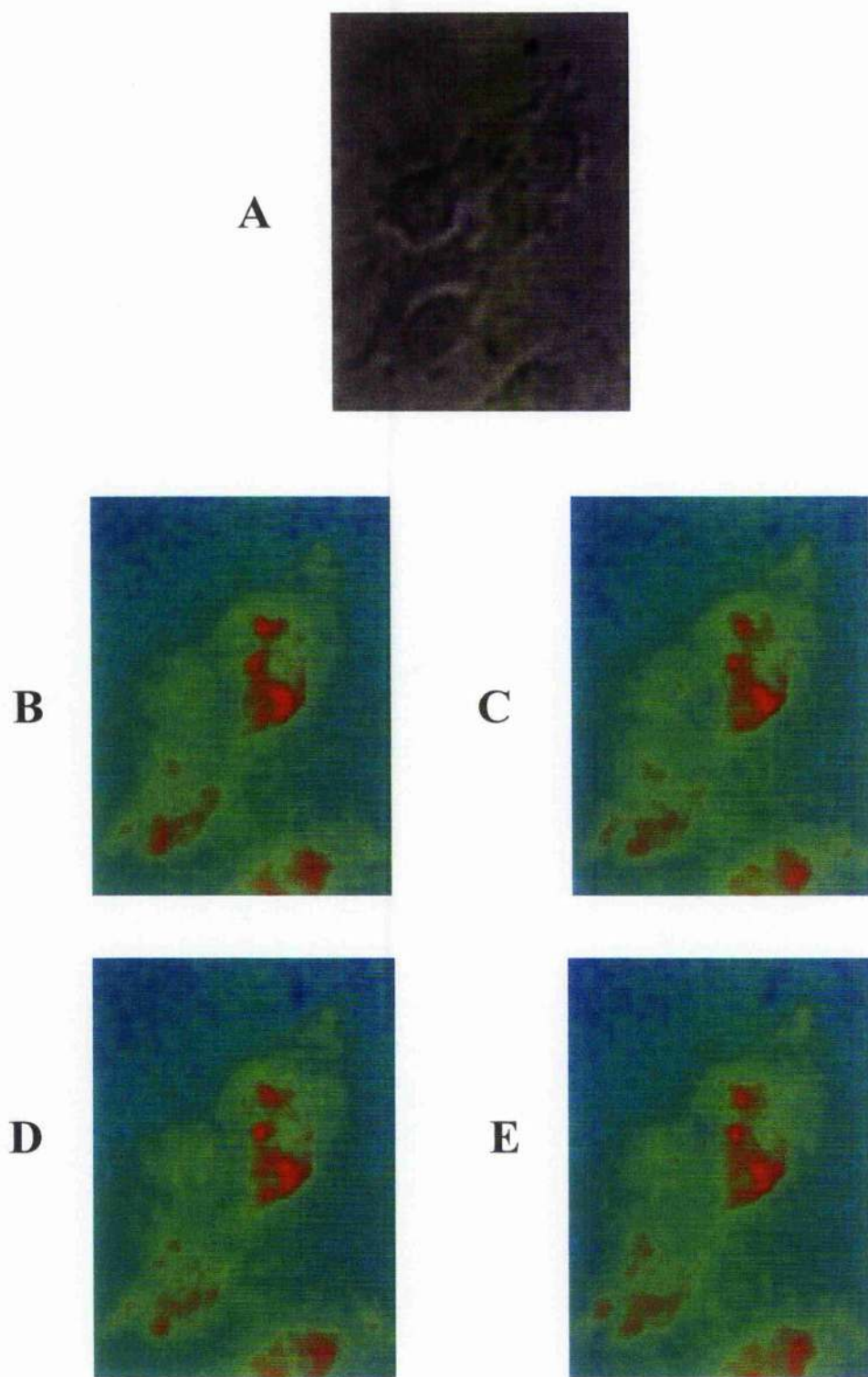


**Figure 3.13** QAPB binding to Rat-1 Fibroblasts expressing the bovine  $\alpha_{1a}$ -AR. **A**, Transmission image of a selected patch of R-1Fs. 4nM QAPB equilibrium binding after **B**, 15 minutes, **C**, 30 minutes, **D**, 45 minutes and **E**, 60 minutes. Red colour indicates areas of high QAPB fluorescent intensity.

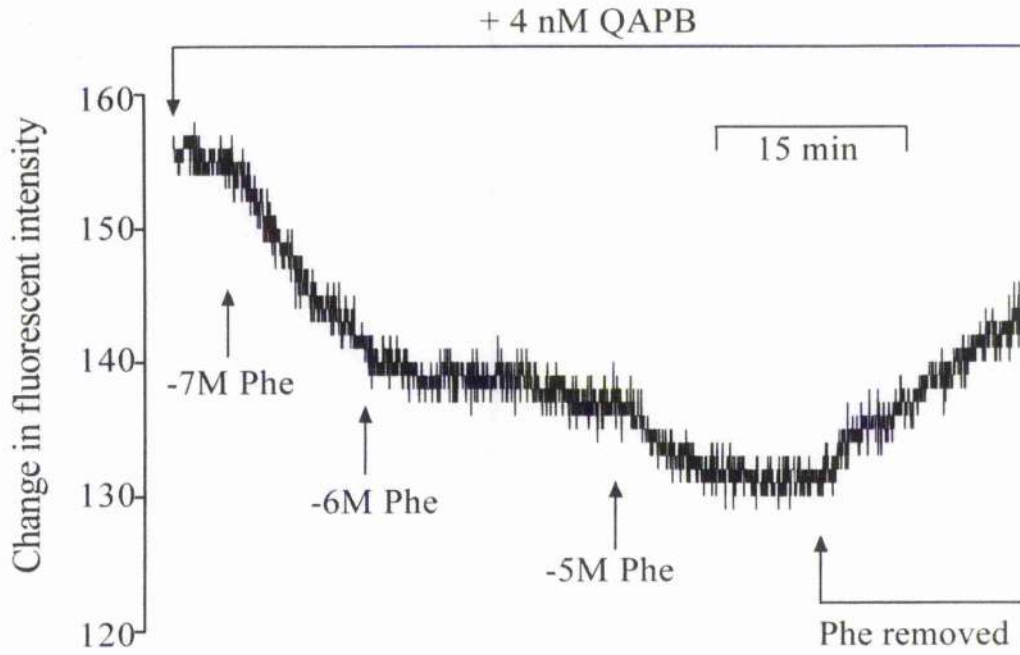


**Figure 3.14** Effect of reverse displacement. Trace shows three 15-minute cumulative applications of phenylephrine ( $0.1 \rightarrow 10\mu\text{M}$ ) following 60-minute incubation of cells with 4nM QAPB. Phenylephrine was removed from the perfusion system and the resultant QAPB fluorescent intensity returned.

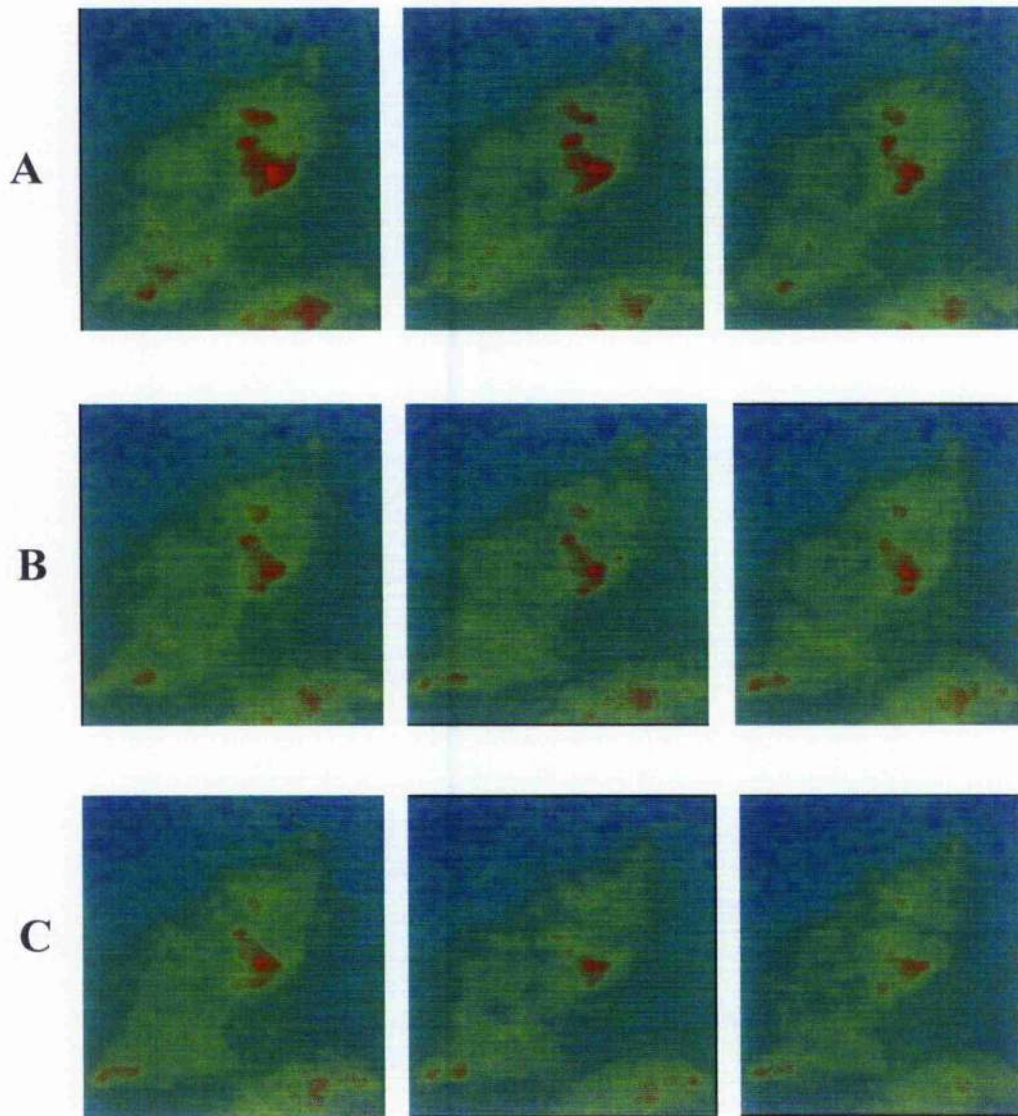


**Figure 3.15** Cells incubated with 4nM QAPB in the presence of increasing concentrations of phenylephrine. Three 15-minute applications of phenylephrine were added cumulatively. **A**, shows 0.1 $\mu$ M phenylephrine causing a large decrease in QAPB fluorescent intensity. **B**, shows 1 $\mu$ M phenylephrine having little effect and **C**, shows 10 $\mu$ M phenylephrine producing a further decrease in QAPB intensity. Changes in QAPB intensity represented above by a decrease in the red colour intensity.

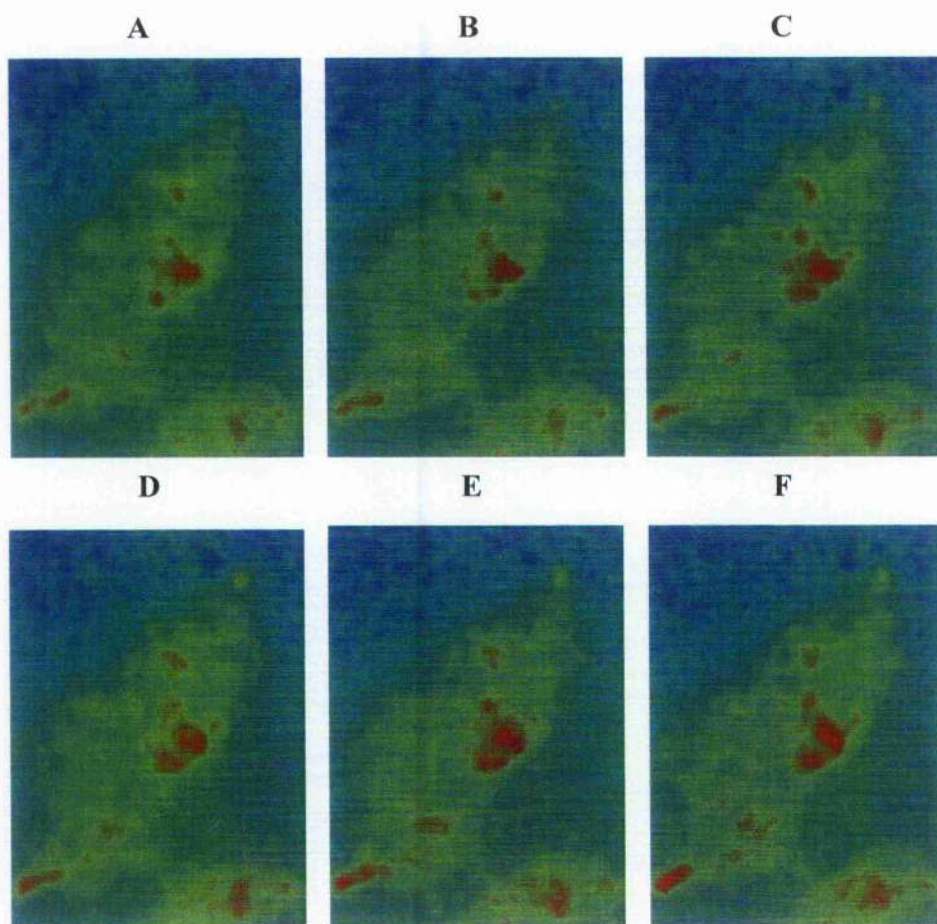


**Figure 3.16** Binding of QAPB was reversible. When phenylephrine was removed from the perfusion system, a reversal of 4nM QAPB fluorescent intensity was observed. This is represented above by an increase in red colour intensity.

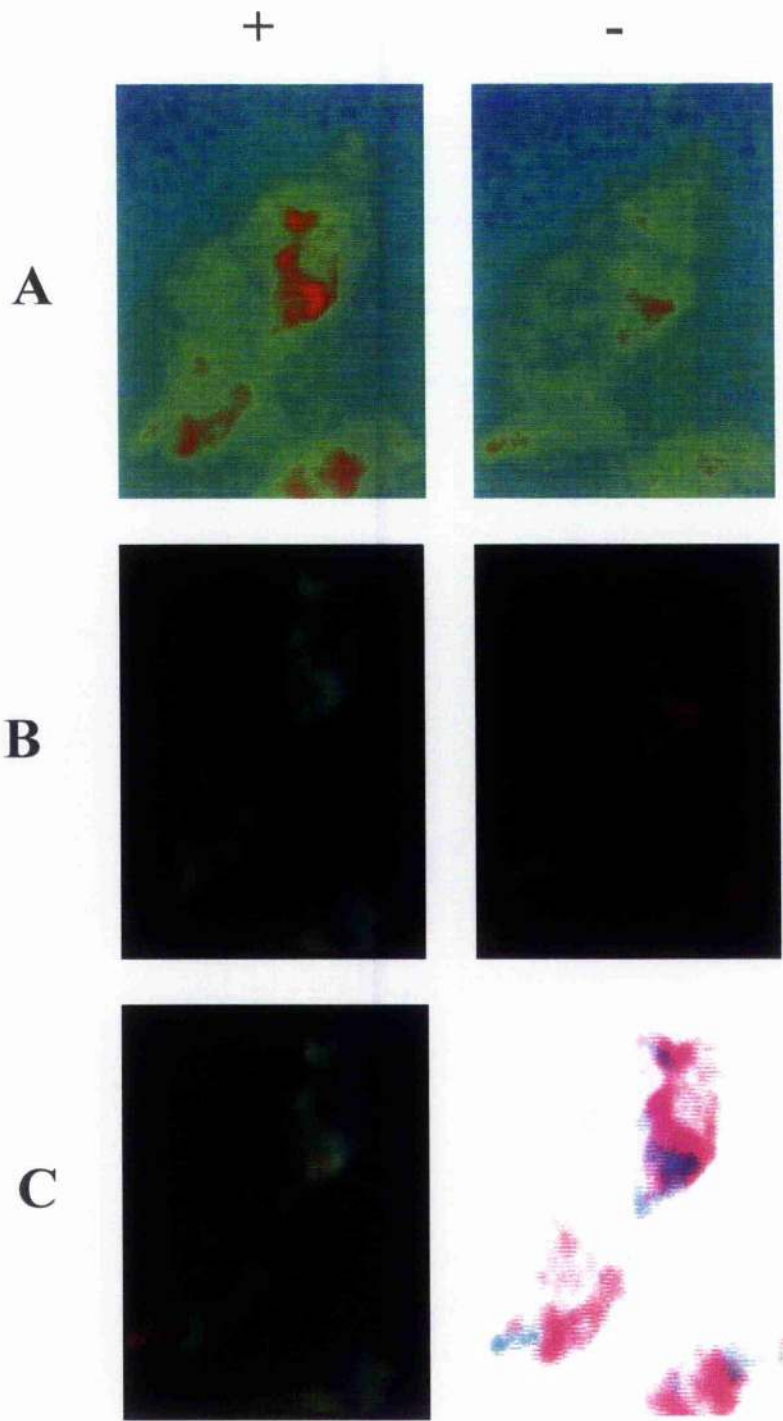


**Figure 3.17** QAPB displacement by phenylephrine. **A** (+), shows cells in the presence of 4nM QAPB alone with fluorescence at optimal intensity and also (-) after 3 cumulative applications of phenylephrine and the resulting decrease in fluorescent intensity. **B**, shows the corresponding threshold images where green (+) represents QAPB binding before addition of phenylephrine and red (-) represents QAPB binding following 3 cumulative applications of phenylephrine. **C**, shows the overlay (+) of both green and red images and also the inverse colour overlay (-) images.

**A**

**B**

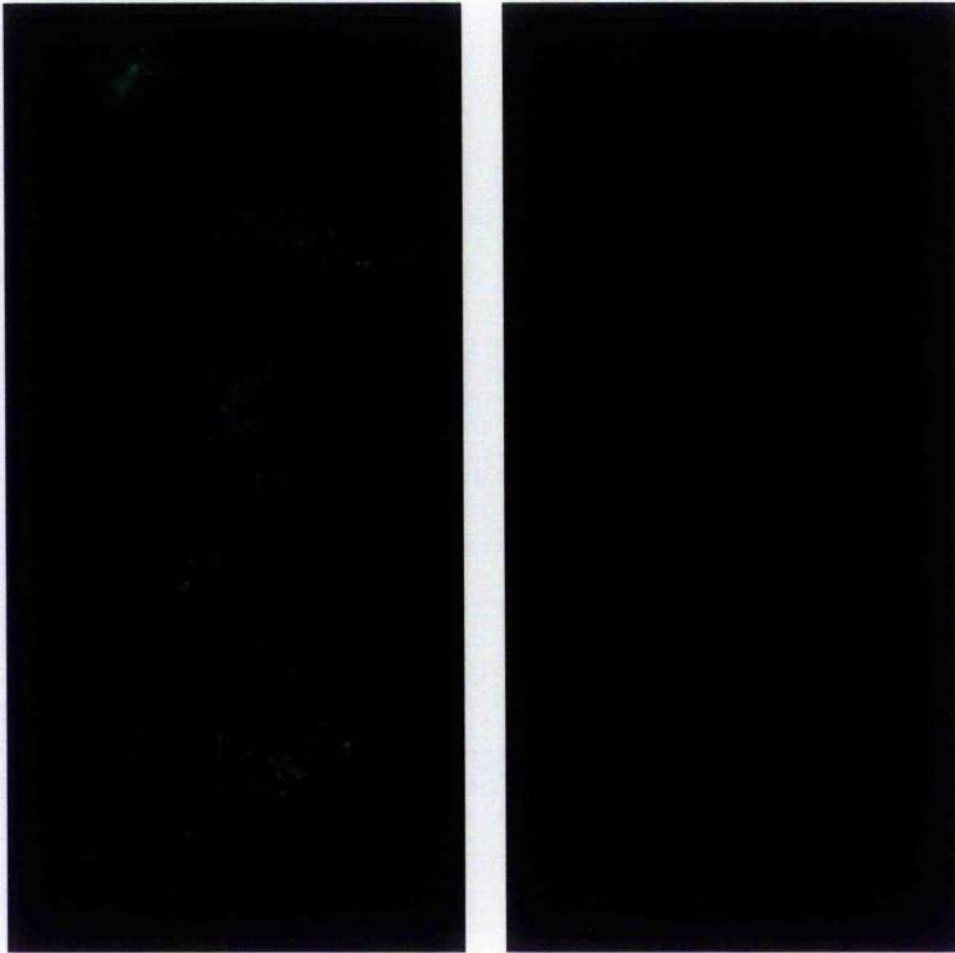


**Figure 3.18** QAPB displacement by phentolamine. **A**, shows a group of Rat-1 fibroblasts expressing the bovine  $\alpha_{1a}$ -AR labelled with 5nM QAPB at equilibrium binding after 75 minutes. **B**, shows equilibrium displacement by 10 $\mu$ M phentolamine after 150 minutes.

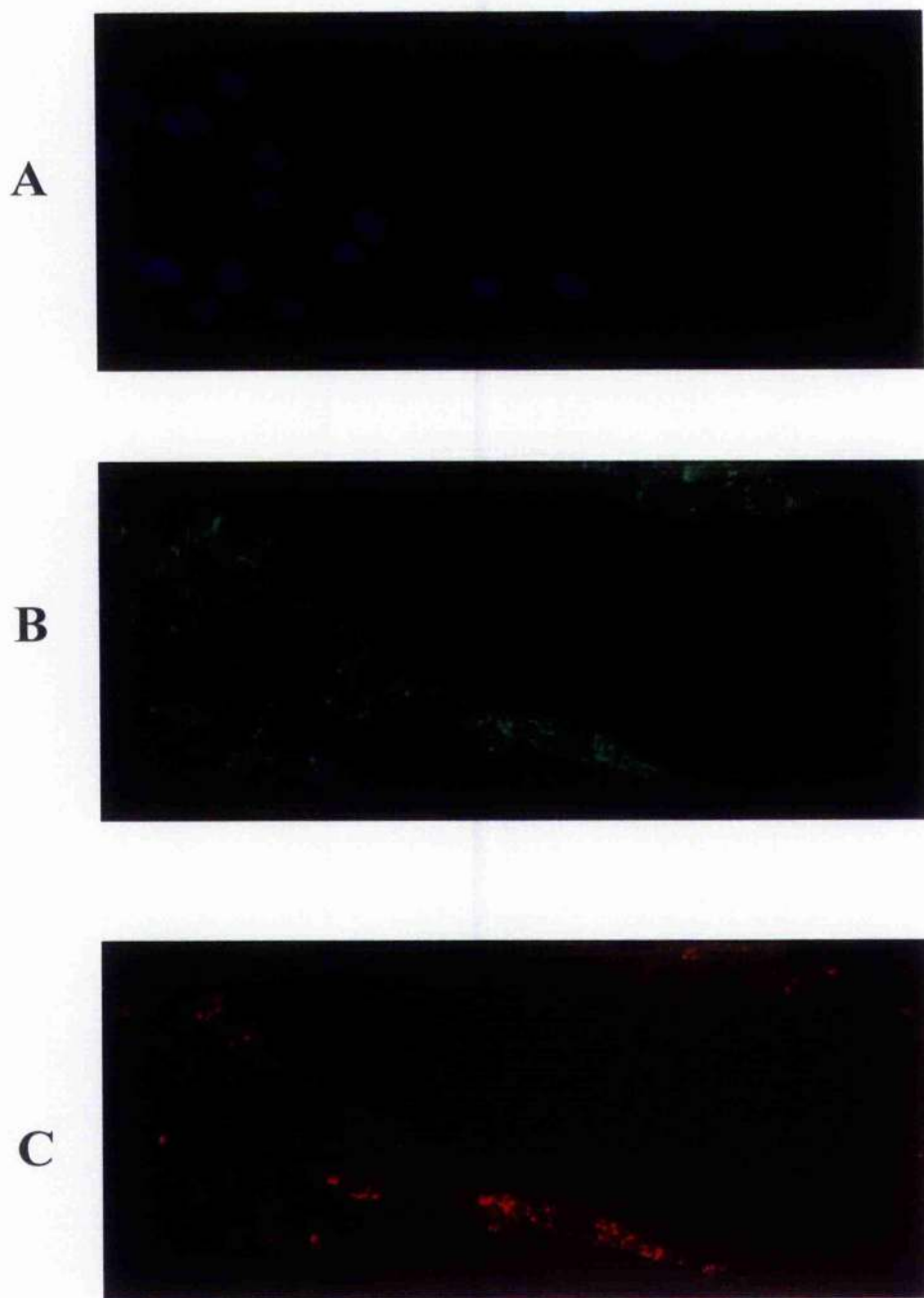


**Figure 3.19** QAPB staining in unstimulated Rat-1 fibroblasts stably expressing the bovine  $\alpha_{1a}$ -AR. **A**, (blue) shows a field of cells stained with the nuclear dye Hoechst 33342. **B**, (green) shows cells labelled with 4nM QAPB after 75 minutes and **C**, (red) shows cells labelled with the fluorescently tagged agonist Transferrin-Alexa Fluor<sup>546</sup> after 75 minutes.

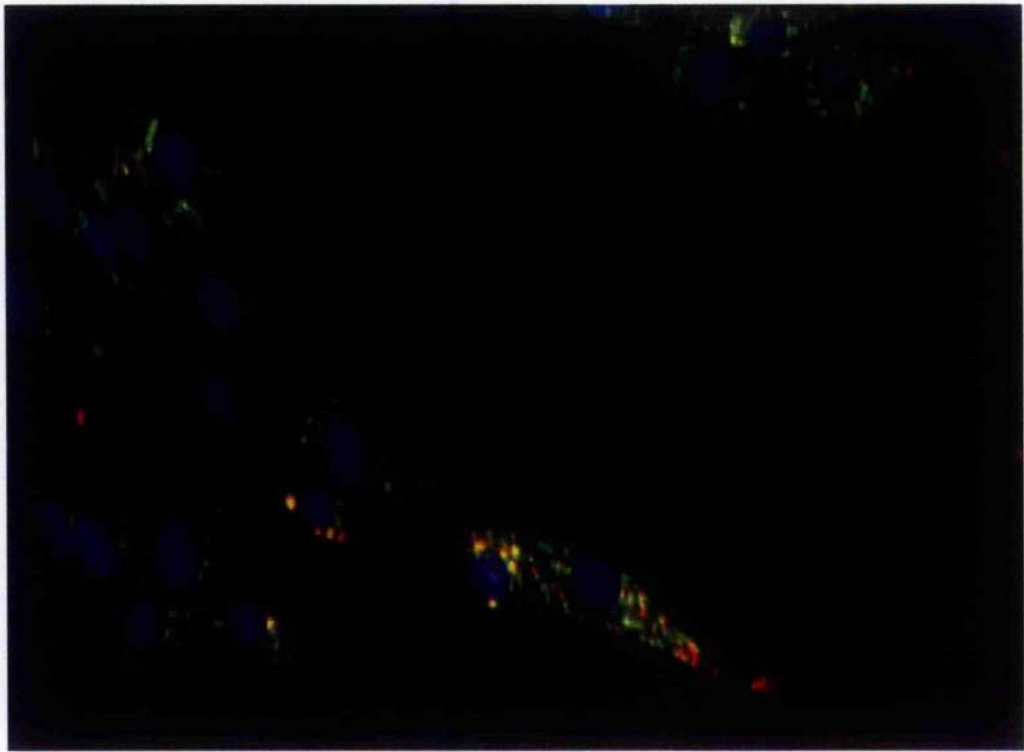


**Figure 3.20** Merged image between internal QAPB-receptor complex and early endosomal marker in Rat-1 fibroblasts. Image of a red (Transferrin-Alexa Fluor<sup>546</sup>), green (4nM QAPB) and blue (Hoechst 33342) overlay. Areas of yellow/orange colour represent co-localisation.

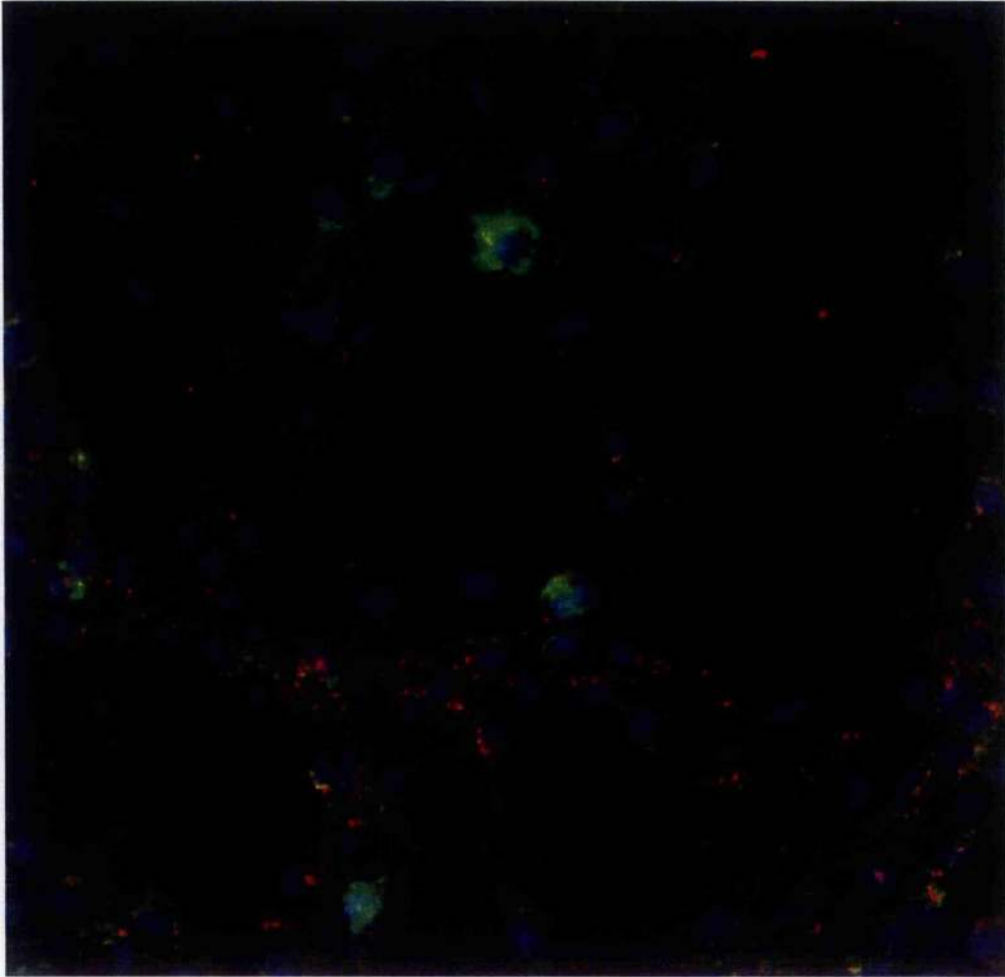


**Figure 3.21** Co-localisation between internal QAPB-receptor complex and early endosomal marker in Rat-1 fibroblasts. Image shows a greater field of cells stained with Hoechst (blue), QAPB (green) and Transferrin-Alexa Fluor<sup>546</sup> (red). Areas of co-localisation represented by yellow/orange colour.

### 3.3 DISCUSSION

#### 3.3.1 Microspectrofluorimetry

The development of molecular cloning of the DNA encoding  $\alpha_1$ -ARs in tissue along with the expression these clones in null cell lines (e.g. R-1Fs which lack endogenous ARs) enables the pharmacological properties of a particular  $\alpha_1$ -AR of defined amino acid sequence to be defined unambiguously.

In most cells, the primary functional effect of  $\alpha_1$ -AR activation is an increase in intracellular  $\text{Ca}^{2+}$  ( $[\text{Ca}^{2+}]_i$ ) (Harrison *et al*, 1991) and this is a result of  $\text{Ca}^{2+}$  release from internal stores and/or the influx of extracellular  $\text{Ca}^{2+}$  into the cell (Minneman & Esbenshade, 1994). Extracellular  $\text{Ca}^{2+}$  can enter the cell via VOCCs (Putney Jnr & Bird, 1993; Berridge, 1995; Clapham, 1995) and via a subgroup of RACCs that have been of interest in recent years called the SOCCs (capacitative  $\text{Ca}^{2+}$  channels) (Putney Jnr & Bird, 1993; Berridge, 1995; Clapham, 1995; Macrez-Lepretre *et al*, 1997; Barritt, 1999). These are defined as plasma-membrane  $\text{Ca}^{2+}$  channels that are opened in response to a decrease in the concentration of  $\text{Ca}^{2+}$  in the lumen of the ER ( $[\text{Ca}^{2+}]_{er}$ ) (Putney Jnr & Bird, 1993) (Fig. 3.22).

Han and colleagues (1987) worked with isolated smooth muscle and reported evidence for two types of  $\alpha_1$ -ARs. They proposed that the  $\alpha_{1A}$ - and  $\alpha_{1B}$ -AR could raise intracellular  $\text{Ca}^{2+}$  levels by different mechanisms, with the  $\alpha_{1A}$ -AR primarily elevating intracellular  $\text{Ca}^{2+}$  levels by gating  $\text{Ca}^{2+}$  influx through VOCCs, whereas the  $\alpha_{1B}$ -AR evoked this effect by mobilising stored  $\text{Ca}^{2+}$ . There are now numerous exceptions to proposals such as Han's. Putative  $\alpha_{1A}$ -AR elevate  $\text{IP}_3$  formation and/or liberate stored  $\text{Ca}^{2+}$  in many primary tissues (Han *et al*, 1990; Macrez-Lepretre *et al*, 1997) which suggests that this subtype of receptor can regulate  $[\text{Ca}^{2+}]_i$  by mobilising intracellular  $\text{Ca}^{2+}$  stores via the PLC- $\beta$ / $\text{IP}_3$  mechanism. Expressed receptors in COS-1 cells demonstrate that all three  $\alpha_1$ -AR subtypes can mobilise intracellular calcium and increase  $\text{Ca}^{2+}$  influx via voltage-operated  $\text{Ca}^{2+}$  channels (Perez *et al*, 1993; Lomansey *et al*, 1993).

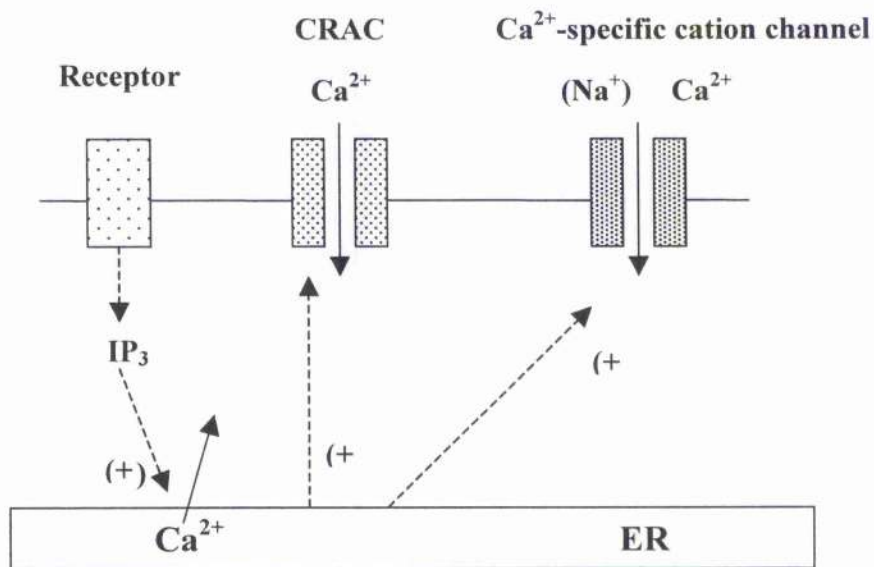


**Figure 3.22** Types of RACC: One of the two main types of RACC in animal cells is the store-operated  $\text{Ca}^{2+}$  channel (SOCC), shown above. These plasma-membrane  $\text{Ca}^{2+}$  channels open in response to a decrease in the  $[\text{Ca}^{2+}]$  in the ER lumen (Barritt, 1999).

R-1Fs expressing the bovine  $\alpha_{1a}$ -AR have been previously used as a model system for evaluating homologous  $\alpha_1$ -AR mediated signalling events (Schwinn *et al*, 1995). Activation of this receptor was shown to increase IP formation which strongly suggested that the receptor regulated  $[Ca^{2+}]_i$  by mobilising  $Ca^{2+}$  from internal stores.

The active uptake of  $Ca^{2+}$  into intracellular stores was discovered during studies on the nature of muscle relaxing factor (Kumagai *et al*, 1955; Ebashi & Lipmann, 1962). The active principle is a  $Ca^{2+}$ ,  $Mg^{2+}$ -activated ATPase in the sarco-endoplasmic reticulum (SR/ER) membrane and these enzymes are now referred to as SERCA pumps (sarco-endoplasmic reticulum  $Ca^{2+}$ -ATPases) (Pozzan *et al*, 1994; Mogami *et al*, 1998). The principle of operation is simple: when the  $[Ca^{2+}]_i$  rises due to release from intracellular stores, the SERCA pumps are activated and following the closure of SR/ER  $Ca^{2+}$  release channels, the net  $Ca^{2+}$  reuptake will occur. When  $[Ca^{2+}]_i$  has been reduced to the resting (pre-stimulation) level, the activation of the SERCA pumps stops (Mogami *et al*, 1998).

Since the idea of store-operated  $Ca^{2+}$  inflow was first proposed (Casteels & Droogmans, 1981; Putney Jnr, 1986), there have been further discoveries providing evidence for this phenomenon, including the discovery of a SERCA inhibitor, thapsigargin (Putney Jnr & Bird, 1993). Thapsigargin-evoked depletion of internal  $Ca^{2+}$  stores occurs in the absence of agonist activation of membrane-bound receptors/generation of related second messengers and activates the same  $Ca^{2+}$  entry pathway as that resulting from agonist activation (Putney Jnr & Bird, 1993). These potent SERCA inhibitors can therefore be used to provide an important distinction between  $Ca^{2+}$  entering through SOCCs as opposed to RACCs or VOCCs.

In the present study, the dual excitation  $Ca^{2+}$ -sensitive fluorescent dye Fura-2 AM was used to assess the mechanism of  $Ca^{2+}$  signalling activated by the recombinant  $\alpha_{1a}$ -AR. The first aim was to determine the nature of the  $[Ca^{2+}]_i$  signal and it was initially established that phenylephrine could evoke a rapid rise in the  $[Ca^{2+}]_i$  that could be resolved into two functionally distinct phases. There was an initial transient phase, which was due to  $Ca^{2+}$  release from internal stores, followed by a small-sustained plateau, which was due to the influx of extracellular  $Ca^{2+}$ . In experiments

using rat-tail arteries, Li and colleagues (1993) reported similar results. The group reported fast and transient increases in intracellular  $\text{Ca}^{2+}$  resulting from  $\text{Ca}^{2+}$  mobilization from intracellular stores and  $\text{Ca}^{2+}$  influx through receptor-operated channels following  $\alpha_1$ -AR stimulation.

Intracellular  $\text{Ca}^{2+}$  levels are held at a constant low level by  $\text{Ca}^{2+}$  buffering within the cell and by the balance between  $\text{Ca}^{2+}$  release/influx into the cytosol and the opposing actions of the mechanisms that extrude  $\text{Ca}^{2+}$  from the cytosol (Pediani *et al*, 2000). This balance is temporarily overcome upon receptor activation. A rapid mobilisation of stored  $\text{Ca}^{2+}$  into the cytosol causes a rise in  $[\text{Ca}^{2+}]_i$  during a short exposure to phenylephrine. As the stores are limited, the release rate rapidly declines to a point where it is exceeded by removal processes and the  $[\text{Ca}^{2+}]_i$  declines. This explains the “faded” response during the 30-second phenylephrine application. A 5-minute cycle was sufficient to replenish the stores if extracellular  $\text{Ca}^{2+}$  was present. Any involvement of VOCCs in the regulation of  $[\text{Ca}^{2+}]_i$  was discarded by Pediani and colleagues (2000) who found that a depolarising concentration of KCl failed to evoke any change in the resting  $[\text{Ca}^{2+}]_i$ . The lack of VOCCs indicates  $\text{Ca}^{2+}$  entry must follow receptor occupation rather than a change in membrane potential.

At various phenylephrine concentrations, the time course of the fade varied as described previously. At low phenylephrine concentrations, the responses were slow to rise and did not reach a peak or fade, which is consistent with the  $\text{Ca}^{2+}$  stores not yet having emptied. The  $\text{Ca}^{2+}$  responses rose and peaked more quickly and faded earlier as the phenylephrine concentrations increased. This would be expected, as the  $\text{Ca}^{2+}$  stores would have emptied more quickly. This pattern continued with each phenylephrine application up to an optimal concentration. Beyond this concentration of phenylephrine that produced the maximum response (30 $\mu\text{M}$ ), the concentration-response relationship displayed an inverse phase (i.e., smaller peak  $\text{Ca}^{2+}$  responses to increasing concentrations of phenylephrine).

Although the peak responses decreased as the phenylephrine concentration increased, the initial rate of rise continued to increase. Pediani and colleagues (2000) found a similar trend and suggested the  $\text{Ca}^{2+}$  response had been limited by a reduced release

from the internal stores before they had emptied. They observed that when the peak is reduced, the response takes longer to decline, as it might if  $\text{Ca}^{2+}$  release continued at a lower level for a longer time. This could be attributed to a negative feedback mechanism. High levels of  $[\text{Ca}^{2+}]_i$  can inhibit  $\text{IP}_3$  receptors found on the ER and also the activity of its integral  $\text{Ca}^{2+}$  release channel (Goldbeter *et al*, 1990; Atri *et al*, 1993). The main point regarding such a mechanism is that a very fast response achieves a lesser peak than a slightly lower one. This may explain a result of the agonist-antagonist interaction discovered in the present study in that the presence of antagonist abolished the inverse phase of the concentration-response relationship. This applied to all concentrations of QAPB tested in the present study.

Prior to studying the interaction between phenylephrine and QAPB, a possible "photobleaching" effect by QAPB was addressed. Results showed that no degradation/photobleaching of QAPB intensity existed, hence a steady state equilibrium binding of QAPB could be maintained over a 4 hour time period and without having any effect on the antagonised fura-2  $\text{Ca}^{2+}$  signal.

The equilibrium relationship between phenylephrine, QAPB, receptor pool, and the response depends on the fractional receptor occupancy required by the agonist to achieve a response, and the dissociation equilibrium constants for the  $\alpha_{1a}$ -AR, the agonist and the antagonist. The ratio of the association and dissociation rate constants determines the dissociation equilibrium constant for each drug/receptor. When the antagonist, QAPB, is present at equilibrium (at adequate concentration to occupy a high proportion of the receptors) and the agonist, phenylephrine is added, the initial agonist association rate depends greatly on the QAPB dissociation rate as the agonist can only associate with free receptors (Pediani *et al*, 2000). The resulting rate of formation of agonist-receptor complexes will be slowed.

It was then possible to study antagonism versus phenylephrine by QAPB across the concentration ranges indicated by its RLB affinities. A period of 60 minutes was sufficient for QAPB to reach and maintain steady state equilibrium binding before a series of 3-minute phenylephrine pulses were applied. For each phenylephrine application, there was a gradual decline in the QAPB signal and this fall in intensity

was reversed when phenylephrine was removed. This trend was similar for each concentration of QAPB tested (0.5, 2, 4, 6nM) and only a small amount of the maximal QAPB signal detected was displaced.

It is also clear that in the presence of QAPB, the initial rate of  $[Ca^{2+}]_i$  is slower and that the magnitude of peak  $Ca^{2+}$  responses was reduced/antagonised. For each QAPB concentration tested, the peak of the  $Ca^{2+}$  response occurred prior to equilibrium displacement of QAPB. The binding of QAPB and its antagonistic action upon  $[Ca^{2+}]_i$  in response to phenylephrine was reversible. Following a 60-minute period after the removal of QAPB, the fluorescent signal had maximally decreased. The magnitude and time course for the initial rise in  $[Ca^{2+}]_i$  was then faster when phenylephrine was applied.

By defining the nature of the  $Ca^{2+}$  signal, it was possible to investigate the nature of the agonist-response relationship for the bovine  $\alpha_{1a}$ -AR and to determine the relationship for the interaction of agonists and antagonists. The peak  $[Ca^{2+}]_i$  signal elicited by phenylephrine was short-lived and a result of the rapid movement of stored  $Ca^{2+}$ . The transient nature for the receptor-response coupling process therefore does not permit sufficient equilibrium time to produce a true thermodynamic equilibrium between the agonist/antagonist and receptor (Pediani *et al*, 2000). The  $Ca^{2+}$  responses in the present study could therefore be described as non-equilibrium functional responses.

The present study also predicts a consequence of insurmountable antagonism for competitive antagonists as their concentration increases. During the short time period that the functional response occurs, only a very small amount of QAPB is actually displaced by phenylephrine. As the QAPB concentration increases, the dominant influence becomes the reduced number of available sites and hence the agonist fractional occupancy is reduced in proportion to the fraction of receptors that are not occupied by QAPB. This leads to insurmountable antagonism (Furchgott, 1972), where the concentration- $Ca^{2+}$  response curves produced by QAPB display a rightward shift and fall in maximum.

### 3.3.2 Direct visualisation of fluorescent binding

Studies by Price and Schwinn (1998) reported that a green fluorescent protein-tagged  $\alpha_{1a}$ -AR underwent constitutive cycling between the cell surface and nonlysosomal intracellular compartments suggesting a possible mechanism for continuous  $\alpha_{1a}$ -AR signalling. These results were supported by earlier studies by Hirasawa and colleagues (1997) who found that transiently expressed, green fluorescent protein- or FLAG-tagged  $\alpha_{1a}$ -AR and  $\alpha_{1b}$ -AR subtypes displayed differential sensitivity to CEC as a result of differences in subcellular localisation and not differences in structural determinants. This different subcellular localisation of the  $\alpha_1$ -AR subtypes has been confirmed by other studies (Piascik & Perez, 2001; Sugawara, *et al* 2002), and the intracellular expression of the  $\alpha_1$ -ARs was observed not only in the cloned receptor transfected cells, but also in the endogenous  $\alpha_1$ -ARs expressed in native tissues including prostate smooth muscle cells and vascular smooth muscle cells (McGrath *et al*, 1999; Hrometz *et al*, 1999).

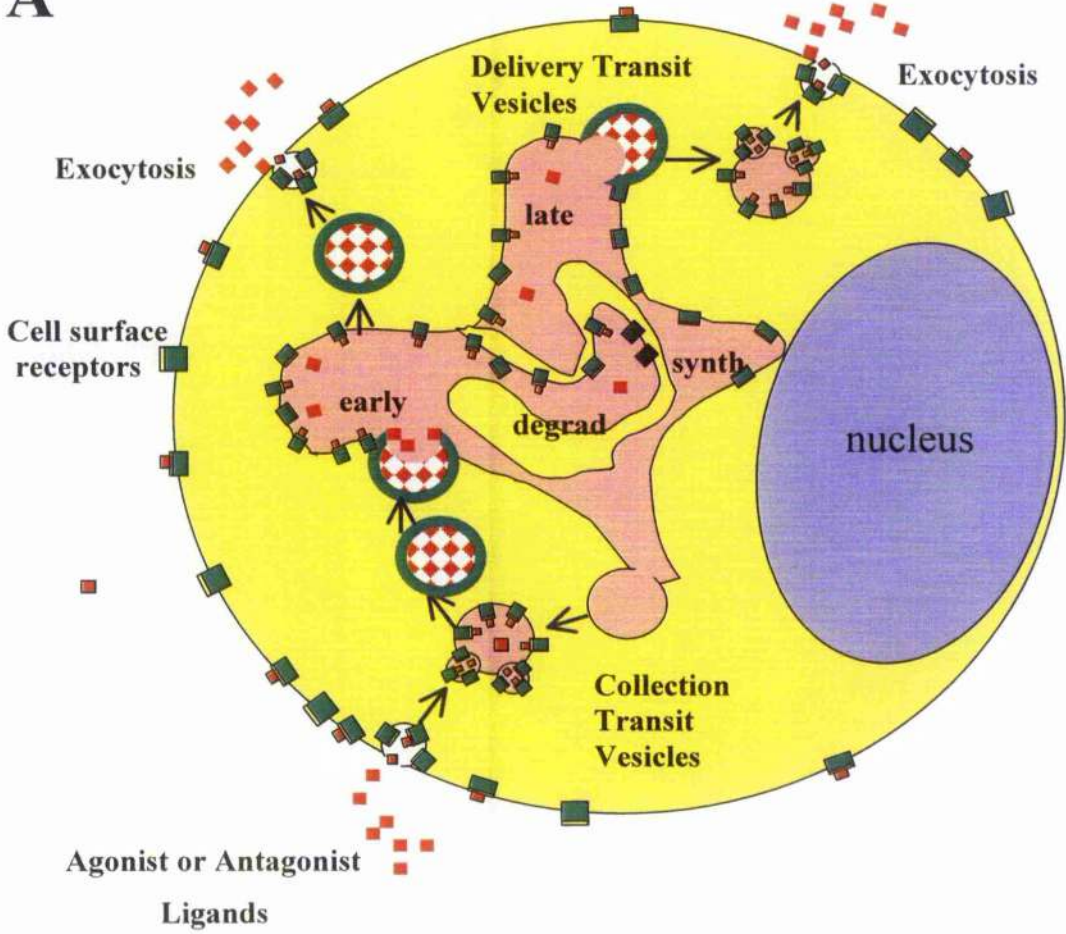
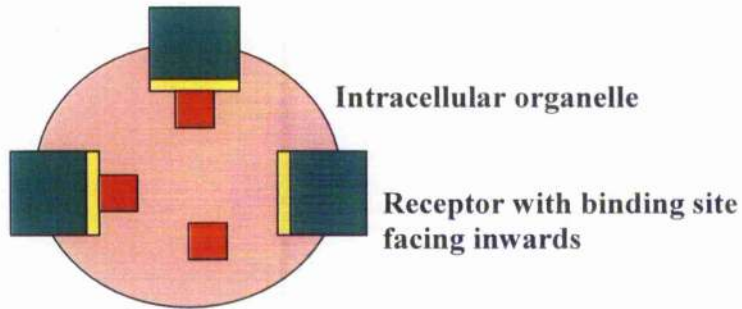
Visualisation of QAPB binding to  $\alpha_{1a}$ -ARs in Rat-1 fibroblasts was used in the present study to determine whether the ligand was internalised with the receptor and to identify subcellular compartments. The “hot spots” emitting the strongest fluorescent signal moved considerably around the cell. Some of these “hot spots” appeared to move in a bi-directional motion over a short range, whereas others moved with great speed. This trafficking of fluorescent “hot spots” suggests a possible endocytotic mechanism. Within minutes of QAPB application, diffuse low intensity fluorescent signals were observed in punctate intracellular sites that were scattered throughout the cell cytoplasm. After a period of 60 minutes, higher intensity fluorescent signals were observed in larger punctate structures. This suggests that the basic units of transport were smaller structures, beyond the resolution of the microscope, characteristic of endocytotic vesicles. These endocytotic vesicles would most likely fuse reversibly with the “hot spots” and exchange a load of plasmalemmal proteins including the ligand-receptor complex. These fluorescent “hot spots” will then move further into the cell towards the perinuclear region where they will fuse with larger structures, delivering ligand-receptor complexes.

The fate of the small fluorescent structures can be decided by three different pathways inside the cell (Fig. 3.23). They can simply traffic inwards via collection transit vesicle structures and fuse with early endosomes. Once fused with the endosomes, a bud forms and subsequently traffics the ligand-receptor complex back towards the cell surface where the ligand will then exit the cell by exocytosis. A second pathway for the ligand-receptor complex is to follow a degradation and synthesis pathway once fused with the early endosomes. A third pathway is for the ligand-receptor complex to traffic from the early endosome through to the late endosome, where a bud will subsequently form a delivery transit vesicle. This transit vesicle will carry the ligand-receptor complex back to the cell surface where it will leave via exocytosis. During all these intracellular transactions, the ligand and its binding site will be restricted to the internal face of the endosomes, so that even if they dissociate, the ligand molecules will be restricted to the compartment and be likely to reassociate.

The present study also confirmed that an agonist could enter the cell and displace QAPB from intracellular compartments. The fluorescent QAPB signal observed in these intracellular "hot spots" decreased in intensity after phenylephrine had been added cumulatively at 15-minute intervals. It would be assumed that phenylephrine would enter the cell and traffic to these "hot spots" in a manner similar to that of QAPB. The binding of QAPB is also reversible. The high fluorescent intensity signal was observed once phenylephrine was removed from the perfusion system.

Antagonists could compete with QAPB fluorescence at the cell surface level and at intracellular compartments. The present study confirmed that the  $\alpha$ -AR antagonist phentolamine could penetrate the cell and almost completely reduce all QAPB fluorescence. The  $\alpha_{1a}$ -AR antagonist RS100329 could also selectively compete at the cell surface. The use of phentolamine is an advantageous tool for fluorescence binding as image subtraction removes the non-specific binding leaving only the image of receptors that have been competitively antagonised by the competitor.

Daly and colleagues (1998) were the first to report the existence of diffuse and clustered populations of  $\alpha_1$ -ARs binding sites in live cells using confocal microscopy

**A****B**

**Figure 3.23** Constitutive recycling of the  $\alpha_{1a}$ -AR in Rat-1 fibroblasts. **A**, shows intracellular compartments and movement of ligand-receptor complexes. **B**, shows receptors on intracellular organelles with binding sites (yellow) facing inwards.

and showed that the affinity of both populations for the ligand were identical. This proved that the environment of the clustered domain left the binding sites accessible to ligands. The group also predicted the relative distribution of receptors between these two domains, stating that although the clusters were visually striking, they represented a relatively small proportion of the receptor population accessible to ligands. This emphasised that subjective visual assessment can exaggerate the relative proportion of receptors that appear to be present in the clusters (Daly *et al*, 1998).

The diffuse binding described by Daly was reduced when phentolamine was added in the present study. After a 75-minute period, QAPB binding had reached and maintained a steady state, showing both areas of diffuse binding and areas of clustered "hot spots". Phentolamine reduced all diffuse binding and a large proportion of intracellular "hot spots" when added for over 2 hours. The ability of antagonists, as well as agonists, to bind competitively to intracellular components in live cells suggests a possibility that they are involved in signal transduction. Al-Damluji and colleagues (1997) previously reported similar findings. Using hypothalamic peptideric neurones, they found QAPB accumulated in a granular distribution, compatible with storage in intracellular vesicles. Using fluorescence microscopy, the group also reported an antagonist, prazosin, could be internalised, possibly by clathrin-coated pits and could inhibit QAPB binding.

To visualise and determine the identity of the intracellular compartments, a fluorescently tagged agonist was employed that would identify subcellular compartments. Many earlier studies using GPCR-GFP chimeras have used red fluorescent markers that label particular cellular organelles or membranes (Kallal & Benovic, 2000). By studying GPCR-GFP and the red fluorescent compound in the same cell, potential co-localisation can be readily ascertained. In addition to visual representations of red and green overlap, it is also possible to quantitate subcellular co-localisation digitally (Tarasova *et al*, 1997, 1998). The present study used Transferrin Alexa Fluor<sup>568</sup>. This labels early endosomes and endocytotic recycling compartments and was used to identify the endocytotic recycling pathway. Transferrin Alexa Fluor<sup>568</sup> also binds to the constitutively active Transferrin receptor,

which localises predominantly in the perinuclear-recycling compartment (PNRC), hence the red dye is ideal for labelling the PNRC. Co-localisation occurred to a small extent between QAPB and Transferrin Alexa Fluor<sup>546</sup>, suggesting a possible perinuclear site for the intracellular components that emit QAPB fluorescence. Although a small proportion of fluorescent sites co-localised with the red dye, there was a large proportion of QAPB binding sites that were spatially distinct from the recycling endosomal marker.

MacKenzie and colleagues (2000) reported similar findings to the present study using confocal microscopy. In Rat-1 fibroblasts expressing all three recombinant  $\alpha_1$ -AR subtypes, they discovered QAPB bound to cell membrane and intracellular perinuclear sites. The perinuclear binding was more obvious in the  $\alpha_{1b}$ -AR subtype. There was no general rule, however, for the localisation of particular subtypes. The group found stark similarities between the intracellular distribution of binding sites in recombinant and native systems. In prostatic SMCs, 40% of specific binding sites were intracellular, particularly around the perinuclear region, which could represent binding in the Golgi apparatus and may include both newly synthesised and recycling stores of receptors (MacKenzie *et al*, 2000). This proves that the vast quantity of intracellular binding sites previously shown in recombinant cells is not an artefact of artificial systems, but a natural phenomenon.

#### 4.0 CONCLUSIONS

The present study used classical and updated radioligand binding techniques to compare binding to isolated cell membranes and whole cells in Rat-1 fibroblasts expressing the recombinant bovine  $\alpha_{1a}$ -AR. The results indicate that both agonists and antagonists can displace a radiolabel ( $^3\text{H}$ -prazosin) from cell surface binding sites and intracellular compartments. Displacement curves of biphasic nature displayed a high affinity component (approx. 20% of binding sites) followed by a slow sustained plateau phase before the low affinity component (approx. 80% of binding sites). The high affinity component suggests a displacement from cell surface receptors and the low affinity component may represent cellular penetration. The uptake of ligands into the cell was found to be time-dependant and temperature-independant. An early hypothesis that the uptake of ligands occurred via an EMT was ruled out after displacement curves demonstrated near maximum displacement of radiolabel by ligands in the presence of a potent EMT blocker, corticosterone.

A more probable explanation of how ligands penetrate cells and access intracellular compartments is via an endocytotic pathway. The present study found that an endocytotic blocker, concanavalin A, exerted an inhibiting effect that could be overcome once a certain amount of antagonist (QAPB) had been applied. A similar result could not be applied to agonists. Concanavalin A displayed little, if any, inhibiting effect on the ability of adrenaline to displace radiolabel. Performing identical experiments at cold temperature ( $4^\circ\text{C}$ ) supports a possible endocytotic mechanism. The endocytotic process is not functional at cold temperatures. The results presented in this study correspond with this theory, as there was little displacement of radiolabel (approx. 20% of binding sites) at cold temperatures. This would imply that due to the non-functioning endocytotic process, the ligands are unable to penetrate the cell and displace the radiolabel. This presents the question of how the radiolabel penetrates the cell. One could speculate that  $^3\text{H}$ -prazosin enters the cells via a separate mechanism, such as a carrier process.

The hypothesis that ligands penetrate cells and access intracellular compartments via an endocytotic mechanism was further tested in the present study by direct

visualisation techniques. The fluorescent  $\alpha_1$ -AR antagonist QAPB could be detected within intracellular compartments throughout the cytoplasm following a sufficient time period. Movement of individual fluorescent signals observed on punctate structures were characteristic of endocytosis. Unstimulated Rat-1 fibroblasts expressing the bovine  $\alpha_{1a}$ -AR were labelled with QAPB, a nuclear dye (Hoechst 33342) and an early/recycling endosomal marker for endocytosis via clathrin-coated pits (Transferrin Alexa Fluor<sup>546</sup>). The latter is ideal for labelling the perinuclear-recycling compartment. When all three labels were merged, the overlapping areas of co-localisation appeared around the perinuclear region, suggesting that  $\alpha_{1a}$ -AR ligand complexes follow the endocytotic recycling pathway, via early and recycling endosomes.

Microspectrofluorimetry techniques were also employed in the present study to investigate whether quantitative pharmacology could be carried out at the single cell level on  $\alpha_1$ -ARs using a Rat-1 fibroblast cell line that stably expresses the recombinant  $\alpha_{1a}$ -AR. The results demonstrate that the dominant  $\text{Ca}^{2+}$  entry pathway evoked by the bovine  $\alpha_{1a}$ -AR is store-operated, in which the  $\text{Ca}^{2+}$  content of agonist-sensitive intracellular  $\text{Ca}^{2+}$  stores governs influx.

Results from the study of antagonism versus phenylephrine by QAPB suggested a consequence of insurmountable antagonism for competitive antagonists as their concentration increases. Although low phenylephrine concentrations produced no rise in  $[\text{Ca}^{2+}]_i$ , there was still a small decrease in QAPB fluorescent intensity. As phenylephrine concentrations increased, the  $\text{Ca}^{2+}$  responses were all transient, followed by small, sustained plateau phases. For each phenylephrine concentration, the maximum rise in  $[\text{Ca}^{2+}]_i$  had occurred before the corresponding decrease in QAPB intensity had started. The QAPB signal also recovered following each washout of phenylephrine.

There are a number of experiments that would have been worth investigating had time not been a factor in the present study. Using direct visualisation studies, the experiments (from Chapter 2) carried out in the presence of concanavalin A could be repeated. Cells would be incubated with concanavalin A for a sustained period of

time, and following the addition of QAPB, there would presumably be a small amount of fluorescence observed in intracellular compartments. Similarly, if cells were incubated with QAPB until steady state binding was achieved, visualisation techniques would reveal clusters of fluorescent “hot spots” around the perinuclear region as shown in Chapter 3. If concanavalin A was introduced following steady state QAPB binding, one could speculate that there would be a large decrease in these areas of high fluorescent intensity.

Other experiments of interest would be to repeat all the updated displacement protocols (Chapter 2) using visualisation techniques to determine the ability of various ligands to displace QAPB. The corticosterone experiments would certainly be worth investigating, firstly with QAPB alone, to determine whether it enters the cell via an EMT. If so, then a series of other agonists and antagonists could be applied to determine their method of uptake.

## 5.0 REFERENCES

- Ahlquist, R.P. (1948). A study of the adrenotropic receptors. *Am. J. Physiol.*, **153**, 586-600.
- Al-Damluji, S., Porter, D., Krsmanovic, L.Z., Knutson, J.R. & Kopin, I.J. (1997). Visual detection of transport-P in peptidergic neurones. *Br. J. Pharmacol.*, **120**, 876-882.
- Alexander, S.P.H. & Peters, J.A. (2000). *TIPS Receptor and Ion Channel Nomenclature Supplement.*, **11**, 15.
- Allen, L.F., Lefkowitz, R.J., Caron, M.G. & Cotecchia, S. (1991). G-protein-coupled receptor genes as protooncogenes: constitutively activating mutations of the  $\alpha_{1B}$ -adrenergic receptor enhances mitogenesis and tumorigenicity. *Proc. Natl. Acad. Sci. USA.*, **88**, 11354.
- Anderson, R.G.W. (1998). The caveolae membrane system. *Ann. Rev. Biochem.*, **67**, 199-225.
- Anderson, R.G.W., Brown, M.S. & Goldstein, J.L. (1977). Role of the coated endocytotic vesicle in the uptake of receptor-bound low density lipoprotein in human fibroblasts. *Cell.*, **10**, 351-364.
- Atri, A., Amundson, J., Clapham, D. & Sneyd, J. (1993). A single-pool model for intracellular calcium oscillations and waves in the *Xenopus laevis* oocyte. *Biophys. J.*, **65**, 1727-1739.
- Attramadal, H., Arriza, J.L. & Aoki, C. (1992).  $\beta$ -Arrestin2, a novel member of the arrestin/ $\beta$ -Arrestin gene family. *J. Biol. Chem.*, **267**, 17,882-17,890.

- Avakian, O.V. & Gillespie, J.S. (1968). Uptake of noradrenaline by adrenergic nerve, smooth muscle and connective tissue in isolated perfused arteries and its correlation with the vasoconstrictor response. *Br. J. Pharmacol. Chemother.*, **32**, 168-184.
- Babich, M., Pedigo, N.W., Butler, B.T. & Piascik. (1987). Heterogeneity of  $\alpha_1$  receptors associated with vascular smooth muscle: evidence from functional and ligand binding studies. *Life Sci.*, **41**, 663-673.
- Balboa, M.A. & Insel, P.A. (1998). Stimulation of phospholipase D via  $\alpha_1$ -adrenergic receptors in Madin-Darby kidney cells is independent of PKC $\alpha$  and - $\epsilon$  activation. *Mol. Pharmacol.*, **53**, 221.
- Barker, F.L., Westphal, R.S., Schmidt, D. & Sanders-Bush, E. (1994). Constitutively active 5-hydroxytryptamine<sub>2C</sub> receptors reveal novel inverse agonist activity receptor ligands. *J. Biol. Chem.*, **269**, 11687-11690.
- Barritt, G.J. (1999). Receptor-activated Ca<sup>2+</sup> inflow in animal cells: a variety of pathways tailored to meet different intracellular Ca<sup>2+</sup> signalling requirements. *Biochem. J.*, **337**, 153-169.
- Bennett, D.L., Bootman, M.D., Berridge, M.J. & Cheek, T.R. (1998). Ca<sup>2+</sup> entry into PC12 cells initiated by ryanodine receptors or inositol 1,4,5-trisphosphate receptors. *Biochem. J.*, **329**, 349-357.
- Benning, C.M. & Kyprianou, N. (2002). Quinazoline-derived  $\alpha_1$ -Adrenoceptor antagonists induce prostate cancer cell apoptosis via an  $\alpha_1$ -Adrenoceptor-independent action. *Cancer Research.*, **62**, 597-602.
- Berman, D.M. & Gilman, A.G. (1998). Mammalian RGS proteins: barbarians at the gate. *J. Biol. Chem.*, **273**, 1269-1272.

- Berman, D.M., Wilkie, T.M. & Gilman, A.G. (1996). GAIP and RGS4 are GTPase-activating proteins for the Gi subfamily of G protein alpha subunits. *Cell.*, **86**, 445-452.
- Berridge, M.J. (1997). Elementary and global aspects of calcium signalling. *J. Physiol.*, **499**, 291-306.
- Berridge, M.J. (1995). Capacitative calcium entry. *Biochem. J.*, **312**, 1-11.
- Berthelsen, S. & Pettinger, W.A. (1977). A functional basis for the classification of  $\alpha$ -adrenergic receptors. *Life Sci.*, **21**, 595-606.
- Berts, A., Zhong, H. & Minneman, K.P. (1999). No role for  $Ca^{2+}$  or protein kinase C in  $\alpha_{1A}$ -adrenergic receptor activation of mitogen-activated protein kinase pathways in transfected PC12 cells. *Mol. Pharmacol.*, **55**, 296.
- Birdsall, N.J.M. & Lazareno, S. (1997). To what extent can binding studies allow the quantification of affinity and efficacy? *Ann. N.Y. Acad. Sci.*, **812**, 41-7.
- Blue, D.R., Daniels, D.V., Ford, A.P.D.W., Williams, T.J., Eglen, R.E. & Clarke, D.E. (1997). Pharmacological assessment of the  $\alpha_1$ -adrenoceptor ( $\alpha_1$ -AR) antagonist tamsulosin. *J. Urol.*, **157**(4), 190.
- Blue, Jr, D.R., Craig, D.A., Ransom, J.T., Camacho, J.A., Insel, P.A. & Clarke, D.E. (1994). Characterization of the alpha-1 adrenoceptor subtype mediating [ $^3$ H]-arachidonic acid release and calcium mobilization in Madin-Darby canine kidney cells. *J. Pharmacol. Exp. Ther.*, **268**, 588-596.
- Bockaert, J., Brand, C. & Journot, L. (1997). Do recombinant receptor assays provide affinity and potency estimates? *Ann. N.Y. Acad. Sci.*, **812**, 55-70.

Boer, R., Grassegger, A., Schudt, C. & Glossman, H. (1989). (+)-Niguldipine binds with very high affinity to Ca<sup>2+</sup> channels and to a subtype of alpha-1 adrenoceptors. *Eur. J. Pharmacol.*, **172**, 131-145.

Bond, R.A., Leff, P., Johnson, T.D., Milano, C.A., Rockman, H.A., McMinn, T.R., Apparsundaram, S., Hyek, M.F., Kenakin, T., Allen, L.F. & Lefkowitz, R.J. (1995). Physiological effects of inverse agonists in transgenic mice with myocardial overexpression of the  $\beta_2$ -adrenoceptor. *Nature.*, **374**, 272-276.

Bouvier, M., Haudsdorff, W.P. & DeBlassi, A. (1988). Mutations of the  $\beta_2$  adrenergic receptor which remove phosphorylation sites delay the onset of agonist promoted desensitisation. *Nature.*, **333**, 370-372.

Braell, W.A., Schlossman, D.M., Schmid, S.L. & Rothman, J.E. (1984). Dissociation of clathrin coats coupled to the hydrolysis of ATP: role of an uncoating ATPase. *J. Cell Biol.*, **99**, 734-741.

Brodin, L., Low, P. & Shupliakov, O. (2000). Sequential steps in clathrin-mediated synaptic vesicle endocytosis. *Curr. Opin. Neurobiol.*, **10**, 312-320.

Bunemann, M., Lee, K.B., Pals-Rylaarsdam, R., Roseberry, A.G. & Hosey. (1999). Desensitization of G-Protein-coupled receptors in the cardiovascular system. *Ann. Rev. Physiol.*, **61**, 169-92.

Burch, R.M., Luini, A. & Axelrod, J. (1986). Phospholipase A2 and phospholipase C are activated by distinct GTP-binding proteins in response to  $\alpha_1$ -adrenergic stimulation in FRTL5 thyroid cells. *Proc. Natl. Acad. Sci. USA.*, **83**, 7201.

Buscher, R., Heeks, C., Taguchi, K. & Michel, M.C. (1996). Comparison of guinea-pig, bovine and rat  $\alpha_1$ -adrenoceptor subtypes. *Br. J. Pharm.*, **117**, 703-711.

Buxton, I.L. & Brunton, L.L. (1985). Action of the cardiac alpha1-adrenergic receptor: activation of cyclic AMP degradation. *J. Biol. Chem.*, **260**, 6733-6738.

Bylund, D.B., Eikenberg, D.C., Hieble, J.P., Langer, S.Z., Lefkowitz, R.J., Minneman, K.P., Molinoff, P.B., Ruffolo Jr, R.R. & Trendelenburg, U. (1994). International union of pharmacology nomenclature of adrenoceptors. *Pharm. Reviews.*, **46**, 121-136.

Bylund, D.B. & Toews, M.L. (1993). Radioligand binding methods: practical guide and tips. *Am. J. Physiol.*, **265**, (Lung Cell. Mol. Physiol. 9) L421-L429.

Cannon, W.B. & Rosenbleuth, A. (1933). Studies on conditions of activity in endocrine organs. Sympathin E and sympathin I. *Am. J. Physiol.*, **104**, 557-574.

Castells, R. & Droogmans, G. (1981). Exchange characteristics of the noradrenaline-sensitive calcium store in vascular smooth muscle cells or rabbit ear artery. *J. Physiol.*, **317**, 263-279.

Catterall, W.A. (1995). Structure and function of voltage-gated ion channels. *Annu. Rev. Biochem.*, **64**, 493-531.

Cavelli, A., Fanelli, F., Taddei, C., de Benedetti, P.G. & Cotecchia, S. (1996). Amino acids of the  $\alpha_{1B}$ -adrenergic receptor involved in agonist binding: differences in docking catecholamines to receptor subtypes. *FEBS (Letters)*., **399**, 9-13.

Chalfie, M. & Kain, S.R. (1998). Green fluorescent protein properties, applications and protocols. Wiley-Liss Press, New York., 385pp.

Chang, D.J., Chang, T.K., Yamanishi, S.S., Salazar, F.H., Kosaka, A.H., Khare, R., Bhakta, S., Jasper, J.R., Shieh, I.S., Lesnick, J.D., Ford, A.P., Daniels, D.V., Elgen, R.M., Clarke, D.E., Bach, C. & Chan, H.W. (1998). Molecular cloning, genomic characterization and expression of novel human  $\alpha_{1A}$ -adrenoceptor isoforms. *FEBS Lett.*, **422**, 279-283.

Chen, S., Xu, M., Lin, F., Lee, D., Riek, P. & Graham, R.M. (1999). Phe310 in transmembrane VI of the  $\alpha_{1B}$ -adrenergic receptor is a key switch residue involved in activation and catecholamine ring aromatic bonding. *J. Biol. Chem.*, **274**, 16320-16330.

Cheng, Y. & Prusoff, W.H. (1973). Relationship between the inhibition constant (K<sub>I</sub>) and the concentration of inhibitor which causes 50 per cent inhibition (I<sub>50</sub>) of an enzymatic reaction. *Biochem. Pharmacol.*, **22**, 3099-3108.

Chuang, T.T., Iacovelli, L., Sallèse, M. & DeBlasi, A. (1996). G protein-coupled receptors: heterologous regulation of homologous desensitisation and its implications. *Trends Pharmacol. Sci.*, **17**, 416-421.

Clapham, D.E. (1995). Calcium signalling. *Cell.*, **80**, 259-268.

Clapham, D.E. & Neer, E.J. (1993). New roles for G-protein beta gamma-dimers in transmembrane signalling. *Nature.*, **365**, 403-6.

Coge, F., Guenin, S-P., Renouard-Try, A., Rique, H., Ouvry, C., Fabry, N., Beauverger, P., Nicolas, J-P., Boutin, J.A. & Canet, E. (1999). Truncated isoforms inhibit [<sup>3</sup>H]prazosin binding and cellular trafficking of native human  $\alpha_{1A}$ -adrenoceptors. *Biochem. J.*, **343**, 231-239.

Conrad, P.A., Smart, E.J., Ying, Y.S., Anderson, R.G.W. & Bloom, G.S. (1996). Caveolin cycles between the plasma membrane caveolae and the Golgi complex by the microtubule-dependant and microtubule-independent steps. *J. Cell. Biol.*, **131**, 1421-1433.

Cotecchia, S., Schwinn, D.A., Randall, R.R., Lefkowitz, R.J., Caron, M.G. & Koblika, B.K. (1988). Molecular cloning and expression of the cDNA for the hamster  $\alpha_1$ -adrenergic receptor. *Proc. Natl. Acad. Sci.*, **85**, 7159-7163.

- Cubit, A.B., Heim, R., Adams, S.R., Boyd, A.F., Gross, L.A. & Tsien, R.Y. (1995). Understanding, improving and using green fluorescent proteins. *Trends Biochem. Sci.*, **17**, 416-421.
- Daaka, Y., Luttrell, L.M., Ahn, S., Della Rocca, G.J. & Ferguson. (1998). Essential role for G Protein-coupled receptor endocytosis in the activation of mitogen-activated protein kinase. *J. Biol. Chem.*, **273**, 685-88.
- Daaka, Y., Luttrell, L.M. & Iefkowitz, R.J. (1997). Switching of the coupling of the beta 2-adrenergic receptor to different G proteins by protein kinase A. *Nature.*, **390**, 88-91.
- Daly, C.J., Milligan, C.M., Milligan, G., MacKenzie, J.F. & McGrath, J.C. (1998). Cellular localization and pharmacological *Alpha-1* adrenoceptors by fluorescent ligand binding and image analysis reveals identical binding properties of clustered and diffuse populations of receptors. *J. Pharmacol. Exp. Ther.*, **286**, 984-990.
- Daniels, D.V., Gever, J.R., Jasper, J.R., Shannon Kava, M., Lesnick, J.D., Meloy, T.D., Stepan, G., Williams, T.J., Clarke, D.E., Chang, D.J. & Ford, A.P.D.W. (1999). Human cloned  $\alpha_{1A}$ -adrenoceptor isoforms display  $\alpha_{1L}$ -adrenoceptor pharmacology in functional studies. *Eur. J. Pharm.*, **370**, 337-343.
- Davis, R.J. (1993). The mitogen-activated protein kinase signal transduction pathway. *J. Biol. Chem.*, **268**, 14553-14556.
- DeBlasi, A., O'Reilly, K. & Motulsky, J. (1989). Calculating receptor number from binding experiments using same compound as radioligand and competitor. *Trends Pharm. Sci.*, **10**, 227-229.
- De Duve, C. (1963). Lysosomes in: *Ciba Foundation Symposium*, edited by A.V.S. de Reuck and M.P. Cameron. London: Curchill, 411-412.

- Dicker, F., Quitterer, U., Winstel, R., Honold, K. & Lohse, M.J. (1999). Phosphorylation-independent inhibition of parathyroid hormone receptor signalling by G protein-coupled receptor kinases. *Proc. Natl. Acad. Sci.*, **11**, 5476-5481.
- Dolman, H.G. & Thorner, J. (1997). RGS proteins and signaling by heterotrimeric G proteins. *J. Biol. Chem.*, **272**, 3871-3874.
- Drew, G.M. (1985). What do antagonists tell us about alpha-adrenoceptors? *Clin. Sci.*, **68** (suppl.10), 15s-19s.
- Dunlap, K., Luebke, J.I. & Turner, T.J. (1995). Exocytotic  $Ca^{2+}$  channels in mammalian central neurons. *Trends Neurosci.*, **18**, 89-98.
- Eason, M.G., Moreira, S.P. & Liggett, S.B. (1995). Four consecutive serines in the third intracellular loop are the sites for  $\beta$ -adrenergic receptor kinase-mediated phosphorylation and desensitisation of the  $\alpha_{2A}$ -adrenergic receptor. *J. Biol. Chem.*, **270**, 4681-4688.
- Ebashi, S. & Lipmann, F. (1962). Adenosine triphosphate-linked concentration of calcium ions in a particulate fraction of rabbit muscle. *J. Cell Biol.*, **14**, 389-400.
- Eckert, R.E., Kartsen, A.J., Utz, J. & Ziegler, M. (2000). Regulation of renal artery smooth muscle tone by  $\alpha_1$ -adrenoceptors: role of voltage-gated calcium channels and intracellular calcium stores. *Urol. Res.*, **28**, 122-127.
- Eisenhofer, G., McCarty, R., Pacak, K., Russ, H. & Schomig, E. (1996). Disprocynium24, a novel inhibitor of the extraneuronal monoamine transporter, has patent effects on the inactivation of circulating noradrenaline and adrenaline in conscious rat. *Naunyn-Schmiedeberg's Arch. Pharmacol.*, **354**, 287-294.
- Eltze, M., Konig, H., Ullrich, B. & Grebe, T. (2001). Failure of A111110A to functionally discriminate between  $\alpha_1$ -adrenoceptor subtypes A, B and D or between  $\alpha_1$ - and  $\alpha_2$ -adrenoceptors. *Eur. J. Pharmacol.*, **415**, 265-276.

Eltze, M., König, H., Ullrich, B. & Grebe, T. (1999). Buspirone functionally discriminates tissues endowed with  $\alpha_1$ -adrenoceptor subtypes A, B, D and L. *Eur. J. Pharmacol.*, **378**, 69-83.

Fain, J.N. & Garcia-Sainz, J.A. (1980). Role of phosphatidylinositol turnover in  $\alpha_1$ - and adenylyl cyclase inhibition of  $\alpha_2$ - effects of catecholamines. *Life Sci.*, **26**, 1183-1194.

Fain, J.N. & Berridge, M.J. (1979). Relationship between hormonal activation of phosphatidylinositol hydrolysis, fluid secretion, and calcium flux in the blowfly salivary gland. *Biochem. J.*, **178**, 45-58.

Fasolato, C., Innocenti, B. & Pozzan, T. (1994). Receptor-activated  $\text{Ca}^{2+}$  influx: How many mechanisms for how many channels? *Trends Pharmacol. Sci.*, **15**, 77-83.

Faure, C., Pimoule, C., Vallancien, G., Langer, S.Z. & Graham, D. (1994). Identification of  $\alpha_1$ -adrenoceptor subtypes present in the human prostate. *Life Sci.*, **54**, 1595-1605.

Ferguson, S.S.G. (1998). Using green fluorescent protein to understand the mechanisms of G-protein-coupled receptor regulation. *Braz. J. Med. Biol. Res.*, **31**, 1471-1477

Ferguson, S., Zhang, J., Barak, L.S. & Caron, M.G. (1997). Pleiotropic role for GRKs and  $\beta$ -arrestins in receptor regulation. *News Physiol. Sci.*, **12**, 145-151.

Flavahan, N.A. & Vanhoutte, P.M. (1986).  $\alpha_1$ -Adrenoceptor subclassification in vascular smooth muscle. *Trends Pharm. Sci.*, **7**, 347-349.

Foglar, R., Shibata, K., Horie, K., Hirasawa, A. & Tsujimoto, G. (1995). Use of recombinant alpha 1-adrenoceptors to characterize subtype selectivity of drugs for the treatment of prostatic hypertrophy. *Eur. J. Pharmacol.*, **288**, 201-207.

Ford, A.P.D.W., Chang, D.J., Clarke, D.E., Daniels, D.V., Eglén, R.M., Gever, J.R., Jasper, J.R., Kava, M.S., Lachnit, W.G., Lesnick, J.D., Meloy, T.D., Stepan, G.T. & Williams, T.J. (1998). Alpha-1A-versus alpha-1L-adrenoceptors: A pharmacological comparison. *Pharmacol. Toxicol. Suppl.*, **83**, 12-14.

Ford, A.P.D.W., Daniels, D.V., Chang, D.J., Gever, J.R., Jasper, J.R., Lesnick, J.D. & Clarke, D.E. (1997). Pharmacological pleiotropism of the human recombinant  $\alpha_{1A}$ -adrenoceptor: implications for  $\alpha_1$ -adrenoceptor classification. *Br. J. Pharmacol.*, **121**, 1127-1135.

Ford, A.P.D.W., Williams, T.J., Bluc, D.R. & Clarke, D.E. (1994).  $\alpha_1$ -Adrenoceptor classification: sharpening Occam's razor. *Trends Pharmacol. Sci.*, **15**, 167-170.

Franke, R.R., König, B., Sakmar, T.P., Khorana, H.G. & Hoffman, K.P. (1990). Rhodopsin mutants that bind but fail to activate transducin. *Science*, **250**, 123-125.

Freedman, N.J. & Lefkowitz, R.J. (1996). Desensitisation of G protein-coupled receptors. *Rec. Prog. Horm. Res.*, **51**, 319-351.

Freissmuth, M., Casey, P.J. & Gilman, A.G. (1989). G proteins control diverse pathways of transmembrane signaling. *FASEB J.*, **3**, 2125-31.

Furchgott, R. (1972). The classification of adrenoceptors (adrenergic receptors): An evaluation from the standpoint of receptor theory. *Handbook of Exp. Pharm.*, **33**, 283-355.

García-Sainz, J.A., Vázquez-Prado, J. & del Carmen Medina, L. (2000).  $\alpha_1$ -Adrenoceptors: function and phosphorylation. *Eur. J. Pharm.*, **389**, 1-12.

García-Sainz, J.A., Vázquez-Prado, J. & Villalobos-Molina, R. (1999).  $\alpha_1$ -Adrenoceptors: Subtypes, Signalling, and roles in health and disease. *Arch. Med. Res.*, **30**, 449-458.

Garcia-Sainz, J.A. & Torres-Padilla, M.E. (1999). Modulation of basal intracellular calcium by inverse agonists and phorbol myristate in rat-1 fibroblasts stably expressing  $\alpha_{1d}$ -adrenoceptors. *FEBS (Letters)*, **443**, 277-281.

Garcia-Sainz, J.A., Gottfried-Blackmore, A., Vazquez-Prado, J. & Romero-Avila, M.T. (1999). Protein kinase C-mediated phosphorylation and desensitisation of human  $\alpha_{1B}$ -adrenoceptors. *Eur. J. Pharm.*, **385**, 263-271.

Garcia-Sainz, J.A. (1995).  $\alpha_1$ -Adrenergic action: receptor subtypes, signal transduction and regulation. *Cell Signal.*, **5**, 539-547.

Garcia\_Sainz, J.A., Romero-Avila, M.T., Alcantara-Hernandez, R. & Olivares-Reyes, A. (1993). Different sensitivity to methoxamine and oxymetazoline of hepatocytes expressing  $\alpha_{1A}$ -,  $\alpha_{1B}$ -, and  $\alpha_{1C}$ -adrenoceptors. *Pharmacol. Commun.*, **2**, 339-44.

Gaurino, R.D., Perez, D.M. & Piascik, M.T. (1996). Recent advances in the molecular pharmacology of the  $\alpha_1$ -adrenergic receptors. *Cell Signal.*, **8**, 323-333.

Giardina, D., Crucianelli, M., Romanelli, R., Leonardi, A., Poggesi, E. & Melchiorre, C. (1996). Synthesis and biological profile of the enantiomers of [4-(4-amino-6,7-dimethoxyquinazolin-2-yl)-cis-octahydroquinoxalin-1-yl]furan-2-ylmethanone (cyclazosin), a potent competitive alpha (1B)-adrenoceptor antagonist. *J. Med. Chem.*, **39**, 4602-4607.

Gluchowski, C., Forray, C., Chiu, G., Brancheck, T.A., Wetzel, J. & Hartig, P.R. (1994). The use of alpha-1C specific compounds to treat benign prostatic hyperplasia. *International Patent Application No. WO 94/10989*

Goetz, A.S., King, H.K., Ward, S.D.C., True, T.A., Rimele, T.J. & Saussy Jr, D.L. (1995). BMY 7378 is a selective antagonist of the D subtype of  $\alpha_1$ -adrenoceptors. *Eur. J. Pharm.*, **272**, R5-R6.

- Goldbeter, A., Dupont, G. & Berridge, M.J. (1990). Minimal model for signal induced  $\text{Ca}^{2+}$  oscillations and for their frequency encoding through protein phosphorylation. *Proc. Natl. Acad. Sci. USA.*, **87**, 1461-1465.
- Gonzalez-Espinosa, C., Romero-Avila, M.T., Mora-Rodriguez, D.M., Gonzalez-Espinosa, D. & Garcia-Sainz, J.A. (2001). Molecular cloning and functional expression of the guinea pig  $\alpha_{1a}$ -adrenoceptor. *Eur. J. Pharm.*, **426**, 147-155.
- Goodman, O.B.Jr., Krupnick, J.G., Santini, F., Gurevich, V.V. & Penn, R.B. (1996). Beta-arrestin acts as a clathrin adaptor in endocytosis of the beta 2-adrenergic receptor. *Nature.*, **383**, 447-50.
- Grady, E.F., Bohn, S.K. & Bunnett, N.W. (1997). Turning off the signal: mechanisms that attenuate signaling by G protein-coupled receptors. *Am. J. Physiol.*, **273**, G586-G601.
- Graham, R.M., Perez, D.M., Iiwa, J. & Piascik. (1996).  $\alpha_1$ -adrenergic receptor subtypes: Molecular structure, function and signalling. *Circ. Res.*, **78**, 737-749.
- Greengrass, P. & Bremner, R. (1979). Binding characteristics of  $^3\text{H}$ -Prazosin to rat brain  $\alpha$ -adrenergic receptors. *Eur. J. Pharmacol.*, **55**, 323-326.
- Grohmann, M. & Trendelenburg, U. (1984). The substrate specificity of uptake<sub>2</sub> in rat heart. *Naunyn-Schmiedeberg's Arch. Pharmacol.*, **328**, 164-173.
- Gross, G., Hanft, G. & Rugevics, C. (1988). 5-methyl-urapidil discriminates between subtypes of the alpha-1 adrenoceptor. *Eur. J. Pharmacol.*, **151**, 333-335.
- Gruenberg, J. & Maxfield, F.R. (1995). Membrane transport in the endocytic pathway. *Curr. Opin. Cell Biol.*, **7**, 552-563.

Grundemann, D., Schchinger, B., Rappold, G.A. & Schomig, F. (1998). Molecular identification of the corticosterone-sensitive extraneuronal catecholaminic transporter. *Nature neurosci.*, **1**, 349-351.

Grundemann, D., Koster, S., Kiefer, N., Breidert, T., Engelhardt, M., Spitzenberger, F., Obermuller, N. & Schomig, E. (1998). Transport of monoamine transmitters by the organic cation transporter type 2, OCT2. *J. Biol. Chem.*, **273**, 30915-30920.

Grynkiewicz, G., Poenic, M. & Tsien, R.Y. (1985). A new generation of  $Ca^{2+}$ -indicators with greatly improved fluorescence properties. *J. Biol. Chem.*, **265**, 3440-3450.

Gudermann, T., Kalkbrenner, F. & Schultz, G. (1996). Diversity and selectivity of Receptor-G Protein interaction. *Annu. Rev. Pharmacol. Toxicol.*, **36**, 428-459.

Hamada, H., Damron, D.S., Hong, S.J., Van Wagoner, D.R. & Murray, P.A. (1997). Phenylephrine-induced  $Ca^{2+}$  oscillations in canine pulmonary artery smooth muscle cells. *Circ. Res.*, **81**, 812-823.

Han, C., Esbenshade, T.A. & Minneman, K. P. (1992). Subtypes of alpha 1-adrenoceptors in DDT1 MF-2 and BC3H-1 clonal cell lines. *Eur. J. Pharmacol.*, **226**, 141-148.

Han, C. & Minneman, K.P. (1991). Interaction of subtype-selective antagonists with  $\alpha_1$ -adrenergic receptor binding sites in rat tissues. *Mol. Pharmacol.*, **40**, 531-538.

Han, C. Wilson, K.M. and Minneman, K.P. (1990).  $\alpha_1$ -Adrenergic receptor subtypes and formation of inositol phosphates in dispersed hepatocytes and renal cells. *Mol Pharmacol.*, **37**, 903-910.

Han, C., Abel, P.W. & Minneman, K.P. (1987).  $\alpha_1$ -Adrenoceptor subtypes linked to different mechanisms for increasing intracellular  $Ca^{2+}$  in smooth muscle. *Nature.*, **329**, 333-335.

Hancock, A.A. (1996).  $\alpha_1$ -Adrenoceptor subtypes: a synopsis of their pharmacology and molecular biology. *Drug Development Res.*, **39**, 54-107.

Hao, M. & Maxfield, F.R. (2000). Characterization of rapid membrane internalization and recycling. *J. Biol. Chem.*, **275**, 15279-15286.

Harrison, J.K., Pearson, W.K. & Lynch, K.R. (1991). Molecular characterisation of  $\alpha_1$ - and  $\alpha_2$ -adrenoceptors. *Trends Pharmacol. Sci.*, **12**, 62-67.

Hatano, A., Takahashi, H., Tamaki, M., Komeyama, T., Koizumi, T. & Takeda, M. (1994). Pharmacological evidence of distinct  $\alpha_1$ -adrenoceptor subtypes mediating the contraction of human prostatic urethra and peripheral artery. *Br. J. Pharmacol.*, **113**, 723-728.

Hebert, T.E. & Bouvier, M. (1998). Structural and functional aspects of G protein-coupled receptor oligomerization. *Biochem. Cell Biol.*, **76**, 1-11.

Hein, L. & Kobilka, B.K. (1997). Adrenergic receptors: from molecular structure to in vivo function. *Trends Cardio. Med.*, **7**, 137-145.

Hein, L., Ishii, K., Coughlin, S.R. & Kobilka, B.K. (1994). Intracellular targeting and trafficking of thrombin receptors. A novel mechanism for resensitization of a G protein-coupled receptor. *J. Biol. Chem.*, **269**, 27719-27726.

Hein, P., Goepel, M., Cotecchia, S. & Michel, M.C. (2000). Comparison of [ $^3$ H]tamsulosin and [ $^3$ H]prazosin binding to wild-type and constitutively active  $\alpha_{1B}$ -adrenoceptors. *Life Sciences.*, **67**, 503-508.

Heximer, S.P., Cristillo, A.D. & Forsdyke, D.R. (1997). Comparison of mRNA expression of two regulators of G-protein signalling, RGS1/BL34/1R20 and RGS2/G0S8, in cultured human blood mononuclear cells. *DNA Cell Biol.*, **16**, 589-598.

Hieble, J.P., Bylund, D.B., Clarke, D.E., Eikenburg, D.C., Langer, S.Z., Lefkowitz, R.J., Minneman, K.P. & Ruffolo Jr, R.R. (1995). International Union of pharmacology. Recommendation for nomenclature of  $\alpha_1$ -adrenoceptors: Consensus update. *Pharm. Reviews.*, **47**, 267-270.

Hille, B. (1992). G protein-coupled mechanisms and nervous signalling. *Neuron.*, **9**, 187-95.

Hirasawa, A., Sugawara, T., Awaji, T., Tsumaya, K., Ito, H. & Tsujimoto, G. (1997). Subtype-specific differences in subcellular localization of  $\alpha_1$ -adrenoceptors: Chlorethylclonidine preferentially alkylates the accessible cell surface  $\alpha_1$ -adrenoceptors irrespective of the subtype. *J. Pharmacol. Exp. Ther.*, **52**, 764-770.

Hirasawa, A., Shibata, K., Horie, K., Takei, Y., Obika, K., Tanaka, T., Muramoto, N., Takagaki, K., Yano, J. & Tsujimoto, G. (1995). Cloning, functional expression and tissue distribution of human alpha 1C-adrenoceptor splice variants. *FEBS Lett.*, **363**, 256-260.

Holck, M.I., Jones, C.H.M. & Haeusler, G. (1983). Differential interactions of clonidine and methoxamine with the postsynaptic alpha-adrenoceptor of rabbit main pulmonary artery. *J. Cardiovasc. Pharmacol.*, **5**, 240-248.

Honner, V. & Docherty, J.R. (1999). Investigation of the subtypes of  $\alpha_1$ -adrenoceptor mediating contractions of rat vas deferens. *Br. J. Pharmacol.*, **128**, 1323-1331.

Hrometz, S.L., Edelman, S.E., Mccune, D.F., Olges, J.R., Hadley, R.W., Perez, D.M. & Piascik, M.T. (1999). Expression of multiple  $\alpha_1$ -adrenoceptors on vascular smooth muscle: Correlation with the regulation of contraction. *J. Pharmacol. Exp. Ther.*, **290**, 452-463.

- Hu, Z-W., Shi, X.Y., Lin, R.Z. & Hoffman, B.B. (1999). Contrasting signalling pathways of  $\alpha_{1A}$ - and  $\alpha_{1B}$ -adrenergic receptor subtype activation of phosphatidylinositol 3-kinase and ras in transfected NIH 3T3 cells. *Mol. Endocrinol.*, **13**, 3.
- Hu, Z-W., Shi, X.Y., Lin, R.Z. & Hoffman, B.B. (1996).  $\alpha_1$ -Adrenergic receptors activate phosphatidylinositol 3-kinase in human vascular smooth muscle cells. Role in mitogenesis. *J. Biol. Chem.*, **271**, 8977.
- Hunt, T.W., Fields, T.A., Casey, P.J. & Peralta, E.G. (1997). RGS10 is a selective activator of G alpha i GTPase activity. *Nature.*, **383**, 175-177.
- Hunyady, L., Merelli, F., Baukal, A.J., Balla, T. & Catt, K.J. (1991). Agonist-induced endocytosis and signal generation in adrenal glomerulosa cells. A potential mechanism for receptor-operated calcium entry. *J. Biol. Chem.*, **266**, 27783-2788.
- Hwa, J., Graham, R.M. & Perez, D.M. (1995). Identification of critical determinants of  $\alpha_1$ -adrenergic receptor subtype selective agonist binding. *J. Biol. Chem.*, **270**, 23189-23195.
- Hwa, J. & Perez, D.M. (1996). The unique nature of the serine interactions for  $\alpha_1$ -adrenergic receptor agonist binding and activation. *J. Biol. Chem.*, **271**, 6322-6327.
- Ikeda, S.R. (1996). Voltage-dependent modulation of N-type calcium channels by G-protein beta gamma subunits. *Nature.*, **380**, 255-8.
- Iversen, L.L. & Salt, P.J. (1970). Inhibition of catecholamine Uptake<sub>2</sub> by steroids in the isolated rat heart. *Br. J. Pharmacol.*, **40**, 528-530.
- Iversen, L.L. (1965). The uptake of catechol amines at high perfusion concentrations in the rat isolated heart: A novel catechol amine uptake process. *Br. J. Pharmacol.*, **25**, 18-33.

Jarajapu, Y.P.R., Coats, P., McGrath, J.C., Hillier, C. & MacDonald, A. (2001). Functional characterization of  $\alpha_1$ -adrenoceptor subtypes in human skeletal muscle resistance arteries. *Br. J. Pharmacol.*, **133**, 679-686.

Johnson, R.D. & Minneman, K.P. (1987). Differentiation of alpha-1-adrenergic receptors linked to phosphatidylinositol turnover and cyclic AMP accumulation in rat brain. *Mol. Pharmacol.*, **31**, 239-246.

Johnson, R.D. & Minneman, K.P. (1986). Characterisation of  $\alpha_1$ -adrenoceptors which increase cAMP accumulation in rat cerebral cortex. *Eur. J. Pharmacol.*, **129**, 293-305.

Kallal, L. & Benovic, J.L. (2000). Using green fluorescent proteins to study G-protein-coupled receptor localization and trafficking. *Trends Pharm. Sci.*, **21**, 175-180.

Kanaseki, T. & Kadota, K. (1969). The "vesicle in basket". A morphological study of the coated vesicle isolated from the nerve endings of the guinea pig brain, with special reference to the mechanism of membrane movements. *J. Biol. Chem.*, **42**, 202-220.

Kanterman, R.Y., Felder, C.C., Brennerman, D.E., Ma, A.L., Fitzgerald, S. & Axelrod, J. (1990). Alpha 1-adrenergic receptor mediates arachidonic acid release in spinal chord neurons independent of inositol phospholipid turnover. *J. Neurochem.*, **54**, 1225-1232.

Karhunen, T., Tilgmann, C., Ulmanen, I., Julkunen, I. & Panula, P. (1994). Distribution of catechol-O-methyltransferase enzyme in rat tissues. *J. Histochem. Cytochem.*, **42**, 1079-1090.

- Kenny, B.A., Miller, A.M., Williamson, I.J.R., O'Connell, J, Chalmers, D.H. & Naylor, A.M. (1996). Evaluation of the pharmacological selectivity profile  $\alpha_1$ -adrenoceptor antagonists at prostatic  $\alpha_1$ -adrenoceptors: Binding, functional, and in-vivo studies. *Br. J. Pharmacol.*, **118**, 871-878.
- King, H.K., Goetz, A.S., Ward, S.D.C. & Saussy Jnr, D.L. (1994). AHH1110A is selective for the  $\alpha_{1B}$  subtype of  $\alpha_1$ -adrenoceptors. *Soc. Neurosci. Abstr.*, **20**, 526.
- Kirby, R.S. (1999). Clinical pharmacology of  $\alpha_1$ -adrenoceptor antagonists. *Eur. Urol.*, **36**, 48-53.
- Klijin, K., Slivka, S.R., Bell, K. & Insel, P.A. (1991). Renal  $\alpha_1$ -adrenergic receptor subtypes; MDCK-D1 cells, but not rat cortical membranes possess a single population of receptors. *Mol. Pharmacol.*, **39**, 407-413.
- Knepper, S.M., Buckner, S.A., Brune, M.E., DeBernardis, J.F., Meyer, M.D. & Hancock, A.A. (1995). A-61603, a potent  $\alpha_1$ -Adrenergic receptor agonist, selective for the  $\alpha_{1A}$  receptor subtype. *J. Pharmacol. Exp. Ther.*, **274**, 97-103.
- Ko, F.N., Guh, J.H., Yu, S.M., Hou, Y.S., Wu, Y.C. & Teng, C.M. (1994). (-)-Discretamine, a selective  $\alpha_{1D}$ -adrenoceptor antagonist, isolated from *Fissistigma glaucescens*. *Br. J. Pharmacol.*, **112**, 1174.
- Koenig, J.A. & Edwardson, J.M. (1997). Endocytosis and recycling of G protein-coupled receptors. *Trends Pharm. Sci.*, **18**, 276-287.
- Kopin, I.J., Rundqvist, B., Friberg, P., Lenders, J., Goldstein, D.S. & Eisenhofer, G. (1998). Different relationships of spillover to release of norepinephrine in human heart, kidneys, and forearm. *Am. J. Physiol.*, **275**, R165-R173.
- Koshimizu, T., Yamauchi, J., Hirasawa, A., Tanoue, A. & Tsujimoto, G. (2002). Recent progress in  $\alpha_1$ -Adrenoceptor pharmacology. *Biol. Pharm. Bull.*, **25**, 401-408.

Krueger, K.M., Daaka, Y., Pitcher, J.A. & Lefkowitz, R.J. (1997). The role of sequestration in G Protein-coupled receptor resensitisation: regulation of  $\beta_2$ -adrenergic receptor dephosphorylation by vesicular acidification. *J. Biol. Chem.*, **272**, 5-8.

Krupnick, J.G. & Benovic, J.L. (1998). The role of receptor kinases and arrestins in G-protein coupled receptor regulation. *Annu. Rev. Pharmacol. Toxicol.*, **38**, 289-319.

Kumagai, H., Ebashi, S. & Takeda, F. (1955). Essential relaxing factor in muscle other than myokinase and creatine phosphokinase. *Nature.*, **176**, 166.

Laduron, P.M. (1994). From receptor internalization to nuclear translocation. *Biochem. Pharmacol.*, **47** (1), 3-13.

Lands, A.M., Arnold, A., McAuliff, J.P., Lunduena, F.P. & Brown, T.G. (1967). Differentiation of receptor systems activated by sympathomimetic amines. *Nature.*, **214**, 597-598.

Langer, S.Z., Pimoule, C., Faure, C. & Graham, D. (1994). Evidence that the classical  $\alpha_1$ - and cloned  $\alpha_{1C}$ -adrenoceptors are the same subtype. *Can. J. Physiol. Pharmacol.*, **72**, 554.

Langer, S.Z. (1974). Presynaptic regulation of catecholamine release. *Biochem. Pharmacol.*, **23**, 1793-1800.

Laz, T.M., Forray, C., Smith, K.E., Vacsse, P.J.J., Hartig, P.R., Gluchowski, C., Branchek, T.A. & Weinshank, R.L. (1993). Recombinant rat homolog of the bovine  $\alpha_{1C}$ -adrenergic receptor exhibits an  $\alpha_{1A}$ -like receptor pharmacology. *Soc. Neurosci. Abstr.*, **19**, 1788.

Lazareno, S. & Birdsall, N.J.M. (2000). Effects of contamination on radioligand binding parameters. *Trends Pharm. Sci.*, **21**, 57-60.

Leff, P. (1995). The two-state model of receptor activation. *Trends Pharm. Sci.*, **16**, 89-97.

Lefkowitz, R.J., Pitcher, J., Krueger, K. & Daaka, Y. (1998). Mechanisms of beta-adrenergic receptor desensitisation and resensitisation. *Adv. Pharmacol.*, **42**, 416-420.

Lefkowitz, R.J., Cotecchia, S., Samama, P. & Costa, T. (1993). Constitutive activity of receptors coupled to guanine nucleotide regulatory proteins. *Trends Pharmacol. Sci.*, **14**, 303-307.

Lencer, W.I., Hirst, T.R. & Holmes, R.K. (1999). Membrane traffic and the cellular uptake of cholera toxin. *Biochem. Biophys. Acta.*, **1450**, 177-190.

Li, X-F., Kargacin, M.E. & Triggle, C.R. (1993). The effects of  $\alpha$ -adrenoceptor agonists on intracellular  $\text{Ca}^{2+}$  levels in freshly dispersed single smooth muscle cells from rat tail artery. *Br. J. Pharmacol.*, **109**, 1272-1275.

Libert, F., Parmentier, M., Lefort, A., Dinsart, & Van Sande, J. (1989). Selective amplification and cloning of four new members of the G protein-coupled receptor family. *Science.*, **244**, 569-572.

Ljung, B. & Kjellstedt, A. (1987). Functional antagonism of noradrenaline responses to felodipine and other  $\text{Ca}^{2+}$  antagonists in vascular smooth muscles. *J. Cardiovasc. Pharmacol.*, **10**, 82-88.

Llahi, S. & Fain, J.N. (1992).  $\alpha_1$ -Adrenergic receptor-mediated activation of phospholipase D in rat cerebral cortex. *J. Biol. Chem.*, **267**, 3679.

Lohse, M.J., Benovic, J.L., Codina, J., Caron, M. & Lefkowitz, R.J. (1990).  $\beta$ -Arrestin: a protein that regulates  $\beta$ -adrenergic receptor function. *Science*, **248**, 1547-1550.

Lomansey, J.W., Allen, L.F., Capel, D. & Lefkowitz, R.J. (1993). *Clin. Res.*, **41**, 264A.

Lomansey, J.W., Cotecchia, S., Lefkowitz, R.J. & Caron, M.G. (1991a). Molecular biology of  $\alpha$ -Adrenergic receptors: implications for receptor classification and for structure-function relationships. *Biochem. Biophys. Acta.*, **1095**, 127-139.

Lomansey, J.W., Cotecchia, S., Lorenz, W., Leung, W.Y., Schwinn, D.A., Yang-Feng, T.L., Brownstein, M., Lefkowitz, R.J. & Caron, M.G. (1991b). Molecular cloning and expression of the cDNA for the  $\alpha_{1A}$ -adrenergic receptor: the gene for which is located on human chromosome 5. *J. Biol. Chem.*, **266**, 6365-6369

MacKenzie, J.F., Daly, C.J., Pediani, J.D. & McGrath, J.C. (2000). Quantitative imaging in live human cells reveals intracellular  $\alpha_1$ -Adrenoreceptor ligand-binding sites. *J. Pharmacol. Exp. Ther.*, **294**, 434-443.

Macrez-Lepretre, N., Kalkbrenner, F., Scultz, G. & Mironneau. (1997). Distinct functions of  $G_q$  and  $G_{11}$  proteins in coupling  $\alpha_1$ -adrenoreceptors to  $Ca^{2+}$  release and  $Ca^{2+}$  entry in rat portal vein myocytes. *J. Biol. Chem.*, **272**, 5261-5268.

Marshall, I., Burt, R.P. & Chapple, C.R. (1995). Noradrenaline contractions of human prostate by  $\alpha_{1A}$ -( $\alpha_{1C}$ -) adrenoreceptor subtype. *Br. J. Pharmacol.*, **115**, 781-786.

Maruyama, K., Nakamura, T., Yoshihara, T., Fukutomi, J., Sugiyama, K., Hattori, K., Ohnuki, T., Watanabe, K. & Nagatomo, T. (1998). Tamsulosin: Assessment of affinity of  $^3H$ -Prazosin bindings to two  $\alpha_1$ -adrenoreceptor subtypes ( $\alpha_{11}$  and  $\alpha_{1L}$ ) in bovine prostate and rat heart and brain. *Gen. Pharm.*, **31**, 597-600.

McCune, D.F., Edelmann, S.E., Olges, J.R., Post, G.R., Waldrop, B.A., Waugh, D.J.J., Perez, D.M. & Piascik, M.T. (2000). Regulation of the cellular localization and signalling properties of the  $\alpha_{1B}$ - and  $\alpha_{1D}$ -adrenoreceptors by agonists and inverse agonists. *Am. Soc. Pharm. Exp. Ther.*, **57**, 659-666.

- McGrath, J.C., MacKenzie, J.F. & Daly, C.J. (1999). Pharmacological implications of cellular localisation of  $\alpha_1$ -adrenoceptors in native smooth muscle cells. *J. Auton. Pharmacol.*, **19**, 303-310.
- McGrath, J.C., Arribas, S. & Daly, C.J. (1996). Fluorescent ligands for the study of receptors. *Trends Pharm. Sci.*, **17**, 393-399.
- McGrath, J.C. & Daly, C.J. (1995). Viewing adrenoceptors; past, present, and future; commentary and a new technique. *Pharmacol. Commun.*, **6**, 269-279.
- McGrath, J.C. (1982). Evidence for more than one type of post-junctional  $\alpha$ -adrenoceptor. *Biochem. Pharmacol.*, **31**, 467-484.
- McWhinney, C., Wenham, D., Kanwal, S., Kalman, V., Hansen, C. & Robishaw, J.D. (2000). Constitutively active mutants of the  $\alpha_{1a}$ - and the  $\alpha_{1b}$ -adrenergic receptor subtypes reveal coupling to different signalling pathways and physiological responses in rat cardiac myocytes. *J. Biol. Chem.*, **275**, 2087-2097.
- Medgett, I.C. & Langer, S.Z. (1984). Heterogeneity of smooth muscle alpha adrenoceptors in rat tail artery in vitro. *J. Pharmacol. Exp. Ther.*, **229**, 823-830.
- Meyer, M.D., Altenbach, R.J., Hancock, A.A., Buckner, S.A., Knepper, S.M. & Kerwin, J.F. (1996). Synthesis and in vitro characterization of *N*-[5-(4,5-dihydro-1*H*-imidazol-2-yl)-2-hydroxy-5,6,7,8-tetrahydro-naphthalen-1-yl]methanesulfonamide and its enantiomers: a novel selective alpha 1A receptor agonist. *J. Med. Chem.*, **39**, 4116-4119.
- Michel, M.C. & Goepel, M. (1998). Differential  $\alpha_1$ -adrenoceptor labeling by [<sup>3</sup>H]prazosin and [<sup>3</sup>H]tamsulosin. *Eur. J. Pharmacol.*, **342**, 85-92.
- Michell, R.H. (1975). Inositol phospholipids and cell surface receptor function. *Biochem. Biophys. Acta.*, **415**, 81-147.

- Michclotti, G.A., Price, D.T. & Schwinn, D.A. (2000).  $\alpha_1$ -Adrenergic receptor regulation: basic science and clinical implications. *Pharm. & Ther.*, **88**, 281-309.
- Milligan, G. (1999). Exploring the dynamics of regulation of G protein-coupled receptors using green fluorescent protein. *Br. J. Pharmacol.*, **128**, 501-510.
- Minarini, A., Budriesi, R., Chiarini, A., Leonardi, A. & Melchiorre, C. (1998). Search for  $\alpha_1$ -adrenoceptor subtypes selective antagonists: design, synthesis and biological activity of cystazosin, an  $\alpha_{1D}$ -adrenoceptor antagonist. *Bio. Med. Chem. Lett.*, **8**, 1353-1358.
- Minneman, K.P., Theroux, T.L., Hollinger, S., Han, C. & Esbenshade, T.A. (1994). Selectivity of agonists for cloned alpha 1-adrenergic receptor subtypes. *Mol. Pharmacol.*, **46**, 929-936.
- Minneman, K.P. & Esbenshade, T.A. (1994).  $\alpha_1$ -Adrenergic receptor subtypes. *Annu. Rev. Pharmacol. Toxicol.*, **34**, 117-133.
- Minneman, K.P. (1988).  $\alpha_1$ -Adrenergic receptor subtypes, inositol phosphates and sources of cell  $Ca^{2+}$ . *Pharm. Reviews.*, **40**, 87-119.
- Mogami, H., Tepikin, A.V. & Petersen, O.H. (1998). Termination of cytosolic  $Ca^{2+}$  reuptake into intracellular stores is regulated by the free  $Ca^{2+}$  concentration in the store lumen. *EMBO J.*, **17**, 435-442.
- Montesano, R., Roth, J., Robert, A. & Orci, L. (1982). Non-coated membrane invaginations are involved in binding and internalisation of cholera and tetanus toxins. *Nature.*, **296**, 651-653.
- Moran, N.C. & Perkins, M.E. (1958). Adrenergic blockade of the mammalian heart by a dichloro analogue of isoproterenol., *J. Pharmacol. Exp. Ther.*, **124**, 223-237.

Morrow, A.L. & Creese, I. (1986). Characterization of  $\alpha_1$ -Adrenergic receptor subtypes in rat brain: A reevaluation of [ $^3$ H]WB4104 and [ $^3$ H]Prazosin binding. *Mol. Pharmacol.*, **29**, 321-330.

Mukherjee, S., Palczewski, K., Gurevic, V., Benovic, J.L., Banga, J.P. & Hunzicker-Dunn, M. (1999). A direct role for arrestins in desensitisation of the luteinizing hormone/choriogonadotropin receptor in porcine ovarian follicular membranes. *Proc. Natl. Acad. Sci. U.S.A.*, **96**, 493-498.

Mukherjee, S., Ghosh, R.N. & Maxfield, F.R. (1997). Endocytosis. *Physiol. Rev.*, **77**, 759-803.

Muramatsu, I., Ohmura, T., Hashimoto, S. & Oshita, M. (1995). Functional subclassifications of vascular  $\alpha_1$ -adrenoceptors. *Pharm. Comm.*, **6**, 23-28.

Muramatsu, I., Oshita, M., Ohmura, T., Kigoshi, S., Akino, H., Gohara, M. & Okada, K. (1994). Pharmacological characterisation of  $\alpha_1$ -adrenoceptor subtypes in the human prostate: functional and binding studies. *Br. J. Urol.*, **74**, 572-578.

Muramatsu, I., Ohmura, T., Kigoshi, S., Hashimoto, S. & Oshita, M. (1990). Pharmacological subclassification of  $\alpha_1$ -adrenoceptors in vascular smooth muscle. *Br. J. Pharmacol.*, **99**, 187-201.

Nambi, P., Peters, J.P., Sibley, D.R. & Lefkowitz, R.J. (1985). Desensitisation of the turkey erythrocyte  $\beta$ -adrenergic receptor in a cell-free system. *J. Biol. Chem.*, **260**, 2166-2171.

Nebigil, C. & Malik, K.U. (1992). Comparison of signal transduction mechanisms of alpha-2C and alpha-1A adrenergic receptor-stimulated prostaglandin synthesis. *J. Pharmacol. Exp. Ther.*, **263**, 987-996.

Neer, E.J. (1995). Heterotrimeric Proteins: Organizers of Transmembrane Signals. *Cell.*, **80**, 249-257.

Neubig, R.R. (1994). Membrane organization in G-protein mechanisms. *Faseb J.* **8**, 939-946.

Newman-Tancredi, A., Conte, C., Chaput, C., Spedding, M. & Millan, M. (1997). Inhibition of the constitutive activity of human 5-HT<sub>1A</sub> receptors by the inverse agonist, spiperone but not the neutral antagonist WAY 100,635. *Br. J. Pharmacol.*, **120**, 737-739.

Nishio, E., Nakata, H., Arimura, S. & Watanabe, Y. (1996). Alpha 1-adrenergic receptor stimulation causes arachidonic acid release through pertussis toxin-sensitive GTP-binding protein and JNK activation in rabbit aortic smooth muscle cells. *Biochem. Biophys. Res. Commun.*, **219**, 277-282.

Offermanns, S. & Schultz, G. (1994). Complex information processing by the transmembrane signaling system involving G proteins. *Naunyn-Schmiedeberg's Arch. Pharmacol.*, **350**, 329-338.

Ohmura, T., Sakamoto, S., Hayashi, H., Kigoshi, S. & Muramatsu, I. (1993). Identification of alpha-1 adrenoceptor subtypes in the dog prostate. *Urol. Res.*, **21**, 211-215.

Oliver, G. & Schaffer, F.A. (1895). The physiological effects of extracts from suprarenal capsules. *J. Physiol.*, **18**, 230-237.

O'Neill, A.B., Buckner, S.A., Brunc, M.E., Milicic, I., Daza, A.V., Gauvin, D.M., Altenbach, R.J., Meyer, M.D., Williams, M., Sullivan, J.P. & Brioni, J.D. (2001). Pharmacological properties of A-204176, a novel and selective  $\alpha_{1A}$  adrenergic agonist, in *in vitro* and *in vivo* models of urethral function. *Life Sciences.*, **70**, 181-197.

Oshita, M., Kigoshi, S. & Muramatsu, I. (1993). Pharmacological characterisation of two distinct alpha 1-adrenoceptor subtypes in rabbit thoracic aorta. *Br. J. Pharmacol.*, **108**, 1071-1076.

Patane, M.A., Scott, A.L., Broten, T.P., Chang, R.S.L., Ransom, R.W., DiSalvo, J., Forray, C. & Bock, M.G. (1998). 4-Amino-2-[4-[1-(benzyloxycarbonyl)-2(S)-[[[(1,1-dimethylethyl)amino]carbonyl]-piperazinyl]-6,7-dimethoxyquinazoline (L-765,314): A potent and selective  $\alpha_{1b}$  adrenergic receptor antagonist. *J. Med. Chem.*, **41**, 1205-1208.

Patel, S., Fernandez-Garcia, E., Hutson, P.H. & Patel, S. (2001). An in vivo binding assay to determine central  $\alpha_1$  -adrenoceptor occupancy using [ $^3$ H]prazosin. *Brain Res. Prot.*, **8**, 191-198.

Pediani, J.D., MacKenzie, J.F., Heeley, R.P., Daly, C.J. & McGrath, J.C. (2000). Single-cell recombinant pharmacology: Bovine  $\alpha_{1a}$  -Adrenoceptors in rat-1 fibroblasts release intracellular  $Ca^{2+}$ , display subtype-characteristic agonism and antagonism, and exhibit an antagonist-reversible inverse concentration-response phase. *J. Pharmacol. Exp. Ther.*, **293**, 887-895.

Pelkmans, L., Kartenbeck, J. & Helenius, A. (2001). Caveolar endocytosis of simian virus 40 reveals a new two-step vesicular-transport pathway to the ER. *Nat. Cell. Biol.*, **3**, 473-483.

Perez, D.M., DeYoung, M.B. & Graham, R.M. (1993). Coupling of expressed alpha 1B- and alpha 1D-adrenergic receptor to multiple signalling pathways is both G Protein and cell type specific. *Mol. Pharmacol.*, **44**, 784-795.

Perez, D.M., Piascik, M.T. & Graham, R.M. (1991). Solution-phase library screening for the identification of rare clones: isolation of an  $\alpha_{1D}$ -adrenergic receptor cDNA. *Mol. Pharmacol.*, **40**, 876-883.

Piascik, M.T. & Perez, D.M. (2001).  $\alpha_1$ -adrenergic receptors: new insights and directions. *J. Pharm. Exp. Ther.*, **298**, 403-410.

- Piasecik, M.T., Soltis, E.E., Piasecik, M.M. & MacMillan, I.B. (1996). Alpha-adrenoceptors and vascular regulation: molecular, pharmacologic and clinical correlates. *Pharmacol. Ther.*, **72**, 215-241.
- Pitcher, J.A., Freedman, N.J. & Lefkowitz, R.J. (1998). G Protein coupled receptor kinases. *Annu. Rev. Biochem.*, **67**, 653-692.
- Powell, C.E. & Slater, I.H. (1958). Blocking of inhibitory adrenergic receptors by a dichloro analogue of isoproterenol. *J. Pharmacol. Exp. Ther.*, **122**, 480-488.
- Pozzan, T., Rizzuto, R., Volpe, P. & Meldolesi, J. (1994). Molecular and cellular physiology of intracellular calcium stores. *Physiol. Rev.*, **74**, 595-636.
- Prasher, D.C., Eckenrode, V.K., Ward, W.W., Prendergast, F.G. & Cormier, M.J. (1992). Primary structure of the *Aequorea Victoria* green-fluorescent protein. *Gene*, **111**, 229-233.
- Price, R. & Schwinn, D.A. (1998). Mechanisms underlying human alpha-1a desensitisation. *FASEB J.*, **12**, A452.
- Price, D.T., Schwinn, D.A., Lomasney, J.W., Allen, L.F., Caron, M.G. & Lefkowitz, R.J. (1993). Identification, quantification, and localization of mRNA for three distinct alpha<sub>1</sub> adrenergic receptor subtypes in human prostate. *J. Urol.*, **150**, 546-551.
- Pulito, V.L., Li, X., Varga, S.S., Mulcahy, L.S., Clark, K.S., Halbert, S.A., Reitz, A.B., Murray, W.V. & Jolliffe, L.K. (2000). An investigation of the uroselective properties of four novel  $\alpha_{1a}$ -Adrenergic receptor subtype-selective antagonists. *J. Pharm. Exp. Ther.*, **294** (1), 224-229.
- Putney Jr, J.W. & Bird, G. St. J. (1993). The inositol phosphate-calcium signaling system in nonexcitable cells. *Endocr. Rev.*, **14**, 610-631.

Putney Jnr, J.W. (1986). A model for receptor-regulated calcium entry. *Cell Calcium*, **7**, 1-12.

Ramarao, C.S., Kincade-Denker, J.M., Perez, D.M., Gaivin, R.J., Riek, R.P. & Graham, R.M. (1992). Genomic organization and expression of the human  $\alpha_{1B}$ -Adrenergic receptor. *J. Biol. Chem.*, **267**, 21936-45.

Rang, H.P., Dale, M.M. & Ritter, J.M. (1995). Pharmacology (3<sup>rd</sup> Edition). *Churchill Livingstone*.

Razani, B., Woodman, S.E. & Lisanti, M.P. (2002). Caveolae: From cell biology to animal physiology. *Pharm. Rev.*, **54**, 431-467.

Remmers, A.E., Engel, C., Liu, M. & Neubig, R.R. (1999). Interdomain interactions regulate GDP release from heterotrimeric G Proteins. *Biochem.*, **38**, 13795-13800.

Riek, R.P., Handschumacher, M.K., Sung, S-S., Tan, M., Glynias, M.J., Schluchter, M.D., Novotney, J. & Graham, R.M. (1995). Evolutionary conservation of both the hydrophilic and hydrophobic nature of transmembrane residues. *J. Theor. Biol.*, **172**, 245-258.

Roettger, B.F., Rentsch, R.U., Pinon, D., Holicky, E., Hadac, E., Larkin, J.M. & Miller, I.J. (1995). Dual pathways of internalisation of the cholecystokinin receptor. *J. Cell. Biol.*, **128**, 1029-1041.

Rokosh, D., Stewart, A., Chang, K., Bailey, B., Karliner, J., Camacho, S., Long, C. & Simpson, P. (1996).  $\alpha_1$ -Adrenergic receptor subtype mRNAs are differentially regulated by  $\alpha_1$ -adrenergic and other hypertrophic stimuli in cardiac myocytes in culture and in vivo. *J. Biol. Chem.*, **271**, 5839-5843.

Rossier, O., Abuin, L., Fanelli, F., Leonardi, A. & Cotecchia, S. (1999). Inverse agonism and neutral antagonism at  $\alpha_{1a}$ - and  $\alpha_{1b}$ -adrenergic receptor subtypes. *J. Pharm. Exp. Ther.*, **56**, 858-866.

Roth, T.F. & Porter, K.R. (1964). Yolk protein uptake in the oocyte of the mosquito *Aedes aegypti* L. *J. Cell Biol.*, **20**, 313-332.

Rovati, G.E. (2000). The many faces of binding artefacts. *Trends Pharm. Sci.*, **21**, 168-169.

Rovati, G.F. (1998). Ligand-binding studies: old beliefs and new strategies. *Trends Pharm. Sci.*, **19**, 365-369.

Roy, S., Luetterforst, R., Harding, A., Apollini, A., Etheridge, M., Stang, E., Rolls, B., Hancock, J.F. & Parton, R.G. (1999). Dominant-negative caveolin inhibits H-Ras function by disrupting cholesterol-rich plasma membrane domains. *Nat. Cell. Biol.*, **1**, 98-105.

Ruan, Y., Kan, H., Parmentier, J., Fatima, S., Allen, L.F. & Malik, K.U. (1998). *Alpha*-1A adrenergic receptor stimulation with phenylephrine promotes arachidonic acid release by activation of phospholipase D in rat-1 fibroblasts: Inhibition by protein kinase A. *J. Pharmacol. Exp. Ther.*, **284**, 576-585.

Ruffolo, R.R., Bondinell, W. & Hieble, J.P. (1995).  $\alpha$ - and  $\beta$ -adrenoceptors. From gene to the clinic. 2. Structure-activity relationships and therapeutic applications. *J. Med. Chem.*, **38**, 3681-3716.

Salomonsson, M., Oker, M., Kim, S., Zhang, H., Faber, J.E. & Arendshorst, W.J. (2001).  $\alpha_1$ -Adrenoceptor subtypes on rat afferent arterioles assessed by radioligand binding and RT-PCR. *Am. J. Physiol.*, **281**, F172-F178.

Samama, P., Cotecchia, S., Costa, T. & Lefkowitz, R.J. (1993). A mutation-induced activated state of the  $\beta_2$ -adrenergic receptor. Extending the ternary complex. *J. Biol. Chem.*, **268**, 4625-4636.

- Santha, E., Lendvai, B. & Gerevich, Z. (2001). Low temperature prevents potentiation of norepinephrine release by phenylephrine. *Neurochem. Int.*, **38**, 237-242.
- Saussy, D.L., Goetz, A.S., Queen, K.L., King, H.K., Lutz, M.W. & Rimele, T.J. (1996). Structure activity relationship of a series of buspirone analogs at alpha-1 adrenoceptors: further evidence that rat aorta alpha-1 adrenoceptors are of the alpha-1D-subtype. *J. Pharmacol. Exp. Ther.*, **278**, 136-44.
- Saussy, D.L., Goetz, A.S., King, H.K. & Trute, T.A. (1994). BMY 7378 is a selective antagonist of  $\alpha_{1D}$ -adrenoceptors: Further evidence that vascular  $\alpha_1$ -adrenoceptors are of the  $\alpha_{1D}$ -subtype. *Can. J. Physiol. Pharmacol.*, **72**, 323.
- Sayet, I., Neuilly, G., Rakotoarisoa, L., Mironneau, J. & Mironneau, C. (1993). Rat vena cava alpha 1B-adrenoceptors: characterization by [3H]prazosin binding and contraction experiments. *Eur. J. Pharm.*, **246**, 275-281.
- Schnitzer, J.E., Oh, P., Pinney, E. & Allard, J. (1994). Filipin-sensitive caveolae-mediated transport in endothelium: Reduced transcytosis, scavenger endocytosis and capillary permeability of select macromolecules. *J. Cell. Biol.*, **127**, 1217-1232.
- Schomig, E., Spitzenberger, F., Engelhardt, M., Martel, F., Ording, M. & Grundemann, D. (1998). Molecular cloning and characterization of two novel transport proteins from rat kidney. *FEBS Lett.*, **425**, 79-86.
- Schultz, J. & Daly, J.W. (1973). Adenosine 3',5' monophosphate in guinea pig cerebral cortical slices: Effects of alpha and beta adrenergic agents, histamine, serotonin, and adenosine. *J. Neurochem.*, **21**, 573-579.

Schwinn, D.A., Johnson, G.I., Page, S.O., Mosley, M.J., Wilson, K.H., Worman, N.P., Campbell, S., Fiddock, M.D., Furness, M., Parry-Smith, B., Peter, B. & Bailey, D.S. (1995). Cloning and pharmacological characterisation of human alpha 1 adrenergic receptors: sequence corrections and direct comparison with other species homologues. *J. Pharmacol. Exp. Ther.*, **272**, 134-142.

Schwinn, D.A., Page, S.O., Middleton, J.P., Lorenz, W., Liggett, S.B., Yamamoto, K., Lapetina, E.G., Caron, M.G., Lefkowitz, R.J. & Cotecchia, S. (1991). The  $\alpha_{1C}$ -adrenergic receptor: characterisation of signal transduction pathways and mammalian tissue heterogeneity. *Mol. Pharmacol.*, **40**, 619-626.

Schwinn, D.A., Lomansey, J.W., Lorenz, W., Szklut, P.J., Fremeau, R.T., Yang-Feng, T.L., Caron, M.G., Lefkowitz, R.J. & Cotecchia, S. (1990). Molecular cloning and expression of the cDNA for a novel  $\alpha_1$ -adrenergic receptor subtype. *J. Biol. Chem.*, **265**, 8183-8189.

Sleight, A.J., Carolo, C., Petit, N., Zwingelstein, C. & Bourson, A. (1995). Identification of 5-hydroxytryptamine<sub>7</sub> receptor binding sites in rat hypothalamus: sensitivity to chronic antidepressant treatment. *Mol. Pharmacol.*, **47**, 99-103.

Sorensen, S.D., McEwen, E.L., Linseman, D.A. & Fischer, S.K. (1997). Agonist-induced endocytosis of muscarinic cholinergic receptors: Relationship to stimulated phosphoinositide turnover. *J. Neurochem.*, **68**, 1473-1483.

Strader, C.D., Sigal, I.S. & Dixon, R.A.F. (1989). Structural basis of beta-adrenergic receptor function. *FASEB J.*, **3**, 1825-1832.

Strader, C.D., Sigal, I.S., Register, R.B., Candelore, M.R., Rands, E. & Dixon, R.A.F. (1987). Identification of residues required for ligand binding to the beta-adrenergic receptor. *Proc. Natl. Acad. Sci.*, **84**, 4384-4388.

Strange, P.G. (2002). Mechanisms of inverse agonism at G-protein-coupled receptors. *Trends Pharm. Sci.*, **23**, 89-95.

- Sugawara, T., Hirasawa, A., Hashimoto, K. & Tsujimoto, G. (2002). Differences in the subcellular localization of  $\alpha_1$ -adrenoceptor subtypes can effect the subtype selectivity of drugs in a study with the fluorescent ligand BODIPY FL-prazosin. *Life Sciences.*, **70**, 2113-2124.
- Summers, R.J. & McMartin, L.R. (1993). Adrenoceptors and their second messenger systems. *J. Neurochem.*, **60**(1), 10-23.
- Suzuki, F., Taniguchi, T., Takauji, R., Murata, S. & Muramatsu, I. (2000). Splice isoforms of  $\alpha_{1a}$ -adrenoceptor in rabbit. *Br. J. Pharmacol.*, **129**, 1569-1576.
- Szmigielski, A., Szmigielski, H., Zalewska-Kasubaska, J. & Marczak. (1997). The cooperation between the influx of extracellular calcium and  $\alpha_1$ -adrenoceptor-induced translocation of protein kinase C. *Pharmacol. Res.*, **36**, 211-219.
- Taguchi, K., Yang, M., Goepel, M. & Michel, M.M. (1998). Comparison of human  $\alpha_1$ -adrenoceptor subtype coupling to protein kinase C activation and related signalling pathways. *Naunyn-Schmiedeberg's Arch. Pharmacol.*, **357**, 100-110.
- Takeda, M., Hatano, A., Arai, K., Obara, K., Tsutsui, T. & Takahashi, K. (1999).  $\alpha_1$ - and  $\alpha_2$ -adrenoceptors in BPH. *Eur. Urol.*, **36**, 31-34.
- Takei, K. & Haucke, V. (2001). Clathrin-mediated endocytosis: membrane factors pull the trigger. *Trends Cell Biol.*, **11**, 385-391.
- Tarasova, N.I., Stauber, R.H., Joon Ki, Choi., Hudson, E.A., Czerwinski, G., Miller, J.L., Pavlakis, G.N., Michejda, C.J. & Wank, S.A. (1997). Visualisation of G protein-coupled receptor trafficking with the aid of the green fluorescent protein. Endocytosis and recycling of cholecystokinin receptor type A. *J. Biol. Chem.*, **272**, 14817-14824.

Testa, R., Taddei, C., Poggiosi, E., Destefani, C., Cotecchia, S., Hieble, J.P., Naselsky, D., Bergsma, D., Swift, A., Ganguly, S. & Leonardi, A. (1995). A novel prostate selective  $\alpha_1$ -adrenoceptor antagonist. *Pharmacol. Commun.*, **6**, 79-86.

Tooze, J. & Hollinshead, M. (1991). Tubular early endosomal networks in AtT20 and other cells. *J. Cell Biol.*, **115**, 635-653.

Tsujimoto, G., Tsujimoto, A., Suzuki, E. & Hashimoto, K. (1989). Glycogen phosphorylase activation by two different alpha 1-adrenergic receptor subtypes: methoxamine selectively stimulates a putative alpha 1-adrenergic receptor subtype (alpha 1a) that couples with  $Ca^{2+}$  influx. *Mol. Pharmacol.*, **36**, 166-176.

Uhlen, S., Axelrod, D., Keefer, J., Limbird, L. & Neubig, R. (1995). Membrane organisation and mobility of  $\alpha_2$ -adrenergic receptors in MDCK cells. *Pharmacol. Commun.*, **6**, 155-167.

Uhlen, S. & Wikberg, J.E.S. (1991). Delineation of rat kidney  $\alpha_{2A}$ - and  $\alpha_{2B}$ -adrenoceptors with [3H]RX821002 radioligand binding. Computer modelling reveals that guanfacine is an  $\alpha_{2A}$ -selective compound. *Eur. J. Pharmacol.*, **202**, 235-243.

Vazquez-Prado, J., Carmen Medina, L.D., Romero-Avila, M.T., Gonzalez-Espinosa, C. & Garcia-Sainz, J.A. (2000). Norepinephrine- and phorbol ester-induced phosphorylation of  $\alpha_{1a}$ -adrenergic receptors. *J. Biol. Chem.*, **275** (9), 6553-6559.

Vazquez-Prado, J. & Garcia-Sainz, J.A. (1996). Effect of phorbol myristate acetate on  $\alpha_1$ -adrenergic action in cells expressing recombinant  $\alpha_1$ -adrenoceptor subtypes. *Mol. Pharmacol.*, **50**, 17-22.

Vinet, R., Rojas, F., Luxoro, M., Vargas, F. & Cortes, M. (2000). Catecholamines-evoked cytosolic  $Ca^{2+}$  rise in endothelial cells from bovine adrenal medulla. *Mol. Cell. Biochem.*, **203**, 53-58.

Voigt, M.M., Kispert, J. & Chin, H. (1990). Sequence of a rat brain cDNA encoding an alpha1B adrenergic receptor. *Nucleic Acids Res.*, **18**, 1053.

Von Zastrow, M. & Kobilka, B.K. (1994). Antagonist-dependent and -independent steps in the mechanism of adrenergic receptor internalization. *J. Biol. Chem.*, **269**, 18448-18452.

Waugh, D.J.J., Gavin, R.J., Zuscik, M.J., Gonzalez-Cabrera, P., Ross, S.A., Yun, J. & Perez, D.M. (2001). Phe 308 and Phe 312 in TM VII are a major site of  $\alpha_1$ -adrenergic receptor antagonist binding: imidazoline agonists bind like antagonists. *J. Biol. Chem.* (in press)

Waugh, D.J.J., Zhao, M-M., Zuscik, M.J. & Perez, D.M. (2000). Novel aromatic residues in transmembrane domains IV and V involved in agonist binding at  $\alpha_{1a}$ -adrenergic receptors. *J. Biol. Chem.*, **275**, 11698-11705.

Wayman, C.P., Gobson, A. & McFadzean, I. (1998). Depletion of either ryanodine- or IP3-sensitive calcium stores activates capacitative calcium entry in mouse anococcygeus smooth muscle cells. *Eur. J. Pharm.*, **435**, 231-239.

Wetzel, J.M., Miao, S.W., Forray, C., Borden, L.A., Branchek, T.A. & Gluchowski, C. (1995). Discovery of alpha 1a-adrenergic receptor antagonists based on the L-Type  $Ca^{2+}$  channel antagonist nifedipine. *J. Med. Chem.*, **38**, 1579-1581.

Wikberg, J.E.S., Dambrova, M., Uhlen, S. & Prusis, P. (1998). Conditions for biphasic competition curves in radioligand binding for ligands subjected to metabolic transformation. *Biochem. Pharmacol.*, **56**, 1129-1137.

Willms, E.W., Heiligers, J.P.C., De Vries, P., Tom, B., Kapoor, K., Villalon, C.M. & Saxena, P.R. (2001). A61603-induced vasoconstriction in porcine carotid vasculature: involvement of a non-adrenergic mechanism. *Eur. J. Pharmacol.*, **417**, 195-201.

